Damage Accumulation in High Performance Synthetic Fibre Ropes

Mehran Koohgilani

A thesis submitted in partial fulfilment of the requirements of Bournemouth University for the degree of Doctor of Philosophy

September 1998

Bournemouth University
In collaboration with
Airwave Paragliders

This work is dedicated to

My loving wife **Shahrzad** and son **Arya**
who had faith in me and endured the hardship of my student years

And to

My parents for giving me the opportunity to fulfil a dream

Abstract

This thesis presents the results of an investigation into the process of damage and failure in small diameter high performance synthetic fibre ropes namely Dyneema, Vectran and Technora ropes. This study was prompted by a series of fatal accidents on paragliders as a result of the line failure.

All the different rope materials, including the rope with cover, without cover and the core with different number of strands, have been tensile tested. The transfer of loading and subsequent damage in different rope constituents, fibres and strands, are also discussed. The residual strength of the rope after static and cyclic preloading regimes is discussed and possible mechanisms for the damage accumulation in the rope are given.

The acoustic emission monitoring of the tensile and residual strength tests shows distinctive differences between the different types of rope and permits the identification of characteristic effects of preloading on the tensile damage and failure mechanisms of all three materials. The process of damage in the Dyneema and Vectran is similar, in which damage progresses in steps during the loading history whereas Technora rope accumulates gradual increase in damage until the catastrophic failure. The application of the static preloading improves the strength of Dyneema and Vectran ropes whereas it deteriorates the mechanical properties of Technora rope. The cyclic response of Dyneema rope shows a dramatic downturn at lives in excess of 1000 cycles, but moderate cyclic loading improves the strength.

The variation in surface temperature of Dyneema rope during tensile loading has been measured analysed and related to the process of damage. Dyneema fibres melt and fuse together under loading, since Dyneema is disadvantaged by its low melting temperature.

Rope on rope abrasion tests, carried out on covered and uncovered Dyneema and Technora ropes, show that Dyneema rope has superior abrasion properties compared to Technora. This is due to the low compression properties of Technora, as abrasion process involves compressing the fibres.

The effect of exposure to different environments, including natural weathering, -22°C, +54°C and seawater on tensile performance is discussed. The tensile properties of the Dyneema ropes are little affected by the environmental conditioning except the effect of synthetic sea water, in which case the salt crystals damage the rope fibres, once the water has evaporated.

Acknowledgements

The author is grateful to many people who contributed to the smooth running of this study:

Dr. S.H. Saidpour, for his endless patience and supervision throughout this study.

Dr. K. Tabeshfar and Professor P. Hogarth for the provisions of funds to carry out this project

Mr P. Jones, technician of the School of Design Engineering & Computing

Mr B. Goldsmith and Dr. D. Pilkington of the Airwave Gliders, Isle of Wight, for the support and technical information.

Mr B. Morris, British Hanggliding and Paragliding Association Safety Executive, for his input and technical support.

Mr M.J.N Jacobs, DSM High Performance Fibres, for his technical information and support on Dyneema.

Mr. N. Leefe, Hoechst Celanese, for his technical information and support on Vectran.

Mr. Y. Saito, Teijin Ltd, for his technical information and support on Technora.

Mr. T. Hall, Ibex Ropes, for his technical information and support on the ropes.

Mr. J. Yeardley, Bridon Fibre Ropes, for his technical information and support on ropes.

Mr. J.A. Barron, Cousin Freres S.A, for his technical information and support on ropes.

Mr. S. Banfield, Tension Technology International, for his technical information and support.

Glossary

"A" line: Rope to the leading edge of the wing

AE: Acoustic Emission

Aerodynamics: The study of moving air

Airfoil: A curved surface designed to generate lift when moving through the air

Akzo: Dutch manufacturers of Twaron

Aramid: Aromatic polyamides

Aramid Copolymer: Aromatic Copolyamide

As Received: Rope samples with the polyester cover

Basic yarn: Thousands of individual fibres assembled together

Brake: Control to alter the speed or direction of the paraglider

Big Ear: A certain manoeuvre in paragliding, where the ropes are subjected to rapid shock loads.

Braid rope: To interweave several strands

Breaking Strength: The breaking strength is the maximum force, which the cordage will sustain before rupture occurs

Burrs: Rough edge of rope

Canopy: The material or "sail" of a paraglider that forms the airfoil or wing

Chafe: To make or become worn by rubbing

C.H.S: Cross Head Speed

Coefficient of Friction: When two bodies are in sliding contact, a force is created to oppose the motion, which is known as the frictional resistance

Coiled: To wind or gather rope

C.S.V: Comma Separated Values (Format of the data from the MR1004 Acoustic Emission Analyser)

CTF: Cycles to failure at load level

Dead Time Delay: This is the time between the end of the last record and when a new record is allowed to start

Denier: The weight in grams of 9000 metres of a yarn, tow or roving

DHV: Deutscher Hängegleiterverband e. V im DAeC (the German governing body for Paragliding and hang gliding sport and certification of new models

DSM: Dutch State Mines, Manufacturers of Dyneema

Du Pont: American manufacturer of Kevlar

Dyneema: Gel spun HMPE fibre produced by DSM

Elastic Tension: This is the phenomenon of man made fibre ropes caused by their high extension under load

Event Count: Number of events occurring during sampling

Event Duration: Time taken for each sampling

Fibre: A material form showing high length-to-diameter ratio normally characterised by flexibility and firmness and the basic starting point for a rope

Filament: A single fibre

Gouges: Force the rope out of its position

GPD: Grams Per Denier

Gutesiegel: German governing body for paragliders

HMPE: High Modulus Polyethylene

Hockle: Untwisting in three strands laid hawsers

HPSFR: High Performance Synthetic Fibre Rope

HPPE: High Performance Polyethylene

Hysteresis: Because present man made fibres are non linear their loading and recovery curves do not follow the same path, and a hysteresis loop is generated. The area of this loop is proportional to the energy absorbed by the fibre during the loading cycle.

IPSFRs: Intermediate Performance Synthetic Fibre Ropes

Kevlar: Aramid fibre produced by Du Pont

Kink: A sharp twist or bend in a rope

LASS: Load at Specific Strain

L/D: Length to Diameter ratio

LCP: Liquid Crystal Polymer

Line: Rope, tension member

MR1004: Marandy Acoustic Emission analyser

PA: Polyamide (Nylon)

PAD: Peak Amplitude Distribution

Pararopes: Paraglider Ropes

PE: Polyethylene

Pentex: Super high modulus polyester produced by Allied Signal

Plaited: Several strands twisted or intertwined

Plied yarn: Several basic yarns are plied or twisted together

PP: Polypropylene

RBS: Rated Break Strength

RDC: Ring Down Count

RMS: Root Mean Square Value

Rope yarn: Several plied yarns are twisted together to form rope yarn

Roving: An assembly of compact fibre bundles, or strands usually with no twist. Usually heavier (higher tex) materials, term most often used with glass fibre

SEM: Scanning Electron Microscope

Sheaves: A bundle of fibres tied together

Sisal: Mexican plant, its large fleshy leaves produce a stiff fibre used for making rope

Snag resistance: Resistance to sudden pull

Spectra: Gel spun HMPE fibre produced by Allied Signal

Splice: To join two ropes by intertwining the strands

Strands: A number of rope yarns twisted together

SWoR: Specific Work of Rupture

Technora: Aramid copolymer produced by Teijin

Teijin : Japanese manufacturer of Technora

Tex: The weight in grams of 1000 metres of yarn, tow or roving ($9 \times$ tex = denier)

The Core: Rope samples with the polyester cover removed

Tow: A loose bundle of fibres, having little or no twist

Twaron: Aramid produced by Akzo

Txt: Text format supplied by the Testometric UMT software

UMT: Universal Materials Test

UV: Ultra Violet

Vectran: LCP fibre produced by Hoechst Celanese

WF: Work Factor

WoR: Work of Rupture (Energy)

Yarn: An assembly of fibres, of similar or variable length, held together by twisting

List of Tables

List of Figures

List of Plates

1.0 INTRODUCTION

The dictionary definition of a rope is "A rope is a long, compact, flexible assembly of fibres serving primarily to transmit tensile force or energy". The requirements for any synthetic fibre rope are[1,2]:

- The greatest possible tensile strength
- Flexibility, knotability, ease of handling and gripability
- A compact cross section which retains its form during use
- Elastic behaviour, dampening of shock loads, (absorption of mechanical energy)
- Stable load elongation properties in use
- Light weight
- Fatigue resistance
- Abrasion and cutting resistance
- Resistance to chemicals and corrosion, temperature stability
- Ease of splicing or attaching reliable termination
- Low cost
- Torque balanced or better yet torque free construction

Ropes and chains are bodies, whose symmetrical, mostly circular cross sections, are small compared to their lengths. They are able to transfer loads only along their axes[3]. They can not transfer bending moments or transverse forces of any magnitude and are unstable under compressive loads, they will bend out. While chains hardly stretch at all and wire ropes very little (under 5%) under applied tensile loads, fibre ropes often show considerable elongation. Some fibre ropes can be stretched over 50% of their original length before break. Compared with wire ropes, fibre ropes are very flexible. This accounts for their knotability. Simple ropes are made up from a number of sub-elements called strands; these strands in turn being constructed from a number of rope yarns. Ropes may incorporate several levels of complexity, from single textile filaments to sub-elements, which are themselves, ropes in their own right. Ropes have been around for a very long time and are one of mankind's oldest artefacts and an example of today's advanced engineering. The greatest amount of work done on ropes whether synthetic or wire has been carried out on the ones used in the offshore industry.

There are several international annual conferences, which have marine and offshore industry as their core, and they are:

- Offshore Technology Conference (OTC)
- Marine Technology Society (MTS)
- International Offshore and Polar Engineering (IOPE)
- International Offshore and Arctic Engineering (IOAE)
- Ocean's
- Oil Companies International Marine Forum (OCIMF)
- Tug Convention

Most of the literature on small diameter ropes has concentrated on parachute ropes carried out by the American military on such aspects as the dynamics of parachute opening force or the drag effect[4,5,6,7,8].

There has not been any scientific investigation into small diameter high performance ropes. The only available published data can be found in glossy manufacturer brochures. Although some work was done by paragliding governing body in Germany namely DHV mainly for certification purposes rather than analysis and performance specification. They have published their results in related sports magazines[9,10,11,12].

This thesis presents results of the first systematic study on the ropes used in the paragliding industry, to reduce the risk of rope failure by achieving a better understanding of the rope behaviour. This is very important, as there have been several fatal accidents since the conception of the sport.

One of the difficulties in this study has been the lack of standards for test of high performance fibre ropes. There are no testing guidelines such as what cross head speed to use. However, DSM High Performance Fibres test Dyneema[13] at 100 mm/min and since Dyneema is the most widely used Paraglider rope, and the main rope tested in this study, it was decided to use this testing speed for all the materials tested to enable direct comparison to be made.

It has been the first time that acoustic emission as a tool has been applied to small diameter ropes. It can be seen from the literature that acoustic emission has been successfully applied to wire ropes[14,15,16,17,18,19,20,21,22] as well as large diameter double braid *nylon* ropes[23,24,25,26]. There has not been any published work dealing with acoustic emission and high performance small diameter ropes namely Dyneema, Vectran and Technora making the work done in this research unique. Other non-destructive techniques have only been applied to intermediate fibre ropes[27,28,29,30,31,32,33,34,35,36,37,38].

The closest examples of published works to strand removal tests are the strand pullout test[39,40,41,42,43]. Even then the paper did not address the relationship between the number of strands and strength of rope as well as strand and rope efficiencies.

The effect of preloading as a means of residual strength measurement[44,45,46,47,48,49] has been investigated but no systematic investigation of the effect of preloading on the overall strength of the rope has been conducted in order to estimate the start of damage to the rope. The main objectives of this project are:

1. To investigate the mechanical performance of Dyneema, Technora and Vectran ropes.
2. To investigate the micro & macro mechanical behaviour of these ropes.
3. To determine the rate of damage accumulation and residual strength after a preload conditioning
4. To determine the effect of the strand failure on the breaking strength of the ropes
5. To investigate the failure mechanisms operating in these ropes

All the above objectives have been met by following carefully designed experiments as explained in the section 7.0.

2.0 BACKGROUND TO PARAGLIDING

Parachutes have been around in reality and in the man's imagination for many years. They first started as safety devices to be used as a last resort, however, mankind soon took the idea further by enjoying first the free-fall and finally prolonging the descent.

Paragliding, see Figure 2.1, the latest aeronautical sport in fashion, has become an increasingly popular activity with enthusiast searching for freedom, dynamism and nature. By enabling man to fulfil Icarus' old dream, this evolution of the parachute has given him an affordable means of sharing the skies with the birds. There are now some 250,000 paraglider pilots flying in Europe alone with 4000 registered Paraglider pilots in the UK flying in 1996. The sales over the past ten years exceeded 200,000 units.

A Paraglider can be described as a ram-air, flexible airfoil canopy that can be flown and landed using the wind energy, force of gravity and the pilot's muscle-power.

2.1 History

Back in the 1940's on the East Coast of America, just down the road from the site of the Wright brother's first successful flight- another aviation pioneer was conducting experiments with kites made of pieces of curtain materials. His name was Dr Francis Rogallo and, after much persuasion, his work was eventually followed up by his employers, the North American Space Administration (NASA). It was in 1948 when he filed a patent for his flexible Delta kite. From Dr Rogallo's work came a whole mountain of research, testing, and flexible wing (flex-wing) construction technology[50]. This resulted in both the Ryan aircraft Company's bizarre looking aerial cargo-delivery wings which used a folding "kite" wing and the steerable recovery parachutes used by the Gemini series in the US space programme. But by far the most important offshoot of this research was the utilisation of the Rogallo wing by several latter-day aviation pioneers as an excellent way of getting off the ground, either by means of a tow-launch behind a boat or a car, or by foot-launching. Some of the earliest exponents of "hang gliding" (so-called because, in those days, you literally had to hang on by your armpits)

made their wings from bamboo, polythene and sticky tape. Not surprisingly, the golden rule was never to fly higher than you care to fall[51].

Very soon, the machines were made of stronger material and, as early as 1961, Tom Purcell Junior was tow-launched on a Rogallo wing in the USA. The following year, John Dickenson, a water-skier, began to fly a Rogallo wing in preference to the flat kites that had sometimes been used. It was he who introduced the idea to two men whose names are recognised by hang glider pilots world-wide today-Bill Moyes and Bill Bennett. These two dominated the early development of the sport of hang gliding as is known today, and are still active as manufacturers in Australia and the USA respectively. Meanwhile, in the UK, Walter Neumark was flying new types of parachute, designed by Lemoigne and Pioneer, which were capable of far superior performance and control than the existing types. Even back in 1961 Neumark, a sailplane pilot, could envisage a self-inflating parachute being used for soaring flight. Shortly afterwards, he wrote a manual, Operational procedures for ascending parachutes, and training began in what was to become known as parascending. In 1968 Dan Poynter recorded in an article for the Parachutist magazine that canopies were foot-launched at Lake Placid, in the USA, during the annual parachute competition. In 1973 the British Parachute Association withdrew support for the emerging sport of parascending and the British Association of Parascending Clubs was formed. In 1989, the association changed its name to the British Association of Paragliding Clubs, reflecting its interest in a range of related pursuits, from over-water towing operations, towed parascending and, most recently, foot-launched paragliding[52].

2.2 Paraglider Design

NASA originally conceived a version of Paragliding during the 1950s as a lightweight hybrid of parachute and inflated wing that might have allowed astronauts to manoeuvre the space vehicle to an airfield landing. For a period of three years (1961 to 1964) the United States National Aeronautics and Space Administration (NASA) tried to convert the idea into a practical landing system for the Gemini Spacecraft which would carry the Paraglider safely tucked away until after re-entry when it would be deployed

converting the spacecraft into a makeshift glider. However, NASA abandoned land landings, until the delta shaped Shuttle, because the Russians got ahead in the space race, so they used conventional parachutes for sea landings. The true genesis of Paragliding is from Domina Jalbert who in 1964 developed a ram air-inflating wing, which he named the Parafoil. He then developed the parasledge in 1972 and sold the rights to North American Aerodynamics in 1974. These devices were double surfaced, with inflatable cells and brought about a skydiving "square" revolution that ousted the traditional "round" parachute. The first foot launched Paragliding flights from hills were made on opened jump ram-air parachutes. Paraglider canopies are usually made of ripstop *nylon* with polyester from Teijin Ltd, Japan, being increasingly employed. The very large quantities of suspension ropes are 1 mm to 1.5 mm in diameter. The material originally used as opposed to parachutes was Kevlar[i]. Today ropes are mostly Dyneema, Spectra, Technora and Trevar. Vectran has also been considered. As with many other ideas that originated in either military and space, it was soon taken on by the sports enthusiasts but it was not until the advent of High Performance Synthetic Fibres that true Paragliders could be designed, the same fibres which helped offshore installation to be held securely in very deep waters.

2.3 Paraglider Performance

The landing run for a hang glider is 2-3 paces and it can be retrieved by ordinary car or even by foot. The best parachute has 50% performance of an intermediate paraglider. The minimum sink rate is just 1 m/s with a workable speed range of 25-40 km/h. The Paraglider allows the pilot to soar through the skies catching thermals (hot air pockets) and fly for several hours covering considerable distances, reaching heights of around 4500 metres above sea level. The world Paragliding distance is 281.5 km and was set by Alex Lowe on 31st December 1992 in South Africa. Steve Ham set the UK record at 174 km[53]. The typical competition paraglider has a span of 10 m similar to the hang glider but with a wing area of 30 m^2, about double that of the hang glider. The glide angle is about 7 to 1 and aspect ratios are around 4. The paraglider itself weighs only some 7 kg with a pilot weight range of 45-65 kg for smaller 23 m^2 wing area models

---

[i] In the parachutes due to the large shock loads generated on opening *nylon* is the material used due to its great energy absorbency.

and 85-105 kg for larger 30.7 m^2 versions. Paragliders have the smallest turning circle of all gliding machines; therefore they can be maintained in the centre of a thermal where the lift is greatest. The sink rate of 1.2 m/s is a little higher than the hang glider and the L/D worse; the best having an L/D of 7 and a low speed range of 20-40 km/h. They can be safely landed in tiny spaces.

2.4 Paraglider Components

A Paraglider is basically made of three sections, See Figure 2.2:

1. Canopy
2. Harness
3. Suspension Ropes

The material for the canopy has not changed since the start of the sport as such since the main requirement has been that it should not be porous and not be affected by the environmental effects such as moisture and UV. The material used has been polyester or *nylon*, which meet the necessary requirements and are relatively cheap. However, the design has to be exact so that the precise pilot position can be maintained and hence the flying characteristics. The actual design is very similar to an airfoil with leading and trailing edges, which direct the air over and under the canopy. Entry ports and cross ports inflate the canopy to give it its shape, but, like all flying devices, increased efficiency partly relies on reducing the "parasitic" drag of the air rubbing against canopy and around the ropes.

2.5 Paraglider Rope Requirements

The breakthrough came with the ropes. In order for the average 80 kg man to take to the air the canopy has to be very large around 30 m^2. This was overcome in parachuting in the early part of the century by the use of *nylon* and later in Paragliders with the use

of high performance plastics materials. However, there were certain requirements which were needed to be met for the ropes and they are:

- Create as little a drag as possible
- Dimensionally stable
- High strength to weight ratio
- Good environmental and sun light resistance (UV)
- Good shock loading resistance
- Good flexibility and bend resistance
- Good termination properties when sewn

There is no single material available which would completely satisfy all these requirements but since the early seventies there has been developments in high performance fibres which have paved the way for great advancements in the design of the Paragliders. The main original constraints were the size needed to reduce drag and the high weight to strength ratio. A Paraglider is a symmetrical object with loads being taken by about 500 metres of rope on an average Paraglider starting from the harness and then cascading out to the canopy. The average rope diameters range from 1.1 mm to about 1.6 mm. The ropes are arranged in the form of A, B, C, and D ropes starting from outside inwards, see Figure 2.3. This means that the ropes on the inside carry the maximum load with the ones on the outside the least. However, the maximum load carried under normal flying conditions is approximately 5-7 kg in each rope. This thus gives a great margin of safety of usually 6 because the average 1.1 mm rope has strength of approximately 85 kg.

There are several rope designs available:

- Twisted (4 strands as used in this research)
- Plaited
- 4 Strands
- 6 Strands
- 8 Strands (as used in this research)
- Braided

These are shown in Figure 2.4 and are the ones that are used in this study.

3.0 BACKGROUND TO ROPES

The history of natural fibres converted to yarns for cloth and rope predates recorded history. Twisting the short fibres of cotton or flax and that native to each area created the yarns and continuity for weaving. The manual counter-twisting to form the stranded cord and rope progressed over the millennia to small hand tools and to the rope-walks of the 18th century. Manila hemp became the best commercial fibre, while silk represented the highest quality with its continuous uniform filaments and high strength. The demands of ships and farm in the booming America of 1800 required almost 200 rope-walks to serve the river and ocean traffic. The great sailing ships were rigged by the expanding giants of rope and chain, with huge stranding machines outmoding the miles of walks. A key feature of the rope makers art was his coating of resin or lubricant. To this day no fibre producer will reveal his secret surfactant, oil, binder or coating, but the common additives then were tallow, beeswax, whale oil, pine pitch, coal tar, and later petroleum tars and waxes. The natural petroleum crude was mined for mortaring stones and impregnating rope centuries before the auto and fuel oil demands. The tars were the vital matrix that sealed the ropes and planking and from which the sailors derived their fragrance.

The 3-strand and the braid or plait were the basic rope designs and still are. It has taken centuries of ingenious mechanics to evolve the rotating high decibel machines that to this day are the major mass manufacturing methods. World War II saw the last big surge in natural fibre production and the advent of synthetics. Rayon became the first tonnage fibre for textile and tyre cord. *Nylon* has become a household word and dominates the plethora of synthetics. For ropes the hemp is still a major fibre, but far outclassed and outmoded by *nylon* and polyesters, ethylenes and polypropylenes. Now the high modulus aramids and polyethylene and Vectran are used while natural fibres such as hemp, leather and cork retain their special sectors of the market[54].

The craft of rope making has existed for longer than history can trace. Early ropes were made of hides, climbing plants and grasses and latterly leaf and stem fibres. Until the

middle of the nineteenth century, hemp and flax were the usual materials. Most of the hemp was produced in South East Europe while the flax was produced of indigenous origin. At the time of the Crimean war, hemp became difficult to obtain and did not satisfy demand; thus ropes were made from manila fibres. Manila was a new fibre to Great Britain at this time, although it had been used commonly in the Far East where its reliability was known. So successful was its introduction in Britain that stocks of the fibre were, during the second world war, again difficult to obtain and, partly due to this, and partly due to the improved water repellent treatments which had been developed, sisal fibre made inroads into the manila share of the market. This was further accelerated by the financial position of Britain after the war. Manila fibre was a dollar purchase, and hence was restricted in application by the government.

3.1 Natural Progression of Rope Design

Three thousand years ago the sailor had a simple choice: he could have either papyrus or flax ropes in three-strand construction and could draw on centuries of experience for knowledge of its behaviour. The remains of a nearly 10,000 years old Mesolithic fishing net were found by archaeologists in Finland but this was by no means the oldest example of ropes used by man. By contrast two years ago another net made of ropes of break strength of 4000 kN was put in the Gulf of Mexico 150 miles SW of Morgan City, Louisiana, to protect the oil riser on the Shell's Auger platform. This net used nearly 30,000 kg of polyester yarn produced by Hoechst Celanese and took two years from research to design and production.

While exploring Tura Caves in 1942 on the East Bank of the Nile, British troops found blocks of stone similar to the ones used on the pyramids. There was a papyrus rope round one of them which dated back to 500 BC, see Figure 3.1. Its construction was very similar to a modern three strand rope. It had seven fibres twisted in the cross sections of the yarns, forty yarns were twisted into strands and three strands were twisted to form the rope. The papyrus rope is remarkably similar to a *nylon* rope produced nearly 2500 years later. One of the officers was G.C. Hawkins, a grandson of

the founder of Hawkins & Tipson, rope makers in Sussex in the South of England who are now known as Marlow ropes[55].

Ropes have a long history. In prehistoric times, man found the need for what sophisticated engineers would now call tension systems for mooring, towing, staying, guying, tying, fencing and other similar applications. The technology developed to meet these needs in the ancient civilisations changed little until the second half of the 20th century. Figure 3.2 shows the relative time periods for different rope designs.

Then, as now, the key requirements were strength and durability, and a combination of high resistance to extension with flexibility. It was found that high quality long hard cellulosic fibres, such as manila, hemp and sisal best met these needs, which were extracted from the stems or leaves of plants. Cotton was used where softer, more extensible and cheaper rope was required.

Twist was needed in order to hold these discontinuous fibres together, and this resulted in the development of the traditional 3-strand ropes. In order to provide long lengths, rope-walks were established in most sea-faring and agricultural communities. Here the fibres were spun into yarns, then the bundles of yarns were twisted into strands and finally the strands were twisted or laid into ropes. Reversal of twist at the different levels gave a reasonably stable structure and reduced the torque forces. Variants of the twisted construction included 4-strand and 9-strand ropes. A few made use of circular braid constructions. This was the state of the art in the agriculture; fishing and marine fibre rope markets until man-made fibres appeared on the scene.

Following the industrial revolution a new "engineering" market for ropes and cables developed during the 19th century. Wire ropes, a product of the emerging steel industry, gave great strength and stretch resistance (or high modulus) and found applications as bridge catenaries, and lift cables, hoist, carne, stay and conveyor ropes. They also made massive inroads into the traditional marine and fishing markets previously dominated

by natural fibre ropes. Steel wire ropes and strands remain unchallenged today in a wide range of civil and mechanical engineering applications where technical demands are high.

The first man-made fibres had little impact on either the wire or the natural fibre rope trade. Acetate and the early rayon yarns were too weak to be of interest. The tyrecord rayon yarns found some cordage applications in the 1940s, but had little time to influence a conservative industry before *nylon* appeared as a more serious competitor. Other synthetic fibres quickly followed this. But these first melt-spun synthetic fibres barely surpassed the hard vegetable fibres in dry strength.

However, from the 1950s onwards, their better strength conversion into rope, greater durability, higher energy absorption, consistency of properties and falling price led to a progressive capture of the larger part of the cheaper "commodity" rope market from the natural fibres. Some were also stronger than steel per unit weight. None of these early wave fibres, however, could offer strength or resistance to stretch approaching that of steel rope of equal diameter.

It was the introduction of the second generation of man-made fibres, the high modulus, high tenacity fibres made in the 1970s, which stimulated the advance towards high performance synthetic fibre ropes which could also compete with steel in strength and also resistance to stretch. Indirectly, they benefited from the greater stimulation of rope manufacturers to experiment with more efficient constructions in response to raised market expectations. This also led to improved ropes made from the older man-made fibres, making some polyester ropes competitive in the high performance market.

Although the first wave of man-made fibres displaced natural fibres, the displacement of steel wire ropes by High Performance Synthetic Fibre Ropes will be slow in many markets and improbable in others. To generate substantial volumes in the short to

medium-term, therefore, the second wave of fibres must carve markets either at the expense of the first wave or in entirely new areas[56].

3.2 Chronological Development of Fibres for Ropes

From the earliest civilisations the use of natural fibres, twisted and bound together have been used to suspend loads and translate forces. This is recognised in its basic form as rope. In England, rope making was well established by the 14th century. This can be attributed to the demands of the English maritime fleet and the extensive use of rope used in the maritime industry.

By the 16th century in England, a crown rope works at the Royal Dockyards, Woolwich was set-up. Due to the ever-increasing demand of the seafaring nation, many other crown and privately owned rope works were established in most sea ports.

The first material used appears to have been flax with the later use of soft hemp, cotton and jute. The use of hard fibres such as manila, sisal and coir did not appear until the early 19th century.

By the 19th century the traditional materials limited the development of the fibres and their applications. The manufacture of rope was also based purely upon experience and little investigation into internal factors influencing a rope performance had been done.

To cope with the increasing demands of the industrial revolution and the higher loads associated with heavy industry, larger steel ships, etc.; work began on steel wire ropes during the 1830's in Germany. From about 1850, the manufacture of steel ropes had developed from the initial use of iron wire to the use of high carbon steel wire. It was also recognised that the technical aspects of a rope construction affected the overall rope performance. These technical developments took the form of flattered stranded

rope and the invention of locked coils. Wire rope from the start had important industrial applications in mining and engineering. By the end of the 19th century the UK industry was producing technically sophisticated wire rope for use in mining, bridges and aerial ropeways and was technically the world leaders. In some industrial uses wire rope was the long awaited answer replacing, to a limited extent, fibre ropes.

As fibre ropes were limited by the availability of traditional natural fibres any further development in rope technology was tied into the material advancement. The real breakthrough came with the modern day synthetic fibres.

In 1883, an English man, Joseph Swan extruded the first cellulose nitrate filament whilst searching for a useful material for the new electric lamp. The resulting carbonised filament was also recognised for its potential as a textile fibre but no suitable method of mass production was available at the time.

The first production of a cellulose nitrate fibre on a commercial scale was implemented by count Chardonnet, in France in 1885. The nitrate material is highly flammable and useable fibres were obtained by treatment with ammonium sulphide solution to convert the nitrate back to cellulose. The resulting product was called artificial silk.

In 1891, British chemists, C.F. Cross and E.J. Bevan developed a method of converting cellulose cheaply into a more attractive soluble derivative. This is now known as viscose rayon process. By 1894 Cross and Bevan had developed a second process for cellulose acetate. Their interest also covered the manufacturing of both product and with the co-operation of Mr H. Stearn, patented fibre spinning process. The three developed a crude pilot plant and eventually both processes were brought up to economic industrial scale and superseded the previous Chardonnet process.

The next development was the acetic esters of cellulose. From about 1914 to 1927 in the U.S.A a little fibre called cellulose triacetate was produced. However, between 1919 and 1921 a more successful cellulose derivative called "Celanese", a secondary cellulose acetate was developed by the Dreyfus brothers.

The remarkable feature of fibre development up until that point was that most of the ideas about chemical structure of the fibres were thoroughly inaccurate. During the early years of the 19th century the development of the scientific knowledge and techniques enabled scientists to investigate the molecular structure of more complex natural products.

As greater understanding was acquired as to the structure of many natural materials. It was recognised that the construction of natural materials, such as cellulose, wool, silk and other proteins are composed of macromolecules. The natural macromolecule is built up from small basic repeated units and connected end to end. The concept of the macromolecule marked a recent and important step in the development of chemistry. In the 1920's research in this field was lead by Hermann Staudinger and his theories are the basis for current understanding. He was awarded the Nobel chemistry prize in 1953.

From about 1928 the greatest practical exponent of Straudinger's ideas was with Dr W.H. Carothers within the company E.I. Du Pont de Nemours in the USA. In 1932 he discovered that if certain synthetic polymers of high molecular weight were melted, fibres could be pulled from the surface. After lengthy investigation using many polymers, useful characteristics were discovered in a class known as polyamides. This resulted in the first synthetic fibre called *nylon* 6,6 being launched in the USA in 1938. The practical realisation of Straudinger ideas directed the development of designer synthetic polymers and the rapid development of new polymers.

The other discoveries were the polyester fibres; however, the next big step came in early 1970's when Stephanie Kowleck of Du Pont discovered the aromatic polyamides

which became known as the aramids. Du Pont patented the production process and produced the fibre under the trade name of Kevlar. Akzo Noble in the Netherlands also produced a similar aramid fibre with comparable properties under the trade name of Twaron. However, early uses of these ropes in such applications as yachting proved unsatisfactory, as many sailors did not realise that these fibres suffer from poor compression and UV properties.

A great deal of work were directed at establishing the different properties and performance of ropes made from the aramid fibres since they promised a possible replacement for bulky steel wire ropes and chains.

In the 1980's Teijin of Japan produced an improved aramid fibre which can be better explained as aramid copolymer. It showed an improved resilience of 20% compared to the traditional aramid and an improved strength. Teijin produces the fibre under the trade name of Technora. Hoechst of Germany tried and produced a comparable aramid copolymer under the trade name of Trevar. However, they stopped production possibly due to economical reason.

The next development came in the early 1980's when a new gel spinning process was developed by DSM High Performance Fibres to produce polyethylene fibres with a very high degree of orientation. This fibre showed exceptional strength and excellent weathering properties since it has all the inherent properties of normal polyethylene except the weak strength. It has been produced in Europe under trade name of Dyneema by DSM and in America as Spectra by Allied Fibres. It was soon used in ropes. Its main draw backs have been its low operating temperature and the corresponding creep due to that.

The next development was when Hoechst Celanese developed the Liquid Crystalline Polymers and sold them under the trade name of Vectran[57,58]. These fibres have the same strength as the aramid fibres and suffer from the same environmental attack but

have superior creep properties, which makes them ideal for rope applications and better compression properties.

3.3 Ropes Properties

Some rope properties are dependant on manufacturing techniques and on who manufactures it: Yarn twist for instance gives rise to a number of properties: High yarn twist means tight yarn, more rounded strand, greater abrasion and snag resistance, higher stretch, lower strength and a more dimensionally stable strand[59]. The tightness of the rope lay or braid also affects these properties in the same way and makes the rope less likely to hockle, although more difficult to handle and splice. With each type of material there is a large choice available of yarn type as well as yarn "finishes" which are coating that enhance such properties as abrasion and fatigue resistance. The care taken to make a rope can also give an indication of its strength and durability. A rope whose yarn appear uneven with perhaps some of them protruding, indicates unequal tensions during manufacture and so a reduced service life would be expected. Equal tensioning of yarns, plaits and strands is vital. Tight yarns or plaits will take on a disproportionate amount of tension as the rope is loaded causing a lower rope breaking strength.

3.4 Rope Behaviour

As a general rule the lower the amount of twist the greater the load transfer efficiency. It is known that for a given size of a rope Maximum Strength and Minimum Elongation will be achieved with Parallel Lay Construction at the expense, however, of Flexibility and Cycle over Sheave lifetime. With Braided or Stranded Construction higher Lay Angles (Twist Levels) gives increased Flexibility, better Spoolability and higher Elongation while lowering Strength and Modulus[60]. The rope used in paragliding either has a braided jacket of polyester or in some cases no cover at all. There are some aramid ropes, which have a thermoplastic cover. The cover protects the core from the effects of the environment such as UV and weathering as well as chaffing and abrasion.

Its design and material directly affect the way a rope behaves. The design has to be torque balanced so that the load can be transmitted equally and uniformly. The relationship between the main load bearing section of the rope and the protective part has to be correct. Some designs such as braid on braid ropes are designed such that the upper braided layer is a sacrificial one. In extruded polyurethane coated ropes the cover protects the rope but at the expense of flexibility. In parallel lay ropes the lack of rope twist is translated into a more efficient load bearing structure; however, the need for extruded jacket puts a limit on the flexibility of the rope. Another important factor is the termination and how that would affect the rope performance. In other words selecting a right rope for the right application requires an understanding of the material, design and performance.

3.5 Paraglider Rope Materials

The original material, which met the main criteria, was Kevlar, which is an aromatic polyamide and has twice the strength of steel at a fraction of the weight. Then came the high modulus polyethylene (HMPE) which is even stronger than Kevlar. There have been other aramids developed ever since such as Twaron, Technora and the latest being Trevar[ii]. The two main HMPE types are Dyneema and Spectra. All these fibres are used in the ropes for Paragliders see Table 3.1.

3.6 Fibre Ropes as Textile Structures

Ropes are structures made of textile fibres. Rope structures are designed to obtain the maximum utilisation of fibre strength from a compact rope cross sectional area in order to produce certain rope breaking strength and elasticity while using a minimum amount of fibres. Since fibres are very fine elements, sometimes less than 10^{-3} μm in diameter or width, they have to be set up in large bundles to use their combined strength in a rope. The usual way to obtain strength and compactness in a fibre bundle is to twist the fibres together that are to wind them around one another. A yarn is formed by this

[ii] Heochst AG has stopped production of Trevar due to economical reasons

method. Twisting yarns together to form a multi-ply obtain large structures. Again larger structures are formed by twisting multi-plies together to form strands. Finally by twisting strands together a rope is produced[61,62,63,64,65,66,67,68], see Figure 3.3. Due to the twisting process, the components of the twisted unit form a fairly compact, mainly cylindrical structure at the expense of some of their tensile strength. The rope itself has to be torque free or at least torque balanced. Since the twist can have either a left hand or a right hand turn, torque free structures can be built up by taking the same number of right and left hand components, arranging and interlacing them symmetrically into a cross section. This is the basic construction principle of plaiting and braided rope. Another way to build a rope is to employ three or four equally sized strands having the same twist direction and turn them together to form rope twisted in the opposite direction. This is the principle used to produce a twisted rope. A third way is to combine a larger number of single fibres in a cross section and thus to produce a rope. A fourth way is to arrange parallel fibres in a circular cross section and to keep them there by extruding a hollow plastic jacket over the fibre bundle. In all cases ropes are slender textile structures whose symmetrical, frequently circular cross sections are small compared to their lengths. They are composed of a large number of single fibres. The fibre bundle has to be arranged to form a torque free or torque balanced structures. At the same time the structure has to produce a maximum utilisation of the fibre strength and sufficient flexibility and elasticity.

3.7 Constructions of Rope

Another key factor in determining the performance and rope properties is the construction of the rope. Eventhough in many cases there may appear to be little difference there are subtle variations between the various construction systems employed by the various manufacturers.

Ropes are complex structures and are made of several sub-elements, see Figure 3.3, namely:

- Fibres
- Yarns
- Plied yarns
- Strands

The definitions of these terms are given in the glossary of terms and Figure 3.4 shows several designs of ropes used. In the beginning all rope was laid or twisted from individual fibres. Originally performed on rope walks, long narrow areas where the rope could be laid out full length. Rope making was essentially a manual process. The length of rope that could be produced was limited to the length of the rope walk and production of large ropes was complex and time consuming. Individual fibres were made into yarns; these yarns were twisted into threads, these threads were in turn twisted into strands and finally the strands were twisted together to form the rope. The twist in each thread and strand served to hold the rope tight and a whole tradition of knot work and rope craft was developed to utilise the properties of laid rope. Machine manufacturing followed and with it came the ability to produce infinite lengths.

3.7.1 Three Strand Hawser Laid

Three strands are twisted or laid together to form the rope. This construction is still the most commonly use. It is an easily spliceable, firm rope. It stretches more than equivalent material core and cover constructions and has a tendency to hockle through poor handling. It is a traditional rope and is very cost effective and has an excellent abrasion resistance. Incorporation of reverse twist yarns in the centre of each strand can reduce the tendency to kink and hockle[69,70].

3.7.2 Three Strand Pre-Stretched

This is an advanced 3 strand construction especially useful for polyester. The rope is stretched and heat set during manufacture giving rise to higher strength, lower extension and even better abrasion resistance. It is a firmer rope and still spliceable[69,70].

3.7.3 Four Strand Shroud laid

Four strands are laid normally over a central core. The core may be omitted for ladder ropes where two strands pass on either side of the rungs. The construction was used formerly for running rigging on sailing vessels but today is rare to find ropes made in this manner. The rope is 11% weaker than equivalent size three strand rope[69,70].

3.7.4 Cable Laid Rope

Laying three or more hawser laid ropes together forms this construction. It is some 40% weaker than a similar size of 3 strand rope but is more extensible. Consequently, it was used for springs etc. Before the use of man made fibres but since their inception their use has dwindled[69,70].

3.7.5 Eight Strand Plaited

These ropes are initially made in the same way as the 3 strand ropes except that 8 strands are formed to produce a twist balanced, non rotating, solid plaited tope, comprising of four left hand and four right hand strands. Its properties are similar to the 3 strand construction except that it is a softer rope with a square profile providing a greater wearing surface and should not kink or hockle even if mishandled. 8 strand plaited ropes can continue in service nearly twice as long as the comparable 3 strand rope[69,70].

3.7.6 Braidline Ropes

Braidline rope consists of a plaited hollow core; over, which is, plaited an overlaying sheath. The rope construction is similar to two hoses placed coaxially within one another. This construction utilises more efficiently the aggregate strength of the component yarns and the guaranteed strength is some 15% stronger than an equivalent size 3 strand rope[69,70].

3.7.7 Superline Circular Braid

Superline ropes are circular in cross section consisting of a circular outer braided protective jacket over a central group of parallel low twist; torque balanced 3 strand core. The outer protective jacket is essentially non load carrying and if so completely severed or abraded through, the larger superline ropes will still retain 100% guaranteed minimum breaking strength. They have a much higher strength, lower weight and higher tensile fatigue life than conventional 8 strand plaited or braid on braid ropes, whilst retaining much of the flexibility and ease of splicing which such conventional structures offer[69,70].

3.7.8 Parallel Lay Ropes

These ropes are the most efficient rope design since there is very little twist in the fibres and there is no loss in strength transmission due to the presence of the helix angle. However, the necessary presence of the cover whose primary function is to protect and hold the fibres together limits the amount of flexibility of the rope[69,70].

3.7.9 Core/Cover Ropes

There are a number of variants within this type of construction. The core can be 3 strand, braided, or parallel and the cover 8 or 16 plait. A 3 strand core is the best construction for flex fatigue resistance. Its helical construction assures equal load sharing when stressed round tight radii and low twist levels keeps inter yarn abrasion to

a minimum. When encased in a 16 plait cover it is easily spliceable and stowable and handles very well. A braided core is not as good as 3 strand core for flex fatigue resistance therefore they should only be used where there is a distinct material advantage, for instance braided HMPE core over a 3 strand aramid core. If part of the rope needs to be used with the cover stripped off then a braided core presents no handling problems. A parallel core is simply a group of yarns neither twisted nor plaited aligned in the rope in a parallel fashion. This construction has a poor flex fatigue life and is not easily spliceable, however, it is the strongest of the core constructions and is generally used in small ropes which can be knotted. A rope with this type of core will generally have an 8 plait cover and will be a firmer rope than the braided or 3 strand cored ropes as the spliceability is not normally required. 8 or 16 plait covers are constructed from a number of yarns which come together to form a plait. They produce a more rounded profile rope than 3 strand; multiplait or solid braid ropes and so perform better in stoppers[69,70].

3.7.10 "Thor" Nylon Ropes:

The design is very similar to wire rope construction with six strands laid over a cover. Each strand is made of large *nylon* monofilaments, interspersed with multifilament yarn of conventional design. The monofilaments vary in size from 1.6 mm to 6 mm diameter depending on the size of the final rope. The rope is made stable by using a balanced mix of mono and multifilament both carrying the load[71].

3.7.11 "Viking 7" Polyester Rope:

Parallel arrays of seven long braided rope sub-elements are held together using a protective braided cover. This design overcomes the length limitation problems by utilising the seven sub-ropes rather than a single large strength member, see Figure 3.5[72].

3.8 Performance Prediction of Ropes

If the performance of the rope could be predicted then the right size, material and design rope could be tailor made for particular applications. However, there are several types of ropes and materials available. Due to the varaibilities in the fibre length in the ropes, there are several techniques used for determining the rope performance and they are listed below:

3.8.1 Mathematical Modelling

Mathematical modelling is a powerful tool for investigating the performance of a rope. Principle of virtual work, which is based on the kinematics of deformation to establish the equivalent of static equilibrium, is used to calculate the total virtual work of the rope by the addition of the virtual work of each component fibre. The rate of strength reduction at any tension cyclic load level is a non-linear function of applied cycle, being gradual at first and becoming more rapid as the CTF limit is approached and could be expressed such[61-65]

$$\frac{(100\% - R)}{(100\% - L)} = \left[\frac{n}{CTF}\right]^{B} \qquad \textbf{Eq:}\ 3.1$$

where:

L = Cyclic load level, percent of new strength

CTF = Cycles to failure at load level

n = Number of applied cycles

R = Residual strength after n cycles

B = empirically derived exponent constant

A value of 2 is estimated for the constant B for a particular double braid *nylon* rope[44]. However, the value should be higher[61]. The slope of the CTF rope could be approximated, at least over part of its range as a straight rope on a semi-log plot. The CTF could then be expressed as:

$$CTF = e^{A\,(100 - L)} \qquad \textbf{Eq:}\ 3.2$$

where:

A = Slope of the CTF rope on semi-log plot

Thus the equation for the residual strength could then be written as:

$$R = 100\% - (100\% - L)\left[\frac{n}{e^{A\,(100 - L)}}\right]^{B} \qquad \textbf{Eq:}\ 3.3$$

An analysis is developed to take into account the fact that residual strength curve equation is not enough because it is based on cycling at constant load level and in reality the typical load history would not be a regular series of loads to a constant peak but is a random record composed of many low level loads combined with a few relatively high peak loads. This method is known as strength reduction summation method and uses the above equation. The residual strength due to cycles at first load level is calculated. The equivalent number of cycles, which produce this strength reduction at a second, load level is then determined. The number of additional cycles applied at the second load level was added to this equivalent number preceding cycles to determine the total number of cycles at the second load level. The strength reduction due to this total effective number of cycles at the second load level is then determined[45,61-65,].

These formulae were first considered in order to investigate if they could be used or modified. However, after consideration of the parameters involved it was decided against using them as there was not enough relevance to the project. There is no indication of the material used and they were primarily useful for testing of ropes subject to cyclic fatigue.

3.8.2 Abrasion

Abrasion behaviour is very important since it is one of the elements of rope failure and its understanding would help define the rope performance. A model for the wear rate of *nylon* has been developed and it is found that the wear rate for *nylon* 6 is about five times higher than that of *nylon* 6,6. The abrasion model fits the data well down to 5% of the new strength for *nylon* 6. The applicability of the creep-rupture based prediction from fibre and yarn studies to large ropes at high stresses implied that the ropes failed by creep-rupture process. By this model, the accumulating rope creep strains brings some of the local fibres to their failure strain, initiating failure of the rope. If the failure mode (position) remains consistent for static and cyclic tests, then the cumulative rope strain at failure should be similar in all cases. Furthermore, since the fibres and yarns fail in a sudden death manner, with little loss in residual strength until very close to failure, the ropes are expected to show the same trend[75].

3.8.3 Bending

Bending is a parameter, which occurs when the cover is extended. It also occurs when the rope sub-elements interact making the axial compression fatigue an important criterion. The axial compressive fatigue of twisted ropes has been modelled[46]. This mode of failure is observed in use and testing of ropes. It is characterised by sharp co-operative kinking of yarns, which lead to flex fatigue breakage of fibres. A model of pipeline buckling has been modified to allow for plasticity in bending. The axial and lateral restraints, which influence the buckling, are derived from the existing rope mechanics model. Axial compression is introduced into the total computational model, in order to predict the form of buckling and the consequent fibre failure.

3.8.4 Hysteresis

Hysteresis is important since there is a build up of heat as the ropes are loaded due to the movements of the rope sub-elements on each other. This heat build up become more pronounced and important in thermoplastic ropes therefore the dynamic stiffness (called the apparent spring constant) and hysteresis of *nylon* and polyester double braid ropes 1-30 and 50 mm in a series of laboratory tests are determined[73]. The experimentally determined apparent spring constant and hysteresis are treated analytically to calculate the Viscoelastic parameters of the three parameter model of a synthetic rope. The apparent spring constant and hysteresis stabilises (i.e. change by less than 10%) after approximately 10,000 cycles of loading. The hysteresis decreases by approximately 30-50% between approximately 100 cycles and 10,000 cycles of loading. The apparent spring constant increases by approximately 20% between approximately 100 and 10,000 cycles of loading. The concept that the apparent spring constant is 2-4 times greater than the quasi-static spring constant is confirmed. Also the load-elongation curves for the ropes are not significantly affected by the loading conditions applied in these tests. The tensile strength of 30 mm *nylon* ropes and 50 mm polyester ropes are not significantly affected by the dynamic loading, whereas the strength of 50 mm *nylon* and 30 mm polyester diameter ropes exhibit a significant loss of strength. A thermal model for hysteresis heating of synthetic fibre ropes for the condition of tension cycling around a mean tension between fixed displacement limits and a constant frequency has been developed[74,75].

The mean tension correspond to the hawser load required to tow a given ship at a fixed speed with constant wind velocity and vessel heading. The displacement limits correspond to that between ship displacements induced by wave action. Under these conditions, a thermal steady state can exist where the heat generated due to rope hysteresis is removed by convection to environment. Hysteresis[74,75] is first measured from the load displacement curve obtained during actual dynamic loading experiments. The thermal model is then used to predict rope temperature rise based on the hysteresis data. Rope thermal properties are also measured. When a synthetic fibre rope is used at sea to tow a load, the rope is subjected to a dynamic, cyclic tensioning due to ship displacement induced by wave action. Under such a cyclic loading, the rope as a

Viscoelastic structure, absorbs energy. Part of this energy is dissipated in form of heat, which results from plastic deformation and the interfilament friction between rope fibres. This energy is absorbed by the rope, or the hysteresis, causes temperature rise inside the rope. For a small or medium sized rope under windy or wet (when the rope is under sea water) conditions, the heat can be effectively removed from the rope. In some circumstances where heat transfer conditions are poor, the rope temperature becomes so high that the mechanical strength of rope fibres is degraded. Most of physical properties of the rope fibres are temperature dependent. The temperature rise can cause the rope fibres to operate at a different mechanical regime and therefore reduce the reliability of rope failure predictions.

3.8.5 Structural Model

Modelling how the different rope elements interact with each other can give an understanding of the way the rope carries the load and how different sub-elements fail as the rope fails. The slippage criterion and model of synthetic double-braid ropes, particularly, for the partial frictional conditions have been formulated[41,76]. Such constraint is closest to reality, and contributed to most failure cases in marine service due to abrasion / wear. The slippage criterion proposed is based on the measured frictional resistance of individual rope strands from a newly devised pull-out test. Emphasis is on straight ropes as well as rope termination, the latter either an eye splice or a continuous loop on bollard like pin. The experimental results agree well with the predictions of the partial friction case for 0.64 cm *nylon* ropes. However, for PET ropes, the predictions of the infinite friction case agree better with the experiments due partially to high frictional constraints. The pullout load displacement curves of the PET (Du Pont 68) strands (subjected to same loading conditions) show maximum forces almost twice that of *nylon* (Du Pont 707).

A statistical model for the strength of long, slender, fibrous structures such as yarns and cables are described[47]. Emphasis is on the effect of strong mechanical interactions among fibres that arise from the presence of friction or a binding matrix. Basic features are that the structure is viewed as long chain of statistically and structurally

independent bundles whose length depends on the local mechanics of fibres at breaks. Within each bundle, localised load sharing occurs among non-failed fibre elements depending on the local mechanics and fibre spatial geometry. Key conclusions are:

- Weibull distribution describes the statistical strength of yarns and cables.
- The coefficient of variation of fibre strength has very little effect on the variability of strength of the yarn or cable. The "effective" Weibull shape parameter for the yarn or cable typically ranges between 25 to 40, even when that for the fibre varies widely between 5 and 30.
- An increase in the variability in fibre strength, as reflected by a decrease in the Weibull shape parameter for the fibre, causes large decreases in the median strength of the yarn or cable.
- As the localised load sharing among non-failed fibres become more diffuse as a result of changes in fibre spatial geometry or interfibre mechanics, the median strength of the yarn or cable rises moderately while the variability in strength is virtually unaffected. The increase is most pronounced when the coefficient of variation for fibre strength is 15 to 20%, and it slowly decreases as this coefficient decreases.
- The size effect in strength for yarns and cables is much milder than that for single fibres. The size effect diminished slowly as the number of fibres in the yarn or cable is increased.
- The median strength of the yarn or cable diminishes very slowly as the ineffective length of the fibre is increased. The effect is milder than the size effect for the fibres.

A model has been presented based on a common elementary system, which can be termed a helical wire strand, generally consisting of a core surrounded by one or several wire layers[42]. Depending on strand geometry, loading type (axial or bending), and also, on the required specifications (stiffness, strength, damping), a wide variety of hypotheses can be made. To address this problem, the following tentative classification is presented: fibre models, taking into account only axial wire forces; curved rod

models, which include wire bending stiffness and in the most general case, twisting stiffness; and semi-continuous models, in which each wire layer is replaced with an equivalent elastic orthotropic medium. The different models are compared, together with the corresponding experimental data when available. The review is restricted to the elastic behaviour under small deformations, which may include contact conditions, with or without friction, and possible stick-slip behaviour.

3.8.6 Fibre Bundle Theory

In modelling the performance of parallel lay ropes the following conclusions can be made[77,78]:

1. The variability in the element stiffness, cross sectional area and random slacks affect the bundle strength. The introduction of variable random slack reduced the strength of the rope (bundle). The scatter in the element cross sectional area increased the bundle strength slightly; however, this increase was only significant at very high variability and therefore the effect can be considered to be practically insignificant. The effect of the variability in the stiffness had different effects on the ropes, whereas type G rope gained strength, type A rope lost strength with increasing scatter in element stiffness.
2. Increasing the length of the rope reduced the strength; larger ropes lose strength less rapidly than smaller ones as the length increases. Typically, a 60 tonne Type G rope loses only about 2% of its characteristics strength over 3 km.

A theory for predicting the strength of a bundle of sufficiently large number of elements, if the average breaking load and the breaking elongation distribution of these elements are known has been developed[79]. The usefulness of the theory is illustrated with data on cotton fibres. The tenacity of a bundle of textile strands is always less than the average tenacity of the individual components. The poor strength realisation in the bundle results from the unequal extensibility of individual strands. The strength of the bundle can nevertheless be calculated from single fibre load extension data.

Many successful structural models have been developed[80,81] to predict the static tensile behaviour of ropes. These models assume that spatial locations along individual strands can be described by a helix with a sinusoidal undulation in their radius direction. Thus the local strand strain can then be calculated on the basis of the differential geometry of strand segments before and after the rope is stretched. Strand load is readily determined through the load strain relationship. By converting the individual strand load into the rope axial load and summing up the contributions from different strands, a load/strain curve is generated.

3.8.7 Weakest Link Theory

Suppose the strength could be determined at every point along the length of the sample and it is found to vary from point to point, as shown in Figure 3.6.

If a gradually increasing load is applied to the whole specimen, it will break at its weakest point, giving the strength S_1, but if the specimen is tested in two half lengths, each will break at its own weakest place, one giving the value S_1, and the other a value S_2, which is necessarily greater than S_1. The mean strength, $S_{1/2}$, measured on half-length, is the mean of S_1 and S_2, and must therefore be greater than the strength measured on the whole length. Similarly, going to quarter length, the strength values are, S_1, S_2, S_3, S_4, and the mean strength $S_{1/4}$, is greater still. This increase will continue until at very short lengths the mean strength tends to the value S_0, which gives equal areas of the curve above and below the line $S = S_0$. Thus the following conclusions could be made:

- As the test length increases, the mean measured strength of a specimen decreases.
- The more irregular the fibre is the more rapid will be the decrease in the mean measured strength.
- The order of ranking of specimens may alter if the test length is altered.

In order to estimate the strength that would be obtained at some greater test length than actually used, the simplest method in principle is to group the results together in the appropriate numbers and to take the mean of the lowest value in each group. The weak-link effect also affects breaking extension. If a fibre breaks under a low load owing to the presence of a weak place, the rest of the specimen will have comparatively small extension and the breaking extension will be low. The mean breaking extension will decrease as the specimen length increases[3].

In order to establish the effect of test gauge length on yarn properties[43,82], yarns of varying gauge lengths were tensile tested and the data were fitted into two-parameter Weibull distributions and corresponding shape and scale parameters were determined. Strength increases as gauge lengths decreases, a trend indicated by the weakest-link theory. At very short gauge lengths, however, the data deviates from prediction based on the weakest-link theory, thus suggesting a change in the yarn failure mechanism, as gauge length decreases.

A mathematical description of a weakest-link model for fibre strength in which there is no assumption regarding the test length with respect to the link length has been developed[83]. The model describes well the filament strength mean and coefficient of variation response to test length of three commercial Kevlar Aramid yarns samples. The significant increase in coefficient of variation at the longest test length (254 mm) is most likely to be a result of deviation of the link strength distribution from the Weibull in the low strength tail portion which become very influential in determining the observed distribution of strengths when test length become substantially larger than the link length.

3.8.8 Energy Method

An energy method to predict the static tensile strength of double braided ropes which are composed of two separable layers based on the actual constitutive relationship of individual rope components is employed[84], so this approach is valid for predicting the

whole stress/strain curve of ropes. Extremes of zero friction and infinite friction conditions are explicitly considered. Experimental results agreed with the predictions for small *nylon* and polyester fibre ropes. In particular, experimental-failure strains lie between the limits predicted by the above two extreme conditions owing to a realistic partial-frictional constraint.

3.9 Rope Performance Analysis

The way a rope performs depends on the design, material and the environment that it is operating in. Computer stress analysis tools such as finite element analysis, which has conventionally been used for other products, could also be applied to ropes.

3.9.1 Finite Element Analysis

The incorporation of the micromechanics in a finite-element model of a uniform rope of initially untwisted fibrous material is described. The response of the whole model to combined external and torsional stresses such as occurred during twist insertion is then described. Detailed analyses of the stresses and strains in the deformed model shows that fibre packing in the yarn is predicted to quickly become non-uniform. The inner regions become most densely packed, and the fibres are subjected to the highest stress levels. Fibres further from the centre largely avoid being stressed by moving toward the yarn axis[85].

A basic model, which treats a yarn as a true three-dimensional solid object, is proposed. This approach is first applied to three yarns twisted together to form a rope-like bundle. Next, it is used to model a woven fabric[86]. An abstraction to visualise the effects of yarn compressibility and then studied the results of applying the new model on a final object that was primarily one-dimensional in nature, a rope like structure composed of a twisted bundle of individual yarns was also proposed. There is a theoretical maximum volume fraction for the elliptical cross-section, one dimensional, rope like fibrous

structure composed of twisted outer bundle of yarns. This maximum volume fraction was about 87% and occurred for 3 yarns[87].

3.10 Parameters Affecting Rope Performance

The behaviour of a rope is directly affected by certain factors. Ropes for example lose some strength due to termination. The construction could also have a bearing on the performance of the rope. How the ropes are tested could also affect the rope performance as there will be some compression of the fibres round the pulleys.

3.10.1 Construction

Study of the influence of the role of the jacket on strand lifetime shows that unjacketed Kevlar strands have their lifetime reduced by a factor of about 6 to 8 times as compared to strands with a braided jacket. For Vectran and Technora strands the lifetime of unjacketed strands is reduced only by a factor of about 3 times as compared to strands with a braided jacket. A study of the effect of silicone coatings over the cords for both jacketed and unjacketed Kevlar strands, or over the jackets when such exist show no enhancement for the cycle lifetime. In fact these coatings seemed to have a detrimental effect. For all unjacketed strands more localised damage is observed, sudden failure with pronounced fibrillation, crushing, abrasion, as well as fibre flattening just as for jacketed strands. Strands made of Vectran fibre have about 10 to 15 times longer lifetimes than strands made of Kevlar fibre and about 2 to 3 times longer lifetimes than strands made of Technora fibres. Strands made of Technora cords have better performance than strands made from Technora twisted yarns both in terms of residual strength at half the lifetime. Both Vectran strands and Technora strands show longer lifetimes and superior abrasion resistance as compared to Kevlar strands. These are strong candidates for ropes subjected to high tensile force and lateral sheave loads[88].

3.10.2 Effect of Pulleys

There are a number of significant variables in designing equipment in which hawsers must pass over components such as rollers, pulleys or static fairleads while under load. These variables include pulley diameter, pulley groove shape, fleet angle of hawser onto pulley, ratio of roller to hawser diameter, contact angle of hawser over rollers, frequency of applied loading, magnitude of applied loading and whether the hawser is wet or dry. The main conclusion of the tests was that significant improvement of hawser life could be achieved by careful selection of hardware details[89].

3.10.3 Termination

Any rope has to have some sort of end fitting. In many large ropes, such as mooring hawsers the rope has an eye splice or in parallel lay ropes the fibres are fanned out and a bullet is trusted in to hold the rope fibres. All these techniques are called termination, i.e. ending the rope such that there are no loose fibres and there is also a workable end. However, due to the small size of paragliding ropes the termination techniques are different from other applications, originating in parachuting ropes. The main techniques are:

- Stitching
- Epoxy Potting
- Finger trapping, Figure 3.7

Stitching, see Figure 3.8, is the commonest technique used, however, several factors have to be considered and they are:

- Speed of stitching
- Size of needle
- Shape of needle tip

The stitching process involves a sharp needle penetrating the rope. HMPE fibres shrink slightly during this process due to the heat generated which is directly related to the speed of stitching and the size of the needle. The biggest problem is with aramid ropes. The stitching process causes localised compression fatigue. The best way to minimise this, is to make sure that stitching occurs along the same length of the same fibre. The stitching holes in the protective cover, no matter how small to start with, will get larger with loading use and allow more light in leading to possible UV degradation.

Other termination techniques such as epoxy potting and finger trapping are usually used with micro ropes[iii]. No matter what type of termination is used the failure in the ropes usually occurs where the termination ends due to the maximum stress concentration. The maximum bending stress also occurs where stitching finishes because that is where the ropes bend in flight and during take off and landing, see Figure 3.8.

3.10.4 Environmental Testing

57 new, aged and wet para lines were tested. The ropes were loaded to 2 kg in mid October at an altitude of 2700 metres above sea level being exposed to the Sun for 310 hours. The temperature ranged from -16 to -5 °C with 11 to 98% RH (Relative Humidity) in wind velocities of 0 to 57 km/h. The extensions were between 0.2% and 0.5%. Dyneema shrank within these temperature ranges. Frozen ropes did not suffer any reduced breakage resistance. At the end of a seam it proved a negative effect to use tightening stitching. This was a big problem especially with Kevlar[90].

3.10.5 Paraglider Ropes Design

More than 70% of the load is carried by A and B ropes in a Paraglider. This load, over a period, stretches the ropes, moving the canopy position back thus increasing the angle of attack hence changing the flying characteristics of the Paraglider. Since HMPE ropes tend to shrink, it is recommended to pre stretch the ropes by a minimum of 15.0 kg. Even when the ropes are pre-stretched to 20 kg they would still shrink by an average of

[iii] Micro ropes have no cover and are as small as 0.3 mm in diameter. They are primarily used on competition gliders.

0.3% unless they are periodically loaded to 5 kg or more. A 0.3% shrinkage on a rope 5 metres long equals 15 mm. A difference of 15 mm between front and rear risers could move the canopy position back by as much as 50 mm. Ropes A and B which are heavily loaded stretch more than the less loaded ropes[91].

One of the most common methods of rope construction is the sheath and core method. Modern glider ropes are built with materials such as Dyneema and Kevlar. The function of the outer sheath is to provide abrasion resistance, not to carry any load. So, as a very general example, a 1.3 mm rope might have a 0.7 mm load-carrying inner. For users of "micro" ropes the protection of the outer sheath is dispensed with, as well as some strength in the inner core. If the inner core is broken, then it will be observed by very high extension in the rope. The paraglider manufacturer has to cut the suspension ropes with the sheath and core difference in mind, making sure the sheath and core are together and that subsequent sewing gathers them both. The sheath should remain in situ and should not extend when sewn into a loop. The trick for the manufacturer is balancing out how tight to braid the sheath over the core. If it the braid is too tight, it will grip the core and contract on it, which will effect the initial extension. So the requirement is for a core that will lie fairly slack within the sheath so that when the whole rope is extended the core is properly loaded. Strength of the rope is known from several calculations and from load testing.

The braiding process reduces the strength of the raw yarn as the helical braiding does not result in straight vertical rope suspension, the yarns being at the helix angle. Therefore a very loose structure braid retains more of the original yarn strength whereas a tighter braid, where the helix angle is closer to 90°, will reduce the strength. The sewing process, which forms loops, reduces strength by needle damage, and abrasion during use can seriously weaken the rope. Damage to the inner core is damage to the load bearing structure of the rope. Extension, lumps and obvious cuts are indications that the rope may be extremely close to total failure. Kevlar is not as resistive to damage by bending as other materials. Among the criteria for rope specification from paraglider manufacturers are low extension, high strength and small diameter. Ropes do have a useful lifetime after which they weaken. The current trend is towards regular

examination and replacement, possibly of key load-bearing ropes. For example the Gutesiegel examination at 100 hours or two years measures the ropes strength against the original manufacturers specification and if less than 50% residual strength were left then the rope would have to be changed[92].

3.11 Rope Deformation

The way a rope fails has to be understood in order to be able to formulate the behaviour of it. Ropes are complicated structures and the failure is a combination of the interaction between the rope sub elements.

As the rope is loaded taking into account the loading history of the rope, the rope goes through a series of steps. As the load is taken on, the rope sub-elements start to interact. The load carrying action can lead to damage accumulation and finally to failure. The rate of damage accumulation depends on the material and design of the rope. The greater the number of strands the greater the amount of rope sub-element movement, the greater the chance of failure due to abrasion. There is also the effect of the cover which becomes evident as the rope takes on load which can lead to damage and ultimately failure by pressing on the rope leading to exaggerated interfibre/strand abrasion and as the rope sub-elements try to realign themselves and finally fail.

The rate of damage accumulation also depends greatly on the way the rope is torque balanced. The original rope is torque balanced but as the loading continues and a sub-element fails, the remaining elements are no longer carrying equal loads which would indicate that the failure procedure would be even more exaggerated as one sub-element would probably carry more load and therefore it would creep more leading to differential friction and abrasion between the fibres and unequal structural realignment and hence a more rapid final failure.

3.11.1 Failure Analysis

There are five principal modes of rope failure[93,94, 95,96]:

- Creep, is the permanent increase in length as a result of loading and takes place in all synthetic fibres at low loads and its rate decreases with time until it becomes virtually indiscernible. However, in some materials at high load, significant creep continues and eventually causes failure.
- Hysteresis, is the loss of energy during load cycle. Friction due to relative slippage of adjacent elements causes loss of energy and build-up of heat.
- Fibre Fatigue, is similar to metal fatigue and crack propagation due cycling and buckling of the fibres.
- Internal Abrasion, is the relative sliding between the various rope elements, fibres, yarns and strands which contribute to the abrasion of the fibres. As wear progresses, fibres fail. Abrasion is most severe at points in the rope where high contact pressure is accompanied by considerable relative movements between elements. The rope elasticity also influences internal abrasion.
- Rope Structural Realignment, is the progressive redistribution of stresses and strains among the load bearing elements within the rope due to tension cycling. Redistribution of stresses and straining among the elements increases rope strength.

It is difficult to define bounds for the conditions in which various rope failure mechanisms occur. Effects could vary with material type, rope structure, environment and cyclic conditions. Thus a rope material/structure could have excellent resistance to internal abrasion and thus give good performance at low load level. This same rope could have poor creep or hysteresis performance and thus fail rapidly at higher load levels than another rope, which has poor internal abrasion but good creep and hysteresis performance. As an example approximate ranges for a *nylon* rope are:

1. Internal abrasion dominates in tension cycling at upper load ranges up to 40% in dry *nylon*. Where the rope temperature is controlled by the cooling effect of continuous application of water, abrasion continues to dominate above about 70%.
2. Fibre fatigues in tension cycling at low levels up to about 40% but is not a dominant mechanism.
3. Hysteresis dominates between 40 to 70% in dry *nylon* and also if wet *nylon* is allowed to dry out. Hysteresis is not important if loading is intermittent or the loading rate is very slow.
4. Creep also dominates.
5. Structural realignment occurs each time an element fails. However, the effect of realignment is normally only significant at high loads.

3.11.2 Paraglider Rope Failure Criteria

The conditions that the paraglider ropes are subjected to necessitates certain precautions which are[9-11]:

- The aramid ropes are affected by the sun light thus a braided polyester cover protects the aramid core.
- The cover also protects the core against chaffing
- The HMPE ropes are temperature/time dependent, i.e. the ropes can extend under load or as heat is built up in the ropes as they are loaded.
- The loading process generates heat in HMPE ropes which leads to their shrinkage and localised stress concentration.
- The ropes are not always under static load, in certain manoeuvres such as Big-Ears they are subjected to very large shock loads, which can lead to complete cascade failure of the ropes. This is because a rope, which fails at 100 kg under static load, will fail at fraction of that under shock or dynamic loads.
- The mechanism of cascade failure occurs because the Paraglider is a symmetrical object and the loads are shared equally and as one rope fails the load is transferred to the next and the shock load increases and that rope fails even faster transferring

the load to the next rope which will fail even faster and the process continues until all the ropes have failed.

- There can be certain amount of extension under load in the rope, which can lead to alteration of pilot position causing the flight characteristics of the Paraglider to change.

Understanding the performance and behaviour of the rope material is very important as the life of the pilot depends on these ropes. In the offshore industry the size and cost of the rope takes second place to the performance as the main purpose is moor the installation in deeper and deeper waters whereas in Paragliding the cost is very important as is the size of the rope. By reducing the diameter of the ropes you decrease the drag and weight and improve the performance and speed of the Paraglider. This has the effect of reducing your static safety margin from around 90 kg to around 10 kg since the ropes can be as thin as 0.3 mm in diameter on racing competition gliders. These micro ropes are also uncovered which increases the risks of degradation due to sun light (UV) and others.

3.12 Applications

Through the ages ropes have been used for many applications such as shipping, farming, primitive bridges, climbing, around home, towing, and even art forms. The original ropes were made from natural fibres until about 150 years ago when steel wire ropes dominated the market for demanding applications such as mooring and bridges. However, in the last fifty years man-made fibres have taken almost 99% of the natural fibres market and the new High Performance Synthetic Fibres Ropes (HPSFR) have even been threatening the dominance of steel wire ropes and cables in applications such as catenary mooring and tension leg platforms. For example Petrobras of Brazil will replace steel wire ropes with polyester ropes in the taut leg mooring system for Petrobras 13, a floating production platform in the Marlin Field in the Campos Basin off the coast of Brazil followed by three more polyester moorings on new platform in 1997 and 1998. Water depths in the Marlin field ranges from 600 to 1,050 metres but

the real challenge will come in the exploitation of the nearby Albacora field with depths down to 2,500 metres. Ropes have many applications, some of which are listed below.

3.12.1 Single Point Mooring (SPM)

Basic design information for sizing for single point mooring (SPM) and related mooring applications has been developed[97]. Extensive testing of scaled hawsers from 5 combinations of materials and construction is carried out to determine initial strengths in the wetted condition, the characteristics of degradation resulting from cyclic loading. The results indicate that for hawsers configured as grommets, the double braid is superior to the 8 strand rope construction, and the importance of the assembly details, such as the splices and the protective arrangements at the eye, is amplified

Strengths of new and used large synthetic ropes used as hawsers at SPMs have been determined. Almost 70 tests were run on size 15 and size 6 double braid *nylon* ropes. Most of the tests involved cyclic loading to determine cycles to failure or residual strength after cycling. In addition, seven used SPM hawsers were tested to determine breaking strength after service. Test results indicate rate of strength reduction during cyclic loading is non-linear becoming more rapid as the cycles to failure is approached. The cycles to failure limit for large ropes are less than that for small ropes when cycled at the same percentage of new strength. The actual new strength of size 15 rope is found to be lower than the rated breaking strength, but strength is increased by improvements in splice quality[48].

3.12.2 Guy Towers

Synthetic fibre ropes can be used for guying broadcasting towers provided the following conditions are fulfilled[98]:

- The core of the rope has to be made of high modulus fibre, its dielectric strength should be the highest and the water absorption coefficient the lowest.
- The jacket of the rope must be smooth but thick enough to protect the core against mechanical damages. Its dielectric strength should be the highest and the water absorption coefficient the lowest. A spirally-shaped jacket with smooth surface is particularly suitable where air is polluted and higher transmitting powers are involved.
- Tower design engineers should by all means have evaluated the natural frequencies of construction
- Synthetic rope could be tensioned at a level, which is lower than normal for steel guys.
- For risks of fire and for safety's sake, it is advisable to use a steel rope for the first few metres of guying above the ground.
- Synthetic fibre rope must be protected against the corona effect with properly designed funnel like connections.
- It is advisable to further protect the ropes either by ceramic egg insulators or additional corona rings. This is particularly necessary when higher transmitting power or complex antenna systems with extreme electric field strengths are involved.

3.12.3 Tension Leg Platforms (TLP)

Parallel-lay or low twist angle constructions with high modulus Kevlar ropes can be used as alternatives to steel in the construction of mooring ropes for deep-water compliant structures such as tension leg platforms (TLP). Steel is not an optimum mooring rope material for deep water compliant structures because of its low specific

strength and modulus. For deep water (beyond 300 m), steel mooring ropes require complicated tensioning, handling and floatation systems[99,100].

3.12.4 Buoy Mooring

A study on stranded Aramid ropes deployed as low tension buoy mooring ropes yields the following conclusions[101,102]:

1. 6 strand construction inherently have excellent survivability
2. Rope durability can be increased substantially by increasing the compliance or freedom for fibre movement in the rope, such as using multiple twist levels.
3. Rejacketing over the splice region can be critical to survivability. Particularly to be avoided are discontinuities in flexibility which lead to extensive working and strength loss in regions of highest flexibility. For plastic jacketed ropes, the benefit of a tapered elastomeric covering over the splice to provide bending strain relief in the splice to rope transition is demonstrated.
4. Wet strength of stranded Aramid ropes is 0-15% lower than dry and appeared to be related to rope construction, with 6 strand rope the most sensitive.

Typical rope uses in the ocean are:

- Buoy moorings
- Offshore ship and rig moorings
- Moorings for floating breakwaters, oil spill barriers
- Moorings for sensor and array installations.
- Ropes and handling systems
- Tow ropes

Two types of ropes are used and they are:

- Wire ropes:

1. Mild plow steel
2. Plow steel
3. Improved Plow steel

The strength increases as flexibility decreases in that order. Stainless steel wires are rarely used because they show a tendency to crevice corrosion in saltwater. The wire ropes used for ocean applications are either twisted or laid construction. Mostly six equally sized strands are arranged with a long pitch around a centre core, Each strand is formed from 7 to 55 wires. the larger the number of wires per strand, the more flexible is the wire rope, but the more susceptible to external abrasion and crushing.

- Fibre ropes:

1. *Nylon*
2. Polyester
3. Polypropylene
4. Kevlar 29

Fibre ropes are highly elastic and have little viscous behaviour and high tenacity. Fibre rope construction for ocean applications are either 8 strand plaited, double or single braided or parallel fibre core ropes with encapsulating jackets either from fibre braids or extruded jackets. In fibre ropes, the construction could greatly modify the load elongation behaviour of the fibres used. Except for the parallel fibre core ropes all rope constructions show more elongation than the composing fibre or yarn elements but less combined strength. This behaviour is caused by the fibre or yarn and strand arrangement in multihelical configurations at different helix angles. The multihelical arrangement is necessary to contain the fibres in compact cross section. This assures an

optimum load sharing of all fibres and components, and provides for flexibility and ease of handling of the rope. Some of the rope constructions can triple the elongation of the composing fibres. Studies and experiments performed so far lead to the following conclusions on the synthetic ropes[103]:

- Synthetic ropes of *nylon* and polypropylene recover faster upon load reduction than they creep.
- At low loads, creep depends both on the rope material and construction.
- Wet testing and temperature differences do not appear to have significant effect upon creep in *nylon* ropes.
- The testing sequence employed in determining the dynamic characteristic is critical due to load history dependence in synthetic ropes.

3.12.5 Towing

A method has been developed to simulate tow conditions with emphasis on constant strain amplitude dynamic loading[104]. The change in the dynamic modulus, or stiffness, of the rope when subjected to varying loading conditions has been investigated leading to the following conclusions:

1. The stabilised stiffness, K, is found to be considerably higher than the quasi-static stiffness of uncycled ropes.
2. The internal rope temperature is higher in polyester rope than in a comparable *nylon* rope, become significant in dry ropes subjected to high strain amplitudes and high frequencies. A reduction in dynamic modulus accompanies the high temperature increases.
3. Both polyester and *nylon* rope exhibit increasing hysteresis per cycle with increasing strain amplitude and frequency, reflected in increased mechanical energy input and a corresponding increase in rope temperature.
4. *Nylon* experiences less hysteresis than a comparable polyester rope.

The dynamic response of straight ropes and of towing catenaries at 'excitation' periods in the 0.6 second range is considered[105]. The dynamic stiffness at wave period of conventional construction *nylon* and polyester ropes exceeds their quasi-static stiffness by upwards of 3/1, though damping losses are similar to quasi-static values. Wet quasi-static fatigue life of conventional hawsers is rated in the order 'typical' polyesters (best), 'typical' polypropylenes and 'typical' *nylon*s (worst), though wide variations occurred within these global descriptions reflecting the wide range of yarns available. In dynamic fatigue, internal rope temperatures sufficient to cause yarn strength degradation on 'typical' polyester and *nylon* yarns are shown to occur in wave period cycling of size 6 ropes between 10% and 50% of break. On size 24 ropes such heat damage is predicted in cycling between 25% and 35% of break. Ropes based on parallel low twist cores have higher strength and tension fatigue life and show lower wave period damping than the conventional constructions.

3.12.6 Paragliding

Poor mechanical stitching at termination can reduce the strength by as much as 30%. The effect of UV, Moisture and Temperature could also reduce the strength by as much as a further 30% . The failure types could be placed into two distinct categories, i.e. Dimensional instability for HMPE Ropes and Breakage for Aramid Ropes**.** With the High Modulus Polyethylene Ropes this dimensional instability is a direct result of the low melting point and manifested itself in the form of either Shrinkage or Stretching. On the other hand with the Aramid ropes it is the brittle fracture failure which is the main cause of failure in the form of work hardening together with poor UV resistance. Most of the failures due to breakage occur at the pilot end, where the rope exits the polyester sheath protecting the termination (i.e. the stitching). This is the point where the rope is very often sharply bent leading to high mechanical stresses being built up in the rope thus causing the rope breakage . This type of manoeuvre due to sharp bending can reduce the strength of a new rope specially aramid ropes by as much as 30% and 50% after two years for normally used Paraglider and maybe as much as 75% for heavily used Paraglider. One method of protecting the stitching has been to use shrink wrap hard plastic namely for aramids. However, this only pushed the centre of stress concentration further down to a new place. There are no visual signs to warn of the loss

in strength of these ropes except in laboratory tests. Other modes of failure are spirals i.e. when partially loaded sails could cause overloading which can lead to cascade failure or if a pilot falling at 15m/s is caught by a sail, it can produce high shock loads then lift rupture can occur. This kind of failure could occur even with new ropes[9-11].

The bending behaviour of Kevlar, Dyneema and Vectran have been determined with material samples mounted on to a hinge and bent 1000 times at ± 180°. These samples are then tensile tested and it is found that Kevlar is left with 60% of its stability. Dyneema was hardly changed but tore apart in most cases at the bending. Vectran remained with its good tearing stability and in fact tore apart at a spot other than the bending. In another experiment the same three rope types are exposed to the sun for 1 months (about 200 hours of Sun) and then tear stability tested. The proportional decrease in firmness is the same for all rope types used. However, Vectran turned out to be the best as it had a higher stability in the first place. Dyneema shrinks by as much as 3% when wet, due to capillary attraction of the water pushing the fibres apart thus they become shorter. However, with little burden the water will be pushed out and the fibre goes back to the original state. This very low coefficient of friction may be the reason for hysteresis effect. It is also found that it takes longer to go back to its original length than Kevlar. When Dyneema samples are cut using a hot knife or terminated they shrink and this is attributed to the heat generated due to the needle penetrating the fibre and the hot knife. It is determined that by simply tensioning the ropes before cutting them the shrinkage can be minimised. The shrinkage can be due to the fact that there is a differential shrinkage between the fibre core and the cover as well as the fibres slipping on each other. Same type of ropes are tested under 1.5 kg load going at 90° over a knife edge until the core is torn apart. It is found that Kevlar performs worst followed by Vectran and Dyneema[12].

4.0 FIBRES

The only constituents of a rope are the fibres, which make up the rope. Therefore it is very important to understand what they are and how they perform. In composites, the mechanism of load transfer depends on the relationship between the matrix and the fibre and how they interact. However, since there is no binding matrix in ropes, then it is difficult to decide when the rope has failed. Would it be when the fibres within one strand have failed? What percentage of the total building fibres has to fail before the rope is considered unsafe and how much more indicates total failure.

No work has been done to address this issue. Almost all the work conducted so far concentrates on the residual strength after mechanical loading or after weathering or UV exposure.

4.1 Fibres for Ropes

In the ancient pictures, the Theban rope makers were using strips of leathers. Vines can be twisted together to make hanging bridges. Any fibres from plants or animals that come easily to hand, can be twisted into yarns and stranded into ropes. For special purposes cotton gave soft ropes, silk gave luxurious ropes, and Rapunzel used hair in the fairy story, but the commonest cordage material was hemp. Fibres for ropes can now be classified into three main categories, see Table 4.1:

- Commodity ropes with adequate properties for common use
- Intermediate performance Fibres (IPF)
- High Performance Fibres (HPF)

The deciding factors for ropes are:

- Price
- Strength
- Extensibility
- Durability

Table 4.2 shows the comparison of different fibre ropes with break strength of 500 kN. *Nylon* is the leader when high elastic extension is needed but polyester and high performance fibres are better to limit extension. Depending on the application the total system response has to be evaluated. For example in climbing ropes the primary requirement is to have a high enough energy to break (work of rupture) to take up the kinetic energy of the falling body, which equals the loss of potential energy (weight height of the fall); this is given by the combination of the strength and extensibility. A low modulus also reduces the peak force experienced by the body. *Nylon* is the preferred fibre. But for support of a working platform or for the positive rather than protective uses of ropes in acrobatic exercises of modern rock climbing, it is better to minimise movements by keeping extensions small with higher modulus rope. Similarly, in mooring applications, a high modulus best maintains station but a low modulus reduces the forces imposed by wave motions.

4.2 The Viscoelastic Nature of Fibres

Synthetic and natural fibres are Viscoelastic. They react to loads or strains with spring elastic recoverable deformation and viscous non recoverable stretch. Part of the fibre reaction follows the elastic performance of a spring. Part of it follows the behaviour of a viscous fluid. The term *elastic* describes that property of a body by virtue of which it tends to recover its original size and shape after deformation. The opposite performance, retaining a deformed size and shape after stretching is called *Plasticity.* All fibres consist of large macromolecules, which by drawing processes become

oriented parallel to the fibre axis. The Viscoelastic behaviour of macromolecules under stress and strain is very complex. It depends on the type of polymer, the degree of polymerisation, the attracting forces between molecules and the degree of orientation. The response of a fibre to applied stress and strain is time depended, since all position changes within the macromolecular fibre substance need time to take place. Temperature, humidity and previous load history also influence the load elongation behaviour of the fibres. Any fibre could be used to make a rope, but since ropes are mainly strength carrying, energy absorbing "connection links", high tenacity fibres with various degrees of low stretch are used:

- *Nylon*
- Polyester
- Polypropylene
- Aramid
- HMPE
- LCP

Similar rope behaviour can be achieved by arranging highly stretchable fibres in a low stretching structure or low stretching fibres in a highly stretching structure. Synthetic Fibre Ropes fall into two main categories:

- IPSFRs. (Intermediate Performance Synthetic Fibre Ropes)
- HPSFRs. (High Performance Synthetic Fibre Ropes)

4.3 Intermediate Performance Synthetic Fibre Ropes (IPSFRs)

The main bulk of ropes used, is made from intermediate performance fibres. They are used in most applications such as mountaineering, parachuting and mainly in mooring of offshore installations and ships. Their only limitation is their lower strength.

However, in some recent applications where high performance ropes would have been the initial choice such as mooring of offshore installation in very deep waters, it was found that by doubling the size, the desired strengths could be achieved at a lower cost than the high performance ropes.

4.3.1 Nylon

This was the original high strength synthetic fibre for rope applications. It is characterised by having the greatest elasticity of all of the synthetic fibres, good strength and good abrasion resistance when dry but is susceptible to UV. It absorbs water (in an intermolecular sense) which causes the fibre to swell, losing upto 10% to 20% of its strength and adversely affects its abrasion resistance. Fibre swelling causes ropes to increase in diameter and shorten in length, causing the phenomenon in the rope to called "*shrinkage*". It is suitable in applications where there is relative movement between the tow ends of the rope and energy needs to be absorbed. Its flexibility is unaffected by temperature although it does shrink when wet. In repeated loading conditions it has good tension-tension fatigue and flex fatigue resistance[106], see Figures 4.1 and 4.2 as well as Table 4.3.

4.3.2 Polyester

New high grade polyesters are as strong as *nylon* (dry) however, since polyester does lose strength when wet, it is actually 15% to 20% stronger than *nylon* but has about one-half the elongation of *nylon*. It holds colour superbly and it's the most suitable material for yachting rope covers. It doesn't shrink when wet. It has better UV resistance than *nylon*. There are two types of polyester used in rope construction: the spun staple polyester which is made from relatively short and very fine fibre spun together, but a far softer one with a matt finish. Continuous filament polyester has a shiny surface and is generally a harder rope. It is stronger and has less stretch than spun fibre rope. Polyester is generally easier to splice and knot, depending on construction, see Figure 4.2 and Table 4.3.

4.3.3 Polypropylene

Polypropylene rope is rope making's modern answer to sisal. It is even made on the same machine that once made sisal ropes. Polypropylene has a density lower than water and 60% strength of polyester and *nylon* but almost the same extension as polyester. It is susceptible environmental stress cracking at low temperatures It has poor fatigue resistance and is subject to creep under sustained load, and can be degraded by severe sunlight exposure even if inhibitors are used. Polypropylene is generally stiff and slippery in texture, but there are high grade versions that are almost as supple as polyester. Polypropylene is difficult to splice due to its texture and is difficult to Knot. The fibre does float and it is significantly less expensive than *nylon* and polyester. It is a good economic fibre for utility type rope, especially if the rope needs to float, see Figure 4.2 and Table 4.3.

4.5.4 Mechanical Testing

The relative performances of polyester and *nylon* 6,6 fibres and yarns, both dry and in aqueous solutions, primarily synthetic sea water have been investigated[107,108,109,110]. Fibre failure over a range of loading conditions and frequencies is found to occur at a critical cumulative strain governed by a creep rupture process. Polyester is more resistant to creep rupture and consequently outperforms *nylon* 6,6 in cyclic fatigue. The advantage of polyester is considerably greater in aqueous solutions, where the performance of the *nylon* is diminished. Other comparisons indicate that the particular polyester fibres studied have higher stiffness and strength, lower strain to failure, and much lower hysteresis energy absorption compared with the *nylon*.

4.4 High Performance Synthetic Fibre Ropes (HPSFRs)

High Performance Synthetic Fibre Ropes have become more and more important. They offer excellent strength to weight ratio and therefore in applications where that property is important they have found their uses such as paragliding. Also within the marine industry steel chains and wire ropes could be replaced with these materials eliminating the problems of corrosion and weight, see Figure 4.2.

4.4.1 Poly(p-phenylene Terephthalamide) (PPTA) Aramid Fibres

Aramid fibres have a higher strength than *Nylon* and polyester but with lower energy operation capacity. They have a higher density than Polyester and the lowest extension of all man-made fibres. Ropes manufactured from this material are available in braided construction with abrasion resistance outer braid of Polyester or other fibre depending on application[111], see Figures 4.2 & 4.3 as well as Table 4.3.

The original method for producing high molecular weight PPTA was patented by Du Pont's Stephanie Kowleck in 1971[112]. This fibre is now known as Kevlar aramid fibre and the significance of the processing breakthroughs that permitted its use in the automotive, military and aerospace applications have been recognised as a great achievement in processing. Indeed, in 1985, Kowleck was one of the charter inductees into the University of Akron's Polymer Processing Hall of Fame for her work in this area[113]. Prior to 1985, DuPont was the only company producing commercial quantities of PPTA. Since then, however, the Dutch-German fibres manufacturer Akzo Group, in conjunction with a Dutch-state operated co-operative, have begun producing PPTA based fibre under the trade name of Twaron. At the same time, the third largest fibre manufacturer in Japan, Teijin, has begun pilot scale production of a modified PPTA, HM-50 under the trade name of Technora. These companies will thus be responsible for defining and refining the m markets for PPTA based fibre and composites[114].

Aramid fibres have exceptional low stretch and immense strength. Typically, they have three times the strength of polyester. They are highly susceptible to UV light. In general aramid fibres form the core of a rope, being protected from light and chafe by a braided polyester sheath. They are difficult to splice, particularly in smaller sizes, and do not take kindly to knotting. The creep rates are low relative to *nylon* and polyester and only slightly higher than those of steel wire. They are essentially unaffected by long-term exposure to extreme temperatures in the -40 °C to 160 °C range. At low temperatures there is a modest increase in tensile strength and slight reduction in elongation. Their modulus is much higher than those of traditional fibre (60,000 - 120,000 N/mm²) and consequently the rope must be designed and fabricated to obtain even load sharing

between the elements. Helix, or braid angles should be low in order to maximise strength translation. The aramid polymers are made from aromatic diamine and terephthalic acid. One of these aramid polyamides is polyparaphenylene terephthalamide. During production monophase paracrystalrope structures are formed with crystal length of 200 to 700 Å and with a high stiffness and low deferability at elevated temperatures. Aramid fibres have:

- low weight
- corrosion resistance
- high tensile strength
- high dimension stability
- high modulus

Aramid fibre's high tenacity, low creep, thermal resistance and low elongation play an important role in its application in ropes and cables. Due to their slight light/UV stability, the unprotected surface of cable and rope made of this material will be attacked. The effect depends on the exposed area, the intensity and time. However, in large rope constructions, the rope can be self screening, i.e. as the surface fibres are affected, they begin to decompose and in turn blocking the sun light from entering further into the core of the rope and affecting the rest.

The synthesis of PPTA to high molecular weight polymer appears simple on paper but when production quantities are needed, the problems that arise are tremendous. PPTA is generally synthesised via an acid chloride condensation of terephthaloyl chloride (TPC), with p-phenylene diamine (PDA). The reaction involves dissolving PDA in hexamethylphosphoramide/N-methylpyrollidone (HMPA/NMP) solution and cooling followed by addition of powdered TPC. The mixture is stirred and then washed with water to remove the solvent and HCl. Because of the environmental concerns over HMPA, a known carcinogen, later work has shown that NMP with dissolved $CaCl_2$ can generate high enough molecular weights without the stringent controls on recapture of

solvent. The major difficulties involved with this synthesis are keeping the reactants and solvents clean and extremely dry prior to synthesis. Impurities, particularly water, in the reaction mixture adversely affect the products molecular weight, and if not carefully controlled, will impair the formation of high molecular weight PPTA polymer necessary for successful spinning of high strength fibres. After a polymer of correct molecular weight is synthesised (inherent viscosity ≥ 4 in 98% H_2SO_4 at 30°C),fibres are extruded at temperatures less that 90°C using a dry jet-wet spinning technique, see Figure 4.4. The approximately 20% PPTA, 80% H_2SO_4 spinning dopes are spun at rates between 0.099 and 6 m/s into a cold (~1°C) water bath. The air gap between spinneret tip and the bath is on the order of 0.5 mm. Following the formation of the as spun fibre, the fibre is washed, dried and given post treatment depending on the particular properties being sought. Indeed, it is post fibre processing that differentiates the three types of aramid from each other. Figure 4.5 outlines a simplified process flow sheet based on some of Du Pont's original patents for production of a specific Kevlar[115].

4.4.2 Aramid Co.-polymer

The next logical step was to produce a more resilient aramid fibre and Technora was developed and patented by Teijin Ltd in 1974 under the development name of HM-50, see Figures 4.2 and 4.3. Hoechst A.G. of Germany also has produced a new breed of aramid fibre under the development name of HMA, which is now known under the trade name of Trevar. However, the Trevar production has stopped due economic reasons. They are organic fibres, which exhibit good mechanical characteristics in high tensile strength and modulus and good chemical characteristics with regard to both hydrolytic and chemical resistance (seven times as strong as that for steel and three times stronger than glass or polyester of the same weight). They have the following characteristics :

- Excellent impact resistance, applicable for soft and hard anti-ballistic use.
- High cut resistance, suitable for protective clothing.
- Compared with other high tenacity fibres, Their close structure presents excellent fatigue resistance to abrasion, flexure and stretching.

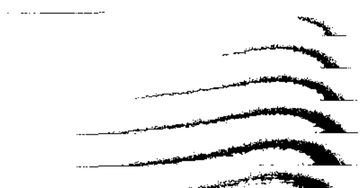

- Their stiff and highly oriented molecular structure makes creep and stress relaxation extremely low. Moreover, thermal shrinkage is undetectable at up to 200°C (392°F).

Because of their high thermal stability, even at 250°C (482°F) they maintain more than half of their room temperature tensile strength and modulus. This high heat resistance allows it to keep 75% of its strength after 1000 hours in 200°C (392°F) hot air, while for a short time, it remains durable even up to 500°C (932°F). see Table 4.3.

Technora aramid fibre is easily differentiated from other PPTA fibres. It is composed of three starting monomers, terephthalic acid PDA and 3,4-diaminodiphenyl ether. The ether monomer creates a greater flexibility in the main chain backbone and results in final properties exhibiting slightly greater compressive strength than for PPTA. Technora is also produced using a condensation reaction in highly acidic solvents[116].

The manufacturing process for Technora is schematically depicted in Figure 4.6[117,118]. It takes full advantages of the 50 mol% coply-terephthalamide of *p*-phenylenediamine and 3,4'-ODA (HM-50). The polymer is soluble in a single solvent like *N*-methyl-pyrrolidone. The solution when neutralised, is stable enough to carried out directly to the spinning process, where it is introduced into an aqueous coagulation bath. The gel fibre formed is then subjected to solvent extraction, drawing, and finish to give the final product. Since only one solvent is used throughout the process and there is no isolation of the polymer, the process becomes simple and straightforward. No use of a strong acid not only greatly simplified the solvent recovery, but also makes Technora fibres free of residual acid[119].

4.4.3 High Modulus Polyethylene (HMPE)

HMPE are also known as High Performance Polyethylene (HPPE). They are best known by the trade name **"Dyneema"** and **"Spectra"** which currently have near identical performance. HPPE is derived from Ultra High Molecular Weight Polyethylene (UHMWPE), a grade having much longer molecules than most usual

commercial products, see Figure 4.7a & b and Table 4.3. The UHMWPE is then spun using a special process called gel spinning process, which aligns all the molecules along the length of the filaments. This methods produces fibres with exceptionally good mechanical properties and also retaining many of the intrinsic advantages of polyethylene (PE), namely excellent chemical/light resistance and lower density than water. The main disadvantages are also inherited from regular PE. These are:

1. poor high temperature performance.
2. a certain degree of creep.
3. very low coefficient of friction.

When measuring a materials performance, units, which account for the weight of the fibre (so called "specific" units) are the most useful. This is especially true for rigging applications where reduction of weight aloft is one of the most important factors. Since the density of aramid is higher than that of HPPE, on a size for size basis ropes made of either material have similar stretch and strength performance. When weight is considered however, HMPE rope has a clear advantage. The resistance a fibre presents to stretching is shown by the "specific modulus". The tenacity of the HMPE fibres is the highest of all synthetic fibres and can be up to 15 times that of high tensile steel. The free breaking length gives perhaps the best illustration of its unique combination of high strength and low weight,[120], see Figure 4.8. This is the theoretical length of a fibre at which it will break under its own weight. The free breaking length is independent of the size of the fibre or rope and is determined only by the material properties. This is obtained by dividing the breaking strength (lbs-wt or kg-wt), by the weight per unit length (lbs-wt/ft or g-wt/m). The result is the breaking length in ft (or km), the length of suspended rope or chain which will break under its own weight[121]. HMPE fibres have a chemical and crystalline structure that gives them very good resistance against environmental influences. Solvents and chemicals scarcely effect their performance. For ropes, the resistance to UV radiation, sea water, weathering and temperature cycles are of major importance and HMPE fibres have excellent long-term properties.

a) The Gel spinning Process

Figure 4.9 gives a diagram of the gel spinning process used to produce a high performance polyethylene fibre. A short explanation of the main points of the process is as follows:

- The continuous extrusion of the solution of ultra high molecular weight polyethylene (UHMWPE) with a huge jump in viscosity when the solution is formed.
- Spinning of the solution and gelation / crystallisation of the UHMWPE. This can be done either by cooling and extraction or by evaporation of the solvent.
- Ultra drawing and removal of remaining solvent. Ultra drawing is of course the "heart" of the process but the other steps are essential in the production of a fibre with good characteristics. It is this process which gives HMPE fibres their high degree of orientation and crystallisation. See Figure 4.10.

4.4.4 LCP (Liquid Crystal polymer)

Vectran is a high performance thermoplastic multi filament yarn spun from liquid crystal polymer and is manufactured by Hoechst Celanese Corporation. There are three types of Vectran fibres products available namely Vectran HS, a high-strength fibre; Vectran M, a thermoplastic matrix fibre; and a combination of HS and M and of S-2 Glass. Vectran ropes have a similar load extension performance to those made from aramid but display lower stretch. Vectran ropes have a similar density to aramid and require the same protection from UV light. Vectran has a flex resistance six times that of aramid and an abrasion resistance 10 -12 times better. A unique property of Vectran is its resistance to creep, at load up to 50% of its break strength. Vectran displays no creep, even at high temperatures, a feature that any other rope making material can match including steel. See Figures 4.11 and 4.12.

4.5 Factors Affecting Performance of Fibres

For the same reasons that the factors that affect the ropes are important the factors that affect the fibres are just as important. However, these are more fundamental since the fibres are the building blocks of ropes. Almost every rope and cable requirement has its own unique design requirements, which are normally dependent on application and environmental severity. The mechanical properties of aramids offer high strength to weight ratios, low elongation, low creep, and non-corrosive ropes and cables. The physical constraints within which a rope or cable must function may create design criteria that can not be met by utilising Kevlar or Twaron. Technora exhibits many of the same physical properties as other aramids with a molecular structure which imparts higher break strength and elongation, lower moisture adsorption, and an intrinsically higher abrasion resistance[122,123].

4.5.1 UV and Weathering

Nylon and Kevlar yarns were subjected to degradation under high temperature and humidity conditions and after 26 weeks of exposure, smog cause approximately 50% strength loss in *nylon* and approximately 25% strength loss in Kevlar yarns. Ozone had little effect on both yarns[124]. The exposure to full natural weathering over a period of about a year caused changes in the shape of the stress-strain curves for yarns extracted from cordage made from *nylon* 6,6, Aramid, acrylic, polyester and polypropylene fibres. The shorter time of exposure to sun only, together with longer periods of storage, caused some truncation of the curves. The rate of strength loss while exposed to the sun was higher than the overall rate for full weathering, which included periods without sun and periods of darkness. Aramid fibre yarns and medium and high tenacity *nylon* yarns were most affected. Acrylic fibre yarns were least affected after exposure to full weathering or sun only but suffered the highest reduction by a combination of periods of immersion in water at 20°C followed by conditioning at 20°C, 65% relative humidity. Storage for approximately one year did not cause any noticeable deterioration for any of the fibre types[125].

Three methods of protecting the Twaron fibre from the effect of light have been investigated. In the Twaron yarns covered with cotton/polyester, optically tight sheaths were obtained that still do not protect the yarns from the harmful radiation. A possible method of improving light stability is to dye the sheath layers. The light stability of the sputtered fabrics is limited, owing to the unavoidable effects of processing resulting in uncoated places being laid bare. An appropriate anti-slip finish may achieve an improvement. The stacking of woven fabrics with films having different transmission ranges demonstrated that para-aramids are damaged not only by UV radiation, but also by visible light; therefore, the generally recommended UV protection alone is not sufficient[126]. The effect of ultraviolet radiation on the tensile properties of Kevlar 149 and Technora fibres types causes considerable loss in strength, but the former also exhibits a significant and unexpected fall in modulus. Electron microscope examination of the virgin and extended fibres reveals the structural reasons for the observed mechanical behaviour[127].

The presence of moisture in a polymer often accelerates the creep process, presumably through a plastision effect. Studies on wool, wood and wood products indicated that the creep and dynamic loss significantly increased for conditions of changing moisture content. Similar trends occur in certain man-made fibres and their composites. This suggests that not only the moisture content, but also the sorption history are important for determining the Viscoelastic properties of polymeric fibres and composites. Also the logarithmic creep rate of Kevlar 29, 49, and 149 fibres subjected to 2-h wet/dry cycles increase by as much as a factor of 3 over the creep occurring under constant, saturated moisture conditions[128,129,].

5.0 TESTING

The testing of the ropes and fibres is an important tool in understanding the performance of the rope. There are several destructive tests available for the evaluation of a rope and recently there has been some movement towards non-destructive testing of ropes. In order to define the behaviour of the fibre rope, it has to be tested. Testing has always been a powerful tool in determining the performance of any material. However, it is important to decide on the right testing regime that would yield the desired data. The biggest use of ropes has always been the marine industry and it has grown drastically as new demands have grown with new development in new materials. However, the bulk of testing carried out has been for the marine applications where such parameters as the cycles to failure are important. There is distinct lack of work aimed at small diameter ropes for specific applications such as paragliding, which makes this research very important.

5.1 Destructive Testing of Ropes

The commonest and the oldest testing technique have been the destructive testing, where the results are obtained at the expense of destruction of the test sample. It has the advantage of being able to be tailor made for any test regime.

5.1.1 Mechanical Testing

a) Fatigue

Accelerated flex-fatigue tests on gel-spun ultra-high-modulus, high-performance polyethylene (HPPE) fibres, under the influence of an applied tension has been carried out. The study concludes that failure occur mainly as a result of axial splitting and/or fibrillation[130]. Ultra-high-strength linear polyethylene monofilaments that are produced by solution spinning and subsequent hot drawing at 120°C have been studied. Some salient features of a polyethylene filament with a draw ratio of 31.7 are[131]:

- tensile strength at break = 3.0 GPa
- Young's modulus = 90 GPa
- DSC melting point at a scan speed of 10° C/min = 145.5°C

The modulus is found to depend linearly on the draw ratio. The tensile strength tends by contrast, to approach an upper limit at high draw ratios. Additional morphological and X-ray studies reveal an extremely good orientation of the macromolecules in the fibre direction of the highly drawn polyethylene monofilament.

The stress relaxation behaviour of high-modulus oriented polyethylene fibre with regard to the response to successive small strain increments imposed on an initial relatively large strain deformation can describe satisfactorily some of the stress relaxation experiments on the oriented polyethylene fibres. However, it is unsatisfactory once the strain increments have exceeded a certain size, and it is at variance with stress recovery experiments. Both the present stress relaxation and stress recovery experiments could be interpreted in terms of a model comprising two thermally activated processes acting in parallel. Furthermore, the parameters obtained for the stress relaxation data are consistent with those required to fit creep data obtained in a comparable stress range. The essential feature of the mechanical behaviour, which was previously attributed to strain hardening, can now be seen to arise from the transfer of stress between the two thermally activated processes in the two-process model[132].

The production scheme for extended chain polyethylene have been reviewed and compared with other high performance materials. Particular emphasis has been placed on the wide range of physical properties, which are achieved, and the extraordinary stability of "second generation" products to relatively high temperatures and long term stresses. An overview of the potential applications and representative end use products and properties has been presented[133].

The tensile creep and recovery behaviour of a range of drawn linear polyethylene monofilaments with temperature ranges from 20° C to 70°C and varying loading times ranging from 80 hours to 2 years have been described. It is found that creep and recovery behaviour depends strongly on draw ratio and molecular weight as well as on irradiation cross-linking prior to or subsequent to drawing and copolymerisation. Optimum performance is found in high molecular weight homopolymer, copolymer and homopolymer irradiated prior to drawing. Homopolymer, which is irradiated subsequent to drawing, displayed higher creep compliance than the as drawn homopolymer, but a superior recoverability from creep[134,135].

The fatigue data for *nylon* and polyester marine ropes from several testing programs in Europe and the US have been compared. A model based on the creep-rupture behaviour of individual fibres and yarns could predict failures at loads above 30-40% of the new breaking strength for *nylon* or 60-70% for polyester. Failures at lower loads and higher cycles usually occur by external or internal abrasion. Polyester outperforms *nylon* under wet conditions in both regimes. Rope failures in tests tend to occur in or at the end of the splice, at the tangent of the eye and the bollard, or at the back of the eye. The failure position appears to depend on the ratio of the rope to bollard diameter, the type of eye protection (if any), and the rope construction. Important factors in rope fatigue tests are the environment and the test period. Test on dry ropes at high loads, unless run at very low frequencies (long periods), fail due to hysteretic heating[136]. If the specimen is immersed in water or sprayed with water during testing, heat build-up does not appear to be a problem. The additional effects that complicate the rope behaviour include:

1. Fibre shrinkage with long term water exposure
2. Transverse loading
3. Abrasion (internal or external)
4. Recovery periods between loading
5. Hysteretic heating
6. Photochemical degradation.

Comparing *nylon*, polyester, polypropylene and Kevlar it is found that wet *nylon* frequently fails at about 40% of its new strength at 1000 cycles. Long term survival seems to be at about 10% of breaking strength range. For wet polyester, frequent failures at 1000 cycles appears at about 70% breaking strength range. Long life appears possible below 40% of breaking strength. One test by Samson Ropes cycles the rope between 15% and 30% of breaking strength for 200,000 cycles. The rope has a residual strength of 110% of new. *Nylon* can be used at 10% of break strength while polyester at 20%. The smaller polyester rope would have about the same elasticity as the larger *nylon* since elasticity ratio was also about 2 to 1. Stranded Kevlar have nearly the same strength as wire rope for the same diameter. This meant that it could replace wire on a direct basis[137,138,139,140,141,142,143,144,145].

Kevlar and polyester parallel lay ropes are subjected to high, medium and low-load cyclic tension fatigue tests. Both ropes survive 2,000,000 cycles without failing at low load cyclic tensions of 8% to 25% of breaking strength. Results indicate that ropes with non-parallel constructions have superior bending fatigue lives over parallel constructions. Where upper limits are placed on sheave and rope diameter, ropes constructed of high strength fibres contributed to longer bending fatigue lives because they allow smaller diameter ropes to be constructed which perform better than a larger diameter rope on a given sheave diameter. Thus, there is confidence that a long-term mooring rope is realistic. Residual strengths are 70% to 77% for the Kevlar rope and 93% for the polyester rope. Interfibre abrasion is the primary failure mechanism for ropes in bending fatigue[146].

In tension-bending tests intended to produce failures at the mouth of the termination on Kevlar 49 parallel lay ropes most failures occur at the deflector; one test was stopped after 1 million cycles. No curvature in the rope could be measured at the termination, indicating that the rope was acting as a bundle of individual fibres of negligible stiffness. With a pre-load of 300 kN on a rope with an ultimate load of 600 kN, a life in excess of 240,000 cycles can be expected at an offset of ±1.5° (3° range) at the termination. The sheave bending tests produce lifetimes of about 4000 cycles when

tested at up to 50% of the static breaking strength (600 kN/2 =300 kN), and about 20,000 cycles with a load range of 200 kN, using a pulley with a D/d ratio of 23[147].

The performance of two reduced-scale prototype rope constructions: a 1-inch diameter 6-strand and a 2.1-inch diameter 36-strand rope have been evaluated. Tensile tests revealed the rope elongation and diameter versus tension characteristics. Cyclic- bend-over-sheave fatigue tests using either a single sheave or three or five sheaves in a reverse-bend configuration reveal the rope fatigue life and failure mechanisms for various sheave diameters and trolley weights. The tests include both lubricated and unlubricated ropes. Teflon and aluminium conformally grooved "sliders" are also evaluated as a possible substitute for test platform support sheaves. The results of these tests reveal the superiority of the 36-strand rope construction[148].

Cycles-to-failure tests on small-diameter ropes (diameters up to 18 mm) revealed considerable differences between *nylon*, polyester and polypropylene, between dry and wet ropes and between the temperatures reached during cyclic loading. In comparison with *nylon* and polyester, Aramid show promising dynamic properties[149].

A method for measuring pressures and friction within textile structures and its use on four ropes made of two different man-made fibres has been developed. The method employs a novel pressure-sensing 'yarn' element built (or pulled) into the rope and a separate measurement of the force is needed to pull a short length of rope yarn out of the rope. The coefficient of friction is then simply found from the pull-out force divided by the pressure force acting on the surface area of the yarn. Two wire-rope-construction Kevlar ropes and two multi-rope polyester fibre ropes are compared, at a variety of mean axial loads (1%, 5% and 10% of the ultimate axial load). By using built-in sensors, coefficients of friction are found to range from 0.10 to 0.14 for the Kevlar 960 and from 0.24 to 0.31 for the Kevlar 961 ropes, with variations at low loads. Because of technical difficulties with the pulled-in sensor used for the polyester-fibre ropes, the friction results for these ropes are unreliable[150].

b) Realistic Cyclic Testing

In most laboratory experiments the cyclic tests are either carried out in dry or wet conditions but in order to simulate the environment that a rope is subjected to, it has to be cycled both dry and wet one after each other. This is as close to the realistic situation as possible. However, since the numbers of variables in the process are enormous because it is difficult to define how long the rope is immersed in the water and how often . It is also difficult to establish if all of the rope is realistically cycled or only parts of it. However, realistic in this context refers to wet and dry cycles. Some synthetic fibre ropes are cyclically loaded and creep tested. The final master hysteresis loops are obtained and permanent elongation and elastic ones are estimated. Vectran and Tekmilon are pre-eminent in strength, though not in elasticity. Young's moduli are estimated from the master hysteresis loops. It is shown that they increase with the external load. The wet *Nylon* rope test specimens show a strength drop[151].

Cyclic loading endurance properties of continuously wetted braid-on-braid, eight strand(square) and parallel lay polyamides, polyester and polypropylene ropes have been studied. Rope sizes researched were 100 kN nominal breaking force and up to 1.0 MN nominal breaking force. The test results indicate the superior bollard abrasion resistance and interstrand friction wear resistance of polyester and polypropylene over the polyamides[152].

Cyclic endurance at sea wave frequency of 0.16 Hz (6 second period) of *nylon* 6 fibres ropes exhibit loss in performance at the higher frequency rate when identical ropes are compared. However, ropes produced from filaments with a resistant finish (so-called "superfinished" filaments) have considerably better endurance performance than those of otherwise similar ropes without the resistant finish. The results of tests on ropes made from filaments with resistant finishes show their performance at high cyclic loads to be little improved on their non-resistant finished counterparts, but at low cyclic loads the improvement in endurance performance is very large indeed[153].

It has been noted that it may not be the maximum load that causes rope failure as much as the combination of the minimum load and the maximum load. During cyclic loading, if the minimum tension is zero, the rope fails at a much lower maximum tension than it would if the minimum is above zero. The wet strength of *nylon* actually increases after 200,000 cycles to the point where it equals the new, dry strength of the rope. In other words, *nylon* rope loses 10-12% of its strength when immersed in water; after cyclic loading in which some tension is always in the rope (i.e., 3% Rated Break Strength RBS), the original dry strength is regained. Both *nylon* filaments and stranded fibre ropes fail in fatigue when the maximum tension peak exceeds approximately 30% RBS. *Nylon* rope cyclically loaded between 3% RBS and 62% RBS show no statistical reduction in break strength after 200,000 cycles[154].

c)Abrasion

Kevlar braided cord provides high strength and excellent thermal isolation in a compact geometry. Calculations based on their measured value of Young's modulus, agrees well with measured values of the resonant frequencies of their support system. The strength of the support under prolonged vibration seemed to be limited by abrasion of the Kevlar cord against the pulley. Nevertheless, the results of their vibration tests indicate that their design is adequate for supporting large loads during launch. The support is expected to become stronger with higher resonant frequencies at lower temperatures[155].

Two essentially identical *nylon* yarns are wet breaking strength and cyclic-load tested. The only difference in the yarns is the type of finish, an ordinary marine finish and an improved finish. Yarn-on-yarn friction and abrasion test methods, developed by the Goksoy et al, is used to investigate the yarn properties. The *nylon* rope made with ordinary-finish yarn exhibits the usual 20% reduction in wet breaking strength. The *nylon* rope made with improved-finish yarn has a very unusual 13% wet strength increase. The wet breaking strengths of the yarns are the same. The improved-finish yarn has a lower wet friction coefficient. This lower fiction coefficient allows fibres, yarn, and strands to adjust and share tension loads more evenly, and thus result in a higher rope breaking strength. The *nylon* rope made with the improved-finish yarn exhibits much better cyclic-load performance. Internal abrasion is the principal form of

cyclic-load damage in each rope. Wet yarn abrasion tests show that the improved-finish yarn can survive many more abrasion cycles than could the ordinary-finish yarn. The better wet yarn abrasion resistance results in longer cyclic-load rope life[156].

A yarn-on-yarn abrasion test for use on continuous-filament rope yarns has been developed. It involves application of a reciprocating motion to two yarn sections wrapped helically together under tension. Different modes of behaviour are found under more severe and less severe conditions yielding reproducible results with acceptably low variability. Tests are made on two *nylon* and two polyester-fibre yarns. Results are presented for the influence of tensioning weight, number of wraps, wrap angle, cyclic stroke, and cyclic speed on the cycles to failure of two *nylon* and two polyester-fibre yarns, both wet and dry. The measurements made are dry as received, in tap-water, in distilled water, in synthetic sea-water, and in Sodium Chloride (NaCl) solution and also after drying from these environments. The effects of pre-soaking are studied. The different wet environments do not give large differences in abrasion life, but *nylon* has a lower life wet than dry. Severe reduction of life occurs in yarns dried from the salt solutions[157,158,159].

A test facility for determining the slip forces and friction characteristics between large rope strands or sub-ropes as used in large polyester, *nylon* and Kevlar ropes have been developed. The device used in the test is modelled on that used by Goksoy et al[123,124,125,126] but is developed to simulate motions within different rope geometries. It is concerned with the sawing action between pairs of strands to give an estimate of the friction forces and to qualify it as a function of contact pressure, slip rate and twist geometry. Also considered is the sliding within three strand polyester ropes and sliding between sub-ropes in six strand polyester sheathed Kevlar ropes. The aim of the investigation is to identify the frictional behaviour of the relative motion between these components to measure the friction force thus giving the work done or energy loss in hysteresis thus giving an estimate of the heat generated between components[160].

Small diameter double braids using poly (p-phenylene terephthalamide) (PPTA) as the core material and *nylon* 66 and polyester (PET) as the braided sheath materials have been fabricated. The degree of deterioration due to abrasion is characterised by residual strength measurements, while the number of cycles to failure is used to determine fatigue resistance. Tensile testing of both the sheathed braid and unsheathed core revealed that the sheath improved load-bearing capabilities, but pre-conditioning the braids before testing decreased strength. Abrasion testing of the sheathed samples do not result in a strength loss within the number of cycles tested, but when the unsheathed core was tested at a moderate number of cycles, a 60% loss of strength resulted. The sheath also improved the lifetime when the braids are subjected to cycling around a capstan. Lifetimes are short due to sensitivity of the PPTA core to lateral compressive forces and the high loading force (~50% UTS). SEM investigation of the failure zones for both the abrasion and fatigue samples result in similar topographies. Surface abrasion of the PPTA core resulted in fibrillation. Splitting is evident in the morphologies of both *nylon* and polyester sheaths. There is little evidence of self-abrasion of the PPTA in the braided structure, indicating low relative strand movement[161].

d) Bending Test

The bending fatigue (formation of kinkbands and cracks in the individual filaments) and abrasion due to the relative movements during bending of Twaron ropes have been studied. The number of cycles to failure, as a function of loading level, depends strongly on internal parameters such as rope construction, lubrication, type of jacket and on external parameters determined by the (field) test conditions of the rope. Under optimal circumstances a TWARON rope (diameter range up to 30 mm) suffered one hundred thousand cycles at a 20% loading level up to one million cycles at 10% loading[162].

Bending fatigue tests on Kevlar 49 parallel lay (parafil) ropes and helically laid ropes of Kevlar 29 and high-modulus polyethylene (HMPE) have been reported. The parafil ropes were subjected to three different regimes: free bending-tension tests intended to

produce failures at the mouth of a termination, sheave bending through 45° under varying axial load, and sheave bending through 180° at constant axial load. The Kevlar 29 and HMPE ropes were tested over a 180° sheave. Although the free bending-tension tests were intended to produce failures at the mouth of the termination, most failures occurred elsewhere: one test was stopped after one million cycles. The 45° sheave bending tests produce lifetimes of about 4000 cycles when tested at up to 50% of the static breaking strength. The 180° sheave bending test gives lives of 157 cycles at 25% of the static breaking load (SBL) for the parafil ropes, and 100 to 400 cycles at about 40% SBL for the helically laid Kevlar 29 ropes. The HMPE rope give nearly 6000 cycles at a load of 40% SBL[163].

The performance of a 68 mm diameter six strand Twaron rope with polyester cover has been assessed. The loading conditions were chosen to approximate those, which the rope would experience if used for a particular deep water salvage operation. When subjected to bend over sheave conditions, keeping it wet with ordinary tap water considerably enhances the life of the rope. The average life of three dry ropes when subjected to bend over sheave is 933 cycles whereas the wet rope reached 2800 cycles without failing. Reduction in diameter in order of 5% occurs during bend over sheave test. During a tension-tension fatigue test around sheaves the ropes, one wet and one dry achieved 311 580 cycles without failure. The coefficient of wet friction for the rope in contact with steel sheave is in the order of 0.3 for the static condition and 0.2 for the sliding condition. A total of 508 bend over sheave cycles were conducted with induced tension differences between 150 and 260 kN being attained without failure of the rope. When conducting bend over sheave tests under wet conditions with a fleet angle of 1.5° the endurance of the rope is 752 cycles[164].

e) Torsional Testing

Synthetic fibre ropes are often used under circumstances that result in a rotational displacement (twist) of the rope due to either inherent torque imbalance or the application of an external torque to the end of the rope[165]. The ability of a rope to tolerate this twist without experiencing a significant reduction in strength or service life

depends on both the rope construction and the material of which the rope is manufactured. The development of several new high strength, high modulus synthetic fibres, such as Dyneema, Kevlar, Technora, Vectran, Twaron, Spectra and Zylon[iv] has led to the evolution of new rope designs which took advantage of the special properties of these materials. For instance they can with intelligent design replace traditional wire ropes for mooring of offshore installations as the water depths increase. However, these new ropes are much less twist tolerant than the conventional ropes made from common low modulus synthetic fibres such as polypropylene, *nylon*, and polyester.

f) Creep Testing

Type G parafil parallel-lay Kevlar 49 rope has been creep tested over a period of up to 580 days. The applied stress varied from 24.5%-81.6% ultimate tensile strength. The results of the experimental investigation conducted on ropes of 1.5 and 3.0 tonne nominal breaking load show[166]:

- Creep and recovery in parallel-lay ropes could be adequately described using a logarithmic time law.
- The creep rate at any time increases with stress
- The creep coefficient for parallel-lay aramid ropes can be considered as stress independent.
- The comparison between the creep rate values for parallel-lay ropes and Kevlar 49 fibres indicated that the application of pre-tensioning load has the effect of reducing the creep strain in subsequent loading.

Creep properties of five non-metallic strength members have been studied. A mechanical contact method of creep testing based on accurate LASS data is made possible by the use of a modified strain gauge arrangement. Material yarn log secondary creep rates and cable log secondary creep rates are found to be constant and

---

[iv] Zylon is the trade name for new PBO fibre produced by Toyobo of Japan

the same. Fatigue testing based on the same LASS data identifies abrasion as a key mechanical strength loss parameter[167].

g) Stiffness

After 4-5 years in the ocean, the dynamic stiffness increases significantly- approximately 100% for *nylon* double braid rope and 30% for polyester 8 strand plaited rope. This can result in the *nylon* rope being stiffer than the polyester after exposure to the marine environment. As the rope ages, the variability of the dynamic stiffness also increases. This indicates that it is more difficult to predict how a mooring would perform after a period of time. The dynamic stiffness of *nylon* rope is more dependent on the magnitude of the load amplitude than the rate of load variation. The mean load has a much greater effect on the dynamic stiffness than both the frequency and load amplitude[168].

h) Residual Strength

Tensile fatigue and residual strength test on braid-on-braid small size aramid rope show that the strength reduction of aramid rope by cyclic loading in dry condition starts early and proceeds gradually. At 20% load level the values of the average residual strength for 20% at each test number of cycles is larger than the value of the average breaking strength, and it indicates no strength reduction even after 200,000 cycles. Before the beginning of the gradual decrease of residual strength, the data shows that the strength of the aramid rope increases at first, which is similar to that of *nylon*[49].

i) Energy

Kevlar ropes, due to their lower stretch, store less potential energy than equivalent *nylon* or polyester ropes. In addition, Kevlar is less efficient at transferring its stored potential energy to kinetic energy as the broken ends propel at rope failure. Thus Kevlar ropes are inherently less lethal and therefore, are more amenable to snap-back reduction or control. Three-strand Kevlar ropes show evidence of snap-back reduction by cascading, that is, breaking one strand at a time, allowing elongation and load relaxation[169].

5.2 Destructive Tests for Fibres

Destructive testing of fibres gives an indication of what may be the strength of the full rope. However, it is not as straight forward as that, since the effect of the twist needs to be taken into account in order to be able to directly relate the strength of strands and fibres to that of the full rope.

5.2.1 Mechanical Testing

The chemical and physical changes reported at sliding interfaces when homogeneous or composite polymers are involved in sliding situations are examined[170].

The change in the properties of Twaron and Spectra 900 fibres exposed to radiation have been investigated. The fibres were first treated under radiation and the mechanical property changes, which occurred after treatment, were compared with the fibres, which were not treated. The radiation source used in this investigation is (Ra-Ba) source of neutron. Breaking strength of these fibres decreased at the beginning then a significant increase in breaking strength was observed[171].

Kevlar 29,49, and 149 of 12 μm nominal diameter and 216 mm nominal fibre length have been tested. The average denier and strength of the fibres are about 1.45, and 300 MN respectively. The average elastic modulus is 86.9 GPa for Kevlar 29, 113.6 GPa for Kevlar 49 and 205.6 GPa for Kevlar 149. Before start of each test, a fibre was conditioned in the glass chamber with a nominal relative humidity of 95% and 60°C for about 12 hours for the fibre to reach its equilibrium moisture content. After this preconditioning stage, the test was started with the same relative humidity and temperature as in the preconditioning stage so that during the first two hour period the moisture content in the fibre was constant. After the first two hours, the humidity levels were cycled between 5% and 95% to observe the mechano-sorptive behaviour. In this way, the creep rates at constant humidity level and cyclic humidity levels could be compared on the same fibre to minimise data scattering due to fibre variability. Three tests on each type of aramid fibres result in the average values of the mechano-sorptive

parameter as 4.2 for Kevlar 29, 2.9 for Kevlar 49 and 1.9 for Kevlar 149 fibres. These results suggest that the transient moisture conditions could have substantial effects on the creep of aramid fibres[172].

Single Kevlar-29 fibres have been subjected to a variety of tensile cyclic and steady loading conditions. The dispersion of tensile strengths of the samples tested is found to be inherent to the fibre due to the distribution of defects in it and not due to variations of diameter between samples. Cyclic loading is found to produce both longer and shorter lifetimes than those recorded under steady loads equal to the maximum cyclic load. Longer lifetime indicates failure due to creep mechanisms whereas shorter lifetimes, seen with greater load amplitudes, suggesting a fatigue mechanism. No difference is noted in the fracture morphologies of the aramid Kevlar-29 fibres broken under simple tensile fatigue and creep conditions because of the complex splitting which occurred in all cases. The origin of the splitting might have been a defect on the surface or inside the fibres[173]. The tensile stress-strain properties of twisted para-aramid fibres have been measured by three experimental procedures:

1. Twist at constant length followed by extension
2. Initial extension followed by twist
3. Twist at constant small tension with contraction followed by extension

Additionally a fourth procedure of twisting and untwisting is used to examine the act of twisting, not the presence of twisting. The strength and breaking extension of aramid fibres decrease at much lower twist factors than *nylon* and polyester. The effect is severe, with a steep reduction occurring beyond a twist factor of 10 $tex^{1/2}$ cm^{-1} and falling to half the initial value by 30 $tex^{1/2}$ cm^{-1}. The corresponding values for *nylon* and polyester would be 40 and 70 $tex^{1/2}$ cm^{-1}. This more rapid reduction with Kevlar is presumably associated with failure by axial splitting, which is encouraged by the shear stresses in a twisted fibre. Even though the para-aramid fibres are more sensitive to twist, the fact that they are used as very fine filaments reduces the likelihood of this problem in practice[174].

The deformation of equivalent size and shape glass, asbestos and Kevlar aramid fibrils, when subjected to bending or longitudinal compressive loads have been estimated. Kevlar fibrils deform more easily than glass or asbestos fibrils. This behaviour is a direct result of the lower compressive modulus and compressive yield strength of Kevlar fibres. Among the Kevlar fibres studied, those with higher molecular orientation and crystalline perfection (Kevlar149 >Kevlar49 >Kevlar29) are more flexible and deform more easily. Compressive yielding occurs more easily in fibrils stripped from the spun filament surface and promoted fibril breakdown through chemical degradation[175].

The creep behaviour of ultrahigh-modulus polyethylene monofilaments over the temperature range 20-70°C has been studied. Permanent flow creep arise from a combination of two creep processes, one of which is associated with the crystalline regions of the oriented structure and the other with a molecular network. Two thermally activated processes acting in parallel describe the steady-state creep behaviour of oriented polyethylene. One process has a comparatively small activation volume and appears to be primarily affected by the draw ratio, but not by the polymer molecular weight, copolymerisation, or crosslinking. It is therefore concluded that the process relates to a deformation process in the crystalline regions of the polymer. The second process has a comparatively large activation volume, which is not significantly affected by changes in structure or chemical composition. However, the contribution of this process varies markedly for different samples, and is greatest for samples of high molecular weight, the copolymer and crosslinked polymer. Solution-spun fibre shows very different behaviour from the melt-spun and drawn monofilaments. This relates to fundamental differences in structure between two kinds of ultra high-modulus polyethylene[176,177].

Static and dynamic mechanical testing have been used to study the time-dependent deformation behaviour of a commercial grade of high-performance polyethylene fibres (Dyneema SK66). A mathematical model is proposed, where the total deformation of the fibre is regarded as being composed of a stress-linear delayed elastic component

and a non-linear plastic flow contribution. The thermo-rheological characteristics of the delayed elastic contribution are obtained using dynamic mechanical thermal analysis. The non-linear plastic flow component is characterised separately using long-term creep experiments. Model predictions of stress relaxation and tensile experiments are in good agreement with the experimental data. Evaluation of the model in stress relaxation and constant-strain-rate experiments (up to impact rate) shows that the deviation between calculated and measured stresses are within 10%[178].

The performance of poly(vinyl alcohol) (PVOH) fibres and their composites has been described. PVOH fibres are studied, with the emphasis on long-term properties. Results indicate that the long-term properties of PVOH fibres are superior to those of high-performance polyethylene (HP-PE) fibres leading to the conclusions that[179]:

- The short-term properties of PVOH fibres are relatively poor compared with those of HP-PE, Whereas the long-term properties (creep) are far superior due to absence of plastic flow.
- With increasing stress and/or strain levels the mechanical properties of PVOH fibres become less dependent on temperature and/or strain rate , i.e. the fibre displays a more elastic behaviour.
- The compressive strength of PVOH fibres is approximately three times that of HP-PE but only one third of that of Aramid fibres.

Vectran fibre has excellent mechanical properties, property retention over a wide range of temperatures, excellent chemical resistance, and low moisture absorption. In addition, single-thread rope evaluation confirmed by end-product testing shows that Vectran has no measurable creep when loaded up to 50% of the breaking load and excellent abrasion-resistance with an appropriate finish[57,58].

Torsional moduli and damping factors have been measured on a number of polymeric [Kevlar, poly(p-phenylene benzobisoxazole) (PBO), poly (p-phenylene benzobisthiazole) (PBZT) and Vectran] and carbon fibres [pitch and PAN based , and one bromine interacted pitch based carbon fibre] as function of vacuum level (1.1-80 × 10^3 Pa). In general PAN based fibres have a higher torsional moduli than pitch based carbon fibres. Kevlar 149, PBO and PBZT fibres have a comparable room temperature torsional moduli, while the torsional modulus of Vectran fibre is very low, probably due to the torsional flexibility of the -COO- group. In the same temperature range, torsional moduli of both pitch and PAN based carbon fibres do not change significantly, while for polymeric fibres they decrease; a small decrease is observed for PBO and PBZT, and a significantly higher decrease is observed for Vectran[180].

5.3 Non-Destructive Testing

Over the past 20 years there has been a huge growth of interest in what are generally called non-destructive testing (NDT) and non-destructive evaluation (NDE) techniques. These are methods for probing inside the materials that are used to construct structures, manufacturing plants, etc. The aim is to characterise the material and defects present, but without damaging, or disturbing the material or structure. The main motivation for NDT has been increased safety standards, but economic considerations are equally important, especially when quality control of a material product is at issue. Material defects such as surface cracks, laps, pits, internal inclusions, burst, shrink, seam, hot tears, and composition analysis can be detected. Sometimes their dimensions and exact location can be determined. Such tests can usually be made more rapidly. Processing results such as hardness, case depth, wall thickness, ductility, decarburization, cracks, apparent tensile strength, grain size, and lack of weld penetration or fusion may be detectable and measurable. Service results such as corrosion and fatigue cracking may be detected and measured by non-destructive test methods. In many cases imperfections can be automatically detected so that parts or materials can be classified. NDT techniques for locating damage, i.e. ultrasonic (particularly time of flight diffraction, acousto-ultrasonics, X-radiography, computer aided tomography and electronic speckle pattern interferometry are discussed, quantification of the damage along with the need to adopt a repair design strategy. Practical problems of repair

specification were highlighted demonstrating the need to take into account the complicating factors of laminate moisture penetration, time dependent chemical changes in resins, high temp. operating requirements and composite joint technology[181].

5.3.1 Non-Destructive Testing Techniques Applied to Synthetic Fibre Ropes

Magnetic flux leakage method is limited to the case of ropes made of ferromagnetic materials and requires that either the rope is run through the magnetic test device or the instrument is hauled along the rope. Radiography is useful once a trouble zone has been localised. In principle, the induced wave propagation method offers considerable advantages, since it yields information on the overall wear, corrosion or broken wires in a very efficient, rapid manner[27].

The technical feasibility of applying Internal Friction Damping (IFD) as a non-destructive evaluation technique for synthetic ropes is discussed. Marine applications of interest for synthetic ropes include mooring ropes and towing hawsers with specific emphasis in this paper on ropes for Single Point Moorings (SPM) in Deep Water Ports (DWP). The theory of internal friction damping is briefly presented here as it has been historically applied to metallic materials. The methodology for application of IFD technique to synthetic rope material and construction is also discussed. The experimental apparatus and specific laboratory technique are then discussed as applied to 150 and 200 mm circumference ropes. Experimental results are presented and related to the feasibility of employing this technique as a monitoring method for the real world assessment of rope deterioration/performance. The characteristics of ropes when tested in both wet and dry conditions are discussed. A comparison of the effect of IFD to various synthetic rope failure mechanisms is presented[28]. Applications of ultrasonic to ropes could lead to the following conclusions[29,30]:

- The output signal appears as a complicated wave packet. The maximum amplitude peak of this wave packet arrives much later than the first detectable peak.

- The wave speed corresponding to the arrival of the first peak increases with increasing rope tension or rope strain. For the 0.635 cm (¼in) rope, this wave speed ranges from 1700 ms^{-1} at very low loads to 4500 ms^{-1} near the breaking strength.
- For any given rope tension or rope strain, the wave speed corresponding to the arrival of the first peak is dependent upon the loading history of the rope. Wave speed at a given tension increases with cyclic loading. However, this loading history dependence becomes pronounced at higher rope tensions. The incremental change in wave speed with each loading cycle decreases as the number of loading cycles increases; and, the wave speed stabilises after approximately three loading cycles.
- At any given strain, the wave speed corresponding to the arrival of the first peak is nearly independent of the rope diameter, to within an average standard deviation of 4.1%.
- The wave speed corresponding to the arrival of the first peak is the function of the path angle of propagation through the interior of the rope. The wave speed along the generator on the surface of the rope is 2.33 times as large as the wave speed across the rope diameter.
- If the rope is assumed to act as a uniform elastic rod, the longitudinal wave speed predicted consistently underestimates the measured wave speed corresponding to the arrival of the first peak. The average percentage deviation of predicted wave speed from observed wave speed is 13.2% for the range of rope sizes and tensions used. However, the percentage deviation decreases with rope tension.
- If the rope is assumed to act as a uniform taut string, the transverse wave speed predicted is lower than the apparent wave speed corresponding to the arrival of the maximum amplitude peak. The average percentage deviation of the predicted wave speed from the apparent wave speed is 47.9% for the range of rope strains used. This percentage deviation decreases with increasing rope tension.
- The wave speed corresponding to the arrival of the first peak is much faster than the apparent wave speed corresponding to the arrival of the maximum amplitude peak. For the range of rope strains used in that study, the average ratio of the two wave speeds was 4.1.
- No significant difference in wave speed versus tension is observed between rope samples in the dry and wet conditions. In general, there is no significant reduction

in tensile strength of wet polyester ropes. However, there is a reduction in the tensile strength of wet *nylon* ropes, between 7 and 15%.

- Little difference in wave speed versus tension is observed between rope samples obtained from different spools of the same rope construction and material.
- Little difference in wave speed versus tension is observed between 3-strand and double-braided ropes of the same diameter. There is little difference in the breaking strength between 3-strand and double-braided *nylon* ropes of the same diameter. However, the breaking strength for double-braided polyester ropes is large than that for 3-strand polyester ropes of the same diameter by 20 to 40%.

A non-destructive test scheme which, is sensitive to the cumulative effect of the various degradation mechanisms on the mechanical properties of the rope, has been developed. Their use of mechanical spectroscopy is keyed to measuring the wave propagation characteristics of rope under tension and correlating differences in those characteristics with the state of degradation. Reproducible differences in the magnitude spectra of new and "used" ropes under load using mechanical spectroscopy are found. These differences change reproducibly with time at load and change even faster as loads are increased, ultimately achieving a sort of equilibrium condition. Their preliminary measurements show this is best achieved using low loads, loading quickly, and making measurements quickly[31].

The feasibility of the non-destructive evaluation (NDE) of wire and synthetic ropes using a transverse-impulse vibrational wave has been experimentally investigated. The experiment was conducted using a 2.38 mm diameter stainless-steel wire rope and a 6.35 mm diameter double-braided *nylon* rope. Each sample was approximately 14m long. Broken strands produce readily detectable particle reflection of the wave. The velocity of the wave propagation followed the well-known equation.

$$\sqrt{\frac{F}{M}} \qquad \textbf{Eq:}\ 5.1$$

where F is the applied load and M is the mass per unit length of the rope. The results indicate that the transverse-impulse vibrational wave method can provide a fast and simple means of detecting flaws and determining both the load level in and the average mass per unit length of a rope[32,33].

Laboratory investigations indicate that the AE technique is well-suited to the non-destructive evaluation of cables due to their location and size. Crack extension and breakage of wires, as well as crack growth in the cable connectors, are possible sources of AE in the cables[34,35]. Methods for evaluating the structural health of mechanical cables and detecting their imminent failure could prevent the loss of valuable equipment and, more importantly, the possible loss of human life. The non-destructive test methods available are: thorough visual examination and measurement of the external diameter; X-rays; (induced) wave propagation; acoustic emission; magnetostrictive sensors; infrared detection. A new method, which employs, a commercial optical fibre for detecting the breakage of individual wires in a rope is available[36].

A wire rope non-destructive testing technique has been introduced concentrating mainly on the magnetic method and indicated how this is used in conjunction with visual inspection methods[37]. Wire fractures have been found near the socket neck in suspension bridge hanger cables. They have been attributed to bending fatigue, possibly accentuated by corrosion. A programme of tests is undertaken to compare the behaviour of seven different types of steel cable when subjected to transverse bending at the socket. Each cable is held under an axial load and a cyclic transverse load is applied at the mid-point of the cable to induce wire fractures at or near the socket neck. the fracture of outer wires is easily detected by visual inspection, but there is a need for a method of detecting internal wire failures[38].

6.0 ACOUSTIC EMISSION

6.1 Introduction

The phenomenon of acoustic emission has been known for centuries, but it is only recently that materials testing have made use of acoustic emission techniques. Acoustic emission is very different from conventional NDT tools, which tell of dynamic generation and growth of defects, rather than their static presence. Acoustic emission testing is strictly 'slightly destructive testing' since some deformation occurs. If, however, acoustic emission techniques are applied to the first loading experienced by a structure or component, data comes from the normal in-use load levels, and no extra damage is caused. In effect, the structure is being interrogated to find its response to a specific applied load. In general, the presence of acoustic emission indicates damage is occurring in the structure. Acoustic emission can be used in conjunction with other methods of materials analysis, e.g. microscopy, to study the details of deformation processes in materials such as metals, rocks, plastics and composites, see Table 6.1. The technique has one of its major applications in NDT work such as structural integrity evaluation. During proof testing of structures such as pressure vessels growing cracks will emit recordable stress waves well before final failure. The use of a number of detectors on a structure allows the position of a growing flaw to be fixed using triangulation techniques based on time of travel of the signal at the individual detectors. Many structures, such as nuclear pressure vessels and materials have been evaluated this way.

The term acoustic emission is used to describe both a technique and the phenomenon upon which the technique is based. Acoustic Emission (AE) or stress wave emission is the phenomenon of transient elastic wave generation due to a rapid release of strain energy caused by a structural alteration in a solid material. It should be emphasised that, unlike ultrasonic, acoustic emission is a passive monitoring system. Signals are not injected into the structure except for calibration purposes. Generally speaking, the proportion of the energy that is released as elastic wave rather than heat, depends on the nature of the source, how localised it is and how rapidly the releases takes place. Localised rapid energy releases give rise to elastic waves in the ultrasonic frequency

regime that can be detected by microphones or transducers attached to the surface of the specimen, see Figure 6.1, provided the waves are of sufficient amplitude. This whole process is known as acoustic emission, each source being an AE event. The signals detected by the transducers are also some times called acoustic emission or AE signals. Figure 6.2 shows a casual AE cycle. Generally, these structural alterations are the results of either internally generated or externally applied mechanical or thermal stresses. Numerous mechanisms have been proposed and confirmed as sources of AE. A partial listing, see Table 6.2, of reported sources include movement of dislocations and grain boundaries[182,183] formation and growth of twins, generation and propagation of cracks[184,185,186], fracture of brittle inclusions and surface films[187,188], fibre breakage and delamination in composites[189,190], phase transformations[191,192] microseismic and seismic activity in geological materials[193] etc. The phenomenon of AE was scientifically in investigated in 1948 by Mason[194].

However, Joseph Kaiser made the first clearly documented and serious investigation of AE in 1950 at the Technical University of Munich. The Kaiser effect is simply that loading which cause no more damage are essentially quiet, an example being repeat loading to a previously applied stress level within the elastic limit. the Kaiser effect tends to hold only for real emissions whilst frictional sources are active for all loading. The first successful application of AE technique to a practical problem, was achieved in the establishment of integrity assurance of fibre wound rocket-motor cases[195]. Monitoring AE during proof-tests predicted the burst pressures of test vessels to within ten percent of actual values. Since then, the applications of AE techniques in the nuclear, chemical, petroleum and aerospace industry have increased rapidly.

6.2 Discussion of the Kaiser and Felicity Effects

Historically, the term "Kaiser effect" honours J. Kaiser[196] and his original observations of reloading phenomena in several metals. The important points here is that these are physical observation not immutable laws. Fowler[197] originally conceived the term felicity ratio, for the observed behaviour of many composite materials. Over the past

several years, several inaccurate notions have arisen regarding these phenomena including:

- All metals exhibit the Kaiser effect (e.g. materials which exhibit twinning do not exhibit this effect.
- All composites exhibit the felicity effect
- If a material exhibit the Kaiser effect for a particular test condition, it will exhibit the Kaiser effect for all conditions and geometries.

The Kaiser effect has been shown to be valid only for unflawed polycrystalline metals tested under uniaxial loading conditions where reloading was immediate. However, if not, (the time is dependent on the material and the temperature) some AE activity can be observed. This is principally attributable to the migration of dislocations, the readhesion of cracked particulates, or the reformation of oxide coatings in the in the intervening time period. It should be also mentioned that most tests are conducted under uniaxial test conditions while most structural materials are actually subjected to biaxial or triaxial loading conditions. In these conditions it is plausible to expect that the results would be path dependent, i.e. if one were to change the manner in which the load was applied on reloading, eventhough the final stress state was the same (e.g. tension followed by torsion initially vs. torsion followed by tension) the Kaiser effect would probably not be seen. For these materials, local material failure (either via matrix cracking, fibre matrix debonding, fibre friction, etc.) is the principal AE source not dislocation motions. Upon reloading AE can still be generated at these microfunction sites, principally by rubbing of mating crack surfaces. In this regard, composites are similar to flawed metals where the Kaiser effect is not nearly as evident[198,199]. Both the above effects refer to the presence or the absence of AE activity upon reloading of a sample. If no acoustic emission is observed, the Kaiser effect is said to hold. Any deviation from this behaviour is known as the Felicity ratio. Fowler has introduced a measure of this deviation as the Felicity ratio, defined to be:

$$Felicity\ Ratio = \frac{load\ at\ which\ AE\ is\ observed\ on\ reloading}{previously\ applied\ \max imum\ load} \qquad \textbf{Eq:}\ 6.1$$

Obviously, a felicity ratio of one would correspond to the Kaiser effect. Ratios greater than one, while possible, would also indicate that the Kaiser effect was present. It should be noted that Japanese researchers use the term Kaiser ratio in place of Felicity ratio.

6.3 Generation of AE by Source Events

The source of the elastic waves is an event inside the body. In many cases it is no trivial matter understanding what the source events are in practical materials or what the generation mechanism is. In the case of a growing crack, still arguably the most important AE source and the formation of new crack faces must be accompanied by sudden changes in stress and displacement of material in the vicinity of the crack. Varying stresses and strains must by definition act as sources of stress (elastic waves), see Figure 6.3.

6.4 Emission Types and Characteristics

Traditionally[200] the AE signals have been classified into two different types:

- Continuous type
- Burst type

The difference between these two types, see Figure 6.4, is in the average repetition rate. Above certain values of average repetition rate, the length of the bursts exceeds the time interval between them leading to the inability of the instrumentation to resolve two successive burst emissions. This results in the superposition of bursts giving the appearance of continuous emission. Actually discrete processes generate both. The amplitude of continuous emission is usually lower than that of burst emission. Generally, the amplitude of an acoustic emission process will have some correlation with the volume of the region producing it. Since continuous emission is a

superposition of many bursts, the volume of each region producing a burst is necessarily small. Therefore, the amplitude of each burst and thus the continuous emission is low.

6.5 Detection of Acoustic Emission

6.5.1 AE Instrumentation

a) Transducer

A transducer is a device , which generates an electrical signal when it is stimulated by AE waves. Transducers connected to the specimen surface collect the stress waves information as it is emitted from its source. These transducers fall into two general types:

- Resonant e.g. piezoelectric materials
- Non-resonant e.g. electromagnetic, strain or capacitance gauges.

Non-resonant transducers can be used to detect stress waves with frequencies ranging from dc to 20 MHz. Piezoelectric devices are usually used to detect waves with frequencies centred on a particular resonant frequency, e.g. 100-300 kHz is a bandwidth often used in practice. Most applications of acoustic emission have used piezoelectric detectors principally because of their high sensitivity, low sensitivity to mechanical noise and robustness. They can also easily be designed to respond to particular wave types e.g. shear waves, which is an advantage for certain applications. The signal from the transducer is first fed into a pre amplifier which usually establishes the systems electrical noise level. It is then filtered to remove unwanted frequencies such as low frequency vibrations from mechanical equipment, etc. that are filtered out below about 100 kHz.

Most transducers used in conventional AE systems are piezoelectric crystals and have been developed for high sensitivity at frequencies in the range of 50 kHz-1 MHz. Their response is relatively of narrow band and resonant type. However, broadband transducers are also available, whose frequency response band-width is extended up to 2 MHz. Two other types of transducers that have been considered are: (Capacitive type, and (b) Optical probe based on optical interferomenty. Transducer is the most critical component any AE measuring system. As a result, if any meaningful source characterisation is to be carried out, the response of the transducer should be extremely satisfactory[201]. Following are some of the basic requirements of an AE transducer for its satisfactory performance.

b) Detection threshold

The detection threshold, sometimes called sensitivity, of an AE transducer is best defined as the minimum level of the signal amplitude that can be detected above the background noise. Since the incoming signal cannot be intensified and the noise cannot be reduced by signal averaging because the signal is changing with time, it is important that transducer and preamplifier combination generate the minimum of background electronic noise. Needless to say, every effort must also be made to reduce ambient acoustic noise, and radio frequency interference.

c) Frequency response

In order to characterise a defect source fully in terms of its time scale and/or frequency content, the transducer bandwidth must cover the source bandwidth. This is a difficult condition to fulfil because source bandwidths extend typically from DC to 10 MHz[202].

d) Directionality

Transducer should have omnidirectional response unless otherwise specified[203]. This is essential for source location.

e) Reproducible

It is also important that the response of the transducer should be reproducible to obviate the need for repeated recalibration.

f) Ease of Application

Finally, it is important to be able to use the transducer for a range of applications, both in the laboratory and for industrial monitoring. The transducer must be readily mountable on the sample or structure with a minimum of surface preparation.

6.5.2 System Calibration

Transducer calibration must be done in absolute units of displacement if it is to be correlated with dynamic phenomenon[204]. It is also necessary to calibrate the frequency response of the transducer. The following are some methods used often for calibration of AE sensors.

a) Laser Transducer Calibration

A laser pulse is applied to an aluminium block of known dimensions and the signal is registered at the other end by the sensor. By knowing the frequency of the laser and the range of the sensor as well as the time taken for the signal to travel along the specimen the sensor could be accurately calibrated.

b) Face to Face Transducer Calibration

A pre-calibrated sensor is used as transmitter. Known voltage signal at different frequencies is fed to this as input. The sensor to be calibrated is coupled with the transmitter face to face and the output voltage signal is measured to obtain the frequency response of the transducer. This is the conventional ultrasonic method and generally used for transducers commercially available today.

c) Pencil Lead Breakage

This method was developed through experimentation by Arved Nielsen and is sometimes called the Nielsen lead break method. A 2H pencil lead of 0.5 mm diameter is usually utilised. The lead field button is pressed repeatedly to protrude a definite length of lead and then it is made to break against an even surface to which the AE transducer to be calibrated is coupled. To obtain repeatable constant AE source, the lead is broken at a fixed distance from the sensor, maintaining the same length and angle of contact of the lead with the surface.

6.5.2 Acoustic Emission Signals

a) Signal Processing

There are several ways to process the AE signal[205,206]. Most of them measure the characteristics of the individual burst emission and all of them can give useful information in an AE experiment. The main aim of the signal processing and display is to identify the character and significance of the event. Following are the more common ways by which signals are processed:

- Ring down Counting Analysis
- Event counting
- Energy Analysis
- Amplitude Distribution Analysis
- Frequency Analysis

b) Ring Down Counting (RDC) Analysis

This type of analysis is one of the easiest and reliable method analysing AE signal. The principle of RDC is to count the number of times a threshold voltage is crossed by oscillating transducer output caused by acoustic emission. Table 6.2 states various parameters associated with the AE signal. The parameters and ring down counts are indicated for two AE events in Figure 6.5. Advantages claimed by RDC are that the count obtained from a given event increases with signal amplitude and there is

consequently some weight in favour of events of larger energy. Secondly RDC automatically improves noise rejection[207]. However, results obtained by this analysis are strongly influenced by the geometry of the specimen, the properties of the transducer and its coupling to the specimen, the precise detection threshold and the performance of amplifiers and filters. Therefore, there are difficulties in the use of this approach for fundamental studies. The values quoted in ringdown count are not quantitative but rather qualitative. In other word the numbers could not be used to measure anything but the level could be used to compare the performance of two ropes. If another sensor is used then the values would be different but the overall pattern would be the same.

c) Event Counting

This is technique for counting the number of events that have occurred over the duration of the test.

d) Frequency Analysis

The most common method of the determination of the frequency content of AE signals is to measure their power spectrum. Both frequency spectral analysis[208] and auto-correlation analysis[209] has been employed. Since the predominant frequency present in the power spectrum is inversely proportional to the duration of dynamic event, these measurements can provide information on the time scale of an AE process. This in turn may be used to characterise the evolution of the dynamic source event[210]. Frequency analysis of AE signal is usually complicated by uncertainties in our knowledge of frequency and mode responses of the experimental system. In general, the spectra of the detected signal may be considered as the original source spectra weighted by the frequency response of the propagation path, transducer and other electronics. However, if a single process is known to be dominating, even considering the modulating effect as above, frequency spectrum analysis may still be used if components can be considered as linear in the frequency domain and the original source spectra are multiplied at each frequency by the frequency response of the transfer function[211]. In practice therefore, it can be considered that spectral analysis does provide some guidelines in selecting instrumentation components, optimising AE delectability,

isolating background noise or extraneous AE, detecting and locating the peak at low pressure under noisy environment and providing qualitative insight to the AE source mechanism[212].

6.5.3 Factors Influencing Reliability AE Signal

There are several factors which, affect the reliability of AE signals and they are:

- Source characteristics
- Structural characteristics of the medium
- Location, type and sensitivity of transducer
- Frequency passband
- Gain of amplifiers and threshold level

The effect of transducer location is interlinked with the effect of structural characteristics. The stress waves undergo extensive changes between the time the waves leave the source and appear at the transducer. These changes can be described by reference either to the frequency or to the time domain. Transducer type is a more subtle and less well understood factor. In general, a given source event in a structure will produce markedly different wave forms from different transducer types. From the viewpoint of practical application, however these complications are not that important. The most important variable is sensitivity which needs to be characterised of quantitative emission data are to be meaningful.

6.6 Acoustic Emission Literature

6.6.1 Acoustic Emission Applied to Composites

The characteristic features of acoustic emission diagnostics of welded joints are studied. Methods of deformation identification and fracture stages on the basis of

statistical analysis of the average energy and the median frequency of AE signals spectra are considered. The possibility of estimating locality degrees of plastic deformation during the testing of a large-sized tube specimen using statistical parameter-entropy of the energy spectrum of the AE signals is shown[213].

The Kernco model VIB-10 vibration monitor, AMSY4 system, Peak Value and the Fracture Wave Detector are examples of the state-of-the-art vibration analysers and monitors. Kernco's[214] model is designed as a diagnostic tool for preventive maintenance and has monitoring methods based on the recommendations of ISO and equivalent national standard organisations. The AMSY4, on the other hand, can be used as either an acoustic emission analyser or a transient recorder. The Peak Value empowers vibration analysis to uncover machine defects that may go undetected with current demodulation techniques, especially in slow speed machinery. The Fracture Wave detector detects and locates cracks, delamination, and fibre breaks in thin structures in real time.

A well-consolidated composite consisting of aluminium alloy[215] reinforced with continuous alumina-based fibres has been made by liquid metal infiltration and its mechanical behaviour investigated by destructive and non-destructive means. The methods involve monotonic and unload/reload tensile testing, and include acoustic emission and slip-rope studies to monitor deformation. The longitudinal composite subjected to tensile stress showed three-stage stress-strain behaviour. Stages I and II are linear and associated with elastic and plastic deformation of the matrix, respectively, whilst stage III is related to fibre damage. With the transverse specimen, the stress-strain curve show a linear stage I and a progressively decreasing slope in stage II as plastic deformation continues, but no well-defined stage I/II transition: some degree of damage is again associated with fibre breakage. Differences of yield stress in directions parallel and perpendicular to fibres are attributed to residual stress in the matrix produced during manufacture of the composite. Heat treatment increases the yield stress of the composites but the heat treatment of the matrix alloy is not fully realised because of increased brittleness of the age hardened matrix.

The dynamic features of the peeling of an adhesive tape from the roll have been analysed[216]. Two sets of experiments are carried out. In the first the unwinding force of an adhesive tape at several constant peel velocities is measured. Analysis of the force-time series, show that the oscillations are deterministic. In the second set of experiments the acoustic emission generated by unwinding at constant peel force is studied. Power spectra analysis of the acoustic emission time series reveal the existence of two frequency domains; lower frequencies are associated with stick slip and higher frequencies are related to the massive rupture of adhesive fibrils.

An acoustic emission technique for in situ monitoring of damage development in ceramic-matrix composites has been developed. Damage initiation is detected and can be evaluated using acoustic emission. Comparing the acoustic emission activity characteristics in simple lay-ups with those of more complex lay-ups allows discrimination between matrix microcracking, matrix macrocracking accompanied by interface debonding, and delamination cracking[217].

Amplitude distribution acoustic emission monitoring of unidirectional carbon fibre with glass fibre hybrid reinforced plastics is carried out during tests to failure in bending. The acoustic emission count is found to be greater in hybrids than in either monofibre composites, and this noise increases with the intimacy of intermixing of the two fibre species. In amplitude distribution AE monitoring, the fine mix hybrids are found to have a cumulative distribution at failure which closely match that predicted by averaging the histograms from the two monofibre composites. The appearance of a hump in the curve corresponding to the intermediate amplitudes, associated with delamination in GRP, is found to occur immediately prior to failure[218].

It has been demonstrated that the Kaiser effect occurs in Kevlar cord reinforced rubber compositions. This is of significance value in assessing the structural integrity of cord/rubber pressure vessels. It has also been suggested that the felicity ratio must be considered whether all emissions had subsided at the previous peak load or maximum

deflection and that the values should be reported at a stress equivalent to ≈60% of the ultimate strength[219].

6.6.2 Acoustic Emission Applied to Wire Ropes

It has been revealed that it is possible to detect and discriminate the difference between the failure of constituent wires from background noise sources under both rising load and fatigue conditions. Near one-to-one correlation exists between wire breaks and events occupying given amplitude ranges. Linear source location techniques allow wire breakage to be located with a good degree of accuracy over a distance of 1.1 m under rising load conditions. Experiments to determine the attenuation of the signals resulting from wire breakage under rising load conditions result in the detection of wire breaks over a distance of 29.5 m. The amplitude of wire breaks at given distances along a rope can be calculated once the attenuation constant for a given rope has been determined experimentally[14-20]. The relation of damage processes to the acoustic emission (AE) parameter called the Felicity ratio for fibre composites under cyclic load and time under load has been discussed. The mechanisms, which can generate the acoustic emission associated with the Felicity effect, are divided into two categories[21]:

- Frictional mechanism
- new damage mechanisms

The application of acoustic emission monitoring to rope, wire and cable has been reviewed. The acoustic emission response of multi core strain cable is studied both in quasi-static and in sine-wave amplitude loading regimes. The Kaiser and Felicity effects are found to be inapplicable as the structural noise in the cable swamped the low amplitude material AE. High amplitude AE events are good indicators of strain members failing[22].

6.6.3 Acoustic Emission Applied to Synthetic Fibre Ropes

The principles of distributed optical fibre sensor for monitoring the integrity of large parafil ropes in offshore applications has been described. By studying a particular property of the light, it is possible to detect and locate a short transient signal such as the acoustic emission caused by a yarn snapping. This sensor could be applied in ambitious offshore projects such as deep-sea oil platforms and submerged tube bridges[220].

The applicability of the stress wave emission phenomena from synthetic ropes can give an to indication of the imminent failure by an increase of at least an order of magnitude in the slope of the curve. Comparison of the number of stress wave emissions with the applied load is a good indicator of impending catastrophic failure. However, no significant differences in the stress wave emission characteristics, were observed for the three types of materials considered[23].

Acoustic emission has been applied to a new Samson double-braided 2-in-1, 6.35 mm diameter *nylon* rope in the dry condition at room temperature using AE transducers with resonant frequencies at 375 kHz. Cutting various numbers of yarns in the core of the rope simulated flaws in the rope. Also, knotted ropes were tested as a means of introducing stress concentrations. It is observed that the spatial location of AE sources at low load levels could be used to identify the location of a flaw and the probable eventual rupture location of the rope. A parameter called the "AE load delay" is defined, as the tensile load producing a specified low baseline level of AE activity. The two competing mechanisms are the decreasing transducer-rope contact area with increasing rope tension and the increasing rope compaction versus increasing rope tension[24,25]. Applications of the acoustic emission method from the point of view of the non-destructive evaluation of wire and synthetic ropes and monitoring their mechanical status while in operation has been reviewed[26].

7.0 EXPERIMENTAL DETAILS

The literature review has shown that the importance, of understanding the behaviour of high performance ropes, which can best satisfy the ever increasing, demands on the modern rope systems. The aim of the experimental work was therefore to investigate the extent of damage and failure on covered and uncovered small diameter synthetic fibre ropes under laboratory conditions. To fulfil the aim the following tests have been carried out on the selected modern paraglider line materials.

i) Static tensile test

ii) Residual strength test after different pre-loading conditions

iii) Residual strength test after different cyclic loading conditions

iv) Strand-rope efficiency test

v) Rope on rope abrasion test

vi) acoustic emission

vii) Determination of temperature distribution during tensile loading

Ranges of rope samples were prepared in which 3 different rope materials in 2 different size constructions were used. This enabled the effectiveness of rope performance in different materials and constructions to be examined. Ideally it would be useful to be able to predict rope performance from the fibre properties using an appropriate theoretical mechanics. Although the properties of fibres are relatively well characterised, but when the fibres are put together as a rope, the performance is less well understood. The aim of the experimental work is to provide sufficient data to explain the effect of changing materials on the strength of the rope. The following sections cover the experimental details involved in preparing and testing of rope samples.

7.1 Rope Materials used

The fibre rope materials used in this research are listed in Table 7.1. These include 1.1 mm Dyneema, 1.6 mm Vectran and 1.1 mm Technora ropes. They are normally used as

paraglider lines. The fibre materials were supplied direct from the producers, using the same batches, which therefore eliminated the production variability. The ropes were all eight strand plaited construction except for Technora which was also available in both 4 strand twisted and 8 strand plaited, allowing comparison of changes in rope construction as well as materials. The ropes had a braided polyester cover and were produced under the same conditions for conventional rope making process, manufactured by Ibex Ropes, UK.

7.2 Samples Preparation

Three main types of sample were used in this investigation:

a) Rope samples (with cover) for assessing static tensile strength, residual strength, rope on rope abrasion, weathering resistance, acoustic emission and thermal analysis.
b) Rope core samples (without cover) for assessing static tensile and acoustic emission.
c) Strand samples (without cover) with different number of strands in each sample for assessing strand- rope efficiency and acoustic emission.

Sample preparation is an important aspect of any research programme. The quality of the samples must be usually high if confidence is to be placed in the results of the measurements.

Before preparing the test samples, the rope materials were visually checked for any signs of defects. Only the ropes that showed high quality in terms of surface consistency were accepted for testing. Every sample was cut to the length of 1400 mm. In order to further maintain the consistency, all the ropes were cut under the same pre-load of 5 kg. It was necessary to apply a pre-load to prevent the ropes from shrinking after the cutting process[91]. They were also cut using the same equipment and under the

same applied load. In order to conduct the three types of tests needed on the ropes, it was necessary to prepare the samples further.

7.2.1 Preparation of Dyneema and Vectran samples

With one end firmly secured, the other end was loaded to 5 kg. Whilst maintaining this load the ropes were cut using a very hot knife, see Figure 7.1. This operation also sealed the ends of the rope. This technique could be on both Dyneema and Vectran because they are thermoplastic and have a sufficiently low melting point to be cut using the hot knife. The same hot knife was used for both materials and it was allowed to heat up for 30 minutes before the cutting process was started.

7.2.2 Preparation of Technora samples

Technora ropes were also pretensioned to 5 kg and prepared in the same way as the Dyneema and Vectran ropes but were cut using a very sharp knife, see Figure 7.2. The knife blades were changed for each set so that all the lines were cut using similarly sharp knife.

7.2.3 Preparation of Samples for Static Tensile, Residual Strength and Abrasion Tests

a) Covered Samples:

These samples were cut using the technique mentioned in the previous section. These ropes all had a polyester cover and were tensile tested to failure to determine their breaking load. This load was given in Newton and it was this, which was used for the basis of the residual strength calculations.

b) Uncovered Samples (Core Only):

Once the samples were cut, the polyester cover was then carefully removed so that the rope structure was not disturbed. These ropes were then loaded to failure to determine

the their maximum breaking load. It was these values that were used for comparison of strand strength and efficiencies. All the samples had their cover removed 24 hours prior to testing in order to allow the ropes to reach equilibrium as well as preventing undue damage to the ropes from being left uncovered for long time.

c) Polyester Cover only

To assess the contribution of the cover to the total performance of the rope, the braided polyester cover, which was removed from the rope, as outlined in the previous section, was prepared in the same way ready for testing.

7.2.4 Preparation of Samples for Strand- Rope Efficiency Test

Once the ropes were cut and the cover removed, single strands were taken out of the rope taking care not to damage the rope structure. The strands were removed from opposite sides so the rope would stay torque balanced[68]. This was achieved by using a template as shown in Figure 7.3. This procedure was followed until all the strands were removed; therefore it was possible to achieve rope samples with varying number of strands ranging from 1 to 8 strands. The different samples are listed in Table 7.2.

7.3 Pre-test Environmental Conditioning

The performance of rope samples can be affected by the storage or testing environment, parameters such as moisture, temperature or UV radiation can influence the properties. It is therefore of great importance to equilibrate the moisture content of the test specimens to a known moisture, temperature and UV level prior to testing so that comparison of results can be justified. In this study four different conditioning have been used, see Table 7.3.

7.3.1 Room Temperature Conditioning

The samples were all kept in the same environment free from contaminants and away from degrading conditions such as UV and weathering. Each sample was left in the controlled laboratory environment next to the test equipment for at least 24 hours (at 22°C & 60% RH) in order to allow the rope to reach the equilibrium temperature. These results are the ones from the static test results section.

7.3.2 Natural Weathering

The weathering was done on an in-house made weathering rig, which was erected on the roof of the University where no shadow fell on it. The conditions were monitored daily and then double-checked by the reports for the area from the Met Office. The conditions and the duration times are listed in Table 7.3.

7.3.3 Hot water immersion conditioning

An electric oven was used to heat and maintain the water and the ropes samples immersed at 54°C. The duration times are listed in Table 7.3

7.3.4 Dry Heat

The same electric oven was used to heat and maintain the rope samples at 54°C. The duration periods are listed in Table 7.3.

7.3.5 Sub-zero conditioning

Low temperature was achieved by using a Zanussi deep freezer to achieve -22°C and the exposure duration are listed in Table 7.3

7.3.6 Synthetic Sea Water

Rope samples were immersed in synthetic seawater, which was made according to BS 23900 part F4 Clause 6.1. The immersion duration is listed in Table 7.3.

7.4 Mechanical Testing

Since there are no standards for mechanical testing of high performance synthetic fibre ropes. It was decided to modify and follow the testing regime based on testing of intermediate ropes suggested by British Standards Institute (i.e. BS4928). The cross head speed was set at 100 mm/min in accordance with the procedure suggested by DSM High Performance Fibres, manufacturer of Dyneema fibres. In order to be able to directly compare the results of the different materials used in this research the cross head speed was kept constant for all the samples. However, in order to eliminate the possibility of cross head speed effect several Dyneema and Vectran samples were tested at varying speeds.

All the mechanical tests were carried out using the Testometric Micro 350 testing machine. Figure 7.4 and Table 7.4 show the testing equipment set up, which consists of a tensile test machine, test rig and acoustic emission analyser. The tensile testing machine used was a screw driven upstroke machine. The load cell was chosen to be 2500 N and this setting was used throughout all the mechanical tests so eliminating the possible errors due to the range and sensitivity of different load cells.

As there are no set standards for rope testing rigs of such small diameter ropes, A special test rig was designed and manufactured to test the samples in tension. This consisted of two capstan and bollard grips (41 mm nominal diameter made of EN58J stainless steel) to reduce the stress concentration in the rope around the grip areas, see Figure 7.5 .

The use of this rig allowed the sample to go round each bollard a total of four times giving a gauge length of 200 mm between each bollard, see Figures 7.6 & 7.7. It was found, through trial and error that any sample length less than 200 mm or less than four turns round the bollards would result in failure of rope outside the valid region of the gauge length.

Due to the explosive nature of samples, it was necessary to stay well clear of the test equipment during the experiment. As some fragments of fibre could be released even though these fibres are considered non-toxic, paper face masks were worn as well as safety goggles. The samples, which were going to be tested were kept in the laboratory in order that the they would all, reach the same temperature at the time of testing.

7.4.1 Static Tensile Testing

Strength or tenacity gives a measure of resistance to steady forces. It will thus be the correct quantity to consider when a specimen is subject to a steady pull, as for example, in a rope used for hoisting heavy weights. The breaking elongation gives a measure of the resistance of the material to elongation. It is thus important when a specimen is subjected to stretching. All samples were tensile tested immediately after the environmental conditioning. Acoustic emission activity was monitored on most tensile samples. Extension was measured from the machine cross head movement. The rope sample was wrapped a total of four times around the top and bottoms bollards and then clamped at each end to prevent slippage. The cross head speed was kept constant at 100 mm/min throughout the test. In most physical and engineering applications, load is replaced by *stress*. The SI unit of stress is Newton per square metre (N/m^2), which is also called a Pascal (Pa). Since the area of the cross-section is not well defined, a relationship between the mass and the load is used in the textile technology and it is called the ***Specific stress***. It is defined as:

$$\textit{Specific Stress} = \frac{\textit{Load}}{\textit{Mass Per Unit Length}} \qquad \textbf{Eq: } 7.1$$

The consistent unit for specific stress is N m/kg (or Pa m^3/kg). However, in order to fit in with Tex system for linear density, it is better to use Newton per tex (N/tex), which is 10^6 times larger than N m/kg. For comparing different materials, the value of the specific stress at break is used and is called ***tenacity*** or ***specific strength.*** Tables 7.5 and 7.6 show the various component masses used in the calculations of the specific stress.

7.4.2 Work of Rupture

The work of rupture, which is also sometimes called the toughness, is the energy needed to break the material and gives a measure of the ability of the material to withstand sudden shocks of given energy. The units are joules and it is the area under the load extension plot. If the rope obeyed Hooke's law, the load-elongation curve would be a straight line, and the work of rupture would be given by:

$$Work\ of\ Rupture = \frac{Breaking\ Load \times Breaking\ Elongation}{2} \qquad \textbf{Eq:}\ 7.2$$

The work of rupture is proportional to mass per unit length due to the effect of the load and its length. Thus to compare different materials, ***Specific Work of Rupture*** is used which is defined as:

$$Specific\ Work\ of\ Rupture = \frac{Work\ of\ Rupture}{(Mass\ per\ Unit\ Length) \times Initial\ Length} \qquad \textbf{Eq:}\ 7.3$$

The units of the specific work of rupture are N m/kg or N/tex.

7.4.3 Work factor

It is convenient to define a quantity, the ***Work factor***, dependent on the difference from this ideal state:

$$Work\ Factor = \frac{Work\ of\ Rupture}{Breaking\ \ Load \times Breaking\ \ Elongation} \qquad \textbf{Eq:}\ 7.4$$

In the ideal state, the work factor will be 0.5. If the load-elongation curve lies mainly above the straight line, the work factor will be greater than 0.5: if below, it will be less than 0.5. This is illustrated in Figure 7.8. For materials breaking at the same point, the work of rupture will be greater the higher the work factor.

7.4.4 Residual Strength Testing of Pre-loaded Samples

This testing regime was chosen to satisfy one of the objectives i.e. to find out the relationship between the rate of damage accumulation in a rope and if it is directly related to the design criteria and the loading regime. Since all the ropes are the same design the material is the only variable. In order to determine the residual strength build up as well as the possible start of the irreversible damage, all the ropes were pre-loaded to a series of predetermined values. These loads were then removed, see Table 7.7. The ropes were then taken to failure. By using this technique it was hoped that it could be determined if the pre-loading had any detrimental effect on the performance of the ropes. As it will be explained later some ropes were taken to 500 N, 600 N and 650 N and held under that load for 15 minutes to investigate the effect of relaxation. The loads were then released and the ropes were allowed to relax for 15 minutes before loading to failure. The following formulae were used to calculate the residual strength for pre-loaded samples:

$$Strength\ \ Loss\ (\%) = \left[\left(F_{PL} \times \frac{100}{F_{AR}} \right) - 100 \right] \qquad \textbf{Eq:}\ 7.5$$

$$Extension\ \ \ Loss\ (\%) = \left[\left(E_{PL} \times \frac{100}{E_{AR}} \right) - 100 \right] \qquad \textbf{Eq:}\ 7.6$$

$$Rope\ Efficiency\ (\%) = \left(\frac{F_{PL}}{F_{AR}} \right) \times 100 \qquad \textbf{Eq:}\ 7.7$$

Where F_{AR} = Breaking load of as received sample

F_{PL} = Breaking load of pre-loaded sample

E_{AR} = Maximum extension to failure of as received sample

E_{PL}= Maximum extension to failure of pre-loaded sample

7.4.5 Residual Strength Testing of Cyclically Loaded Samples

Dyneema was the only sample, which was cyclically tested. This was because the cyclic process would create heat, which exaggerates creep. This is a more significant event in Dyneema than in the Technora and Vectran ropes due to its lower operating temperature range. In this study only covered Dyneema samples were subjected to different cyclic loading for further analysis, see Table 7.8. These tests were carried out in order to investigate the effect of cyclic loading at a constant cross head speed of 100 mm/min.

7.4.6 Strand - Rope Efficiency Testing

The following formulae were used to determine the efficiency of the rope with different number of strands, assuming the strand efficiency for one strand is 100%.

$$Strength\ \ Loss\ (\%) = \left[\left(F_{str} \times \frac{100}{F_{core}} \right) - 100 \right] \qquad \textbf{Eq:}\ 7.8$$

$$Extension\ \ Loss\ (\%) = \left[\left(E_{str} \times \frac{100}{E_{core}} \right) - 100 \right] \qquad \textbf{Eq:}\ 7.9$$

$$Rope\ Efficiency\ \ (\%) = \left(\frac{F_{str}}{F_{core}} \right) \times 100 \qquad \textbf{Eq:}\ 7.10$$

$$Strand\ \ \ Efficiency\ \ \ (\%) = \left[\frac{\left(\frac{F_{str}}{N} \right)}{F_1} \right] \times 100 \qquad \textbf{Eq:}\ 7.11$$

Where F_{core} = Breaking load of core sample

F_{str} = Breaking load of multi-strand sample

F_1 = Breaking load of one-strand sample

E_{core} = Maximum extension to failure of core sample

E_{str} = Maximum extension to failure of multi-strand sample

N = Number of strands in the multi-strand rope

7.4.7 Rope on Rope Abrasion Testing

Abrasion is one of the major elements of rope failure. Thus its understanding is important in order to evaluate a rope performance as it is loaded. During the loading process the rope sub-elements rub against each other leading to abrasion of fibres and compression failure. Rope on rope abrasion test was carried out on Dyneema and Technora ropes only. Dyneema and Technora ropes were abrasion tested using a specifically designed abrasion testing rig based on the Goksoy[157-159] apparatus. The set-up consisted of a reciprocating motor and four pulleys, see Figure 8.44. The arrangement is such that to allow the ropes to be abraded against themselves and count the cycles taken to failure. The ropes were tested under a preload of 2 kg to 4 kg, see Table 7.9. The rope lengths tested were 1400 mm and they were twisted upon themselves twice in order to encourage surface on surface abrasion. The pulley diameter used in all the cases was 21.6 mm. The stroke of the motor was 15 mm and the speed was 42 cycles/min. The starting abrasion area was 10 mm long but as the abrasion process continued the abrasion area increased and the rate of increase accelerated with increasing number as the final cycles to failure approached. The covered ropes had a greater abrasion resistance since the polyester cover had to be abraded first before the fibres could be exposed.

7.5 Acoustic Emission Analysis

Several NDT techniques are available for use in conjunction with both wire and synthetic ropes. However, the most readily available is acoustic emission. The principle has already been successfully applied to composite materials and wire ropes. But very limited work has been conducted on synthetic fibre ropes and virtually none on the small diameter high performance synthetic fibre ropes. Hence the choice was clear. The second major reason was the simplicity of the use. The only equipment needed were the acoustic emission analyser, PC, sensor and silicon grease. The most difficult parts of the process have been the placement of the sensor and the post processing and analysis of the results. In this section a detailed description of the technique used for AE testing of samples is given, and the basic principles of operation of AE analysers are discussed.

Acoustic emission was used in this project in order to:

- Investigate the micromechanical events that occur during the loading process
- Detect the damage mechanisms such as:

  Fibre failure

  Abrasion damage
- Predict the maximum breaking load
- Compare the new and damaged ropes
- Detect plastic deformation

Acoustic emission analysis was performed during the following mechanical tests.

- Static tensile of covered and uncovered roped.
- Rope-strand efficiency.
- Residual strength of pre-loaded sampled.

The data gathered by the transducer were qualitative rather than qualitative. Since the whole system was not calibrated to a specific standard. Therefore the results should not be used quantitatively which means that if another transducer with different frequency spectrum was used the values could not be compared but would yield a comparable plot profile.

7.5.1 Acoustic Emission Analyser Used

The acoustic emission equipment used was a MR1004 AE analyser, which consisted of a single channel system with event counting and ring-down analysis capability Tables 7.10a-e describes the system specifications and Figures 7.9a &b Show the equipment set-up. The system was interfaced to an IBM compatible Pentium P90 computer with 16 MB RAM and 1GB hard disk. In this way the data was collected sequentially and in

a chronological order, in real time and stored on the hard disk from which it could be retrieved for post test analysis.

In this work attention has been paid to the analysis of ring down counting (RDC) rather than other AE parameters. An AE event in this unit, defined in terms of the instrument threshold, had a fixed *"dead time"* of 100 microseconds. If the *"dead time"* elapsed since the last threshold crossing, the next threshold crossing was taken as the beginning of a new event.

The threshold voltage was adjustable from 10 mV to 69.18 mV, which corresponded with levels 0 to 7. The AE event amplitude was defined as the maximum AE signal level relative to 10 mV. The amplitude detector unit of the MR1004 sorted the AE events into 25 levels, each 2.4 dB wide. Level zero corresponded with the amplitude above 10 mV and below 13.18 mV. Events with amplitude larger than 10 volts were registered in level 25 (over-range). For ring-down counting, the amplitude of the signal was compared with the threshold voltage, and the number of times the signal amplitude exceeded the threshold level gave the total ring-down count for each event. Throughout the whole period of this project the same AE analyser and transducer were used.

The data gathered by the transducer were qualitative rather than qualitative. The value could not be used to do any calculations but were there for observation. Therefore if another sensor were to be used the values could not be compared but the shape of the plotted values would be able to be compared.

7.5.2 The AE Transducer

In order to find the most suitable position for the AE transducer, several experiments were conducted. The most commonest technique has been to attach the transducer directly to the sample. However, the most obvious problem was the physical size of the

rope samples. The first approach was to attach the transducer directly to rope by using one of the following:

- Masking tape
- Paper clips
- Bulldog clips

In none of the techniques used the transducer, did the transducer stay in contact with the rope sample at all times during the loading cycle. And in all the cases the rope always failed at a lower breaking load and under the transducer.

Thus the technique had to be revised. The next step was to drill a hole in a hollow plastic tube large enough to house the transducer. The tube was then filled with RS494-124 silicon grease and the rope sample was pushed through it. The major difficult was to make sure that the traducer stayed in contact with the rope and the tube did not slip down the length of the rope. None could be achieved successfully eventhough clips and tapes again were used and in all the cases the rope samples again failed prematurely.

The final choice was to attach the sensor onto the test rig, see Figure 7.10. By keeping the transducer at the same place throughout the whole research it was possible to maintain consistency and accuracy.

The acoustic coupling of the transducer to the surface of the test rig was achieved with a thin layer of silicon grease. Couplant is very important; nearly 100% of the energy incident normal on a metal/ air interface is reflected. A Couplant with the appropriate acoustic impedance will greatly improve the energy transfer from material to transducer.

In this study the same PZT5 (MRTB-500) piezoelectric transducer and silicone grease, i.e. RS454-124 silicone grease, were used through making the comparison of all the results possible.

7.5.3 AE System Check

The performance of the AE System was checked using the pencil lead break technique. In this process a 2H, 0.5 mm pencil lead was broken on the surface of the transducer and the subsequent signal amplitude recorded was adjusted accordingly. The analyser setting was kept to 1. This proved to be the most suitable value since the system did not respond to any higher setting values, the i.e. signal readings were too low and the it was not registering any noticeable readouts. On the other hand the use of zero setting would result in machine noise being recorded. Thus throughout the tests this value was kept at one. Also it has been found that the results were fully reproducible using this set-up procedure.

7.5.4 Processing of Data

The AE data used to analyse the behaviour of the ropes were obtained using two techniques:

- Real Time Data collection
- Post Processing

a) Real Time Data collection

The data was logged, real time, using the Testometric machine software, Universal Materials Testing (UMT), via the RS232 port, Figure 7.9b. The load was recorded directly from the 2.5 kN load cell. The data were logged into the computer in the data and text format. The UMT used the data files to plot its own load extension plots and

make the calculations based on the data inputted into the system at the beginning of the test. The text files were used in the post processing.

The stress waves generated due to the loading process were picked up by the MRTB-500 piezoelectric transducer and fed into the MR1004 Acoustic Emission analyser via the MRP-01 Preamplifier through the RS232C port. They were then displayed as histograms of events occurring as the loading continued.

b) Post-Processing:

In order to make use of the UMT and MR1004 results some post processing had to be done, see Figure 7.11. The first step was to import the text files into Microsoft Excel 7.0 and convert them into XLS format. They were then exported to the Easyplot software and load extension results were then plotted. The acoustic emission data had to be converted into a recognisable format for the Microsoft Excel. Thus they were converted into Comma Separated Values (CSV) format using the MR1004 software and then imported into Excel to change them into XLS format. They were then exported to Easyplot to plot RDC- time curves.

7.6 Measurement of Rope Temperature

To assess the rate of heat build up in Dyneema ropes, the surface temperature was measured using the infrared camera, CYCLOPS T135, manufactured by Land Thermal Imaging Systems, UK. In this process the whole length of the rope sample was scanned and a series of thermograph images were obtained, at a rate of 10 images per second, while the sample was being loaded in tension. The system had a temperature scanning range of -20 to 1500°C, with a sensitivity of 0.1°C

7.7 Microscopy of Rope Samples

Samples of rope, both untested and selected tested samples, were subject to further investigation using a scanning electronic microscope (SEM) in order to determine the start of the irreversible damage. The SEM used was a Hitachi S-450. Double-sided adhesive carbon pads were used to mount the samples on the steel spools, prior to locating the samples in the SEM, taking care to protect the already damaged fibres. Due to the non-conducting nature of the rope samples it was necessary to gold plate the samples and the carbon pad in order to achieve conductive surface. This was performed by the use of an Agar Auto Sputter Coater. Permanent records were achieved using black and white photographs.

7.8 Quality Control of the Experiments

In every case utmost attention was given to the quality of the experimental procedures. This included every process from sample preparation to final result analysis. Care was taken when preparing the samples that no contamination of the samples occurred. The consistency was further maintained by keeping the test conditions such as cross head speed and the gauge lengths constant. Any sample, which was not cut properly or was too short, was not included in the testing. All the samples for particular tests were cut 24 hours prior to testing to allow them to reach an equilibrium state.

The results were fully reproducible and were demonstrated by the work of two researchers within the Department who carried out limited experiments on some of the ropes[221,222]. In order to achieve consistent results, the cross head speed was kept to 100 mm/min throughout the experimental section. All the samples came from the same batch eliminating the production variability. All the samples were conditioned to the same environment, i.e. were placed next to the test equipment 24 hours prior to testing. Protective clothing namely goggles, paper face masks and lab coats were worn. All the samples were prepared under the same 5kg load. The cutting equipment were checked prior and throughout the cutting process. The hot knife was allowed to heat up for 30

minutes before being used and the knife blades were replaced after each set of sample preparation in order to achieve the same clean cut for all the samples.

8.0 RESULTS AND DISCUSSION

This chapter presents and discusses the results of the experimental work and investigates the mechanisms of damage and failure in high performance synthetic fibre ropes under different loading conditions. It will consider the more important factors to arise from experimental results and will also provide a link between the various tests carried out. The way in which variation in rope material and construction affected the mechanical properties of the ropes was investigated by determination of static tensile strength, and residual strength after a series of preloading applications. To assess the different failure mechanisms in high performance small diameter ropes, samples from different types of modern paraglider ropes were used. Table 7.1 lists different variations of ropes used in this study. Total of 1,956 samples, equivalent to approximately 4,200 metres of different ropes were used in all the tests. To gain a high confidence in the results, minimum of 20 samples were used in each case. The different experimental tests carried out in this study are as follows:

- Static tensile test- on all rope samples
- Static tensile test after harsh weathering conditions - on Dyneema rope samples
- Residual strength test after different preloading conditions - on all rope samples
- Residual strength test after cyclic loading conditions - on Dyneema ropes
- Rope-strand efficiency measurement
- Determination of the effect of loading rate on the mechanical properties of ropes
- Acoustic emission monitoring of ropes during static tensile tests
- Acoustic emission monitoring of preloaded ropes during residual strength tests
- Acoustic emission monitoring of ropes after different number of strands subjected to tensile loading removal measurements
- The effect of clamp pressure on rope damage
- Scanning electron microscopy of the damaged and undamaged ropes
- Thermograph measurement of the heat released by Dyneema ropes during static tensile testing
- Rope on rope abrasion tests - on Dyneema and Technora ropes

For brevity reasons the above results are classified according to the type of tests carried out, therefore where deemed appropriate, only the average results for sets of samples are given in this section.

8.1 Parameters Affecting the Quality and Reliability of Results

The mechanical behaviour of a material depends on the nature of the molecules and the condition of the material. The condition of the material depends on its previous history, including the processes to which it has been subjected to and the environment it has endured including the amount of moisture and the temperature[223].

Thus in every case, utmost care was taken to present the most accurate results that closely reflect the true nature of the rope behaviour. In this respect, the following procedure was followed to ensure the validity and accuracy of the results.

- The quality of as-received ropes was monitored prior to sample preparation to ensure that the ropes are free from processing defects and material inconsistency. Occasionally defects in the rope construction were observed by visual inspection in which case the defects were localised, the rope section was cut and discarded. Every rope material used was taken from the same batch to reduce the processing variability.
- During sample preparation, all the different ropes were cut and prepared under the same procedure as detailed in the Experimental Section. In the early stages of this study, it was noted that many parameters such as the temperature of the cutting knife or the load applied on the rope could affect the quality of samples. Only after spending a considerable amount of time and effort, it was possible to master the sample preparation technique.
- Prior to testing all the samples all were stored under the same pre-test conditioning to minimise the effect of environment such as temperature and humidity on the strength.

- During mechanical testing all the samples were tested using the same testing procedures. However, as there is no unified standard for testing small diameter ropes, attempts were made to standardise the testing method. In this respect, the effect of all the parameters including gauge length, total length of the rope, clamping pressure, test rig position and the loading rate were carefully studied before an optimum test procedure was adopted. Occasionally, rope samples failed outside the gauge length. In these circumstances the samples were critically analysed to investigate the causes. In most cases the excessive clamping pressure caused this type of failure mode. All the samples that failed outside the gauge length (about 3% of all the samples tested) were not included in the final results.

- The dimensions of the specimen will, of course, have a direct effect on the results; for example the breaking load depends on its area of cross-section, and the elongation depends on the gauge length. The gauge length can also affect the strength since there is greater chance of the occurrence of a very weak place in a long length, and since a fibre breaks at its weakest place, the mean breaking load of long lengths will be less than that of short ones[224]. Therefore the same gauge length was chosen such that the total length of the rope samples from clamp to clamp was set to 1400 mm. This length was sufficient to allow the rope samples to be taken round the bollards a total of four times and have enough separation distance between the bollards. It has been observed that a decrease in the number of turns would result in a great deal of slippage round the bollards. Also if the separation distance between the bollards was decreased then the rope would usually fail at the bollards or very close to them. However, any longer rope length would not significantly affect the performance or the behaviour of the rope under tensile loading except using more material. Thus the standard throughout the project was set to a length of 1400 mm including the four turns round the bollards.

- All the results were carefully analysed before post processing by the computer. Any sample, which led to a suspect result, was discounted in the final analysis.

8.1.1 The Effect of Loading Rate on the Mechanical Properties

The mechanical performance of a textile fibre is not only dependent on the applied load, but it also depends on the length of time for which the load, and any previous loads, have been applied. If a constant load is applied to a fibre, it will alter its instantaneous extension , continue to extend for a considerable time and, if the load is great enough, it will eventually break. The load necessary to cause breakage will vary with the speed of the test, a rapid test requiring a greater breaking load than a slow one. Thus the results of experiments will be affected by the time allowed and by the way in which the load is applied, whether it is by constant rate of loading, constant rate of elongation, reduction form a higher load, or any sequence of events[224]. As there are no standards for the testing of high performance ropes, in the early trial stages of the present study, it was decided to investigate the effect, if any, of the loading rate on the mechanical performance of the ropes. In this process Dyneema and Vectran ropes were tensile tested under different loading rates.

The British Standards (BS 4928) suggests 250 mm/min as an appropriate cross head speed (C.H.S) for intermediate performance fibres. However DSM High Performance Fibres[13], a well known manufacturer of high performance ropes, have tested Dyneema ropes at 100 mm/min. However, in order to investigate the effect of varying the C.H.S on the viscoelastic behaviour of the Dyneema fibres, a series of tests were conducted with increasing C.H.S in the range of 100 mm/min to 800 mm/min. Figure 8.1 shows the differences in load extension plots for Dyneema rope subjected to different C.H.S.

It can be seen that increasing the C.H.S does not drastically affect the performance of the rope in terms of breaking strength, extension or loading profile. Neither does it affect the appearance, size and the position of the knee point. Knee point features will be discussed in details later in this chapter. In order to examine the performance at the other extreme, Dyneema rope samples were also tested at 1 mm/min and 10 mm/min. Figures 8.2 and 8.3 show the load-extension plots for C.H.S of 1 mm/min and 10 mm/min respectively.

It is evident from Figure 8.2 that existence of the knee point disappears when the C.H.S is 1 mm/min. However, this slow loading speed has increased the interfibre/strand movement and the relative movement of the core and the cover as the load increases. This can be detected as ripples on the load extension plots. These ripples are due to the sufficient time and space for the rope components to move and relax, therefore the rate of heat build up is not high enough to cause stiffness increase and hence preventing the rope from becoming a more efficient load bearing system. However, with a C.H.S of 10 mm/min, see Figure 8.3, the pattern is a mix of standard 100 mm/min and 1 mm/min. The overall pattern is the standard profile but it also has the ripples, which corresponds to the slippage of the interfibre/strand and their relative movement against the cover. The overall profile also shows the knee point and the standard 3 zone behaviour (the 3 zone behaviour will be discussed in details later). The ripple pattern seems to end as the knee point ends and the AE profiles show clear step rise. There are small steps in the AE plot corresponding to the knee point which is caused by stress waves generated as the fibres started to realign themselves but since the speed was slow they had time to elongate more while the cover was trying to grip the core. There was a sudden rise after 400 N corresponding to the changing of the zones.

Covered Vectran samples were also tensile tested using different C.H.S ranging from 100 mm/min to 1000 mm/min, the load-extension plots are shown in Figure 8.4. It can be seen that there is very little variation in performance as the C.H.S is altered, indicating that the testing could be conducted at higher speeds but in order to maintain consistency the C.H.S was kept at 100 mm/min throughout the study. The procedure of altering the C.H.S was not applied to Technora ropes as it was thought that they were not as susceptible to temperature variation as the thermoplastic ropes namely Dyneema and Vectran.

8.1.2 Effect of Clamping Pressure on the Mechanical Properties

To achieve realistic data on the performance of any rope sample under tensile loading, it is essential to secure the rope firmly in the testing clamps. But excessive pressure on the rope will cause higher stress concentration on the rope in the clamp area during

tensile loading. This will lead to premature failure of the rope in the clamp. On the other hand if the clamp applies insufficient pressure, the rope will slip away from the testing rig, due to the low coefficient of friction between the rope fibres.

Therefore at an early stage of this investigation it was decided to optimise the clamping pressure, in order to achieve realistic mechanical properties of the different ropes under tensile loading. In this process acoustic emission was monitored while constantly increasing the clamp pressure on the rope, until the rope was fractured under the clamp. The variation in AE against time for a constant rate of increase in clamp pressure is shown in Figure 8.5. It can be seen that any increase in the number of ring-down counts (RDC) is related to the damage caused by an increase in the clamp pressure for Dyneema rope. In another related experiment Dyneema rope was subjected to different clamp pressures while it was under tension. Figure 8.6 shows the load-extension and AE_extension plots for a lightly clamped sample. In this case the monitored acoustic emission as well as the load extension plot clearly show the abnormal behaviour of the rope, a full explanation of the normal load-extension and AE behaviour of the rope will be given later. It must be borne in mind that eventhough the slippage is a problem, the maximum breaking load does not drastically change provided the slippage does not lead to complete movement out of the clamps. The major problem is the extension measurement.

8.2 Tensile Strength Results

All the rope samples, including covered and core only ropes, were tested under tensile loading allowing comparison of different materials and constructions to be made. For this purpose the ultimate breaking load and the ultimate extension to failure were taken to be the most important criteria for performance comparison. In order to have a high confidence in the results minimum of 20 samples were tested of each individual rope configuration. The ultimate breaking load and extension to failure values including the mean and standard deviation values are listed in Tables 8.1 to 8.4 and are graphically presented in Figures 8.7a, 8.8a and 8.9.

8.2.1 Ultimate Load and Extension

It can be seen from the results that 1.6 mm diameter covered Vectran rope carries the highest load of 1624 N before it fails. Also the polyester cover does not seem to influence the load bearing capability of the rope. It is also evident from the results that the worst performing rope in terms of maximum load before break is 1.1 mm diameter 8 strand Technora with a value of 737.18N core only and 820.40 N with cover, which indicates that the cover takes 10.14% of the total load.

A mediocre performance is shown by the other two ropes namely 8 strand 1.1 mm Dyneema and 4 strand 1.1 mm Technora. Dyneema rope has a maximum load of 795.92 N core only (922.7 N core with cover) and 4 strand Technora rope has maximum load value of 814.19 N, core only (1044.8 N core with cover). In these cases the polyester cover contributed to 22.07% of the Technora rope and 13.74% of the Dyneema rope performance. In terms of the amount of extension to failure Dyneema stretches the most with a value of 44.11 mm core only (47.88 mm covered) and 8 strand Technora stretches the least with an extension of 27.03 mm core only (33.94 mm covered). Other two ropes, namely 8 strand Vectran and 4 strand Technora have a medium extension to failure of 38.71 mm core only (42.00 mm covered) and 28.39 mm core only (39.93 mm covered) respectively. The number of fibres in a rope increases with the square of the diameter therefore a large rope can potentially carry much higher loads but due to the non uniformity of load carried by the fibres with the respect to the rope axis, there is a drop in strength.

A common technique of comparison of different samples is to use the properties, Tenacity, Work of Rupture (WR), Specific Work of Rupture (SWR) and Work Factor (WF), see Tables 8.5 to 8.8[225].

8.2.2 Tenacity

The tenacity of various ropes tested was determined using the Equation 7.1 and the results are presented in Tables 8.5 to 8.8 and shown graphically in Figure 8.10. It can

be seen that uncovered ropes have higher tenacity with lower extension to failure. The tenacity values for both covered and uncovered ropes fall within distinct ranges, i.e. lower than 1.0×10^{13} N/tex for covered ropes and higher than 1.7×10^{13} N/tex for uncovered ropes. 8 strand covered Technora has the lowest tenacity and extension to break compared to other covered samples. 4 strand covered Technora has the highest tenacity of all the covered samples but not the highest extension. Since both 4 strand and 8 strand Technora have the same diameter they have the same tenacity but their breaking load values are different. 4 strand covered Technora has a tenacity of 9.81×10^{12} N/tex and 8 strand covered Technora 8.04×10^{12} N/tex. Both covered Dyneema and Vectran have tenacity values of 8.93×10^{12} N/tex and 9.33×10^{12} N/tex respectively. This is possibly due to the higher breaking load and mass per unit length.

8 strand uncovered Technora has the highest tenacity with 1.99×10^{13} N/tex and the lowest extension to failure. 4 strand uncovered Technora has the lowest tenacity with 1.83×10^{13} N/tex. This can possibly be due to the ratio of the higher breaking load and mass per unit length. This time the tenacity of uncovered Dyneema is greater than uncovered Vectran which can be due to a lower mass per unit length and a lower breaking load.

8.2.3 Work of Rupture

Work of rupture is the energy needed to fracture the rope samples. It is the area under the load extension plots and was calculated using the Simpson's rule. The results are presented in Tables 8.5 to 8.8 and shown graphically in Figures 8.11a & b.

As expected covered rope samples has higher work of rupture values than uncovered ropes. This is simply due to higher breaking load and extension values of covered ropes. Covered Vectran has the highest work of rupture with 25.10 J followed by covered Dyneema with 22.38 J. This is due to higher breaking load of covered Vectran. There is a significant drop in the work of rupture after the removal of the cover as its removal significantly decreases the breaking load and extension. In all the cases

uncovered 8 strand Technora has the lowest work of rupture, which is due to its lowest breaking load and extension values.

8.2.4 Specific Work of Rupture

In order to compare the work of rupture and take into account the size of the ropes tested, specific work of rupture was calculated using Equation 7.3 The results are presented in Table 8.5 to 8.8 and shown graphically in Figures 8.12a & b. The uncovered rope samples have higher specific work of rupture values than covered ropes. Covered and uncovered Dyneema has the highest specific work of rupture and covered and uncovered 8 strand Technora the lowest. These agree well with the previous section. The initial length in all cases was kept constant at 1400 mm thus the only variables in the calculations was the mass per unit length and the work of rupture. This technique shows that the material property is an important factor in the way a rope performs.

Uncovered Dyneema has the highest specific work of rupture with 2.78×10^{11} N/tex and covered 8 strand Technora the lowest with 8.15×10^{11} N/tex. The underlying reason is thought to be the lower work of rupture. Uncovered 4 strand Technora has the second highest specific work of rupture with 1.71×10^{11} N/tex. This technique of comparison has eliminated the size effect. Thus the only variable left is the material. As Dyneema extends to failure more than the other ropes due to its lower melting point, thus its work of rupture is affected. It also has the lowest relative density of all the ropes tested. Hence its mass per unit length is also reduced. All these affect the ultimate specific work of rupture. The same principle is applicable to other ropes tested and thus that's why there is such a variation in specific work of rupture in the ropes and between the covered and uncovered ropes.

8.2.5 Work Factor

In order to establish how closely the rope samples follow a Hookean system, the work factor values were calculated using Equation 7.4, and the results are presented in Tables 8.5 to 8.8 and shown in Figures 8.13a & b. For a perfectly elastic system the work factor would be 0.5. However, as can be seen from the load extension plots that none of the samples actually display a 100% linear behaviour. The work factor values are very close which is possibly because all the ropes tested have shown a linear section at some point during their loading history. The work factor values for all the rope samples are less than 0.5 except for covered Dyneema which is greater than 0.5. Vectran has the lowest work factor value for both covered and uncovered cases. The fact that none of the rope samples displayed a work factor value of 0.5 also supports the analogy that the loading history goes through three zones.

The work factor property can be used in another way to investigate the efficiency of the rope. If a trope has a work factor of 0.5 then it indicates that it is acting very linearly and carrying the load very efficiently. Thus to investigate this phenomena further the percentage of the breaking load was plotted against extension. These plots are shown in Figures 8.14a & b.

8.3 Rope Behaviour under Tensile Loading

The response of fibre ropes to applied forces, energies, and deformations is their most important technical property. The rope as textile structure, reacts to an applied stress or strain with a combination of structural and material deformations. Its reactions thus depend on the structure of fibre material used.

Rope is a fairly complex arrangement of fibres in a multi-helical structure. The rope fibres are arranged in helical structures whose axes form again helixes in a larger structure. Often the larger structure is again arranged in a larger helical structure. These helical structures stretch fairly easily by becoming longer and thinner, as a spring does under tension. They snap back as the tension is removed. At the same time the

structural deformation causes stresses in the fibres to which they respond by stretching. The fibre stretch reaction depends entirely on the load-elongation properties of the fibres used.

In a rope composed of material having very low elongation, nearly all the stretch of the rope will be structural. In a rope constructed the same way of highly stretchable fibres, the material stretch would be an important percentage of the rope elongation. It can be up to 50% of the total elongation. Both construction and material deformation are to be considered in order to understand the rope reaction to applied tension. Both structure and material deformation follow their own particular laws and often interfere with each other. Rope structures usually tighten in use after several loading, but they open by action of the material used, for example swelling or shrinking processes after immersion in water or exposure to heat. The fibre material itself behaves in a viscoelastic manner and thus changes dimensions and load-elongation behaviour due to loading processes and environmental influences.

At the same time these changes interact with the arrangement of the fibres in the rope structure. Fibre ropes change their dimensions and load-elongation properties in use. Therefore, as received and conditioned ropes are discussed separately. Available test data from rope manufacturers usually deal with new ropes only; load-elongation curves mainly show the reaction of new ropes under standard test and environmental conditions. Small ropes show higher strength efficiency than large ropes, the number of fibres in a rope increases with the square of the diameter. They also exhibit greater inclination with respect to the rope axis and thus suffer a drop in strength efficiency.

The load-extension curves obtained from static tensile test results show three stages of the mechanical behaviour of the ropes, see Figures 8.15 to 8.18:

- Zone 1: Initial non-linear behaviour

This zone is defined by the non-linear rise in the load. The main reasons for the non-linear rise are thought to be:

1. The alignment of fibres into a uniform assembly. This agrees well with the literature that during the loading history there is structural realignment of the fibres especially at the start when the fibres have room to move[93-96].
2. The cover extends more than the core, due to the differential extension between the core and polyester cover, but it takes less loads. Hence the rise and fall in load which could be due to slippage. But the literature suggests that it is due to some surface fibres failing as a result of internal abrasion, fibre fatigue and hysteresis. This process of differential extension continues until the cover starts to grip. From this moment onward the core and the cover extend at the same rate, which is the start of the second zone. This also coincides with the onset of acoustic emission[93-96].

- Zone 2: A pronounced knee region, when the curve shows an inflexion. The rope cover and the rope construction are thought to affect the shape and behaviour of the rope. This is only observed in the covered Dyneema ropes, See Figure 8.15.

As the load rises, the cover continues to grip the core. The friction between the fibres leads to an increase in the heat generated. The heat and the radial pressure of the cover will cause the fibres either to fuse together or become very compacted, which is the start of Zone 3. This also corresponds with the second step rise in acoustic emission.

- Zone 3: A complete linear region which precedes to the catastrophic failure of the rope material

Transition from zone 2 to zone 3 is very important since it is the transition from a stage where rope can bear increasing loads, with growing damage, to a stage where the rope fails in a sudden and catastrophic manner. This zone is the linear part that extends from the end of Zone 2 (the curved section of the graph) to the point at which the rope fails. By the time that this stage starts every fibre in the load bearing section of the rope has compacted together, in other word the rope has begun to behave like a single uniform rope. This is reflected in the AE pattern as the final sharp rise in RDC, see Figure 8.15. As the failed end recoils the released stored energy is quickly converted into heat. But the cover prevents this heat from being lost to the environment. This heat causes the fibres to fuse together. It has been observed that parts of the rope away from the fracture there are clear indications of increase in stiffness.

During the tests, apart from the final catastrophic failure, the samples did not emit any audible sound, neither was there any visual sign of failure. However the final failure was always accompanied by a loud sound. The following sections discuss the results and behaviour of each rope material studied.

It can be seen that covered Dyneema displays linear load-extension behaviour at nearly 84% of its breaking load and covered Vectran at nearly 80.05% of its breaking load. The linear part of the 4 strand covered Technora starts at nearly 67.00% its breaking load and at 70.70% of its breaking load for 8 strand covered Technora. The linear part of the uncovered ropes starts earlier than covered ropes. In uncovered Dyneema the linear part starts at nearly 69.10% and in uncovered Vectran at nearly 58.53%. In 4 strand uncovered Technora it starts at nearly 64.85% and in 8 strand uncovered Technora nearly 63.49%.

The significance of these comparisons become clearer when the actual load values is used. The possible indications are that the earlier the linear part is reached the more efficient the rope becomes, the greater the interaction between the rope sub-elements. These comparisons show that the interaction between the rope elements and the cover possibly starts earlier in 8 strand covered Technora compared to other covered ropes,

which would indicate that 8 strand rope is a more efficient system. This could be the reason why Technora produces higher levels of AE than Dyneema and Vectran. The AE activity also is exponential rather than step rise as in the case of Dyneema and Vectran. The fact that the linear part starts earlier can also suggest that the damage also starts early. One of the reasons why the linear part for covered Dyneema and Vectran do not start as early can be due to the fact that covered Dyneema displays a knee point before the relative movement of the rope sub-elements can generate enough heat to fuse the fibres/strands together leading to the linear part. The covered Vectran does not display a pronounced knee point and it has a much higher melting point and breaking load which is why the linear part starts much later.

Uncovered 8 strand Technora again reaches the linear part faster than the rest followed by 4 strand uncovered Technora. This shows that the removal of the cover allows the rope to reach its linear part quicker making it more efficient. This possibly could indicate that the cover achieves its protective function at the expense of a sacrifice in rope efficiency.

It can also be seen that eventhough all uncovered ropes have similar initial rise, the uncovered Technora ropes have a steeper gradient followed by uncovered Dyneema and Vectran. In fact the overall profile for covered and uncovered Vectran seem to be the same. Both uncovered 4 and 8 strand Technora ropes have similar rates of rise but there is a greater difference when their cover is not removed. 8 strand covered Technora has a steeper rise and gradient than 4 strand covered Technora. This is possibly due to the higher number of interacting rope elements indicating that the increase in the number of strands and twist leads to a lower breaking strength but a more efficient system. The actual pattern for both 4 strand and 8 strand covered Technora is the same. There is a significant difference between the behaviour of covered and uncovered Dyneema. The main difference is the existence of the knee point in the covered Dyneema and the overall profile in the load-extension plots. The pattern for the covered Dyneema displays a positive rise compared to the other ropes tested. The existence of the knee point has been linked to the presence of the cover and material.

8.3.1 Behaviour of Dyneema Rope under Tensile Loading

The Dyneema rope samples, both as-received and core only, were static tensile tested to destruction at 100 mm/min. The results of these tests are presented in Table 8.1.

a) Tensile Deformation of Covered Dyneema Rope

The results of the tensile test on covered Dyneema rope (core & cover) including the mean values of breaking load and maximum extension to failure with standard deviation are listed in Table 8.1. The load-extension results are also presented graphically in Figures 8.9 and 8.15. The SEM micrographs showing the fracture surfaces of the covered Dyneema rope failed in tension are shown in the Plates 8.1a & b. The recoiling action of the fractured ends leads to a rapid release of stored energy. This leads to a severe friction and abrasion of the failed ends as they retract. As the process continues, shock waves travel through the rope and a great deal of heat is generated which results in the melting of the failed ends.

The important feature in the load-extension plots is the knee point and the final linear part before failure, as mentioned in the previous section. The size and position of this knee point is thought to be related to the material, cover, diameter and rope design. According to the manufacturer's published literature the function of the cover is only to protect the core and not to affect its load bearing capability. However, it can be seen from the results that the removal of the cover alters the behaviour of the rope somewhat but it still performs a valuable service by virtue of its protective nature[9-12]. The load-extension pattern for covered Dyneema is different at the onset to those of other ropes and the uncovered Dyneema. There is the initial rise, which is in the opposite direction of that of the other ropes tested including uncovered Dyneema. This is thought to be the effect of the cover. As the load is applied, and the interfibre/strand movement begins, the cover starts to grip the core and the knee point begins to form. However, the final part is similar to all the rope samples tested. It is a linear rise which also give rise to its having the only rope sample with a work factor value greater than 0.5.

b) Tensile Deformation of Dyneema Core Only

The results of the tensile test carried out on Dyneema core, after removal of the polyester cover, are presented in Table 8.1. From the results the following observation can be made:

- Removal of the cover leads to a significant reduction in the breaking strength, although the cover is not supposed to contribute to the load bearing performance of the rope.
- The pattern of load-extension curve is more linear and shows no sign of the knee point. This supports the suggestion that the polyester cover is the major contributor to the load-extension inflexion of zone 2. The rope cover used in this study consist of a hollow braided polyester structure which has a maximum extension of 3 to 4 times that of the core, under tensile loading and since it is a hollow structure there is no internal fibre interaction. Therefore the loading action would reduce the internal diameter and as a result the cover will start to grip the core.

- The uncovered rope reaches its linear part faster than the covered rope, which is possibly indicative that the removal of the cover makes the rope a more efficient system. This is possibly true as some extra events, which have to occur in the covered Dyneema rope prior to the formation of the knee point, lower its efficiency. However, this also indicates that the possible irreversible damage also starts sooner in the uncovered Dyneema. Thus making it less damage tolerant. There fore it can be said that the cover not only protects the rope from external damage, it also improves its damage tolerance by forcing the rope to behave in the way it does.

- The fracture surfaces of the failed rope, Plate 8.2a, shows an appearance of 'puffing'. This indicates that the heat generated during the loading process, due to friction, was quickly lost to the environment. Therefore after the fracture, the rope ends rapidly contract and recoil, since there is no arresting cover, the recoiling

strands just collapse on their own giving an appearance of puffing. This becomes more evident in the failure zone, as shown in Plate 8.2b.

8.3.2 Behaviour of Vectran Rope under Tensile Loading

The results of the tensile tests on Vectran rope are listed in Table 8.2 and graphically presented in Figures 8.9 and 8.16. This rope has the same construction as the Dyneema and Technora but with a diameter of 1.6 mm.

a) Tensile Deformation of Covered Vectran Rope

The results show that the covered Vectran rope has a breaking load and a maximum extension of 1624.00 N and 42.00 mm respectively see Table 8.2. There are signs of melting and fusion of fibres in the loaded ropes. The load-extension plot exhibits the three-zone behaviour with no knee point similar to Technora rope, as shown in Figure 8.16. The rate of increase in load is consistent and once the slack due to fibre/strand movement is taken out at approximately 400 to 500 N, the rope efficiently carried the load.

The second zone in load extension curve is relatively small. The start of the final third zone coincides with the instant when the fibres start to fuse together and therefore acting as a single system, with little relative movement between fibres. The failure theory, discussed before, also applies to this rope[93-96]. There are clear signs of melting of fibres near and at the failed ends. There is also clear evidence of fusion of fibres, as shown in Plates 8.3a & b, where the stiffness has increased[101], see also Plate 8.4.

The stiffness increase in rope and fusion of fibres are the result of inter-fibre/strand and rope-cover movement and friction leading to heat generation. The increase in load and extension also leads to a decrease in diameter of the cover, which ultimately exerts a radial compression on the core. The covered Vectran reaches its linear part at 80% of its breaking load, which is lower than the covered Dyneema. This possibly is indicative

that it is slightly more efficient rope. This increase in efficiency can be due to the absence of the knee point and the fact that Vectran has a higher coefficient of friction, which means that the interfibre/strand interaction takes place sooner and hence the rope becomes more efficient. However, this also indicates that the rope becomes less damage tolerant..

b) Tensile Deformation of Vectran Core

The results of the static tensile test on Vectran core are presented in Table 8.2. This uncovered rope has a maximum strength of 1537.7 N and an extension to break of 38.71 mm which shows a slight strength loss due to the absence of the cover. This small loss in strength indicates that the cover does not initially grip the core very tightly, and therefore does not contribute to the load bearing performance of the rope.

The load-extension plot, Figure 8.16, shows the familiar 3-zone behaviour. Which means that the loading process involves the rope taking the slack out, then there are inter-fibre/strands movements realigning themselves so they could carry the load more efficiently and finally the third zone when the helix angle is reduced and the stiffness has increased. The resulting heat generated due to inter-fibre/strand movement and the friction between them is quickly lost to the environment, since there is no cover to keep the heat. Therefore no fusion of the fibres has occurred. Thus the fibre failure follows the failure theory discussed earlier. There is some premature fibre failures in the third zone, which are manifested as ripples in the third zone of load-extension curve. Since the final part starts considerably sooner indicates that the uncovered Vectran is more efficient than the covered rope. But it also indicates that it is possibly less damage tolerant. This is signified by ripples on the load extension plots which could be due to the possible surface fibre failing. The uncovered Vectran is also more efficient than the uncovered Dyneema. It can carry a higher load for lower extension.

8.3.3 Behaviour of 4-Strand Technora Rope under Tensile Loading

The results of the tensile test on 4-strand Technora rope samples are presented in Table 8.3 and presented graphically in Figures 8.9 and 8.17. This rope is made from the same Technora fibres and has the same diameter as the 8-strand rope but with a 4-strand construction.

a) Tensile Deformation of Covered 4-Strand Technora Rope

4 strands Technora has strength of 1044.80 N and maximum extension of 39.93 mm which means that it has a higher strength and lower extension than Dyneema rope. The lower extension is due to the higher temperature resistance leading to a higher creep performance. Because there are only four twisted strands in this rope, the helix angle could be closed much faster than the other ropes, which leads to a more efficient load transfer structure. The higher strength achieved is the result of the lower amount of twist in the rope[54,60,101]. The load-extension plot follows the standard three zones and displays no knee point, see Figure 8.17. The initial zone 1 is very short since the strand movement and realignment[93-96] takes place very quickly and the slack in the rope is taken out once the helix angle is closed. The second zone is a gradual constant rise, which possibly could indicate that the structural realignment and movement round the bollards take place more smoothly than Dyneema. This could be due to the higher frictional contact between fibres / strands and the rope external surfaces with the inner surface of the cover. This limits the inter-fibre/strand movements and as the load is increased the cover grips the core more tightly causing the rope to act as a single more efficient system as the loading curve enters into the third zone.

The final zone 3 is very steep which indicates that the failure is caused by the lateral pressure exerted by the cover, tightening of the strands, together with the helix angle reduction. The failure mode for Technora follows the same pattern as for Dyneema, however, the final explosive release of energy generates a lot of heat, as the rope fails, but since Technora does not melt but decomposes, the fracture leads to a fuzzing effect of the fibres and fanning of the fibres in the failed ends. This behaviour is reflected in the SEM micrograph of the fractured ends, shown in Plates 8.5a & b. This indicated that Technora fibres fail by work hardening and compression of the strands caused by

the external effect of the cover. 4 strand Technora reaches its linear part at nearly 67% of its maximum breaking load, which suggests that it is a more efficient system than both, covered Dyneema and Vectran. This is despite having fewer number of strands. It can carry a larger load over a shorter extension than Dyneema but it also possibly could indicate that the interfibre/strand movement and interaction starts sooner and the compaction of the fibres/strands occurs over a longer extension, thus the damage also starts earlier.

b) Tensile Deformation of 4-Strand Technora Core

The uncovered rope has a strength of 814.19 N and a maximum extension of 28.39 mm, which are considerably lower than the covered ropes. In fact the strength is reduced by 22% when the cover is removed. There is no indication of any knee point and the load-extension plot displays the standard three zone behaviour. The absence of the cover allows the fibres/strands to move against each other more freely and the slack is taken out very quickly. The heat generated during loading, due to the frictional contacts between rope elements (fibres and strands) causes some fibres to fail by fuzzing.

During the transformation from zone 2 to zone 3 there is an increase in tension and compaction of the fibre/strand system[93-96], however since there is no cover, no external lateral compression is applied, therefore the rope elements continue to move against each other right up to the moment of failure. As mentioned in earlier, the fracture region is puffed up after recoiling of the two failed ends causing kink banding. Therefore the cover not only protects the core from the external damage and the environment, it also improves the load bearing performance of the Technora. The drawbacks of having the cover include the presence of the external frictional contact between the surface of the rope and the internal surface of the cover and the lateral compression of the cover on the core. The uncovered 4 strand Technora reaches its linear section at nearly 65% of its breaking load which is close to the same percentage as that of the covered rope. This can possibly suggest that the behaviour of the rope is not significantly affected by the removal of the cover only its strength is reduced. However, the presence of the ripples on the load extension plots of the uncovered rope

indicate a possible failure of some fibres within the strands which is very much limited by the presence of the cover. This is a good example of a rope in which the addition of the cover would simply protect the rope from the external effects.

8.3.4 Behaviour of 8-Strand Technora Rope under Tensile Loading

The covered and uncovered 8-strand Technora ropes were also subjected to the same type of loading as the Dyneema and Vectran ropes. The results are listed in Table 8.4 and graphically presented in Figures 8.9 and 8.18.

a) Tensile Deformation of Covered 8-Strand Technora Rope

Table 8.4 show the results of the tensile test on the covered 8-strand Technora rope, which has a strength of 820.40 N and a maximum extension of 33.94 mm. The results indicate that both strength and extension of the 8-strand Technora are less than that of 4 strand Technora. This agrees well with the principle that the lower the amount of twist the greater the strength[9].

However the load-extension behaviour follows the standard three zone pattern, as mentioned earlier, Figure 8.18. The initial rise is almost at the same rate as the 4-strand Technora, but, as there are more strands, there is more slack to be taken out during the initial stage of the loading, which means that it takes a bit longer for it to take on the load than the 4-strand rope. The transformation from zone 1 to zone 2 occurs faster which could indicate that the interlocking mechanism between fibres/strands due to the tightening of the helix angle is more severe. The linear part starts at nearly 70% of the maximum load. This is lower than both covered Dyneema and Vectran but is greater than 4 strand Technora. This suggests that 8 strand Technora is more efficient than both covered Dyneema and Vectran. However, this time it can carry a lower load over a lower extension.

The SEM micrograph, Plate 8.6, clearly reflects the process of damage. As expected, the fracture surfaces show no indication of melting of the fibres but rather a fanning of the failed ends as the fractured ends recoil. Even the regions where the rope seems to be more stiff, is due to the compaction. The core deforms as the cover continues to press on the core .

The process of compaction causes further damage, accompanied by internal inter-fibre/strand friction and external friction with the inner surface of the cover, which leads to fibres fuzzing and abrasion failure. Upon closer examination of the failed ends the evidence of the final catastrophic failure can clearly be seen. During the loading process the fibres try to untwist and untangle themselves but they are also locked within the strand systems. The fibre ends upon breaking recoil rapidly after being stretched, by releasing a high amount of stored strain energy, causing a collapse of fibres on their own. Plates 8.7a & b reflects the process of damage at the instant of failure.

b) Tensile Deformation of 8-Strand Technora Core

Table 8.4 presents the tensile properties data on the 8-Strand Technora Core (uncovered rope). The results indicate that removal of the cover decreases the strength to 737.18 N load and the maximum extension to 27.03 mm, which implies a lower loss in strength than that of 4 strand Technora. This is because the cover of the 4-strand Technora grips the core much more tightly and thus carries over 20% more load. However, the function of the cover is not to carry significant load but to protect the rope from external damage.

The load-extension plot, Figure 8.18, exhibits the familiar 3 zone behaviour, showing that the absence of the cover has allowed the free movement of the rope elements to take place prior to taking out the rope slack. The load-extension curve also shows that the rate of increase in load is not as steep as the covered rope, due to the difference between the process of fibre/strands realignment. The transformation from zone 1 into zone 2 occurs at around 200 N as opposed to 100 N for covered ropes. This indicates that the covered rope is initially more efficient at load bearing. However, zone 2 is

short-lived before entering zone 3, which indicates that covered ropes become less efficient due to the interference of the cover.

The overall profile of the loading history has been found to be very consistent, with a low scatter. The load-extension displays some ripples in the loading history which are due to the movement between fibre/strands. Since Technora does not melt, there is always inter-fibre/strand movement. The failure in this case is due to the fibre abrasion and the standard failure theory[93-96]. The explosive recoil of the two failed ends led to fanning and fuzzing of the fibres. The absence of the cover allows the fibres to deform in a different manner to the covered rope, The fracture surfaces of the failed ends show clear signs of fibres kinking.

Plates 8.8a & b show the SEM micrograph of the fracture surfaces. There is also no stiffness increase which would have been the case if there was a cover, however, the explosive force of the recoiling failed ends loosen the strands and take apart any area where there may have been any compaction. Plate 8.9 shows the process of rope surface failure, which displays peeling action of the surface of the fibres as they abrade against each other. It reaches its linear part after nearly 64%, which is close to that of uncovered 4, strand Technora. The difference between the percentage load for both covered and uncovered 8 strand Technora to reach their linear part indicates that the existence of the cover is more significant in 8 strand Technora.

8.4 Residual Strength Measurement of Pre-loaded Samples

The residual strength of all the different rope samples was measured after the application of a preload. Dyneema and 4- strand Technora were preloaded to 800 N in increments of 100 N whereas 8 strand Technora was only preloaded to a maximum of 700 N due to its limiting breaking load. The Vectran rope was preloaded to a maximum value of 1400 N since its breaking load was the greatest of all the ropes tested, see Table 7.7. The results of the residual strength measurement are presented in Table 8.1 to 8.8 and shown in Figures 8.19a & b to 8.23a & b, 8.24 to 8.27. After each preloading

programme, the ropes were loaded again but this time to failure in order to measure the residual strength. To have a high confidence in the result minimum of 20 samples were tested of each individual rope configuration.

8.4.1 Results of Residual Strength Measurement of Pre-loaded Samples

Vectran has the highest residual strength compared to the other ropes tested followed by 4 strand Technora and Dyneema. There is also a reduction in breaking extension with increasing preload values. Dyneema has the highest extension followed by Vectran.

There is a consistent loss in strength and extension with increasing preload. However, in Dyneema ropes the strength loss is very small upto 500 N preload and then there is a slightly larger loss after that. However, the overall loss is small with maximum being 8.7% after 800 N. This implies that Dyneema can carry a load safely even though preloaded to nearly 87% of its breaking load. The significant difference between the preloaded Dyneema and the as received besides the strength and extension loss is the load extension behaviour, see Figure 8.20a.

There is an increase in stiffness as the result of fibre/strand movement and compression. This increase in stiffness is a feature of all the preloaded ropes. However, it is manifested differently in Dyneema ropes due to the nature of the Dyneema, namely its lower melting point temperature. The first observation is the way the knee point changes. The knee point position moves higher with increasing preload. The ripples on the load extension plots associated with the knee point and the slippage and movement round the bollards disappear. This is due to the fact that the preloading leaves an imprint of the cover on the core which acts as a friction inducer. This is enough to prevent any slippage of the rope round the bollards. The compression of the fibre/strands also leads to the movement of the knee point.

There is an initial linear part, which is directly proportional to the applied. As mentioned earlier this is only unique to Dyneema. None of the other ropes tested show this behaviour, which may be due to the fact that the preloading action has a more detrimental effect on the Dyneema that the rest by the virtue of the fusion of the rope sub-elements. However, the comparison of the preloaded Vectran with statically loaded Vectran shows that they fall into three main categories, see Figure 8.21a:

- No preload
- 100 N to 400 N
- 500 N to 1400 N

There is a significant drop in extension between the different categories but not the breaking loads. The initial linear rise seems to be the same for all the preloads and there is a trend towards linearity with increasing preload. In Vectran and Technora ropes, there are ripples on load-extension plots after preloading. This is possibly because the preloading compacts the fibres but there are still some interfibre/strand movement as some elements could have been loaded slightly more that the others. Thus upon preloading there are exaggerated structural realignment which would then be manifested as ripples on the load-extension plot. There is a consistent strength loss with increasing preload for Vectran ropes. However, these strength loss values become significant after 400 N preload and even then remain consistent until 1200 N which sees another significant increase in the strength loss.

This is a good indication of the damage tolerance of Vectran. The underlying reason is thought to be Vectran's good creep resistance. As a rope is preloaded, the failure factors come into play and if even one of these factors can be improved then the overall rope performance of the rope can be improved. The higher creep resistance of Vectran implies that when the rope sub-elements go through the processes such as structural realignment and friction, the heat generated does not increase the creep effect thus the damage is less destructive. The strength loss in 4 strand Technora is also less significant

with low preload values but gradually increases to the maximum with 800 N preload. The overall loss in strength is just over 6% which is not very high and shows that 4 strand Technora can carry a safe load even though it was preloaded to over 2/3 of its breaking load. This is thought to be due to Technora's ability to withstand heat generated due to interfibre/strand movement. The overall profile for 4 strand Technora also changes. However, as mentioned earlier not in the same way as Dyneema. Its stiffness increases the load extension gradient increases with increasing preload values, see Figure 8.22a.

This time as the preload increases so does the amount of ripples on the load extension plots. This is possibly indicative that the preloading does not compact the fibre/strand permanently. In fact the rope sub-elements are subjected to structural realignment and interfibre/strands interaction during the loading, unloading and reloading processes. Damage accumulates during these cycles. This is due to the higher coefficient of friction of Technora, which can possibly lead to a abrasion damage during the loading cycles. This abrasion damage is thought to be responsible for the possible failure of some fibres during the loading history of the rope. The process is identical for both 4 strand and 8 strand Technora. The maximum strength loss for 4 strand Technora is just over 6% after 800 N, which is less than Dyneema but is greater than Vectran for the same preload value. This is a possible indication that 4 strand Technora is more damage tolerant than Dyneema. This is further emphasised by the fact that these losses in strength, when the actual load values are compared indicated that Dyneema loses slightly more strength than 4 strand Technora. In the case of comparison with Vectran, the strength loss for the same 800 N preload is again slightly higher than that of 4 strand Technora. In the case of the 8 strand Technora there is also a gradual decrease in strength and extension.

A maximum mediocre loss in strength of nearly 5.29% occurs after 700 N preload. This loss is lower than that for Dyneema and 4 strand Technora for the same preload value. The behaviour is as mentioned previously, see Figure 8.23a. The variation between preload and as received 8 strand Technora is very small which is due to the higher number of strands which indicate that the greater the number of strands, the sooner the

interaction of the rope sub-elements and hence the higher and faster stiffness increase. Thus the rope is more efficient but is at the same time less damage tolerant. This greater interaction of the rope elements can lead to possible failure of some fibres during the loading, unloading and reloading cycles, hence the ripples on the load-extension plots.

a) Tenacity

The tenacity values are listed in Tables 8.5 to 8.8 and are graphically presented in Figure 8.24. The first observation is that 4 strand Technora has the highest tenacity value followed by Vectran and Dyneema. The tenacity values for each rope decreases with increasing preload. However, the initial decrease with increasing preload values is less significant than those of later preload values. In all the cases the only variable was the residual breaking load as the variation in mass per unit length with preload compared to, as received ropes was very small.

The tenacity values of preloaded Dyneema ranges between 8.88×10^{12} N/tex to 8.15×10^{12} N/tex for 100 N to 800 N preload values. There is as mentioned a gradual decrease in the tenacity value from 8.93×10^{12} N/tex for as received Dyneema. However, there is a greater decrease in the tenacity value after 500 N preload. This corresponding to the load range at which the linear part starts in the as received Dyneema. It is also where there is a sharp decrease in residual breaking load. The reason for the reduction in strength of Dyneema have already been discussed.

In the case of Vectran, the behaviour is somewhat different to Dyneema. There is still a gradual decrease in its tenacity values, which range from 9.31×10^{12} N/tex to 8.53×10^{12} N/tex for 100 N to 1400 N preload values. However, the tenacity values fall into three close groups:

- As received to 100 N
- 200 N to 300 N
- 400 N to 1400 N

The variation in the tenacity value is not very large but is still significant enough to show a possible trend. These categories relate to the similar variations in the load extension pattern and values, which have already been discussed.

Vectran is the largest ropes tested and consequently has the highest residual strength of all the ropes tested. However, the ratio used for the tenacity calculations results in a lower tenacity than that of 4 strand Technora which has the highest tenacity values of all the ropes in this research. Its values range from 9.76×10^{12} N/tex to 9.21×10^{12} N/tex for 100 N to 800 N preload range respectively. There is a gradual decrease in its tenacity and it falls into three close categories:

- As received to 200 N
- 300 N to 400 N
- 500 N to 800 N

Again this corresponds to the load and extension values and the groups that they fall into. The underlying reasons why the tenacity values vary as such are similar to those of residual strength. The tenacity values for 8 strand Technora also decrease gradually ranging from 7.92×10^{12} N/tex to 7.61×10^{12} N/tex for 100 N to 700 N preload values. However, the decrease is not very significant within the preloading range and there is no sudden decrease in the tenacity with increasing preload. This is possibly due to the fact that load and extension values of preloaded 8 strand Technora are close. This can also suggest that eventhough the damage in Technora is cumulative, 8 strand Technora is more damage tolerant and its rate of strength loss is not as steep as the other ropes tested.

b) Work of Rupture

The work of rupture values are listed in Tables 8.5 to 8.8 and are graphically presented in Figure 8.25. Vectran has the highest work of rupture but that is as expected since it also has the highest breaking load. Dyneema has the second highest work of rupture followed by 4 strand Technora. The work of rupture of all the ropes tested decrease with increasing preload values due to the resulting decrease in breaking load and extension.

The work of rupture of Dyneema ranges from 22.32 J to 13.91 J for 100 N to 800 N preload. The decrease is significant across all the preload range but is more so after 500 N. This is again thought to be linked to the start of the linear part in the as received ropes. After 500 N, the compression of the fibre/strands is sever enough to cause a larger decrease in the load and extension values and hence decrease the work of rupture.

The work of rupture of Vectran ranges from 24.25 J to 17.29 J for 100 N to 1400 N preload. The work of rupture values decrease gradually with increasing preload. However, the total variation is not very significant. This indicates that the energy needed to fracture the Vectran rope with increasing preload decreases. This decrease is a direct result of the decrease in breaking load and extension. The fact that there are no significant variations in level of the work of rupture compared to Dyneema is an indication that Vectran does not store as much energy as Dyneema.

The work of rupture of 4 strand Technora ranges form 16.12 J to 13.15 J for 100 N to 800 N preloads. The work of rupture values decrease gradually with increasing preload. However, the overall decrease in work of rupture is very small across the preloading range. This is an indication that the rate of strength loss with increasing preload is smaller is smaller than Dyneema. It also indicates that 4 strand Technora stores less energy than both Dyneema and Vectran. This is thought to be the reason why there are greater fibre/strand damage at the fractured ends of the Dyneema ropes and why the

Dyneema fails with a higher audible sound, i.e. Technora has a lower snap back energy level.

8 strand Technora has the same behaviour as the rest. Its work of rupture of decreases with increasing preload and ranges from 11.25 J to 8.64 J for 100 N to 700 N preload. The variation in its work of rupture is not significant and follows the same principle of 4 strand Technora. The underlying reasons for its lower work of rupture is its lower breaking load and extension values.

c) Specific Work of Rupture

The specific work of rupture values are listed in Tables 8.5 to 8.8 and are graphically presented in Figure 8.26. Dyneema has the highest specific work of rupture followed by 4 strand Technora and Vectran. Since the variations in the mass per unit length with increasing preload is very small, the only variable is the work of rupture. The variations in the specific work of rupture for Dyneema is more pronounced than all the other ropes tested. The trend in all the cases is a decrease in specific work of rupture with increasing preload.

The specific work of rupture for Dyneema ranges from 1.54×10^{11} N/tex to 9.62×10^{10} N/tex for 100 N to 800 N preload. The rate of decrease is gradual upto 500 N and then becomes slightly more steep. This is again directly linked to the range at which the fibre/strand compression leads to compaction and start of the linear part. The specific work of rupture for 4 strand Technora and Vectran are closer to each other than the other ropes tested.

The specific work of rupture for Vectran ranges from 9.95×10^{10} N/tex to 7.10×10^{10} N/tex for 100 N to 1400 N preload. There is gradual decrease in the specific work of rupture with increasing preload. The pattern is as mentioned the same as for 4 strand Technora whose specific work of rupture ranges from 1.08×10^{11} N/tex to 8.82×10^{10}

N/tex for 100 N to 800 N preload. 8 strand Technora has a specific work of rupture values ranging from 7.87×10^{10} N/tex to 6.04×10^{10} N/tex for 100 N to 700 N preloads. Its pattern is also the same as Vectran and 4 strand Technora.

d) Work Factor

The work factor values are listed in Tables 8.5 to 8.8 and are graphically presented in Figure 8.27. The preloading leads to compaction and possible fusion of the fibre/strands. The work factor gives an indication of how much is the effect of this compaction/compression. The compaction leads to a stiffness increase, which in turn leads to a more linear behaviour. As mentioned in the experimental section, the work factor is an indication of how closely a rope sample follows Hooke's law. In all the cases there are three variables:

- Work of Rupture
- Breaking Load
- Breaking Extension

It was hoped that the work factor value approach 0.5 with increasing preload. Indeed the values do increase as the preload increases, which is thought to the result of the compaction of the fibres/strands. The work factor values for Vectran show a gradual increase whereas the pattern is not as smooth for the other ropes tested. There is gradual increase for those too but is not as smooth as Vectran. The work factor values for Dyneema range from 0.52 to 0.55 for 100 N to 800 N preload. Dyneema is the only rope tested whose work factor values are always greater than 0.5. The work factor values are very close and gradually increase with a peak at 500 N. However, the small variation range can suggest that the behaviour of Dyneema remains the same, i.e. non linear as the preload increases. This is further supported by the observation of the load extension plots. There is an initial linear rise proportional to the applied preload which can possibly have a work factor value of 0.5. Then there is the second section which is again linear but has a different gradient and can also have a possible work factor value

of 0.5. However, the overall rope loading history has a work factor value which is greater than 0.5.

The work factor values for Vectran gradually increase with increasing preload and range from 0.37 to 0.57 for 100 N to 1400 N preload. The work factor values are close to each other but over a wider range compared to Dyneema and Technora. The work factor values become 0.5 after 800 N preload. This can be the turning point in the behaviour of Vectran, suggesting that possibly preloading Vectran to 800 N could cause it to behave in a fully Hookean manner.

The work factor values for 4 strand Technora also increase with increasing preload and they range from 0.45 to 0.55 for 100 N to 800 N. The work factor values are also close to each other. They could possibly suggest that there is a shift form one type of behaviour to another between 300 N to 400 N preload as there is a jump from a work factor value of 0.49 to 0.51. The 8 strand Technora shows a similar behaviour and its work factor values range from 0.44 to 0.50 for 100 N to 700 N.

8.5 Strand-Rope Efficiency Measurement

All the rope samples have their constituent strands removed one at a time and the remaining structure static tensile tested, see Tables 8.1 to 8.8.

In order to achieve a high confidence in the results a minimum of 20 samples of each rope configuration are tested with their strands removed. The results are also graphically presented in Figures 8.28a & b to 8.32a & b, 8.33 to 8.42. All the samples are 8 strand construction except for Technora ropes, which are also available in 4 strand construction. Care was taken to avoid disturbing the rope structure when removing the strands but some structural disturbance was inevitable and expected.

The ropes were strand tested in reverse in order to see the effect of strand removal on the strength and efficiency of the rope. The procedure involved the removal of one strand at a time. This gave the opportunity to study the effect of the spaces created in order to study the relationship between the balance of the rope sub-elements and the performance of the rope.

8.5.1 Comparison of the Strand Strength for Different Ropes

Tables 8.1 to 8.4 and Figure 8.28a & b show the variations in the breaking load and extension for the various ropes tested in this research. It can be seen that 4 strand Technora has the highest breaking load per strand compared to the other ropes tested despite Vectran being a larger diameter rope. 8 strand Technora and Dyneema have similar breaking load per strand. This is possibly an indication that there is a good correlation between the rope elements in both Dyneema and 8 strand Technora.

A question, which may be asked, is whether a rope with a greater number of strands has a higher breaking load or a rope with less strand but more fibres per strand. The answer lies in the breaking load values of 4 strand Technora, which has more fibres per strand but fewer number of strands. This leads to a lower amount of twist per unit length. The comparison between 4 and 8 strand Technora shows that 8 strand Technora has a lower breaking load which is due to higher amount of twist per unit length and hence the greater the amount of stress raisers.

However, it is a different pattern when the breaking extensions are compared. Dyneema has the highest breaking extension followed by Vectran and 4 strand Technora. The pattern is similar to those of the as received ropes. In all the cases the breaking loads and extensions decrease with strand removal. The relationship of breaking load to number of strands is almost linear but the extension is not as significant. The removal of the strands leaves the gaps which allows the rope sub-elements to move against each other more freely.

8.5.2 Dyneema

The breaking load values for Dyneema range from 110.58 N to 795.92 N for 1 to 8 strands. The values are similar to those of 8 strand Technora but lower than Vectran and 4 strand Technora. The immediate observation of the load and extension behaviour shows that the slop changes and there is no sign of the knee point, see Figures 8.29a. The behaviour also becomes more non-linear as the number of strands increases. The reason for this behaviour is possibly due to the fact that the higher the number of strands the greater the interfibre/strand movement and the greater the twist and hence the greater the crimp[226].

The breaking load values are very linear with number of strands, see Figure 8.28a. This is an indication that once the strands are removed, the Dyneema rope quickly recovers from the spaces created. There is a higher variation in the rate of change of extension with strand removal than other ropes tested. There is a decrease in the extension to break with the strands removed, which is a direct result of ropes decreasing resistance to extension. Comparison of the actual strength with the estimated values of the strands, see Figure 8.33, shows that the initial removal of the first 3 strands is more damaging than the rest. This is interesting since all 8, 6, 4, 3 and 2 strand rope constructions are considered to be torque balanced. However, 6 strands show the highest deviation. The reason could be lying in the fact that the removal of the initial 2 strands created more of a disturbance. The comparison of the load and extension values do not show any thing out of the ordinary.

8.5.3 Vectran

The behaviour of Vectran with strand removal is similar to that of Dyneema, i.e. there is an increase in the non-linear behaviour pattern with increasing number of strands, see Figure 8.30a. However, the patterns are as smooth as Dyneema. The reason for this possibly lies in the property of the material. The coefficient of friction of Vectran is higher than that of Dyneema, thus upon the removal of strands, the gaps left were quickly filled. However, as the interfibre/strand movement continues and they try to realign themselves, some possible fibre/strand damage may have started. This is

manifested as the ripples on the load extension plots. The breaking load values range from 202.40 N to 1537.70 N for 1 to 8 strands. The breaking load values decrease with strand removal, see Figure 8.28a, which is steeper than that of Dyneema. This is thought to be due to the same higher coefficient of friction of Vectran. The removal of the strands allows the remaining rope sub-elements to interact over a larger surface area and the damage starting earlier, which ultimately leads to sharper decrease in breaking load. The breaking extension also decreases as the number of strands decrease, see Figure 8.28b. The decrease range is lower than that of Dyneema but still larger than Technora. The decrease is not as smooth as Dyneema which again indicative of the way the remaining strands overcome the gaps left between them. The maximum decrease is between 5 and 4 strands. This signifies the fact that once four strands are removed, the spaces left are more detrimental than with any number of strands.

The comparison of the actual breaking loads with that of estimated values shows a larger variations and pattern to Dyneema, see Figure 8.34. The removal of the strands seems to have affected Vectran more severely than Dyneema. However, in comparison to Dyneema, the 6, 2 and 1 strand constructions are very close to the estimated values. This possible suggests that the damage continues throughout the loading history. However, at 6 strands the gap left is more quickly closed and in the case of 2 strands the rope acts as two possible ropes in parallel with some twist present due to the strands.

8.5.4 Four Strand Technora

The behaviour of 4 strand Technora is the same as Dyneema and Vectran. The ripples on the load extension plots, see Figure 8.31a, are possibly due to the same reason as Vectran. The trend is towards non-linearity is only evident in the full 4 strand rope. The breaking load values range from 207.47 N to 814.19 N for 1 to 4 strands. The variation in the breaking load with number of strands shows a linear pattern, see Figure 8.28a. This is a good indication that Technora overcomes the spaces left due to strand removal with ease and efficiently. The extension values also decrease with decreasing number of strands, see Figure 8.28b. However, the decrease is not as smooth as the breaking

load. There is a higher decrease in extension between 4 and 3 strands. This possibly suggests that the most damaging part is when the first strand is removed. The comparison of the actual breaking loads with the estimated values, see Figure 8.35, shows a very close correlation between them. The pattern is similar to that of 8 strand Technora where the actual breaking loads are close to that of the estimated values.

In the case of 4 strand Technora, this close correlation shows that the removal of the strands does not affect the performance of the rope. This feature is possibly due to the fact that all the different strand constructions are torque balanced. Also there are only 4 strands to start with which suggests that the removal of the strands does not create any significant disturbance to the rope structure.

8.5.5 Eight Strand Technora

The behaviour of 8 strand Technora is similar to all the other ropes tested and there are ripples in the load extension plots, which are similar to that of Vectran, and 4 strand Technora, see Figure 8.32a. The breaking load values range from 95.11 N to 737.18 N for 1 to 8 strands. The breaking load values are lower than all the other ropes. The comparison of the breaking load values between 4 and 8 strand Technora shows that both vary linearly, see Figure 8.28a. This is also indicative of the fact that the removal of strands is not as damaging thought. This together with the same findings for the other roes tested is encouraging since the removal of the strands can be likened to that of strands failing in the whole rope and the load being transferred to the remaining strands. However, there is a significant difference. The load transfer in a rope whose strands have failed is dynamic. The comparison of the estimated breaking loads with those of the actual values are very close, see Figure 8.36. This behaviour is similar to that of 4 strand Technora. The close variation between the estimated and actual again implies that the removal of strands is not as detrimental to the rope performance as Dyneema and Vectran which can mean that 8 strand Technora is more damage tolerant. This can possibly be as a result of higher coefficient of friction, which leads to the rope sub-elements engaging each other faster.

a) Tenacity

The tenacity values are listed in Tables 8.5-8.8 and are graphically presented in Figure 8.37.

Both Technora ropes have tenacity values, which do not vary significantly with number of strands. The values of tenacity for Dyneema and Vectran vary more significantly than those of Technora. The reason for these lie in the ratios of the breaking load values to the mass per unit length of the strands. The tenacity values for Dyneema ranges from 2.17×10^{13} N/tex to 1.96 10^{13} N/tex for 1 to 8 strands. The variation for Vectran is from 1.91×10^{13} N/tex to 1.82×10^{13} N/tex for 1 to 8 strands. The same variation for 4 strand Technora ranges from 1.85×10^{13} N/tex to 1.83×10^{13} N/tex for 1 to 4 strands and in 8 strand Technora ranges from 2.07×10^{13} N/tex to 1.99×10^{13} N/tex for 1 to 8 strands.

b) Work of Rupture

The work of rupture for different ropes tested are listed in Tables 8.5 to 8.8 and are graphically presented in Figure 8.38. The work of rupture for all the ropes increases with increasing number of strands. This is a direct result of increasing breaking load and extension with increasing number of strands. The rate of increase of work of rupture in both Technora ropes is smoother than in both Dyneema and Vectran ropes. This is again an indication of the more efficient load transfer of Technora and its damage tolerance.

c) Specific Work of Rupture

The specific work of rupture values are listed in Tables 8.5 to 8.8 and are graphically presented in Figure 8.39. Dyneema has the highest specific work of rupture of all the ropes tested. The Technora and Vectran ropes have a closer specific work of rupture. The variation in the specific work of rupture for Dyneema is again more significant than the other rope tested. 4 strand Technora is the only rope, which shows a slight increase in specific work of rupture with increasing number of strands. In the

calculation of the specific work of rupture are the work of rupture and the mass per unit length.

d) Work Factor

The work factor values are listed in Tables 8.5 to 8.8 and are graphically presented in Figure 8.40.

The work factor values in all cases vary with the number of strands between 0.3 and 0.5. The work factor values should theoretically decrease with increasing number of strands because of the increase in the amount of twist and moving rope sub-elements. However, this is not strictly the case. In the Vectran ropes there is a tendency for the work factor to decrease with increasing number of strands but the same is not the case for the other ropes tested. However, the variations are small. Work factor values for 4 strand Technora show an increase with 2 strands but begin to decrease wit more strands. The behaviour possibly indicates that 2 strand Technora is more efficient than 1 strand. In fact the work factor values increase with 2 strands for both Dyneema and 8 strand Technora and decreases slightly with 3 strands. However, in contrast to other ropes tested, 8 strand Technora shows an increase in work factor with 4 strand removed. Its work factor value is still lower than that of 4 strand Technora. This is possibly due to the fact that 4 strand Technora starts as a whole system in this case whereas 8 strand Technora is not a complete rope and its remaining sub-elements have to first fill the gaps left due to the removal of strands..

e) Strand Efficiency Comparisons

The calculation of strand and rope efficiency values based on Equations 7.7, 7.10 and 7.11 show that both Technora ropes have excellent strand efficiencies, see Figures 8.41 and 8.42, indicating that the higher coefficient of friction of Technora quickly overcomes the spaces left due to the removal of the strands. The same can not be observed for both Dyneema and Vectran. Their strand efficiency fluctuates to a higher extent than that of Technora and their values are opposite each other. Dyneema has its highest strand efficiencies with 2 and 4 strands and closely followed by 8 strands.

Vectran too has its highest strand efficiency at 2 strands but then it is followed by 6 strands. The reason for these variations possibly lies in their lower coefficient of friction and how the rope sub-elements interact with each other. In the case of Dyneema the removal of strands allows the movement between the already slippery Dyneema Fibre/strands. The most efficient rope is a rope, which is torque balanced and that means a trope with even number of strands. However, a 7 strand Dyneema seems to be more efficient than 6 strands. This is thought to be due to the higher breaking load, which is still close to the breaking load of the whole rope. The case is true for both Dyneema and Vectran. However, at 6 strands the strand efficiency of Vectran increases whereas that of Dyneema decreases.

This is possibly due to the lower coefficient of friction of Dyneema, which allows the rope sub-elements to move more freely against each other before they interact and lead to the failure of the rope at a lower load. However, in the case of Vectran, the interfibre/strand interaction occurs faster and a since Vectran' strands have more fibres per strand than Dyneema, they fail at a higher load closer to the that of the whole rope.

In the case of 4 strands the pattern is reversed and the strand efficiency of Dyneema increases whereas that of Vectran decreases. The greater spaces left during the strand removal allows the fibres/strands in Dyneema to move even more easily. This possibly allows the interlinking of the elements, which close faster due their lower coefficient of friction. Hence the rope takes on load faster and more efficiently. The pattern is repeated again once four strands are removed which is even better since the rope structure is torque balanced. In the case of Vectran the opposite occurs. This can be attributed to its higher coefficient of friction. The same process, which allows the Dyneema fibres/strands to move quickly into the empty spaces, left. This time it leads to a weakening of the rope due to the abrasion of fibres/strands against each other. Both Dyneema and Vectran have close strand efficiency for 3 strand construction but this signifies a decrease in Dyneema and an increase in Vectran form 4 strands.

3 strand construction is a torque balanced system. 3 strand construction in this case represents a removal of 5 strands which leaves large gaps within the rope sub-elements. The higher coefficient of friction of Vectran overcomes these gaps faster than

Dyneema. Hence the increase in strand efficiency for Vectran as opposed to the decrease in Dyneema. The strand efficiency with 2 strands represents an increase in both cases. This is despite the large gaps created when 6 strands were removed. This possibly supports the theory that remaining gap allows the strands to act like a rope, which has a low twist level, which can be loosely compared to two ropes acting in parallel. This also leads to a higher breaking load.

8.6 Residual Strength of Cyclically Loaded Dyneema Rope

The tests that were conducted as mentioned in the Experimental Details see Table 7.8 and Figure 8.43. As the rope is loaded and unloaded, there is a build-up of heat and release of energy. On the return cycle, the load is taken on again once its value has reached zero "Newton" rather than the extension becoming zero. Therefore there is a residual strength in the rope every time it is cycled leading to ever increasing compaction and elongation. The cycled samples all except the ones, which were cycled for 2000 and 3000 cycles gain strength. The highest gain is at 10 × 300N which is in the zone 2. However, the 100 × 200N has the lowest strength gain. This is due to the same principle, i.e. the increase in elongation after 100 cycles is such that the rope has decreases in diameter and its components have become more compacted and could carry the load more efficiently, but less than 10 × 300N.

The same principle also holds true for 2000 × 300N samples but to a more severe extent resulting in a drop in breaking strength. This complies with the literature that the strength increases as the flexibility decreases. The cause of failure in all cases is a combination of the maximum and minimum loads[101,110,146,152,153] which increase the fibre movement, causing friction and realignment of the fibres[93-96]. The samples, which were cycled to 600, N failed after about 1246 cycles. Increasing the load to 650 N caused the ropes to fail at around 698 cycles, which is about half the number of cycles for 600 N. This is possibly due to the fact that 650 N is well into the third zone, making the damage accumulation faster upon loading and unloading. The cyclic loading increases the extension of the rope over the cyclic process. This is due to the fact that

upon the first cycle the rope goes through an extension. On the second cycle the load is taken on again once its value reaches zero not the extension value. Thus upon reloading there is a further extension. The process is repeated upon subsequent cycles with the extension increasing all the time. This causes the interfibre strand movement to generate frictional heat, which causes the fibre to become fused and thus increase in stiffness.

Acoustic emission was monitored, however, the amount of data accumulated was too great for the memory of the computer. The pattern was an initial step rise for the first cycle followed by a second very high step rise, which is the accumulation of all the consequent cycles. The rate of acoustic emission decreases with cyclic preloading but since Kaiser effect does not apply, there are still some residual acoustic emission signals during the proceeding cycles. The second large step rise corresponds to this accumulation of all the small residual acoustic emission activities.

8.7 Abrasion

As mentioned in the experimental section, the abrasion process is very important since it is one of the major causes of rope failure. This becomes more important in the Technora ropes since their abrasion and compression properties are lower than the Dyneema ropes. However, the heat generated is more detrimental in Dyneema due to its lower operating temperature. This heat produced will accelerate the creep process. Therefore even though the failure process is the same for the ropes, the initial event may be different.

This changes slightly once the cover is removed since most of the heat generated is rapidly lost to the environment, which signifies the significance of the cover. However, the overall pattern should remain the same.

Dyneema and Technora ropes were abrasion tested using a specifically designed abrasion testing rig based on the Goksoy[156-159] apparatus. The set-up consisted of a reciprocating motor and five pulleys. The arrangement was such that to allow the ropes to be abraded against themselves and count the cycles taken to failure. The ropes were tested under a preload of 2 kg to 4 kg, see Tables 7.9 and 8.13 and Figure 8.44. The rope lengths tested were 1400 mm and they were twisted upon themselves once in order to encourage surface on surface abrasion. The pulley diameter used in all the cases was 21.6 mm. The stroke of the motor was 15 mm and the speed was 42 cycles/min. The starting abrasion area was 10 mm long but as the abrasion process continues the abrasion area increases and the rate of increase accelerates with increasing number as the final cycles to failure approaches. The covered ropes have a greater abrasion resistance since the polyester cover has to be abraded first before the fibres could be exposed. Once the fibres are exposed there are several elements that come into play.

As there is a tension in the rope, even though small (2-4 kg), there is some fibre/strand movement and realignment. As the abrasion process continues the exposed areas are heated up due to the frictional contact. Covered Dyneema under 2 kg load took 88653 cycles to failure but under 4 kg load the number of cycles to failure decreased to 49997 which is a reduction of 43.60%. The uncovered Dyneema under 2 kg tension failed after 49441 cycles and under 4 kg failed after 21103 cycles which is equivalent to a reduction in abrasion strength of 57.32 %. This could indicate that the cover is very important since it is making a huge contribution to the service life of the rope. This emphasises the importance of the cover even more once the applied tension is increased. The covered Technora under 2 kg load was subjected to 12216 cycles before failure. This number is reduced to 8320 cycles as the preload is increased to 4 kg. This is equivalent to an abrasion resistance reduction of 31.89%. Comparing the results of 2 kg and 4 kg for covered Technora with covered Dyneema suggests that the abrasion resistance of covered Technora under 2 kg load is 86.22% lower than the equivalent Dyneema.

Under 4 kg load covered Technora has a lower abrasion resistance of 83.36% compared to the covered Dyneema under the same conditions. Uncovered Technora under 2 kg load failed after 1785 cycles and after only 821 cycles under 4 kg load. The increase in the load decreased the abrasion resistance by 54.01%. The absence of the cover caused the abrasion resistance to be decreased by 85.39% for 2 kg load and 90.13% for 4 kg load. The uncovered Technora under 2 kg load has an abrasion resistance of 96.39% lower than the equivalent uncovered Dyneema under the same conditions. Increasing the load to 4 kg decreases the abrasion resistance of uncovered Technora by 96.11% compared to the equivalent uncovered Dyneema under the 4 kg load. In the Dyneema samples the abrasion process leads to the increase in creep rate and heat generated due the friction of the rope constituents. However, no fusion of the fibres was observed, as the heat is quickly lost to the environment. The failure is a combination of surface fibre/strands failing working inwards while the internal fibre/strand movement also weakens the structure.

The abrasion process depends on the movement of the strands against each other, which become more pronounced as the process continues. This is because the abrasion process is progressive, which means that the damage could be accelerated, once the process has started. The failure mechanism is a combination of internal movement and friction between strands and the external abrasion of constituents on each other.

However, the rates of damage are different and it is the external damage caused by the rope surfaces on each other which is the most detrimental. The relative internal movement of the fibres and the external movement of the rope surfaces on each other are linked. As the process continues there is a build up of heat due to the internal events. However, it is the external abrasion, which is the most detrimental. As the surface strands and fibres are abraded the internal surfaces become exposed. These internal fibres have already been weakened during the starting cycles. Therefore they are weaker than the initial surface fibres and have a lower residual abrasion resistance. Thus they abrade and fail quicker. The process is continuous and progressive which ultimately will lead to a stage that the remaining strands and fibres have such a low abrasion resistance that they will fail due to a combination of poor abrasion

performance and static tensile load, i.e. not being able to maintain the applied 2-4 kg load.

The behaviour of Technora fibres are the same as Dyneema except for the number of cycle to failure which is much lower. This is because at the point of abrasion the fibres are also under compression. Aramid fibres are weakest under compression and have a higher coefficient of friction which results in higher rate of localised heat build up as the abrasion process continues leading to a faster localised damage. Thus the role of the cover as abrasion protector is more important in Technora fibres than Dyneema.

8.8 Strength of Conditioned Samples

The weathering was done on a weathering rig, which was erected on the roof of the University where no shadow fell on it. The conditions were monitored daily and then double-checked by the reports for the area from the Met Office. An electric oven was used to heat the samples and the seawater was made according to the BS 3900 part F4 Clause 6.1. Low temperature was achieved by using a Zanussi deep freezer. The ropes were tested using the same apparatus for other testing. The crosshead speed was kept at 100 mm/min. The ropes were taken four times round each bollard before being secured. Tables 8.14 - 8.18 and Figure 8.45 show the results of the tests after the Dyneema rope were subjected to various environmental conditions.

8.8.1 Natural Weathering

As can be seen from the Table 8.14, Dyneema is not highly affected by natural weathering. The strength has decreased with exposure to the cyclic weathering conditions ranging from 896.9 N for 7 days to 823N & for 56 days. The strength loss after 56 days is 8.14%, see Figure 8.45. This is very small considering the number of days, however, Dyneema is a highly oriented polyethylene which clarifies the situation more, since polyethylene has excellent weathering properties. Weathering parameters such as UV posed no problem since polyethylene has also got excellent UV resistance

and the ropes have a polyester cover, which added a further protective barrier. The only time would the cyclic weathering be detrimental if the temperature range was so high as to soften and weaken the rope.

8.8.2 Water at 54 ℃

Table 8.15 shows the results of the Dyneema ropes after immersion in water at 54 °C. The results show a gradual drop in load with increasing exposure. After one day the strength drops to 881.3 N which is equivalent to a strength loss of 1.71%. After maximum exposure of 16 days, the strength drops to 787.4 N indicating a loss of 12.19% in strength, see Figure 8.45. This result shows that after 16 days the strength loss due to water and sea water are very close. However, the causes of failure are different. Here it is the high temperature whereas in the seawater is the salt crystals. The operating temperature for Dyneema is around 70 °C to 80 °C. Therefore, storage in hot water could have weakened the fibres accelerating the creep element of the failure mechanism. This can possibly be observed by comparing the extension values, which increase with increasing exposure period.

8.8.3 Dry heat at 54 ℃

Table 8.16 shows the results of Dyneema ropes heated to 54 °C for the same number of days as hot-water and sea-water exposure. The strength decreases with increasing number of exposure days. After only 1 day, the strength decreases to 832 N indicating a strength loss of 7.22%. This is the greatest loss in all the test done in this section. After the maximum number of days exposure the strength decreases to 788.3 N indicating a strength loss of 12.09%, see Figure 8.45. This is again very close to sea-water and hot-water exposures. It is thought that creep could play a vital role in the failure criteria for these ropes.

8.8.4 Subzero

Table 8.17 shows the results of ropes subjected to temperature of -22 °C. The ropes were kept in the Zanussi deep freezer until the testing. There is a reduction in strength, but it is not as significant as the other conditions. The period of exposures was the same as others. After one day the strength decreases to 865.4 N which is equivalent to 3.49% reduction in strength. After the maximum exposure of 16 days the strength drops to 830.2 N, which is equivalent to 7.42% loss in strength, see Figure 8.45. This suggests that the strength loss due to low temperature is not as significant as high temperatures. This would be explained by the analysis that as the rope is loaded, it takes a longer time and load to reach a critical level for the internal temperature of the rope and start the detrimental creep. However, the fact that there is a loss in strength with exposure to low temperature could indicate that Dyneema has low operating temperature as well as high operating temperature limits.

8.8.4 Synthetic Sea Water

Table 8.18 shows the results of the ropes being immersed fully in synthetic sea water. It can be seen that as opposed to natural weathering that after seven days there was no loss of strength. In this case after only one day the strength drops to 870.3 N, having a loss of 2.94% in strength. The loss in strength increases continuously and after 16 days decreases to 782.9 N, which is a loss of 12.69% in strength, see Figure 8.45. It is not the actual immersion in the water, which weakens the rope because the water is easily pushed out between the fibres as the rope is loaded. However, as the loading process continues, the water is pushed out or evaporated and salt crystals are formed. It is these crystals which physically cut into the fibres and cause the failure of the fibres. In order to see the full impact of the condition the rope samples were not shaken to remove any water, thus maintaining the same condition for all the ropes.

8.9 Thermography

It is stipulated that there is a heat generation as a rope starts to take on load due to the friction caused by the movement of the rope sub-elements against each other and the

cover. This is more evident at the instant of failure when the two failed ends recoil and the stored elastic energy is released. This collapsing fractured ends cause very localised high-speed friction in the vicinity of the fracture. This could explain why there is a maximum heat generated near the failure region, which is manifested by the melting of the fibre at the fractured end. This is more evident with covered Dyneema ropes as they are more temperature sensitive. The removal of the cover would allow the rapid loss of heat to the surrounding.

In order to assess the rate of heat build up, a series of thermograph images were recorded while Dyneema rope was loaded. The failure theory[93-96] states that one of the causes of failure is heat generated due to friction and the recoiling energy. It is hypothesised that once the slack is taken up and the rope takes on load there is a gradual build up of heat. This is due to the internal inter-fibre/strand movement and the inner surface of cover rubbing against them and compressing them. This gradual rise continued until the start of the third zone when there is a sudden increase in rate of heat build up as the failure load approached. At the instant of failure as mentioned in the failure section and literature[93-96] the two failed ends recoiled due to the stored elastic energy as the load dropped. This recoiling, provided that there is a cover to prevent the heat from being lost to the environment, led to a very sharp temperature increase and melting of fibres.

Thus in order to investigate this phenomenon a CYCLOPS T135 Thermal Imaging System[v] with a temperature range of -20° to 1500°C was set-up as Dyneema ropes were tested. It was expected to record temperatures of over 140° C, the melting temperature of Dyneema, however, the registered temperatures were in the range of nearly 30° C to 40° C, see Figures 8.46 and 8.47. This is due to the fact that the camera only recorded only the surface temperature. The polyester cover has shielded some of the heat generated and some have been lost to the environment. Also the camera could not measure the rapid rate of heat build up and could not measure the internal temperature of the rope. In other attempts using uncovered ropes, the recorded temperature is also

[v] The camera was manufactured by Land Thermal Imaging Systems

lower than is expected because of the rapid loss of heat to the surrounding. However, the experiment confirmed that the hypothesis is correct. In order to get a very accurate picture of what is going and measure the rapid rate of temperature rise, the probe must be able to measure both internal and external rope temperature as it is loaded. This would be difficult, as inputting the probe in the rope would interfere with the load bearing performance of the rope leading to inaccurate results.

8.10 Acoustic Emission Monitoring of Rope Samples

The acoustic emission monitoring was undertaken in an attempt to characterise the damage process active at different stages during the loading cycle, with the aim of being able to:

a) identify the fracture processes occurring by the AE signature
b) provide an NDT method for predicting the failure modes of samples from the initial emission activity
c) analyse the performance of different ropes and to investigate the possibility of utilising AE techniques to study rope performance.

To achieve the above objectives AE was monitored during all the mechanical testing of the different rope systems. At the early stages of this study, different AE monitoring systems were used as an attempt to interpret the damage mechanisms. In this process, event counting, amplitude analysis and ringdown counting were used. However, ringdown counting proved to be the best method of achieving enough signal to interpret the micro events occurring during the loading process. The ringdown counting (RDC) results monitored during the different loading conditions are presented in the Tables 8.9 to 8.12. It is evident from the results that RDC can identify successfully the different events happening at early stages of the loading process.

However the system loses resolution when dealing with the pseudo continuous type of emission that is generated during the final phases of rope failure. The catastrophic nature of rope failure is always associated with a large number of RDC and the AE system, used in this study, was found to be unable to handle the high rate of events generated during this phase of the test. In all cases, the tensioned ropes generated most of their emission after the peak load, whilst the major fracture events were occurring.

In this study, the total RDC at any point has been selected to give enough sensitivity with improved resolution of the time scale. In every case the emission data was plotted against extension and the whole curve was superimposed onto the relevant load-extension curve. The RDC-extension curves were used to enable various aspects of the emission to be characterised. The emission sources that we expect to find are:

(i) Fibre fracture
(ii) Fibre yielding
(iii) Inter fibre-strand friction
(iv) Core-cover friction
(v) Irreversible damage
(vi) Fibre buckling

All these mechanisms will have differences in the energy released and their power density spectrum as a function of frequency. We have not attempted any frequency analysis because of the complexity of the equipment required. One of the aims of this work was to see if the relatively simple event counting method could be used to identify the presence of the different damage modes active whilst testing ropes. Data interpretations to this end have not proved an easy task. The static tensile and residual strength tests are somewhat similar in that prior to failure they showed a fairly linear behaviour after a period of non linear load-extension relationship. If we are going to be able to use acoustic emission as an NDT tool (or perhaps more accurately as a slightly destructive testing tool) we can only use the emission produced before failure. It may

be that some fibres will have been stressed beyond their peak load carrying capability. The energy released during fracture mechanisms depends on;

(i) the fracture process (fibre break)

(ii) the fracture surface created

(iii) the interaction between the cracking part and the surrounding part (e.g. fibre buckling)

The preliminary tests on the different ropes, showed that emission versus extension curves fell into the following distinct pattern:

- A slowly rising emission count (RDC), until a critical load was reached, when there was a sudden large increase in the RDC recorded. The linear AE section corresponded to the realignment of the rope sub-elements (fibres, strands and/or cover) whereas the final rise in AE at the critical load was taken to represent the start of the irreversible damage. This final rise in AE normally followed an exponential pattern, which continued, to peak load. This corresponded to compacting of the rope sub-elements prior to catastrophic failure of the rope.

- The above has been observed for all the rope samples tested except covered Dyneema which behaved differently at the final stages of failure. Dyneema did not give rise to the final a sudden increase in emission prior to failure. Instead the emission pattern remained constant after the initial rise in AE due to the realignment of the rope sub-elements

Although presently there is a lack of interest in the literature on the application of acoustic emission technique in testing rope performance but the findings of this study is very encouraging. It is interesting to consider what factors influence the number of RDC produced by a given failure process. Obviously any variation in fibre fracture energy caused by variation in the fibre diameter failure stress or spacing as well as the stress concentration areas caused by the strand cross over points and the compaction of

fibres will influence the stress waves produced by the rope failure. The mechanism of AE propagation, detection and signal processing may also affect the recorded RDC. Until significant advances have been made in the understanding of these effects it will be difficult to explain quantitatively the form of the recorded RDC.

To make full advantage of the AE analysis, the following parameters can be taken to represent a damage event in the loading process:

- Activity level (RDC)
- AE onset and sudden final rise in emission during the loading cycle
- AE_extension curve pattern

8.10.1 AE Analysis of the Static Test Results

Acoustic emission was monitored during tensile testing of all the samples using the techniques shown in Figures 7.9b & 7.11. To determine the process of damage on the rope, the position and the intensity level of AE activity were chosen to represent the different events occurring during the loading process.

The results of the acoustic emission monitored during the tensile testing of the different rope samples are given in Tables 8.9 to 8.12. The AE behaviour of all the ropes tested has been compared and representative plots are presented in Figures 8.7b, 8.8b, and 8.15 to 8.18. The overall shape of the AE-extension curves normally has 3 step zones, which reflects the 3-zone behaviour of load-extension plots with varying degree of emission intensity. In the following sections attempt is made to correlate these events to the AE behaviour of each rope sample.

The difference in ring down activity between Dyneema and Vectran compared to Technora is so great that on a linear scale the pattern for Dyneema and Vectran seems to disappear. The case is true for both covered and uncovered ropes with the covered ropes showing a higher activity. The overall activity follows the pattern explained earlier.

Both Dyneema and Vectran display similar initial patterns which are not as smooth as the one for Technora ropes which can possibly be indicative of events happening at specific moments during the loading cycle, Both designs of Technora ropes display the same behaviour which is possibly indicative of cumulative events during the loading period until such time that there is sudden event that causes a higher activity. The fact that only the gradient changes can also indicate that the possible event is probably the prelude to fracture. The comparison of the shape and position of the ring down for the covered and uncovered ropes shows that the shape does not change but the levels do.

The AE activity after the removal of the cover reduces for Technora ropes. The plots are closer to each other than with the cover and the position of the 4 strand Technora rope change with 8 strand Technora rope. Once the cover is removed from the Dyneema and Vectran ropes they also display a lower AE activity but this time the difference between them is greater than with the cover. As opposed to the case of the Technora ropes. The load and extension values at which the onset of the load occurs are very close. However, the load and extensions at which the final part of the AE occurs are different, see Figure 8.48. The size effect has been eliminated by basing the calculations on the percentage of load rather than the actual.

a) AE from Dyneema Ropes

Representative plots of the onset and the pattern of the AE for Dyneema are presented in Figures 8.15 and 8.48. The results are also shown in Table 8.9. The final part of the AE for the covered Dyneema occurs at 780 N, which is higher that uncovered Dyneema, which occurs at 550 N. However, this time the extension is greater with 42

mm, compared to 32 mm. Both covered and uncovered Dyneema display initial AE profiles. However, their behaviour is somewhat different. The onset is of higher magnitude but a lower load for covered Dyneema. This can possibly be due to the lower coefficient of friction of Dyneema, which lower than all the other ropes tested in this study. The initial high AE activity can be attributed to a combination of the polyester cover; movement round the bollards and the realignment of the fibres/ strands. There are more prominent details in the AE profile of the covered Dyneema that uncovered. This can possibly be an indication of the events, which correspond to various stages, and events occurring during the loading process such as the knee point formation. There are two major differences between the covered and uncovered Dyneema:

- The level

The AE level is greater for covered Dyneema which is possible an indication of more severe or different type of behaviour. The only difference between the two tests is the existence of the polyester cover, which is responsible for the creation of the knee point. The relative initial movement of the cover and core is possibly responsible for the initial higher AE activity of the covered Dyneema. As the cover and core start to take on load at the same time, something unique to covered Dyneema occurs, i.e. the knee point is formed. It is the structural realignment of the rope sub-elements and the cover, which give rise to the second part of the AE. The higher levels of the AE activity are again due to the stress wave generated by the cover as it is being deformed at the same time as the core. The polyester cover not only is a different material it is also of a different design to that of the core. The polyester not only has a higher coefficient of friction that the Dyneema, thus creating higher activity it also has more interacting sub-elements.

- The final section

The major difference in the final part of the AE profile is a reflection of major difference in the behaviour of the covered and uncovered Dyneema. In the case of the covered Dyneema as the loading continues the cover grips the core leading to a

compaction of the fibres and strands causing possible fusion of the fibres/ strands. This is the point at which covered Dyneema acts as a single system. There are no longer any rope sub-elements which can great complicated stress waves. The load at which the fibres/strands begin to compact and fuse together is above 600 N. This is also the load range at which the final part of the AE starts and seems to remain constant. On the other hand, the lack of the cover allows the rope fibres and strands to move against each with greater ease. The fact that there is no knee point indicates a more smooth load transfer and hence a lower AE magnitude. Its low coefficient of friction ensures that it takes longer to overcome the slippage thus stress wave are created. The smooth load transfer is accompanied by a smooth AE profile, which shows less pronounced details until the final section, when there is a sudden sharp rise in the AE activity, which possibly coincide with the prelude to fracture. The fact that any heat generated during the loading process is rapidly lost to the environment, indicates that there will not be any fusion of the fibres/strands. However, slippage is mostly overcome by the tight compaction of the fibre/strands.

There will still be some interfibre/strand movement and possibly some premature failure of some fibres, which will generate increasing stress waves. This is a gradual process eventhough it happens over a very short period of time and is exaggerated as the fracture load is approached. This corresponds with the steep final rise in the AE. The final part of the AE occurs at nearly 85% of actual load, which is greater than all the ropes tested. This is possibly an indication that despite its lower melting point compared to the other ropes tested, the covered Dyneema has the highest damage tolerance. This is possibly due to this lower melting point which allows the fibres/strands to fuse together and hence carry the load more efficiently. On the other hand uncovered Dyneema has its final part starting at approximately 70% of its breaking load. This lower than 8 strand covered Technora but this load occurs at nearly 95% extension.

b) AE from Vectran Ropes

Representative plots of the onset and the pattern of the AE for Vectran are presented in Figures 8.16 and 8.48. The results are also shown in Table 8.10.The load at which the

final AE occurs is highest form covered and uncovered Vectran with 1300 N and 900 N respectively. The extension values also decrease from 35 mm to 28 mm. The AE profile is as described before as the loading process continues. Eventhough the final part of the AE occurs at a higher load and extension for the covered Vectran, the rate of rise is steeper for the uncovered Vectran. This is possibly due to the fact that the cover acts as an organiser; i.e. by its virtue of protection it holds the core together and acts as a damper of the stress waves generated. Also the removal of the cover allows the rope elements to move against each other more freely and thus there is more pronounced structural realignment leading to a more vigorous interaction of the rope sub-elements and hence the compaction of the fibre and strands occurs at a lower load. Thus the lower load at which the final part of the AE occurs. There is also a greater possibility that there are fibres failing at lower loads during the loading process.

Based on the percentage load, it can be seen that the load at which the final part of the AE occurs for covered Vectran is lower than covered Dyneema but for uncovered Vectran is lower that all the other rope samples tested. This is an interesting fining as the actual loads for the final part of the AE for covered and uncovered Vectran are greater than all the ropes tested. This can indicate that the irreversible damage in the uncovered Vectran starts at a lower load than covered Vectran. It can also give an indication of the damage tolerance of Vectran. The fact that the final part of the AE occurs at nearly 80% of breaking load for covered Vectran compared to approximately 60% for uncovered Vectran is possibly an indication that the covered Vectran has a superior damage tolerance. This is higher that all the rope samples tested except covered Dyneema. To complicate the matter further, not only does final part of the AE for uncovered Vectran starts only after 60% load but it also occurs after nearly 73% extension. This is greater than covered Dyneema, 4 strand Technora and covered 8 strand Technora.

c) AE from 4-Strand Technora Rope

Representative plots of the onset and the pattern of the AE for 4 strand Technora are presented in Figures 8.17 and 8.48. The results are also shown in Table 8.11.The AE profile for covered and uncovered 4 strand Technora is similar to that of the covered

and uncovered 8 strand Technora. In all the cases the overall AE profile follows a gradual shallow rise followed by a slight less gradual steep rise. The main difference is the magnitude of the AE, which is greater with the covered ropes.

In the cases of 4 strand Technora the removal of the cover causes the AE to occur sooner. The onset load and extension values are very close in both cases. However, it is a different story for the final part. The final part of the AE occurs at 700 N for covered 4 strand Technora compared to 528 N in the case of the uncovered 4 strand Technora. Eventhough the final part of the AE for the uncovered 4 strand Technora ropes occur at a lower load, it must also be borne in mind that they fail at a lower load and extension values. The fact that the AE profiles are as explained in the form of a shallow rise followed by a steep rise is possibly indicative of the damaging mechanisms involved.

The damage is most probably cumulative. In both Technora ropes namely 4 strand and 8 strand, The damage is exaggerated by the interfibre/strand movement. As Technora does not melt, the loading action causes the compaction of the fibres/strands. This is further exaggerated by the higher coefficient of friction of Technora compared to say Dyneema. Thus the whole interfibre/strand movement is more and more destructive. Hence the greater the applied load the greater the damage caused cumulatively. This is signified by the gradual rise in the AE and especially the final part which possibly correspond the to compaction of the fibres. The percentage load at which the final part of the AE occurs for covered 4 strand Technora is 67% compared to 65% for the uncovered 4 strand Technora. These are lower than all the ropes tested except uncovered 8 strand Technora and uncovered Vectran.

The fact that percentage load values for both cases is very close gives a possible indication that in both situation the rope has similar damage tolerance. However, the extension is at nearly 68% for the covered rope compared to approximately 60% for the uncovered case. The fact the AE starts at a higher load and extension percentage possibly indicates that the rope become a more efficient load bearing systems later but

it is also a more damage tolerant system. The order is similar to that of Vectran except for the values. The order is revered for Dyneema and 8 strand Technora.

d) AE from 8-Strand Technora Rope

Representative plots of the onset and the pattern of the AE for 8 strand Technora are presented in Figures 8.18 and 8.48. The results are also shown in Table 8.12.As mentioned in the previous section the AE behaviour of 8 strand Technora is very similar to that of 4 strand Technora. The overall profile again display the same shape i.e. a shallow gradual rise followed by a steep gradual rise. This is again possibly indicative of the gradual cumulation of damage during the loading process. The damage is exaggerated, as the interfibre/strand movement becomes more and more restricted due to the compaction of the fibres and strands. Thus any further relative movement of the rope sub-elements causes greater damage which creates higher stress wave. This is possibly the reason why the final sharp rise in AE coincides with the start of the linear part of the Load. This is also the point where the compaction of the fibres/strands has started and can be possibly the start of the irreversible damage.

The onset vales of load and extension for both covered Technora ropes are very close. Even the uncovered ropes have similar onset values despite having different number of strands. The main difference between the rope is the final part of the AE. In the case of 8 strand covered Technora, the final section of the AE occurs at a lower load of 580 N as opposed to 700 N for 4 strand covered Technora. This can be attributed to the fact that the 8 strand Technora rope has more twist and stress concentration points per given length than 4 strand Technora. Thus the rope sub-elements interact faster leading to a faster compaction of the rope at a lower load and extension. This in turn, as discussed, would lead to restriction the movement of the rope sub-elements and hence the damage starts sooner.

The fact that final part of the AE also starts sooner corresponds with the start of the linear part of the load-extension plots. The pattern is repeated with uncovered ropes. The percentage load and extension at which the final part of AE occurs are nearly 71%

and 72% respectively compared to nearly 64% and 78% for uncovered 8 strand Technora. The fact that the percentage load at which the covered rope reaches the final part of AE is greater possibly indicates that it is more damage tolerant but it arrives at that stage at lower percentage extension. It also indicates that the covered 8 strand Technora carries the load more efficiently but the damage occurs over a shorter extension.

8.10.2 AE Prediction of the Fracture Load

An important outcome of the Acoustic emission technique used is the possibility of being able to estimate the final fracture load from the value of the percentage load and extension values of the final part of the AE. The process could also be adopted to use the RDC count to achieve the same.

a) The procedure

1. Load the sample until the RDC count reaches a pre-set value
2. That value will correspond to a % load and extension for a specific rope
3. Estimate the maximum breaking load and extension

A computer routine could be written into the system which automatically stop the machine at the given threshold values and generate the desired load and extension values.

This technique if sufficient database of percentage load and extension is built into it and using an expert system has two main uses:

1. It can be tailor made to act as a non-destructive testing feature
2. Estimate the breaking load and extension of a rope of known material and design

The important factor to note is that this technique is an estimation technique. It is based on finding a close correlation between the AE and the load extension. It is also based on conducting several destructive tests and comparing the outcome and measuring the position and percentage load and extension values at which the final part of the AE has occurred.

The technique can be adopted as a way to identify different rope materials and designs. By programming the system with various AE signatures of different rope material and designs, it can be then used to identify a particular signal pattern and estimate its breaking load and extension with a possible given safety factor. The software can be an integrated part of another software such as Campus, which would then be able to supply further information such as mechanical and chemical properties etc.

8.10.3 AE Correlation of Damage in Pre-loaded Rope Samples

The ropes, as mentioned in the experimental section, were subjected to a series of preload values before taking them to failure, see Table 7.7. The values of the onset and the final parts of the AE are shown in the Tables 8.9 to 8.12 and are presented in Figures 8.49a & b.

The first observation is that the application of the preload does not seem to affect the overall profile of the AE but rather the magnitude which decreases with increasing preload values, see Figures 8.20b to 8.23b. The variable which may affect the behaviour of the ropes are the following:

- Material
- Diameter
- Number of strand (design)
- Twist

By basing the calculations of the onset of AE and the final part on the percentage load and extension the effect of the size (diameter) was removed. Three of the ropes used namely Dyneema, Vectran and 8 strand Technora have the same number of strands (design) and hence the amount of twist per given length of the rope was the same. Thus the main variable affecting the performance and the AE is the material and number of strands when comparing 4 strand Technora with the rest of the ropes tested.

It can be seen that the percentage load and extension of the final part of AE after preloading for both 4 and 8 strand Technora does not change a great deal. This is despite the difference in the design and amount of twist in the ropes. This can possibly indicate that material is a stronger factor in the behaviour of the rope. The same comparison shows that Vectran has the highest percentage load and extension. This again is possibly more significant because of the material since it is of the same design as the 8 strand Technora. The percentage load trend for Vectran is decreasing especially for the 100 N preload. The percentage extension trend is also decreasing but it is more significant towards the end rather than the beginning. Dyneema is again the odd one out. The fact that it has the same design as Vectran and 8 strand Technora indicates that again the most significant factor is the material. The percentage load trend at the final part of the AE is also decreasing as in the case of Vectran but more steeply. The greatest drop in percentage load is at 100 N. The trend for percentage extension is also decreasing and this time the maximum drop is with 100 N and 200 N.

a) AE Correlation of damage in Pre-loaded Dyneema Samples

Representative plots of the onset and the pattern of the AE for Dyneema are presented in Figures 8.20b and 8.49a& b. The results are also shown in Table 8.9. Dyneema again displays the same pattern. However, the magnitude of the AE decreases with increasing preload. This is possibly due to the fact that the preloading action leads to possible damage being induced. The higher the applied preload the greater the compaction of the fibres and strands and even fusion of the rope sub-elements. As the preloading action directly reduces the maximum breaking load and extension so does the overall time taken. The onset extension values remain consistently similar but the onset load increases slightly. As in the previous section it is the final part of the AE, which is

important and is possibly linked to a steadily decreasing load. This is due to the fact that increasing the preload causes the compaction of the fibres to occur faster and at a lower load values. This in turn leads to a reduced breaking load and the final part to begin at a lower load. As the final part of the AE is thought to be linked to the start of the linear part of the load-extension thus its value also decreases.

b) AE Correlation of damage in Pre-loaded Vectran Samples

Representative plots of the onset and the pattern of the AE for Vectran are presented in Figures 8.21b and 8.49a & b. The results are also shown in Table 8.10. The behaviour of Vectran is somewhat different to that of Dyneema. The AE profile still display a same pattern but the details are less prominent. In fact the AE profiles if smoothed out can be considered to be similar to those of Technora. Nonetheless there are still steps which can be indicative of the events occurring during the loading history but at a faster rate than as received Vectran.

There is still a loss in both maximum breaking load and extension with increasing preload values but not enough to cause compaction of the rope sub-elements which would ultimately lower the overall magnitude of the AE. In fact during the unloading process the rope sub-elements are allowed to move against each other increasing the possibility of structural realignment and interfibre/strand movement during the reloading which generates higher AE activity. However, the actual final loads and extension at which the final part of the AE occur as in the case of Dyneema, steadily decrease. This can also be an offshoot of the same process as in Dyneema in which the linear part of the load and extension starts sooner with increasing preload. Thus the final part of the AE which is indicative of this also starts at a lower load.

c) AE Correlation of damage in Pre-loaded 4-Strand Technora Samples

Representative plots of the onset and the pattern of the AE for 4 strand Technora are presented in Figures 8.22b and 8.49a & b. The results are also shown in Table 8.11. The behaviour again as explained for Vectran. The overall AE profile remains the same with increasing preload values with only the magnitude changing. The onset load and

extension values are very close. The load at which the final part of the AE occurs decreases gradually. This is again possibly due to the same reasons mentioned for Vectran, i.e. increasing preload leads to compaction of the fibres/strands to occur faster and a lower load, which indicates that the linear part of the graph would start sooner. Therefore the final part of the AE also starts at a lower load with increasing preload.

d) AE Correlation of damage in Pre-loaded 8-Strand Technora Samples

Representative plots of the onset and the pattern of the AE for 8 strand Technora are presented in Figures 8.23b and 8.49a & b. The results are also shown in Table 8.12. The behaviour of 8 strand Technora is similar to 4 strand Technora

8.10.4 AE Correlation of damage in Strands Removed From Rope samples

The ropes are strand tested by removing strands one at a time from the rope construction in order to investigate the effect strand failure in the whole rope. The results are of the AE are shown in Tables 8.9 to 8.12 and shown in Figures 8.29b to 8.32b as well as in Figures 8.50a & b.

The overall AE profiles for all the ropes tested remains unique to the rope. The removal of the strands only affects the AE magnitude. Dyneema and Vectran still display the step rise behaviour compared with the gradual rise of Technora. The AE activity increases with increasing number of strands. This is possibly due to the fact that the greater the number of strands, the greater the amount of twist and the greater the amount of interfibre/strand movement and hence the greater the stress waves generated.

a) AE from Dyneema Rope Strands

The overall AE profiles for one to eight strands Dyneema is similar and all display a step rise, which is possibly indicative of the fact that underlying failure mechanism is the same for the rope to be similar. As the number of strands increases so does the interfibre/strand movement thus the magnitude of the AE rises too.

The onset loads and extension remain very close. However, the loads and extension at which the final part of the AE occurs increases gradually. This is possibly due to the fact that the loading process only leads to the compaction of the fibres, as any heat generated is rapidly lost to the environment. The low coefficient of friction of Dyneema also leads to a greater interfibre/strand movement which ultimately leads to greater stress wave generation and the linear part of the load-extension to occur at higher loads which is why the load and extension values at which the final part of the AE occur gradually increase.

b) AE from Vectran Rope Strands

Vectran also displays similar overall AE profiles for 1 to 8 strands with only the magnitude changing. The behaviour is still step rise which again indicative of the underlying failure mechanism. As in the case of Dyneema the onset load and extension values remain consistent. Only the load and extension values at which the final part of the AE occurs increase. This happens for the same reason as for Dyneema. The magnitude is higher which is probably due to its higher breaking load and extension value.

c) AE from 4-Strand Technora Rope Strands

Again as in the case of Dyneema and Vectran the overall AE profile remains unchanged except for the magnitude as the number of strand increases. The behaviour is still that of a shallow gradual rise followed by a steep rise, which is indicative that the underlying failure mechanism is the same.

Again the load and extension values at which the final part of the AE occurs increases with increasing number of strands for the same reasons mentioned for Dyneema and Vectran. In all the cases the linear part of the load-extension occurs at higher load and extension values as the number of strands increases due to increased interfibre/strand movement. Thus the load and extension values for the final part of AE which correspond to the start of the linear part also increase with increasing number of strands.

d) AE from 8-Strand Technora Rope Strands

The behaviour of 8 strand Technora follows the same pattern as 4 strand Technora in terms of profile and the reasons are the same as those of Dyneema, Vectran and 4 strand Technora. Again the onset value are consistent but the load and extension at which the final part of the AE occurs increase. Again as in the other ropes tested the linear part starts at a higher load and extension with increasing number of strands, which is why the load and extension values for the final part of the AE increase.

8.11 Damage and Failure Analysis

In order to discuss the accumulation of damage in the samples the following model based on the literature is used.

A rope is made of several sub-elements[61-65]. Figures 8.50 and 8.51, shows the events happening from the start of loading to the final failure. In this section an explanation for the failure of the ropes used is presented.

8.11.1 Initial Rise

As the rope is loaded all the components of the rope start moving until slack is taken out. This corresponds to the first zone on the load/extension plots and the onset of the AE, due to the stress wave generation as the helix angle is closed down so that the rope take on load. During this process strands realign themselves as the fibres twist and turn. There is also some movement of the core in relation to the cover.

8.11.2 Second Phase

Once the slack is taken out, there is still movement round the bollards. This movement is probably independent of the central part of the rope between the two bollards. This movement continues until the load exceeds the slippage load. At this stage the fibres

round the bollards are more compressed than the ones in between the two bollards. The cover has gripped the core, and both are carrying the load. This corresponds to the second part of load/extension plot and the AE plot.

8.11.3 Third Phase

Once the cover has gripped the core causing compaction of the fibres/strands and the helix angle decreased enough, the rope begins to act as a single efficient load transfer system. This is also the start of the linear part of the load/extension corresponding to the third part of the AE plot.

8.11.4 Failure Analysis

At this point as the prelude to failure several events take place[93-96]. These events can collectively cause failure to occur. As the third zone is approached the strand and fibres are still moving in relation to each other and the cover. There is the internal inter-fibre/strand movement and the external movement of the surface of fibres/strands against the inner surface of the cover. The internal fiction and realignment leads to heat build up and stress concentration at places where the strands move against each other and cross one another. The external friction generates heat, which can soften the outer surface of Dyneema fibres and strands. The cover at this stage is gripping the core with a greater force as it is loaded leading to a reduction of diameter.

This reduction in diameter would normally be at a different rate to the core because of the difference in materials properties and design but to a certain extent at this stage in loading even lateral compression of the cover is governed by the loading of the core. However, as the surface of the core is heated up due to the external friction of the strand surfaces and the inner surface of the cover, it takes on the imprints of the cover. As the heat is built up increases so does the creep rate. There is a constant temperature rise leading to a stiffness increase and irreversible damage. Once the applied load reaches a critical value, the least critical or the weakest component of the rope failed. At this instant there is a dynamic load transfer the remaining elements of the rope. If the

remaining components can not carry the applied load then the rope fails. However, if they can sustain the load then the process is repeated until the remaining rope element(s) could no longer support the applied load and failed.

8.11.5 Failure Instant

At the instant of failure, the two failed ends recoil explosively due to the stored elastic energy during the loading. The fracture or the failure creates a loud audible noise, which could be used as a basis of sound analysis, see future works, for the analysis of sound signature of different materials. New surfaces are also created. All these also lead to the generation of stress waves, which are inaudible, but could be detected using the acoustic emission and be used to explain the behaviour of the rope at failure.

Finally the shear amount of elastic energy released during recoiling leads to a very sudden frictional movement of the rope components and the cover which generates a great deal of heat which is manifested as the melting of the failing ends. However, this melting is only applicable to the covered Dyneema and Vectran ropes, see Figure 8.51. This is because the cover has a different elongation to failure value to the core so it does not fail at the same time as the core. Therefore as the core recoiled there is a rapid internal friction between the fibres/strand and external friction with the inner surface of the cover. The heat built up can not escape to the surrounding. However, with the uncovered ropes there is no external friction between the fibres/strands and cover, therefore and heat generated is rapidly dissipated and lost to the surrounding as fast as it is generated. Thus there is no sign of any melt down in the Dyneema and Vectran fibres. As the two ends of the uncovered ropes recoil, the strands and fibres move against each other and since not all the strands and fibres are carrying equal loads and possibly there are failures of some strands and fibres before the final failure, the components of the failed end tend to puff up and fuzz out in the failure region.

8.11.6 Further Detailed Failure Analysis

For a given gauge length between the bollards, there are several cross over points, i.e. the places where strands cross each other. There is no localised stress concentration points prior to the application of the load except that which has been built into the rope during fibre and rope manufacture, as well as those created by the sample preparation procedure. As the applied load increases, these cross over points change in size, i.e. **a** decreases and **b** increases. This immediate leads to the start of abrasion between the rope sub elements as they try to realign themselves by taking the inherent twist out. This process continues until the gap **a** has decreased in size so much that it now can be considered to become ≈0 and **b** reaches its maximum length before extending and deformation, see Figure 8.53.

The rope elements have by this time experienced, abrasion, structural realignment and creep. As the loading process increases, there is a relative movement of strands, i.e. the gap **a** is trying to become smaller at the same time as **b** tries to increases. This causes the abrasion of the strands against each other as well as the compression at the cross over points, which act as stress raisers. The greater the load gets, the smaller the gap **a**, the larger the length **b**, the higher the stress concentration, the greater the compression at the same time there is a lateral movement of the rope elements which leads to subsequent abrasion of the fibres and strands. This abrasion generates heat, which can cause the fusion of the fibres and strands. The compression at the cross over points can lead to compression fatigue damage especially in the aramid ropes. As the process continues the weakest link fails and the load is dynamically transferred to the remaining strands.

The remaining strands have already been weakened by the previous loading action, namely abrasion, creep, structural realignment and friction. The load applied to the remaining strands is also of greater magnitude since it is dynamically applied and the ratio of the magnitude of the load divided by the number of strands is greater. It is the case of weakened weakest link taking on load and hence failing again but this time at a lower load since it has already been damaged. At this time there is again the dynamic

load transfer to the remaining strands which have already been further damaged. The strands are weaker and are subjected to a greater load; thus the weakest link will fail at a much lower load. This process continues until the final catastrophic failure.

The length **a** & **b** do not strictly remain constant since not all the strands carry equal amount of the applied load. There is also some movement of the position of the point of **a** & **b**, which leads to the stress concentration points moving. Thus there is a complex combination of stress concentration and abrasion. At the instant of fracture as the two failed ends recoil releasing their stored energy, shock waves are sent through the rope. The magnitude of these shock waves decrease as they move furthers away from the fracture zone. The two fractured ends do not recoil with the same amount of energy as has been observed by the amount of damage at both failed ends. The cover also contributes to the energy release since as the strands collapse, the cover limits their lateral movement. The travelling shock waves cause the strands to collapse decreases in magnitude as they travel along the length of the rope.

The analogy is the swinging balls hitting each other. The first ball has a highest energy and as it hits the next ball it transfers the load to the next ball. The magnitude of the energy has decreased since there is some loss of energy due to transformation of energy. As the process and balls hit each other the last ball has the least energy. If the number of balls used is large enough then theoretically there will a number of balls which no longer is affected by this energy release. This is the possible reason why the maximum damage is at the fracture zone, signified by melting in Dyneema and intermittent stiffness increases along the length of the rope. In the case of Dyneema these stiffness increases are due to the fusion of the rope elements because of the heat generated which is also partly due to the abrasion of the core against the cover. This is also exaggerated after fracture because the recoiling ends rub against the cover at very high speeds creating greater amount of heat. In the aramid ropes the damage at the end has been due to fibre damage and fuzzing and stiffness increase due to sever compression of the strands. It is this complex movement of strand and their relative movement in relation to the cross over points which is the prelude to where maximum

and minimum stiffness occurs bearing in mind that some damage has already occurred during the loading action prior to the final failure.

In the case of covered ropes, there is the added effect of the abrasion between the inner surface of the cover and the outer surface of the core. However, at the start not all the rope is in contact with the cover. Again along the length of the rope only the cross over point are in contact with the cover. As the loading takes place and the strands start to move and try to realign themselves. The inherent twist in the rope and the fibres is taken out. Therefore the abrasion area moves and leads to weakening of the core along its length. This process continues until the cover grips the core such that there is no longer any lateral movement between the cover and the core or until the cross over points become so tight that the length **b** approaches zero. At this point all the length of the rope starts to be abraded. However, the rope has already been weakened. Thus it is a race between the weakest link which is also the most severely abraded member failing and if it will lead to cascade failure.

9.0 CONCLUSIONS

Performance of three different small diameter ropes in two different size and constructions (including the effect of cover) has been investigated. Changes in mechanical properties of Dyneema, Vectran and Technora ropes, as a result of different preloading, strand removal, and environmental conditions have been assessed by means of conventional tensile tests, backed up by non-destructive evaluation techniques such as acoustic emission monitoring and thermography.

9.1 Static Tensile Failure

The present investigation shows that, on the basis of the tests carried out, all the fibre ropes performed satisfactorily under static tensile loading with breaking loads of (Dyneema = 896 N, Vectran = 1539 N, 4-strand Technora = 1023 N, 8-strand Technora = 798 N) and maximum extension to failure of (Dyneema = 48 mm, Vectran = 41 mm, 4-strand Technora = 36 mm, 8-strand Technora = 32 mm).

Changes in the mechanical properties can be identified in terms of the effect of static pre-loading, cyclic pre-loading, and exposure to different environment on controlling the failure mechanisms for a given type of test. All three rope materials undergo 3 stages before the final catastrophic failure namely, realignment of fibres, inter fibre/strand/cover abrasion and fibre compaction/lateral compression. The strand cross exacerbates the accumulation of damage over points and helix angle. Dyneema and Vectran ropes behave in a similar manner during the loading process. The final permanent damage involves melting and the subsequent fusion of fibres whereas Technora suffers a gradual increase in damage, by compaction of fibres, until the final break.

9.2 Residual Strength Measurement

The residual strength of preloaded samples indicate that none of the rope materials loose strength dramatically, in some cases a preload application can even improve the strength. In every case preloaded samples behave more linearly up to the pre-load value. However, an increase in the pre-load value results in an increase in the material stiffness, at the expense of reduced failure extension.

The residual strength of Dyneema rope after cyclic loading is investigated and some relationships between cycles and damage are suggested. It has been established that moderate loading-unloading of up to 300 N and 20 cycles improves the strength of Dyneema by approximately 6%. However the residual strength is dramatically reduced beyond 1000 cycles. This loss in strength is due to the occurrence of fibre damage resulting from hysteresis effect.

9.3 Strand-Rope Efficiency Test

The tensile response of rope samples, with different number of strands, has been studied to investigate the transformation of failure modes and strength efficiency from a single strand rope to multi-strand ropes.

9.4 Acoustic Emission

Acoustic emission monitoring identifies certain obvious damage mechanisms, such as fibre fusion, and distinguishing features characteristic of the permanent (irreversible) damage in different types of rope. It is particularly evident that the AE response of damage in Dyneema and Vectran is in steps whereas in Technora it is a gradual increase in emission. The ability of acoustic emission to detect different stages of damage in both the static tensile and residual strength tests of rope samples is demonstrated. AE is also sensitive to the clamping pressure of the rope samples and has been helpful in identifying the right clamping pressure for an optimum tensile testing

process. Very high RDC emission during the initial stages of tensile testing is responsible for slippage in the test rig clamp. The change from gradual increase to an exponential rise in emission signifies the point of permanent damage in the rope, beyond which the residual strength of the rope is reduced considerably. It has been found that the principle of Kaiser effect does not apply to these rope materials.

9.5 Thermography

Thermography has been shown to be an effective method for assessing the temperature distribution on the rope surface during tensile loading. The results confirm the contribution of elevated temperature in Dyneema rope to fibre melting and fusion before final failure.

9.6 Environmental Conditioning

Changes in mechanical properties of Dyneema rope brought about by different environmental conditioning have been studied by means of tensile testing. It has been established that Dyneema performs well under, natural weathering and cold air of -22 °C but when it is exposed to hot air at 54 °C the strength is reduced, because this temperature is close to the maximum safe operating temperature of Dyneema, which might accelerate creep. When Dyneema is exposed to sea water at 54 °C for 16 days, the strength drops by 12%. Further SEM examination reveals that the salt crystals are the main contributors to the fibre damage.

9.7 Abrasion Failure

Rope on rope abrasion failure of Dyneema and Technora rope samples has been examined, using an in-house abrasion test rig. Different mechanisms of damage have been investigated. The role of cover in providing protection is analysed. The absence of cover reduces the abrasion resistance of Dyneema and Technora ropes by 90% and 96% respectively when the rope samples are under a load of 4 kg.

10.0 SUGGESTIONS FOR FURTHER WORK

In the light of the significant results obtained in this study, the next logical step forward is to investigate more closely into the strength and failure of these high performance rope materials. Hence further research directed towards the following is recommended.

All the fibre ropes tested have shown some interesting features, especially the ability to attain high tensile strength under different loading and environmental conditioning. This is an area for an in-depth investigation into evaluation of damage and failure in high performance ropes.

Possible areas of investigation can be suggested as follows

- Examine the effect of creep on the load bearing capability
- Assess the strength and failure modes under dynamic shock loading conditions
- Investigate the performance of different methods of rope termination in providing an efficient load transfer
- Study the effect of bending and flex resistance on the residual strength of the rope materials
- Investigate the residual strength of ropes with known flight (loading) history.

REFERENCE:

[1] J.E. Smith, Structures in Deep Ocean (Engineering Manual for Underwater Construction), Chapter 7, Buoys and Anchorage systems, US Naval Civil Engineering Laboratory, Port Hueneme, Cal. Oct. 1965, PP3-10.

[2] D. Himmelfarb, Man-made Textile Encyclopaedia, Chapter VII, F. Press, Editor, New York, 1961 (no year given) , P 291.

[3] W.E. Morton and J.W.S. Hearle, Physical Properties of Textile Fibres, Butterworth & Co., The Textile Institute, Manchester & London, 3rd Edition, 1993, ISBN 1 870812 417.

[4] J.S. Preisser and G.C. Greene, Effect of Suspension Line Elasticity on Parachute Loads, Journal of Spacecrafts and Rockets, Vol. 7, No. 10, Oct. 1970, PP1278-80.

[5] E. K. Huckins III, Snatch Force During Lines-First Parachute Deployments, Journal of Spacecraft and Rockets, Vol. 8, No. 3, Mar. 1971, PP298-299.

[6] J. W. Purvis, Prediction of Parachute Line Sail During Lines-First Deployment, Journal of Aircraft, Vol. 20, No. 11, Nov. 1983, PP940-945.

[7] J. W. Purvis, Improved Prediction of Parachute Line Sail During Lines-First Deployment, Aerodynamic Conference, AIAA Paper, (CP843), 1984, Contract No. DE-AC04-76DP00789, Paper 84-0786, PP25-33.

[8] G. A. Barnard, Analysis of the Distribution of Load Among the Lines of an Inflating Cruciform Parachute, , AIAA 9th Aerodynamic Conference, Oct. 7-9, 1986, PP86-91.

[9] K. Tanzler, Rope Breakage, Cross-Country, April/May 1994, P8 & 40

[10] DHV Report published in the Skywings, Sept. 1995.

[11] Skywings Magazine, June 1994, PP9-10.

[12] Dipl. Ing. Karl Bauer, Swing, Vectran Cord Materials, Drachenflieger Magazin, 12/93.

[13] Private communication with Mr Jacobs, R & D, Director, DSM 1995

[14] J.L. Taylor and N.F. Casey, The Acoustic Emission of Steel Wire Ropes., Wire Industry, Vol. 51, No. 601, January 1984, PP79-82.

[15] N.F. Casey and J. L. Taylor, An Instrument for the Evaluation of Wire Ropes: A Progress Report, British Journal of Non-Destructive Testing, Vol. 29, No. 1, January 1987, PP18-21.

[16] N.F. Casey, H. White, and J.L. Taylor, Frequency Analysis of the Signals Generated by the Failure of Constituent Wires of Wire Rope, NDT International, Vol. 18, No. 6. December 1985, PP339-344.

[17] N.F. Casey and J.L. Taylor, The Evaluation of Wire Ropes by Acoustic Emission Techniques, British Journal of Non-Destructive Testing, Vol. 6, No. 7, Nov. 1985, PP351-356.

[18] N.F. Casey, D. Wedlake, J.L. Taylor and K.M. Holford, Acoustic Detection of Wire Rope Failure, Wire Industry, Vol. 52, No. 617, May 1985, PP307-309.

[19] N.F. Casey, K.M. Holford and J.L. Taylor, The Acoustic Evaluation of Wire Ropes Immersed in Water, NDT International, Vol. 20, No. 3, June 1987, PP173-176.

[20] N.F. Casey, K.M. Holford and J.L. Taylor, Wire Break Detection During the Tensile Fatigue Testing of 40 mm Diameter Wire Rope, British Journal of Non-Destructive Testing, Vol. 30, No. 5, Sept. 1988, PP338-341.

[21] M.A. Hamstad, A discussion of the Basic Understanding of the Felicity Effect in Fibre Composites, Journal of Acoustic Emission, Vol. 5, No. 2, April/June 1986, PP95-102.

[22] I. Harrop and J. Summerscales, Acoustic Emission Testing of the Structural Integrity of Multicore Cable, British Journal of Non-Destructive Testing, Vol. 31, No. 7, July 1989, PP383-386.

[23] H.H. Vanderveldt and Quang Tran, Acoustic Emission From Synthetic Rope, Naval Engineers Journal, Vol. 83, No. 6, Dec. 1971, PP65-68.

[24] J.H. Williams, Jr and S.S. Lee, Acoustic Emission/Rupture Load Characterisations of Double Braid *Nylon* Rope, Marine Technology, Vol. 19, No. 3, July 1982, PP268-271.

[25] J.H. Williams, Jr, J. Hainsworth, and S.S. Lee, Acoustic-Ultrasonic Non-destructive Evaluation of Double Braid *Nylon* Ropes Using the Stress Wave factor, Fibre Science and Technology, Vol. 21, No. 3, 1984, PP169-180.

[26] P.A.A. Laura, Acoustic Emissions From Wire and Synthetic Ropes, Shock and Vibration Digest Journal, Vol.17, No. 12, Dec. 1985, PP3-5.

[27] P.A.A, Laura, Evaluating the Structural Condition of Synthetic and Metallic Cables, Ocean Engineering , Vol. 22, No. 6, 1995, PP551-562.

[28] L. Yeager, A.A. Hochrein Jr, J.R. Sherrard, Application of Internal Friction Damping as a Non-destructive Evaluation Technique for Synthetic Ropes Used as SPM Hawsers in Deep-water Ports, Proceedings of the 14th Annual Offshore Technology Conference, Houston, Texas, May 3-6, 1982, Paper OTC 4306, PP61-70.

[29] J.H. Williams Jr, M.J. Connolly, K.M. Malek and S.S. Lee, Ultrasonic Wave Velocity in Double Braid *Nylon* Rope, Fibre Science and Technology, Vol. 21, No. 1, 1984, PP41-57.

[30] J.H. Williams Jr, S.S. Lee, S.G. Lopez-Martinez and H. Sohn, Ultrasonic Wave Speed Tension Characterisations of Synthetic Ropes, Proceedings of the International Offshore and Arctic Engineering Symposium, Vol. 2, 1986, Pub by ASME, PP405-409.

[31] J.M. Winter Jr and R.E. Green Jr, Non-destructive Evaluation of Synthetic *Nylon* Rope Using Mechanical Spectroscopy, Proceedings of the 11th World Conference on Non-Destructive Testing, Las Vegas, ISBN 0 931 40307 3, 1985, PP799-805.

[32] H. Kwun and G.L. Burkhardt, Non-destructive Testing of Ropes Using the Transverse Impulse Vibration Method, Review of Progress in Quantitative NDE Conference, July 31-August 5, La Jolla, California, 1988, PP1-8.

[33] H. Kwun and G.L. Burkhardt, Feasibility of Non-destructive Evaluation of Synthetic or Wire Ropes Using a Transverse-Impulse Vibrational Wave, NDT International, Vol. 21, No. 5, Oct. 1988, PP341-343.

[34] N.L. Sao, Non-Destructive Evaluation of Steel Wire Rope - Part III, Wire Industry, Vol. 63, No. 794, May 1996, PP382-387.

[35] N.L. Sao, Non-Destructive Evaluation of Steel Wire Rope - Part IV, Wire Industry, Vol. 63, No. 755, Nov. 1996, PP382-387.

[36] D. Cortazar, H.A. Larrondo, A.A. Laura and D.R. Avalos, Low Cost Fibre Optic System for Monitoring the state of Structural Health of a Mechanical Cable, Ocean Engineering (Pergamon) Vol. 23, No. 2, Feb. 1996, PP193-199, ISBN: 0080226949.

[37] C.H.H. Corden, Review of Wire Rope NDT, Wire Industry, Vol. 56, No. 669, Sept. 1989, PP583-586.

[38] R.J. Woodward, Detecting Fractures in Steel Cables, Wire Industry, Vol. 56, No. 667, July 1989, PP401-405.

[39] John Flory, Mike Parsey, and Chris Leech, A Method of Predicting Rope Life and Residual Strength, Proceeding of OCEANS 89, Vol. 5, 1989, PP1436-41.

[40] Mathematical Models of Parallel and Twisted Synthetic Fibre Ropes Under Static Loading, Final Report, Phase 1, Validated Response Models For New Rope, For Naval Civil Engineering Laboratory, -Port Hueneme, CA, By Tension Technology International, Weston, MA, 1989.

[41] Hwai-Chung Wu, Frictional Constraint of Rope Strands, Journal of Textile Institute, Vol. 84, No. 2, 1993, PP199-213.

[42] A. Cardou and C. Jolicoeur, Mechanical Models of Helical Strands, Applied Mechanics Review, Vol. 50, No. 1, Jan. 1997, PP1-14.

[43] L.F.E. Hoppe, Modelling the Static Loading behaviour of Dyneema in Wire Rope Construction, DSM Research, Geleen, The Netherlands

[44] John, F. Flory, Hawser Test Report, Data on Large Synthetic Ropes in the Used Condition, Oil Companies International Marine Forum, Witherby and Co., Ltd, London 1982.

[45] J.F. Flory, Strength Reduction Curve Method of Predicting Residual Strength, Proceedings of International Conference on Reliability Stress Analysis & Failure Prevention, San Francisco, August 1980, PP269-274.

[46] J.W.S. Hearle, R.E. Hobbs, M.S. Overington, S.J. Banfield, Modelling Axial Compression Fatigue in Fibre Ropes, Proceedings of the Fifth International Conference of Offshore and Polar Engineering, ISOPE-95-RH-02, The Hague, The Netherlands, June 11-16, 1995, ISBN 1-880653-18-4, PP273-277.

[47] R.E. Pitt and S.L. Phoenix, On Modelling the Statistical Strength of Yarns and Cables Under Localised Load Sharing Among Fibres, Textile Research Journal, Vol. 51, 1981, PP408-425.

[48] J.F. Flory, New and Used Strength of Large marine Hawsers, Proceedings of the 14th Annual Offshore Technology Conference, Houston, Texas, May 3-6, 1982, Paper OTC 4304, PP37-48.

[49] S. Tsurta, Residual Strength of Aramid Rope, Proceedings of 18th Annual Offshore Technology Conference, Houston, Texas, Paper OTC 5189, May 5-8, 1986, PP317-324.

[50] R. Lattin, Ed., History of Rocketry and Aeronautics, CAAS History Series, Vol. 8, 1988, PP11-22.

[51] B.C. Hacker, The Gemini Paraglider, A Failure of Scheduled Innovation, Social Studies of Science, Vol. 22, No. 2, 1992, PP387-406.

[52] British Hanggliding & Paragliding Association (BHPA) Beginner's Manual

[53] Private Communications with Bill Morris, March 1996

[54] E. Scala, Ropes and Cables as Composite Linear Tensile Materials, Conference Proceedings of the 5th International Conference on Composite Materials, Metallurgical Society, ISBN: 0 87339 000 8, 1985, PP483-496.

[55] J.W.S. Hearle, Ropes: From Ancient Craft to Modern Engineering, Part 1: From Hemp to HMPE – New fibres and new constructions, Textile Horizons, April/May 1996, PP12-15.

[56] J.W.S. Hearle and M.R. Parsey, Man-Made Fibre Ropes, the Economic Intelligence Unit, Technical Textile markets, Oct. 1991, PP38-59.

[57] D.E. Beers and J.E. Ramirez, Vectran High Performance Fibre, Journal of Textile Institute, Vol. 81, No. 4, 1990, PP561-574.

[58] D.E. Beers and J.E. Ramirez, Vectran Fibre for Ropes and Cables, Marine Technology Society Conference, MTS'90, Sept. 26-28, 1990.

[59] Marlow ropes, Trade Literature, Marlow Ropes Ltd, Marine & offshore Division, Diplock Way, Hailsham, East Sussex, BN27 3JS, May 1993.

[60] P.G. Riewald, Ropes and Cables From Aramid Fibres for Ocean Systems, Proceedings of the 87th National Meeting of the American Institute of Chemical engineers, Boston, MA, August 19-22, 1979.

[61] Chris Leech, The Assembly and Modelling of Synthetic Ropes Using Microcomputers, Proceedings- Microcomputers in Engineering, ISBN 0906674565, 1986, PP549-559.

[62] C.M. Leech, Theory and Numerical Methods for the Modelling of Synthetic Ropes, Communications in Applied Numerical Methods, Vol. 3, 1987, PP407-413.

[63] C.M. Leech, J.W.S. Hearle, M.S. Overington and S.J. Banfield, Modelling Tension and Torque Properties of Fibre Ropes and Splices Proceedings, 3rd International Offshore and Polar Engineering Conference, Singapore, 6-11 June 1993, PP370-376.

[64] C. M. Leech, Aspects of Modelling of Synthetic Fibre Ropes, Proceedings of Marine technology society, Science and Technology for a New Oceans Decade, MTS'90, Washington D.C. Sept. 26-28, Vol. 1, 1990, PP43-48.

[65] C.M. Leech, The Assembly and Modelling of Synthetic Ropes Using Microcomputers, Communications in Applied Numerical Methods, Vol. 3, 1987.

[66] ASTM D-123-93, Standard Terminology Relating to Textiles, 1993.

[67] BS 3724 : 1991, Glossary of Terms Relating to Fibre Ropes and Cordage

[68] BS 4928 : 1985, Specifications for Man Made Ropes

[69] Marlow ropes trade literature, Offshore Ropes Literature, 1985.

[70] B.J. Dunn, Ropes made from man made fibres, Rope Properties, Bridon ropes, Orange series books, B, 1978

[71] Bridon Marine Trade Literature, Viking Rope Literature, 1986,

[72] J. Yeardley and K. Firth, The Use of Polyester Mooring Line for Ultra Deep-water Applications, Proceedings of the International Two day Conference on Mooring & Anchoring , 10 – 11 June 1996,

[73] K.R. Bitting, Dynamic Modelling of *Nylon* and Polyester Double Braid Rope, Conference Proceeding, OCEANS'85, ISSN 0197-7385, 1985, PP1344-1353.

[74] Shipen Li, E. Curran, S. Backer and P. Griffith Hysteresis Heating of Synthetic Fibre Ropes, Marine Technology Society Conference, MTS'90, Sept. 26-28, 1990, Vol. 2, ISBN 0-933957-06-8, PP295-300.

[75] M.S. Overington and C.M. Leech, Modelling Heat Build-up in Large Polyester Ropes, International Journal of Offshore and Polar Engineering, Vol. 7, No. 1, May 1997, PP63-69.

[76] Hwai-Chung Wu, Moon Hwo Seo, S. Backer and J.F. Mandell, Structural Modelling of Double-Braided Synthetic Fibre Ropes, Textile Research Journal, Vol. 65, No. 11, 1995, PP619-631.

[77] G. Amaniampong and C.J. Burgoyne, Analysis of the Tensile Strength of Parallel-Lay Ropes and Bundles of Parallel Elements by Probability Theory, International Journal Solids Structures, Vol. 32, No. 24, 1995, PP3573-3588.

[78] C.J. Burgoyne and J.F. Flory, Length Effects Due to Yarn Variability in Parallel-Lay Ropes, Marine Technology Society Conference, MTS'90, Science & Technology for a New Ocean Decade, Washington, D.C, Vol. 1, ISBN 0933957068, 1990, PP49-55.

[79] R.P. Nachane and K.R. Krishna Iyer, Prediction of Bundle Strength from Single-Fibre Test, Data Textile Research Journal, Vol. 50, Oct. 1980, PP639-641.

[80] S. Backer and P. Hsu, Applications to Product Design and Process Control, Proceedings of the 3rd Japan-Australia Joint Symposium on Objective Measurement, Kyoto, Japan, 5-7 September 1985, P101.

[81] M.H. Seo, Ph.D. Thesis, Massachusetts Institute of Technology, 1988.

[82] M.L. Realff, M. Seo, M.C. Boyce, P. Schwartz and S. Backer, Mechanical Properties of Fabrics Woven from Yarns Produced by Different Spinning Technologies: Yarn Failure as a Function of Gauge Length, Textile Research Journal, Vol. 61, No. 9, 1991, PP517-530.

[83] W.F. Knoff, A Modified Weakest-Link Model for Describing Strength Variability of Kevlar Aramid Fibres, Journal of Materials Science, Vol. 22, 1987, PP1024-1030.

[84] Hwai-Chung Wu, An Energy Approach for Rope Strength Prediction, Journal of Textile Institute, Vol. 83, No. 4, 1992, PP542-549.

[85] R.G. Djaja, P.J. Moss, A.J. Carr, G.A. Carnaby and D.H. Lee, Finite Element Modelling of an Oriented assembly of Continuous Fibres, Textile Research Journal, Vol. 62, No. 8, 1992, PP445-57.

[86] M. Keefe, D.C. Edwards and J. Yang, Solid Modelling of Yarn and Fibre Assemblies, Journal of Textile Institute, Vol. 83, No. 2, 1992, PP185-196.

[87] M. Keefe, Solid Modelling Applied to Fibrous Assemblies Part I: Twisted Yarns, Journal of Textile Institute, Vol. 85, No. 3, 1994, PP338-349.

[88] P. Petrina, S.L. Phoenix, F.A. Leban and V.J. Pappas, Lifetime Studies of Synthetic Cables Subjected to Lateral Contact Loads From Sheaves, Oceans'95 Conference Proceedings (IEEE), Vol. 2, P1319-1330, 1995, ISSN 0197 7385.

[89] B.H. Markusssen, E.S. Hunt and R.E. Hobbs, Wear of *Nylon* Hawsers on Rollers, pulleys and Fairleads, Proceedings of the 16th Annual Offshore Technology Conference, Houston, Texas, Paper OTC 4765, May 7-9, 1984, PP463-470.

[90] R. Wurgler, The Rope Salad, Paragliding, The Magazine, P27-28, PP40-41.

[91] Private communication with Mr Bruce Goldsmith, Airwave Gliders, Isle of Wight, February 1995.

[92] Bill Morris, Whose Rope is it Any Way, Skywings, Dec. 1994, PP32-33.

[93] Mike, R. Parsey, Fatigue of SPM Mooring Hawsers, 14th Annual Offshore Technology Conference Proceeding, Houston, Texas, Vol. 3, Paper OTC 4307, May 3-6, 1982, PP71-93.

[94] Mike, R. Parsey, John, W, S. Hearle, and Steve Banfield, Life of Polymeric Ropes in the Marine Environment, Polymers In a Marine Environment, Proceedings of the 2nd International Conference, Paper 28, 14-16 Oct. 1987, Institute of Marine Engineers, London 1989, PP205-214.

[95] J.W.S. Hearle and M.R. Parsey, Fatigue Failure in Marine Ropes and Their relation to Fibre fatigue, PRI Fatigue in Polymers Conference, London 29-30, June 1983.

[96] M.R. Parsey, The Fatigue Resistance and Hysteresis of Man-Made Fibre Ropes, Proceedings of Offshore Europe 83 Conference, Sept. 1983, SPE11908/PP1-17.

[97] J.L. Werth, An Evaluation of Materials and Rope Construction for Mooring Hawser Design, Proceedings of Offshore Technology Conference, Houston, Texas, May 5-8, 1980, Paper OTC 3851, PP497-507.

[98] L. Gregoraç, Utilisation of Synthetic Fibre Ropes for Guying Broadcast Towers, International Broadcasting Convention, Brighton, IEE Conference No. 220, ISBN 0 85296263 0, 1982, PP131-134.

[99] M.M. Salama, J.H. Williams, Jr, S.S. Lee and R.M. Vennett, Materials for Lightweight Mooring Systems for Deep-water Compliant Structures, Proceedings of the 4th International Symposium on Offshore Mechanics & Arctic Engineering, ASME, 1985, PP357-364.

[100] E. Scala and F.J. Haas, Synthetic Ropes and Cables: Properties and Analysis, Proceedings of the 17th Annual Offshore Technology Conference, Houston, Texas, May 6-9, 1985, Paper OTC 5062, PP383-400.

[101] P.G. Riewald, Performance Analysis of an Aramid Mooring Rope, Proceedings of the 18th Annual Offshore Technology Conference, Houston, Texas, May 5-8, 1986, Paper OTC 5187, PP305-316.

[102] P.G. Riewald, R.G. Walden, A.S. Whitehill and A.S. Kowleck, Design and Deployment Parameters Affecting the Survivability of Stranded Aramid Fibre Ropes in Marine Environment, IEEE OCEANS 1986 Conference Proceedings, Washington D.C, Vol. 1, Sept. 1986, PP284-293.

[103] W. Paul, S.S. Weidenbaum, K.R. Bitting and P.F. Hartman, Systems Design and Testing of Ropes for Ocean Engineering Applications, The American Institute of Chemical Engineers, AICHE Symposium Series, Vol. 76, No. 194, 1980, PP98-106.

[104] C.J. Toomey, J.F. Mandell and S. Backer, Dynamic Behaviour of *Nylon* and Polyester Ropes Under Simulated Towing Conditions, Proceedings of Marine technology society, Science and Technology for a New Oceans Decade, MTS'90, Washington D.C. Sept. 26-28, 1990, Vol. 1, ISBN 0933957068, PP62-67.

[105] M.R. Parsey, A. Street and S.J. Banfield, Dynamic Behaviour of Marine Hawsers, Proceedings of 17th Annual Offshore Technology Conference, Houston, Texas, Paper OTC 5009, May 6-9, 1985, PP429-443.

[106] H.A. McKenna, Developments in Fibre Rope Technology, Proceedings of the Ocean'83 Conference, IEEE, ISSN: 0197-7385, 1983, PP527-533.

[107] J.F. Mandell, M.G. Steckel, S.S. Chung and M.C. Kenney, Fatigue and Environmental Resistance of Polyester and *Nylon* Fibres, Polymer Engineering and Science, Vol. 27, No. 15, August 1987, PP1121-1127.

[108] B.J. Tabor, The Wear Behaviour of Industrial Yarns, Symposium on High Performance Fibres, Textiles and Composites, department of Textiles, UMIST, June 25-27, 1985, PP175-197.

[109] B.J. Tabor and J.C. Wagenmakers, Some Long-term Behaviour Aspects of Industrial Yarn, Related to Environmental Influence, Techtexil-Symposium, 13-16 May, 1991, Frankfurt.

[110] M.C. Kenney, J.F. Mandell and F.J. McGarry, Fatigue Behaviour of Synthetic Fibres, Yarns and Ropes, Journal of Materials Science, Vol. 20, No. 6, 1985, PP2045-2059.

[111] Viking Rope, Man Made Fibre Ropes, Bridon Fibres Ltd, Trade Literature, 1991.

[112] S.L. Kowleck, U.S. Patent 3,600,350, assigned to DuPont, August 17, 1971.

[113] Plastics Engineering, No. 15, April 1986.

[114] G.R. Hattery and M.E.D. Hillman, High Performance Organic Fibres for Polymeric Composites, High Performance Polymers, Oxford University Press, 1991, ISBN 0-19-520853-6.

[115]T. Otha, Polymer Engineering Science, Vol. 23, No. 697, 1983

[116] Teijin Ltd Technical Literature, Brochure 96,10, 1996.

[117] Teijin Limited, Japan Patent (Tokukai) 51-76386, -134743, -136916, 52-98795 and U.S. Patent 4,075,172 (prior. Dec. 27, 1974)

[118] K. Kazama, Pre-prints for Plastics Engineering Forum, The Society of Polymer Science, Japan, Mar. 1981, P3.

[119] S. Ozawa, A New Approach to High Modulus, High Tenacity Fibres, Polymer Journal, Vol. 19, No. 1, 1987, PP119-125.

[120] Textile Terms and Definitions, 5th Edition, The Textile Institute, Manchester, 1963.

[121] DSM High Performance Fibres Ltd, Dyneema SK60 Trade Literature, Energy saving in Trawl Fishing, Ref. 0-20-08-02, Mar. 1991.

[122] A.H. Driscoll, A Decade of Synthetic Fibres in the Deep Ocean, Proceeding of Marine Technology Society, MTS'90, Washington, Sept. 1990, PP467-472.

[123] J. Stidd, Mechanical Properties of Technora Aramid Fibre and Ropes, Proceedings of Marine Technology Society Conference, MTS'90, Washington, D.C, 1990, PP677-680.

[124] J.W. Mead, K.E. Mead, I. Auerbach and R.H. Ericksen, Accelerated Ageing of *Nylon* 6,6 and Kevlar 29 in Elevated Temperature, Elevated Humidity, Smog and Ozone, Organic Coating of Plastic Chemicals, Vol. 44, March 1981, PP336-342.

[125] M.W. Webb, The Stress-Strain Curves of Yarns Extracted From Cordage Exposed to Weather or Subjected to Immersion in Water, Journal of Textile Institute, Vol. 75, No. 3, 1984, PP219-228.

[126] S. Konrad and D. Schuster, Methods of Protecting Aramid Yarns and Fabrics from the Effects of Light, Journal of Coated fabrics, Vol. 22, July 1992, PP10-25.

[127] M.G. Dobb, R.M. Robson, and A.H. Roberts, The Ultraviolet Sensitivity of Kevlar 149 and Technora Fibres, Journal of Materials Science, Vol. 28, 1993, PP785-788.

[128] J.Z. Wang, D.A. Dillard, M.P. Wolcott, F.A. Kamke and G.L. Wilkes, Transient Moisture Effects in Fibres and Composite Materials, Journal of Composite Materials, Vol. 24, Sept. 1990, PP994-1009.

[129] J.Z. Wang, V. Davé, W. Glasser and D.A. Dillard, The Effects of Moisture Sorption on the Creep Behaviour of Fibres, Proceedings of High Temperature & Environmental Effects on Polymeric Composites- San Diego, CA, 1993, ISBN 0 8031 1491 5, PP186-200.

[130] A. Sengonul and M.A. Wilding, Flex Fatigue in Gel-spun High-Performance Polyethylene Fibre, Journal of Textile Institute, Vol. 85, No. 1, 1994, PP1-11.

[131] P. Smith, P.J. Lemstra, Ultra-High-Strength Polyethylene Filaments by Solution Spinning/drawing, Journal of Materials Science, Vol. 15, 1980, PP505-514.

[132] J. Sweeney and I.M. Ward, A Unified Model of Stress Relaxation and Creep Applied to Oriented Polyethylene, Journal of Materials Science, Vol. 25, 1990, PP697-705.

[133] G.C. Weedon and T.Y. Tam, Properties and Applications of Extended Chain Polyethylene, Symposium on High Performance Fibres, Textiles and Composites, department of Textiles, UMIST, June 25-27, 1985, PP35-75.

[134] M.A. Wilding and I.M. Ward, Routes to Improved Creep Behaviour in Drawn Polyethylene, Plastics, Rubber and Composites Proceedings Applications, Vol. 1, 1981, PP167-72.

[135] I.M. Ward, Recent Developments in the Science and Technology of High modulus Polymers, Proceedings of the 2nd Conference of materials engineering, 1985, PP11-17.

[136] J. F. Mandell, Modelling of Marine Rope Fatigue Behaviour, Textile Research Journal, Vol. 57, 1987, PP318-330.

[137] H.A. McKenna, Polyurethane Coated Fibre Ropes for Mooring Systems, American Institute of Chemical Engineer (AICHE), Symposium Series, ISSN 0065-8812, 1980, PP127-132.

[138] J.F. Flory, M.R. Parsey and H.A. McKenna, The Choice Between *Nylon* and Polyester For Large Marine Ropes, Proceedings of 7th International Conference on Offshore Mechanics & Arctic Engineering, ASME, 1988, PP517-523.

[139] J.F. Flory, The Importance of Balancing the Core and Cover in Double Braid Rope, Marine Technology Society Journal, Vol. 15, No. 3, 1981, PP18-23.

[140] H.A. McKenna, Developments in Fibre Rope Technology, Proceedings of Oceans '83, ISSN 0197-7385, 1983, PP527-533.

[141] H.A. McKenna, Advances in High performance Synthetic Fibre Tension Members, ASME Ocean Engineering Division, Publications, OED, Vol. 12, 1987, PP113-118.

[142] H.A. McKenna, High Performance Polyester Rope, Proceedings of Marine Technology Society Conference, MTS' 90, Washington, D.C., Sept. 1990, PP656-661.

[143] H.A. McKenna, High Performance Polyester Rope, Sea Technology, Vol. 32, No. 7, 1991, PP10-11,13-14.

[144] J.F. Flory, J.W.S. Hearle and M.R. Parsey, Current Issues in the Use of Synthetic Fibre Ropes, Polymers in The Marine Environment Conference, Paper 4, Institute of Marine Engineers, London, Oct. 23-24, 1991, PP37-44.

[145] OCIMF Prototype Rope Testing, Oil Companies International Marine Forum, Witherby & Co. Ltd, London 1987.

[146] S.R. Karnoski and F.C. Liu, Tension and Bending Fatigue Test Results of Synthetic Ropes, 20th Offshore Technology Conference, Houston, Texas, Paper OTC 5720, 2-5 May, 1988, PP343-350.

[147] C.J. Burgoyne, R.E. Hobbs and J. Strzemiecki, Tension-Bending and Sheave Bending Fatigue of Parallel Lay Aramid Ropes, Proceedings of 8th International Conference on Offshore Mechanics and Arctic Engineering, ASME, The Hague, March 19-23, 1989, PP691-698.

[148] M.A. St John Jr, S. Heffelfinger and M. Radosevich, Tensile Bending Performance of Kevlar Ropes, Proceedings of the Marine Technology Society Conference, MTS'92, Global Ocean partnership, 19-21 Oct. 1992, PP899-905.

[149] J.H. Van Leeuwen, Dynamic Behaviour of Synthetic Ropes, Proceedings of Offshore Technology Conference, Houston, Texas, May 4-7, 1981, Paper OTC 4003, PP453-464.

[150] R.E. Hobbs, Pressure Sensitive 'Yarns' and In-rope Friction Measurements, Journal of Textile Institute, Vol. 81, No. 4, 1990, PP549-560.

[151] H. Shin, K. Yamakawa and S. Hara, Laboratory Tests on Synthetic Fibre Ropes, Proceedings of the International Conference on Offshore Mechanics and Arctic Engineering, OMAE, Volume 1, Offshore Technology, ASME, ISBN 0791812624, 1994, PP441-448.

[152] H. Crawford and L.M. McTernan, Cyclic Testing of Continuously Wetted Synthetic Fibre Ropes, Proceeding of the Offshore Technology Conference, Houston, Texas, May 1983, Paper OTC 4635, PP455-466.

[153] H. Crawford and L.M. McTernan, Cyclic Load Testing at Sea-Wave Frequency of Continuously Wetted Man Made Fibre Ropes, Proceedings of the Offshore Technology Conference, Houston, Texas, May 1985, Paper OTC 5061, PP375-382.

[154] K.R. Bitting, Fatigue Failure in *Nylon* Rope, Marine Technology Society Journal, Vol. 14, No. 5, 1980, PP20-22.

[155] L. Duband, L. Hui and A. Lange, Thermal Isolation of Large Loads at Low Temperature Using Kevlar Rope, Cryogenics, Vol. 33, No. 6, 1993, PP643-47.

[156] J.F. Flory, J.W.S. Hearle and M. Goksoy, Yarn Friction and Abrasion Characteristics as Indicators of Rope Performance in Marine Service, Marine Technology Society Conference, MTS'90, Washington DC, Sept. 26-28, 1990, Vol. 2, ISBN 0-933957-06-8, PP313-318.

[157] J.F. Flory, M. Goksoy and J.W.S. Hearle, Yarn on Yarn Abrasion Testing of Rope Yarns, Part I, The Test Method, Journal of Textile Institute, No. 3, 1988, PP417-431.

[158] M. Goksoy and J.W.S. Hearle, Yarn on Yarn Abrasion Testing of Rope Yarns, Part II, The Influence of Machine Variables, Journal of Textile Institute, No. 3, 1988, PP432-442.

[159] M. Goksoy and J.W.S. Hearle, Yarn on Yarn Abrasion Testing of Rope Yarns, Part III, The Influence of Aqueous Environments , Journal of Textile Institute, No. 3, 1988, PP443-450.

[160] H. Kawaguchi and C.M. Leech, A Test Facility for Determining the Frictional Forces Between Components Used in Large Synthetic Fibre Ropes, Proceedings of the Fourth International Offshore and Polar Engineering Conference, Osaka, Japan, April 10-15, 1994, Vol. 2, ISBN 1-880653-12-5, PP289-294.

[161] L.T. Heirigs and P. Schwartz, Properties of Small Diameter Aramid Double Braids: Fatigue Lifetime, Strength Retention after Abrasion, and Strength Modelling, Textile Research Journal, Vol. 62, No. 7, 1992, PP397-402.

[162] IR. Joop H. Van Leeuwen and A.J. Van Der Burg, Bending Fatigue Bending of Twaron Aramid Ropes, Proceedings of Marine Technology Society, "Science and Technology for a New Oceans Decade", MTS'90, Washington , D.C., Sept. 26-28, 1990.

[163] R.E. Hobbs and C.J. Burgoyne, Bending Fatigue in High Strength Fibre Ropes, International Journal of Fatigue, Vol. 13, No. 2, 1991, PP174-180.

[164] N.F. Casey, N.I.D. Robertson and J.R. Wells, The Evaluation of Synthetic Fibre Rope for a Proposed Deep Water Salvage Operation, Proceedings of the International Conference on Offshore Mechanics and Arctic Engineering, ASME, Vol. 3, Part A, 1993, PP341-359.

[165] P.T. Gibson, Rope Reaction to Combined Tension and Rotation, Proceedings of Marine technology society, Science and Technology for a New Oceans Decade, MTS'90, Washington D.C. Sept. 26-28, 1990, Vol. 1, ISBN 0933957068, PP68-73.

[166] G.B. Guimarães and C.J. Burgoyne, Creep Behaviour of a Parallel-Lay Aramid Rope, Journal Of Materials Science, Vol. 27, No. 9, 1992, PP2473-2489.

[167] V.E. Watson, D. Rees and G. White, Examination of Creep and Abrasion Effects on Non-Metallic Strength Members in Optical Communication Cables, Pirelli Cables Ltd, CCD, Newport, Gwent, UK, Internal Report, 1996.

[168] K.R. Bitting, Cyclic Tests of New and Aged *Nylon* and Polyester Rope, Proceedings of the 12th Annual Offshore Technology Conference, Paper OTC 3852, May 5-8 1980, ISSN 0160-3663, PP509-516.

[169] R.C. Swenson, A Snap-Back Restrained Kevlar Mooring Rope, 15th International Annual Offshore Technology, Houston, Texas, May 2-5, 1983, Paper OTC 4636, PP467-470.

[170] M.O.W. Richardson, Chemical and Physical effects Associated with Polymer Tribology, Polymer Science and Technology, for Meeting, Los Angeles, California, April 1-4, Vol. 5B, 1974, PP787-805.

[171] S. Altun, M. Karahan and Y. Ulcay, Investigation of the Effect of Radiation on the Mechanical Properties of the Fibres and Their Usage in Fibre Reinforced Plastic Composites, 20th International BPF Composites Congress'96, 11-12 Sept. 1996

[172] J.Z. Wang and D.A. Dillard, Testing of Viscoelasticity of Single Fibres Under Transient Moisture Conditions, Experimental Techniques, Vol. 15, No. 5, 1991, PP47-49.

[173] M.H. Lafitte and A.R. Bunsell, The Fatigue Behaviour of Kevlar-29 Fibres, Journal of Materials Science, Vol. 17, 1982, PP2391-2397.

[174] J.W.S. Hearle and C.Y. Zhou, Tensile Properties of Twisted para-Aramid Fibres, Textile Research Journal, Vol. 57, No. 1, 1987, ISSN 0040-5175, PP7-13.

[175] W.F. Knoff, Mechanical Behaviour of Respirable Fibrils of Kevlar Aramid Fibre, Glass and Asbestos, Journal of Textile Institute, Vol. 84, No. 1, 1993, PP130-137.

[176] M.A. Wilding and I.M. Ward, Creep and Recovery of Ultra High Modulus Polyethylene, Polymer, Vol. 22, July 1981, PP870-6.

[177] I.M. Ward and M.A. Wilding, Creep Behaviour of Ultrahigh-Modulus Polyethylene: Influence of Draw Ratio and Polymer Composition, Journal of Polymer Science, Part B, Polymer Physics Edition, Vol. 22, 1984, PP561-575.

[178] L.E Govaert, C.W.M. Bastiaansen and P.J.R. Leblans, Stress-Strain Analysis of Oriented Polyethylene, Polymer, Vol. 34, No. 3, 1993, PP534-540.

[179] T. Peijs, R.J.M. van Vught and L.E. Govaert, Mechanical Properties of Poly(vinyl alcohol) Fibres and Composites, Composites, Vol. 26, No. 2, 1995, PP83-90.

[180] V.R. Metha and S. Kumar, Temperature Dependent Torsional properties of High performance Fibres and Their Relevance to Compressive Strength, Journal of Materials Science, Vol. 29, No. 14, 1994, PP3658-3664.

[181] M.O.W. Richardson, Damage Evaluation and Restoration of Mechanically Degraded Polymer Composites, Prog. Rubb, Plast. Technol, Vol. 6, No. 4, 1990, PP329-45.

[182] C.R. Heiple and S.H. Carpenter, Journal of Acoustic Emission, Vol. 6, 1987, PP177

[183] C.R. Heiple and S.H. Carpenter, Report Number RFP-3346, Rockwell International, Colorado, 1982.

[184] H.L. Dunegan, D.O. Harris and C.A. Tatro, Engineering Fractional Mechanics, Vol. 1, 1968, PP105

[185] M. H. Jones W.F. Brown Jr, Materials Research Standards, Vol. 4, 1964, PP120.

[186] C.E. Hartbower, W.G. Reuter, G.F. Morris and P.O. Grimmins, Acoustic Emission ASTM STP-505, p 187, American Society for Testing and Materials, Philadelphia, Pa, 1972.

[187] D. Jaffery, Proceedings of 5th International Acoustic Emission Symposium, Tokyo, Japan, 1980, PP249.

[188] Kanji Ono, R. Landy and C. Ouchi, Report No. ADA-058887, Naval Research Lab, Office of Naval Research, US Department of Commerce, Springfield, Virginia, U.S.A, 1978.

[189] D.O. Harris, A.S. Tetelman and F.A.I. Darwish, Acoustic Emission ASTM STP-505, P238, American Society for Testing of Materials, Philadelphia, Pa, 1972.

[190] F.J. Guild, B. Harris and A.J. Willis, Journal of Acoustic Emission, Vol. 1, P 224, 1982.

[191] G.R. Speich and R.M. Fisner, Acoustic Emission, ASTM STP-505, pp 140, American Society for Testing of Materials, Philadelphia, Pa, 1972.

[192] D. Tseng, Q.Y. Long and K. Tangri, Acta, Metallurgy, Vol. 35, 1987, PP1887.

[193] A.E. Lord Jr and R.M. Koerer, Fundamentals of Acoustic Emission (edited by Kanji Ono), pp 261, Materials Department, School of Engineering & Applied Science, University of California, Los Angeles, California, 1979.

[194] W.P. Mason, H.J. Meskimin and W. Shockley, Physics Review, Vol. 73, No. 10, 1948.

[195] A.T. Green, C.S. Lockman and R.K. Stel, Modern Plastics, Vol. 41, No. 137, 1964.

[196] J. Kaiser, Utersuchungen über das Auftreten von Gerauschen bei Zugversuch, Ph.D. thesis, Technische Hochule, München, Germany, 1950.

[197] T. Fowler, Development of an Acoustic Emission Test for FRP Equipment, ASCE Annual Convention, Boston, MA, 1979, Preprint 3583.

[198] R.A. Kline and D.M. Egle, A Brief Note on the Kaiser and Felicity Effects, Journal of acoustic Emission, Vol. 6, No. 3, July-Sept. 1987, PP205-206.

[199] I.G. Scott, Basic Acoustic Emission, Gordon & Breach Science Publishers, 1991, ISBN 2-88124-352-5.

[200] C.P. Debel, Proceeding of the 5th ISO International Symposium on Metallurgy and Materials Science, pp 19, ISO National Laboratory, Roskilde, Denmark, 1984.

[201] C.B. Scruby, Report No. AERE-R 11328, Atomic Energy Research Establishment, Harwell, U.K, 1984.

[202] C.B. Scruby, H.N.G. Wadley and J.J. Hill, Journal of Physics D, Vol. 16, No. 1069, 1983.

[203] C.B. Scruby, H.N.G. Wadley, R.J. Dewhurst, D.A. Hutchins and S.B. Palmer, Material Evaluation, Vol. 39, No. 1250, 1981.

[204] R.W. Harris and B.R. A wood, Metals Forum, vol. 5, No. 210, 1982.

[205] H.G.N. Wadley, C.B. Scruby and J.H. Speake, International Metals Reviews, Vol. 3, No. 41,1980.

[206] A.G. Evans and M. Lintzer, Annual Review of Materials Science, Vol. 7, No. 179, 1977.

[207] B.J. Brindley, J. Holt and I.G. Palmer, Non-destructive Testing, Vol. 6, No. 299, 1973.

[208] L.J. Graham and G. Alers, Fracture Mechanics of Ceramics (edited by R.C. Bradt, F.F. Lange & D.B. Hasselman), pp 175, Plenum Press, New York 1974.

[209] K. Ono, R. Stem and M. Long, Acoustic Emission ASTM STP-505, pp 152, American Society for Testing of Materials, Philadelphia, Pa, 1972.

[210] Y. Nakamura, C.L. Veach and B.O. Macauley, Acoustic Emission ASTM STP-505, pp 164, American Society for Testing of Materials, Philadelphia, Pa, 1972.

[211] D.G. Eitzen, F.R. Breckenridge, R.B. Clough, E.R. Fuller, N.N. Hsu and J.A. Simmons, EPRI Report NP-2089, National Bureau of Standards, Washington, DC, 1981.

[212] P. Kalyanasundaram, T. Jayakumar, Baldev Raj, C.R.L. Murthy and A. Krishnan, Structural Mechanics in Reactor Technology (edited by Folker H. Wittmann), pp 115, A.A. Balkema Publishers, Brookfield, U.S.A, 1987.

[213] V.V. Ship, G.B. Mauravin, I.S. Samoilova and E.G. Dorokhova, Application of Complex Information Parameters to Acoustic Emission for Diagnostics During the Stages of Fracture, Non-destructive Testing and Evaluation, Vol. 13, No. 2, 1997, PP57-71.

[214] Anon, Acoustic Emission and Vibration, Materials Evaluation, Vol. 55, No. 5, May 1997, PP562-563.

[215] A.S. Chen, R.S. Bushby and V.D. Scott, Deformation and Damage Mechanisms in Fibre Reinforced Aluminium Alloy Composites Under Tension, Composites - Part A: Applied Science and Manufacturing, Vol. 28, No. 3, 1997, PP289-297.

[216] M.C. Gandur, M.U. Kleinke and F. Galembeck, Complex Dynamic Behaviour in Adhesive Tape Peeling, Journal of Adhesion Science and Technology, Vol. 11, No. 1, 1997, PP11-28.

[217] M. Surgeon, E. Vanswijgenhoven, M. Weavers and O. Van Der Biest, Acoustic Emission During Tensile Testing of SiC-Fibre-Reinfoced BMAS Glass_Ceramic Composites, Composites - Part A: applied Science and Manufacturing, Vol. 28, No. 5, 1997, PP473-480.

[218] D. Short and J. Summerscales, Amplitude Distribution Acoustic Emission signatures of Unidirectional Fibre Composite Hybrid Materials, Composites, Vol. 15, No. 3, July 1994, PP200-206.

[219] A.J. Gray and J. Summerscales, Acoustic Emission From Cord-Reinforced Rubber, British Journal of Non-destructive Testing, Sept. 1985, PP300-305.

[220] B.P. Ludden, J.E. Carroll and C.J. Burgoyne, Distributed Optical Fibre Sensor for Offshore Applications, IEE Colloquium (Digest) No. 087, 1995, ISSN: 0963-3308

[221] Mike Kelly, Research Into the Performance of Dyneema Paraglider Ropes, BSc Final Year Project, Bournemouth University, June 1995.

[222] Ameer Raouf, Research into the Behaviour of High Performance Fibre Ropes as Used in Paraglider Ropes, BSc Final Year Project, Bournemouth University June 1996.

[223] W.E. Morton and J.W.S. Hearle, Physical Properties of Textile Fibres, 3rd Edition, 1993, Published by the Textile Institute, P265.

[224] W.E. Morton and J.W.S. Hearle, Physical Properties of Textile Fibres, 3rd Edition, 1993, Published by the Textile Institute, P266.

[225] W.E. Morton and J.W.S. Hearle, Physical Properties of Textile Fibres, 3rd Edition, 1993, Published by the Textile Institute, PP267-273.

[226] W.E. Morton and J.W.S. Hearle, Physical Properties of Textile Fibres, 3rd Edition, 1993, Published by the Textile Institute, P275.

Manufacturer	Material	Trade Name
Du Pont	Aramid	Kevlar
Akzo	Aramid	Twaron
Teijin	Aramid Co polymer	Technora
Hoechst AG	Aramid Co polymer	Trevar
DSM	HMPE	Dyneema
Allied Fibers	HMPE	Spectra
Hoechst Celanese	LCP	Vectran

Table 3.1: *List of high performance fibre manufacturers*

Commodity Ropes	Intermediate performance Fibres	High Performance Fibres
Polypropylene Polyethylene	Nylon 6, 66 Polyester (PET)	Kevlar Twaron Technora Trevar Dyneema Spectra Tekmilon Vectran

Table 4.1: *The most common Synthetic Fibres used for rope making*

Fibre	Rope Type	Weight (kg/100m)	Stiffness kN/1%ext	Price £/100m
manila	3 strand	500	40	600
steel	galvanised	300	360	700
steel	stainless	300	360	2,500
polyester	double braid	220	30	1,500
polypropylene	8 strand	200	20	500
nylon	double braid	150	15	1,200
polyester	parallel	150	40	1,000
carbon	pultruded	70	600	10,000
Aramid	parallel	40	80	1,600
HMPE	stranded	40	80	1,600

Table 4.2: *Comparison of different rope materials with break strength of 500 kN (Courtesy of J.W.S Hearle)*

Material's	Advantages	Disadvantages
Nylon	lightweight resistance to chafe inexpensive it has good load to load fatigue	effected by UV light has a great deal of stretch Loses up to15% of it's strength when wet
Polyester	maintain flexibility it holds colour superbly it does not shrink when wet it is stronger & has less stretch then nylon durable & abrasion resistant excellent tension-tension fatigue ultraviolet resistance	reduces in the presence of steam more expensive than nylon
Polypropylene	inexpensive floats ultraviolet resistance difficult to splice	low elongation lower strength then polyester difficult to knot
Aramid	three times the strength of polyester low creep unaffected to long-term extreme high modulus low weight corrosion resistance high tensile strength high dimension stability excellent handling characteristics high tenacity high cut resistance high thermal stability high resistance to acids and bases	highly susceptible to UV light expensive difficult to knot & splice low elongation sensitive to UV light very expensive very expensive sensitive to UV light Poor compression properties
LCP	Same as aramid fibres with excellent creep resistance	Same as aramid fibres
HMPE	low density - (floats) high tenacity high strength low weight high modulus resistance to UV light resistance to sea water resistance to abrasion resistance to cuts	low melting point very expensive high molecular weight

Table 4.3: *Advantages & Disadvantages of HPSFR & IPSFR*

Metals		Non Metals	
Steel	Cadmium	Ionic crystals	Rocks
Aluminium alloys	Cobalt	Oxide films	Concrete
Zinc	Gallium	Soils	Ceramics
Copper	Iron	Mica	Ice
Lead	Nickel alloys		Glass
Berylium	Vanadium		Wood
Tin	Titanium		Fibre Composites
Brass	Plutonium		Honeycombs
Gold			Plastics
Uranium			Adhesive bonds

Table 6.1: *Some materials that have already been investigated using acoustic emission*

Microscopic Processes	Macroscopic Processes
Creep	Boiling detection and bubble formation
Dislocation movement	Etching
Embrittlement	Crack growth
Luders band formation	Fracture
Phase transformations	Leak detection (hydraulic and pneumatic)
Magnetic transitions	Welding
Ferroelectric transitions	Corrosion
Twining	Thermal Shock

Table 6.2: *Some processes which could be responsible for generating acoustic emission*

Trade name:	Fibre material	No. of Strands	Diameter (mm)	Fibre Producers
Dyneema SK65	HMPE	8	1.1	DSM
Technora	Aramid Co	4	1.1	Teijin
Technora	Aramid Co	8	1.1	Teijin
Vectran	LCP	8	1.6	CELANESE

Table 7.1: *The different rope materials used in this study*

Dyneema	Vectran	8 strand Technora	4 Strand Technora
Number of strands	Number of strands	Number of strands	Number of strands
1	1	1	1
2	2	2	2
3	3	3	3
4	4	4	4
5	5	5	
6	6	6	
7	7	7	
8	8	8	

Table 7.2: *Table showing the number of strands removed from the sample in order to investigate the strand-rope efficiency*

Exposure Conditions	Temperatures (°C)	Exposure periods (days)
Natural weathering	Variable	7,14,28,56
Water immersion	54	1,2,3,8,16
Dry heat	54	1,2,3,8,16
Subzero	-22	1,2,3,8,16
Synthetic sea water	21	1,2,3,8,16

Table 7.3: *Pretest Environmental conditioning of Dyneema rope samples*

Model	Testometric Micro 350, Extended Frame
Manufacturer	Testometric Testing Machinery Co.
Manufacture Date	1994
Cross Head Speed Range	0.1 to 1000 mm/min
Last Calibrated	February 1997
Number of Bollards	Two
Diameter of Bollards	41 mm
Load Cell	2500 N
Load Range	4.00 N to 2500 N

Table 7.4: *Specifications of the Tensile Testing equipment used in this study*

Rope Material	**Mass (kg/m)**		
	Core + cover	**Core only**	**Cover only**
Dyneema	1.033×10^{-3}	0.406×10^{-3}	0.632×10^{-3}
Vectran	1.740×10^{-3}	0.847×10^{-3}	0.890×10^{-3}
4 strand Technora	1.065×10^{-3}	0.446×10^{-3}	0.628×10^{-3}
8 strand Technora	1.021×10^{-3}	0.371×10^{-3}	0.654×10^{-3}

Table 7.5: *Various masses of different rope samples used for specific stress calculations*

Number of strands	**Mass (kg/m)**			
	Dyneema	**Vectran**	**8 strand Technora**	**4 strand Technora**
1	0.051×10^{-3}	0.106×10^{-3}	0.046×10^{-3}	0.112×10^{-3}
2	0.102×10^{-3}	0.212×10^{-3}	0.092×10^{-3}	0.224×10^{-3}
3	0.153×10^{-3}	0.318×10^{-3}	0.138×10^{-3}	0.336×10^{-3}
4	0.204×10^{-3}	0.424×10^{-3}	0.184×10^{-3}	0.446×10^{-3}
5	0.255×10^{-3}	0.530×10^{-3}	0.230×10^{-3}	
6	0.306×10^{-3}	0.636×10^{-3}	0.276×10^{-3}	
7	0.357×10^{-3}	0.742×10^{-3}	0.322×10^{-3}	
8	0.406×10^{-3}	0.847×10^{-3}	0.371×10^{-3}	

Table 7.6: *Mass of the ropes with different strand numbers*

Rope material	Preloading regime (N)	
	Min	Max
8strand Technora	100	700
4 strand Technora	100	800
Dyneema	100	800
Vectran	100	1400

Table 7.7: *Preloading values applied to different Ropes at 100 N intervals in order to measure the residual strength.*

Number of cycles	Applied load (N)
10	100, 200, 300
20	100, 200, 300
100	100, 200, 300
1000	100, 200, 300
2000	100, 200, 300
3000	100, 200, 300

Table 7.8: *The cyclic loading regime, which was only applied to Dyneema rope samples to investigate the residual strength*

Sample type	Applied Load (kg)	No. Of turns
Covered Dyneema	2	2
Covered Dyneema	4	2
Uncovered Dyneema	2	2
Uncovered Dyneema	4	2
Covered Technora	2	2
Covered Technora	4	2
Uncovered Technora	2	2
Uncovered Technora	4	2

Table 7.9: *Rope on rope abrasion test regime for the different rope samples*

Input range	10mV-10V
Input Impedance	50Ω
Level width	2.4dB ± 0.1dB type. (0.2 dB max.)
Frequency range	50 kHz - 1 MHz
Threshold	0-7, set by push index switch
Threshold accuracy	± 0.1 dB type. (0.2 dB max.)
Dead time	100 µS
Ring Down Counter	Range: 8 bit

Table 7.10a: *Specification for the single channel AE equipment used in this project, which has 25 levels amplitude sorter*

Input	±10V
Input impedence	5 Ω
Conversion	12 bits
Accuracy	12 bits
Aperture time	25 nS
Conversion time	28µS/input

Table 7.10b: *Description of Analogue card with 4 analogue inputs with simultaneous data captures for the MR1004 Acoustic Emission analyser*

Processor	68B02 running at 2 MHz
Memory	8k ROM & 8k RAM
Other	68B40 programmable timer
Interface card	16 bit parallel, RS-232 serial

Table 7.10c: *Description of the Microprocessor card for the MR1004 Acoustic Emission analyser*

Gain	60 dB ± 1 dB into 50 Ω
Output	>20 V pp max. into 50 Ω
Noise	<2 mV (1 kHz - 1 MHz)
Frequency response	1 kHz - 2 MHz (-3 dB)
Filtering	100 kHz - 2 MHz 2nd order bandpass
	Upper & lower limits can be set using a plug in DIP
Supply	± 18 V, 50 mV standby current

Table 7.10d: *Description of the MRP-01 Preamplifier used with the MR1004 Acoustic Emission analyser*

Case Material	Stainless steel
Dimensions	Diameter = 6.35 mm Length = 10 mm

Table 7.10e: *Description of the Miniature MRTB-500 broadband PZT5 transducer, which was used in this study in conjunction with the MR1004 Acoustic emission analyser*

Condition	Mean Breaking Load (N)	STD	Mean Extension at Break (mm)	STD	Strength Loss (%)	Strand Efficiency (%)	Estimated Strength (N)	Rope Efficiency (%)
As received	922.70	48.57	47.88	2.30	0			100
Cover	159.10	11.79	211.61	13.58	82.76			18
Core (8 strands)	795.92	8.07	44.11	2.16	13.74	89.91	795.92	86.26
7 strands	662.57	19.58	41.11	2.06	16.75	85.53	696.43	83.25
6 strands	528.38	11.01	39.85	1.97	33.61	79.58	596.94	66.39
5 strands	467.90	42.17	36.42	2.36	41.21	84.57	497.45	58.79
4 strands	398.18	55.47	32.76	6.12	49.97	89.96	397.96	50.03
3 strands	283.85	45.99	29.84	4.27	64.34	85.50	298.47	35.66
2 strands	210.28	16.63	25.11	1.26	73.58	95.01	198.98	26.42
1 strand	110.58	3.19	23.60	1.92	86.11	100	99.49	13.89
1x100N	917.20	58.01	47.18	3.16	0.60			
1x200N	907.20	49.33	45.88	2.69	1.68			
1x300N	901.90	56.46	41.65	2.89	2.25			
1x400N	897.20	35.61	38.75	1.90	2.76			
1x500N	896.80	19.86	36.23	2.04	2.81			
1x600N	868.40	42.89	34.16	3.56	5.88			
1x700N	868.10	20.13	32.18	2.01	5.92			
1x800N	842.40	38.82	30.27	4.34	8.70			
10x100N	918.52		40.72		0.45			
10x200N	917.12		55.04		0.60			
10x300N	913.70		56.3		0.98			
20x100N	910.51		40.85		1.32			
20x200N	908.10		55.33		1.58			
20x300N	903.72		51.58		2.06			
100x100N	900.80		41.39		2.37			
100x200N	898.21		53.37		2.65			
100x300N	891.54		47.33		3.38			
1000x100N	887.24		44.60		3.85			
1000x200N	879.76		46.47		4.65			
1000x300N	865.22		35.43		6.23			
2000x100N	851.39		45.38		7.73			
2000x200N	840.26		42.3		8.93			
2000x300N	836.00		47.66		9.40			
3000x100N	810.30		48.32		12.18			
3000x200N	774.10		50.21		16.10			
3000x300N	768.20		53.00		16.74			

Table 8.1: *Tensile test results for Dyneema samples from all the different tests carried out under dry conditioning*

Condition	Mean Breaking Load (N)	STD	Mean Extension at Break (mm)	STD	Strength Loss (%)	Strand Efficiency (%)	Estimated Strength (N)	Rope Efficiency (%)
As received	1624.00	47.70	42.00	1.32	0		1539.00	100
Cover	295.10	14.30	352.80	15.81	81.83			18.17
Core (8 strands)	1537.70	30.10	38.71	0.89	5.31	94.97	1537.70	94.69
7 strands	1238.70	61.90	38.30	2.20	19.44	87.43	1345.49	80.56
6 strands	1157.70	76.60	34.50	2.58	24.71	95.33	1153.28	75.29
5 strands	874.75	53.20	33.61	1.46	43.11	86.44	961.07	56.89
4 strands	656.30	52.42	27.94	3.82	57.32	81.06	768.85	42.68
3 strands	517.68	50.70	25.64	3.14	66.33	85.26	576.39	33.67
2 strands	393.86	15.73	24.55	2.36	74.39	97.30	384.43	25.61
1 strand	202.40	12.61	21.65	1.60	86.84	100	192.21	13.16
1x100N	1620.00	53.80	40.48	1.36	0.25			99.75
1x200N	1594.70	35.30	37.01	0.97	1.80			98.20
1x300N	1562.90	40.88	35.35	0.93	3.76			96.24
1x400N	1555.40	34.98	33.70	1.52	4.22			95.78
1x500N	1551.60	52.09	30.66	2.68	4.46			95.54
1x600N	1548.80	50.55	29.62	1.60	4.63			95.37
1x700N	1543.80	44.05	27.99	0.75	4.94			95.06
1x800N	1542.48	41.84	26.40	0.96	5.02			94.98
1x900N	1535.90	45.10	24.97	0.91	5.42			94.58
1x1000N	1530.40	33.72	24.49	0.59	5.76			94.24
1x1100N	1526.44	62.11	23.43	1.53	6.01			93.99
1x1200N	1504.10	26.88	23.03	0.95	7.38			92.62
1x1300N	1495.20	62.15	22.70	0.81	7.93			92.07
1x1400N	1484.70	52.90	22.49	0.98	8.58			91.42

Table 8.2: *Tensile test results for Vectran samples from all the different tests carried out under dry conditions*

Condition	Mean Breaking Load (N)	STD	Mean Extension at Break (mm)	STD	Strength Loss (%)	Strand Efficiency (%)	Estimated Strength (N)	Rope Efficiency (%)
As Received	1044.80	22.20	39.93	1.19	0			100
Cover	232.76	10.82	312.08	15.10	77.72			22.28
Core (4 strands)	814.19	57.90	28.39	2.208	22.07	98.11	814.19	77.93
3 strands	618.70	38.15	23.00	1.49	35.60	99.40	610.64	75.99
2 strands	410.00	16.53	21.33	1.23	57.32	98.81	407.10	50.36
1 strand	207.47	16.47	20.62	1.76	78.40	100	203.55	25.48
1x100N	1039.50	5.23	34.31	0.87	0.51			99.49
1x200N	1036.10	16.83	31.96	0.48	0.83			99.17
1x300N	1019.00	20.09	30.94	1.77	2.47			97.53
1x400N	1000.00	26.55	30.24	1.15	4.29			95.71
1x500N	993.60	18.58	29.02	1.39	4.90			95.10
1x600N	990.20	15.75	27.31	1.59	5.23			94.77
1x700N	983.90	15.70	25.92	0.36	5.83			94.17
1x800N	980.50	9.13	24.52	1.06	6.15			93.85

Table 8.3: *Tensile test results for 4 strand Technora samples from all the tests carried out under dry conditions*

Condition	Mean Breaking Load (N)	STD	Mean Extension at Break (mm)	STD	Strength Loss (%)	Strand Efficiency (%)	Estimated Strength (N)	Rope Efficiency (%)
As received	820.40	17.01	33.94	1.03	0			100
Cover	218.31	11.60	298.72	12.40	73.39			26.61
Core (8 strands)	737.18	16.63	27.03	0.78	10.14	96.89	737.18	89.86
7 strands	661.86	25.10	26.17	0.95	10.22	99.41	645.04	89.78
6 strands	566.53	39.77	26.04	1.82	23.15	99.28	552.89	76.85
5 strands	471.31	8.93	23.14	1.64	36.07	99.11	460.74	63.93
4 strands	376.70	14.44	22.12	0.60	48.90	99.02	368.59	51.10
3 strands	280.65	23.44	20.39	1.57	61.93	98.36	276.44	38.07
2 strands	187.75	19.76	19.70	2.72	74.53	98.70	184.30	25.47
1 strand	95.11	3.65	18.25	1.04	87.10	100	92.15	12.90
1x100N	808.80	23.59	31.86	1.08	1.41			98.59
1x200N	806.60	15.74	28.82	1.01	1.68			98.32
1x300N	801.40	19.41	27.56	0.74	2.32			97.68
1x400N	797.70	26.84	25.27	1.48	2.77			97.23
1x500N	796.04	23.51	23.92	1.09	2.97			97.03
1x600N	783.40	14.58	23.34	2.56	4.51			95.49
1x700N	777.02	31.08	22.35	1.54	5.29			94.71

Table 8.4: *Tensile test results for 8 strand Technora samples from all the tests carried out under dry conditions*

Conditions	Tenacity (N/tex)	Work of Rupture (J)	Specific Work of Rupture (N/tex)	Work Factor
As Received	8.93×10^{12}	22.38	1.572×10^{11}	0.51
Core	1.96×10^{13}	15.82	2.78×10^{11}	0.48
100 N	8.88×10^{12}	22.32	1.54×10^{11}	0.52
200 N	8.78×10^{12}	21.56	1.49×10^{11}	0.52
300 N	8.73×10^{12}	20.79	1.44×10^{11}	0.55
400 N	8.69×10^{12}	19.38	1.34×10^{11}	0.56
500 N	8.68×10^{12}	19.13	1.32×10^{11}	0.59
600 N	8.41×10^{12}	16.71	1.16×10^{11}	0.56
700 N	8.40×10^{12}	15.96	1.10×10^{11}	0.57
800 N	8.15×10^{12}	13.91	9.62×10^{10}	0.55
1 Strand	2.17×10^{13}	1.99	2.79×10^{11}	0.42
2 Strands	2.06×10^{13}	3.87	2.71×10^{11}	0.46
3 Strands	1.86×10^{13}	5.35	2.50×10^{11}	0.45
4 Strands	1.95×10^{13}	8.17	2.86×10^{11}	0.41
5 Strands	1.84×10^{13}	9.58	2.68×10^{11}	0.42
6 Strands	1.73×10^{13}	10.23	2.39×10^{11}	0.40
7 Strands	1.86×10^{13}	13.39	2.68×10^{11}	0.49
8 Strands	1.96×10^{13}	15.82	2.78×10^{11}	0.48

Table 8.5: V*arious tensile data for 8 strand Dyneema rope samples derived from Table 8.1*

Conditions	Tenacity (N/tex)	Work of Rupture (J)	Specific Work of Rupture (N/tex)	Work Factor
As Received	9.33×10^{12}	25.10	1.03×10^{11}	0.37
Core	1.82×10^{13}	19.95	1.68×10^{11}	0.34
100 N	9.31×10^{12}	24.25	9.95×10^{10}	0.37
200 N	9.16×10^{12}	23.41	9.63×10^{10}	0.40
300 N	8.98×10^{12}	23.35	9.59×10^{10}	0.42
400 N	8.94×10^{12}	22.84	9.38×10^{10}	0.44
500 N	8.92×10^{12}	22.10	9.07×10^{10}	0.46
600 N	8.90×10^{12}	21.49	8.82×10^{10}	0.47
700 N	8.87×10^{12}	21.12	8.67×10^{10}	0.49
800 N	8.86×10^{12}	20.21	8.29×10^{10}	0.50
900 N	8.83×10^{12}	19.95	8.19×10^{10}	0.52
1000 N	8.80×10^{12}	19.74	8.10×10^{10}	0.53
1100 N	8.77×10^{12}	19.36	7.95×10^{10}	0.54
1200 N	8.64×10^{12}	19.13	7.85×10^{10}	0.55
1300 N	8.59×10^{12}	18.87	7.75×10^{10}	0.56
1400 N	8.53×10^{12}	17.29	7.10×10^{10}	0.57
1 Strand	1.91×10^{13}	1.85	1.25×10^{11}	0.42
2 Strands	1.86×10^{13}	3.92	1.32×10^{11}	0.41
3 Strands	1.63×10^{13}	5.07	1.14×10^{11}	0.38
4 Strands	1.55×10^{13}	6.64	1.12×10^{11}	0.36
5 Strands	1.65×10^{13}	10.05	1.35×10^{11}	0.34
6 Strands	1.82×10^{13}	13.55	1.52×10^{11}	0.34
7 Strands	1.67×10^{13}	15.88	1.53×10^{11}	0.33
8 Strands	1.82×10^{13}	19.95	1.68×10^{11}	0.34

Table 8.6: *Various tensile data for 8 strand Vectran rope samples derived from Table 8.2*

Conditions	Tenacity (N/tex)	Work of Rupture (J)	Specific Work of Rupture (N/tex)	Work Factor
As Received	9.81×10^{12}	16.44	1.10×10^{11}	0.39
Core	1.83×10^{13}	10.67	1.71×10^{11}	0.46
100 N	9.76×10^{12}	16.12	1.08×10^{11}	0.45
200 N	9.73×10^{12}	15.97	1.07×10^{11}	0.48
300 N	9.57×10^{12}	15.61	1.05×10^{11}	0.49
400 N	9.39×10^{12}	15.529	1.042×10^{11}	0.51
500 N	9.33×10^{12}	14.87	9.97×10^{10}	0.52
600 N	9.30×10^{12}	14.62	9.81×10^{10}	0.54
700 N	9.24×10^{12}	13.37	8.96×10^{10}	0.52
800 N	9.21×10^{12}	13.15	8.82×10^{10}	0.55
1 Strand	1.85×10^{13}	1.63	1.036×10^{11}	0.38
2 Strands	1.83×10^{13}	4.25	1.354×10^{11}	0.49
3 Strands	1.84×10^{13}	6.84	1.453×10^{11}	0.48
4 Strands	1.83×10^{13}	10.67	1.707×10^{11}	0.46

Table 8.7: *Various tensile data for 4 strand Technora rope samples derived from Table 8.3*

Conditions	Tenacity (N/tex)	Work of Rupture (J)	Specific Work of Rupture (N/tex)	Work Factor
As Received	8.04×10^{12}	11.65	8.15×10^{10}	0.42
Core	1.99×10^{13}	8.42	1.62×10^{11}	0.42
100 N	7.92×10^{12}	11.25	7.87×10^{10}	0.44
200 N	7.90×10^{12}	11.15	7.80×10^{10}	0.48
300 N	7.85×10^{12}	10.36	7.25×10^{10}	0.47
400 N	7.81×10^{12}	10.07	7.05×10^{10}	0.50
500 N	7.80×10^{12}	9.84	6.88×10^{10}	0.52
600 N	7.67×10^{12}	9.53	6.67×10^{10}	0.52
700 N	7.61×10^{12}	8.64	6.04×10^{10}	0.50
1 Strand	2.07×10^{13}	0.58	8.98×10^{10}	0.33
2 Strands	2.04×10^{13}	1.42	1.10×10^{11}	0.38
3 Strands	2.03×10^{13}	2.15	1.11×10^{11}	0.37
4 Strands	2.05×10^{13}	3.61	1.40×10^{11}	0.43
5 Strands	2.05×10^{13}	4.54	1.41×10^{11}	0.42
6 Strands	2.05×10^{13}	6.34	1.64×10^{11}	0.43
7 Strands	2.06×10^{13}	7.92	1.76×10^{11}	0.46
8 Strands	1.99×10^{13}	8.42	1.62×10^{11}	0.42

Table 8.8: *Various tensile data for 8 strand Technora rope samples derived from Table 8.4*

	Onset of AE				Final part of AE						
Sample	Load (N)	Ext. (mm)	Time (S)	RDC	Load (N)	Load (%)	Ext. (mm)	Ext. (%)	Time (S)	RDC	Final
As received	59	3.5	2	2	780	84.53	32	66.83	31	800	2100
1 strand	30	13.5	8	56	60	54.26	21	88.98	5	56	1245
2 strands	20	3.5	2	25	150	71.33	23	91.60	13	731	3724
3 strands	60	10.5	6	36	190	66.94	28	93.83	12	829	3520
4 strands	40	8	5	46	255	64.04	32	97.68	11	924	3659
5 strands	25	6.5	4	57	320	68.39	34	93.36	12	835	4464
6 strands	25	5	3	73	370	70.03	36	90.34	10	899	3373
7 strands	20	5	3	159	480	72.45	38	92.43	18	820	3091
8 strands	120	13.6	8	69	550	69.10	42	95.22	28	300	656
1 x 100N	85	3.5	2	3	625	68.12	24	50.87	19	956	1232
1 x 200N	75	3.3	2	41	600	66.14	17	37.05	10	621	1960
1 x 300N	80	3.5	2	51	575	63.75	16	38.42	10	484	1740
1 x 400N	50	3.5	2	57	545	60.74	14	36.13	12	700	928
1 x 500N	80	3.5	2	39	530	59.10	13	35.88	16	410	1637
1 x 600N	100	3.5	2	67	480	55.27	12	35.13	11	300	1233
1 x 700N	125	3.5	2	19	450	51.84	10	31.08	10	205	319
1 x 800N	110	3.5	2	31	390	46.30	8	26.43	10	58	504

Table 8.9: *Summary of the acoustic emission data for Dyneema samples for all the tests carried out*

	Onset of AE				Final part of AE						
Sample	Load (N)	Ext. (mm)	Time (S)	RDC	Load (N)	Load (%)	Ext. (mm)	Ext. (%)	Time (S)	RDC	Final
As received	50	3.5	2	1	1300	80.05	35	83.33	21	2306	1206
1 strand	20	5	3	141	100	49.41	13	60.05	7	817	3907
2 strands	30	5	3	1	180	45.70	14	57.03	5	516	5343
3 strands	60	5	3	1	230	44.43	16	62.40	7	775	6780
4 strands	40	5	3	4	300	45.71	18	64.42	7	624	5372
5 strands	20	3.5	2	3	390	44.58	22	65.46	10	703	9304
6 strands	30	3.5	2	52	540	46.64	24	69.57	9	715	8966
7 strands	40	5	3	37	650	52.47	26	67.89	10	935	9710
8 strands	20	3.5	2	1	900	58.53	28	72.33	10	798	6916
1 x 100N	110	3.5	2	11	1150	70.99	32	79.05	18	9309	13096
1 x 200N	130	3.5	2	186	1100	68.98	30	81.06	17	9236	11541
1 x 300N	160	3.5	2	25	1100	70.38	28	79.21	13	9030	17115
1 x 400N	140	3.5	2	9	1075	69.11	26	77.15	14	9237	18093
1 x 500N	200	3.5	2	53	1075	69.28	25	81.54	10	9117	16896
1 x 600N	160	3.5	2	59	1040	67.15	22	74.27	9	9023	12048
1 x 700N	180	3.5	2	55	1010	65.42	21	75.03	11	9403	15302
1 x 800N	200	3.5	2	43	980	63.53	20	75.76	9	9554	15732
1 x 900N	220	3.5	2	39	940	61.20	18	72.09	11	9147	14317
1 x 1000N	200	3.5	2	48	910	59.46	17	69.42	11	8978	15346
1 x 1100N	240	3.5	2	49	880	57.65	14	59.75	9	9030	16487
1 x 1200N	240	3.5	2	36	850	56.51	14	60.79	11	8849	16882
1 x 1300N	220	3.5	2	35	850	56.85	14	61.67	10	8264	12400
1 x 1400N	240	3.5	2	146	850	57.25	14	62.25	5	3000	11840

Table 8.10: *Summary of the acoustic emission data for Vectran samples from all the test carried out*

	Onset of AE				Final part of AE						
Sample	Load (N)	Ext. (mm)	Time (S)	RDC	Load (N)	Load (%)	Ext. (mm)	Ext. (%)	Time (S)	RDC	Final
As received	40	3.5	2	148	700	67.00	27	67.62	17	7189	85549
1 strand	40	3.5	2	108	100	48.20	10	48.58	4	878	26461
2 strands	60	3.5	2	39	220	53.66	12	56.26	6	675	27955
3 strands	80	3.5	2	11	390	63.03	14	60.87	6	794	39103
4 strands	40	3.5	2	105	528	64.85	17	59.88	10	8065	83718
1 x 100N	110	3.5	2	188	680	65.42	24	69.95	15	7746	57056
1 x 200N	120	3.5	2	98	670	64.67	22	68.84	13	7536	63756
1 x 300N	120	3.5	2	48	650	63.79	22	71.11	13	7197	69093
1 x 400N	110	3.5	2	83	650	65.00	21	69.44	12	7336	65733
1 x 500N	130	3.5	2	89	650	65.42	20	68.92	12	8726	81728
1 x 600N	140	3.5	2	59	625	63.12	18	65.91	12	7954	61882
1 x 700N	140	3.5	2	80	625	65.52	18	69.44	12	8458	58478
1 x 800N	140	3.5	2	54	600	61.19	18	73.41	13	7759	55349

Table 8.11: *Summary of the acoustic emission data for 4 strand Technora samples from all the test carried out*

	Onset of AE				Final part of AE						
Sample	Load (N)	Ext. (mm)	Time (S)	RDC	Load (N)	Load (%)	Ext. (mm)	Ext. (%)	Time (S)	RDC	Final
As received	59	3.5	2	107	580	7070	24	70.71	12	7500	95000
1 strand	30	3.5	2	109	30	31.54	11	60.27	5	903	3512
2 strands	30	5	3	100	90	47.94	14	71.07	4	663	15130
3 strands	40	5	3	45	130	46.32	14	68.66	6	225	18894
4 strands	60	5	3	46	280	74.33	17	76.85	7	934	30293
5 strands	60	5	3	64	310	65.77	17	73.47	7	700	25119
6 strands	40	3.5	2	13	350	61.78	19	72.96	7	866	25695
7strands	40	3.5	2	19	400	60.44	19	72.60	7	854	25917
8 strands	40	3.5	2	102	468	63.49	21	77.69	11	7500	62000
1 x 100N	90	3.5	2	29	550	68.00	22	69.05	13	8000	55000
1 x 200N	120	3.5	2	1	550	68.19	21	72.87	12	8227	65000
1 x 300N	120	3.5	2	34	550	68.63	19	68.94	9	8210	66510
1 x 400N	120	3.5	2	26	525	65.81	18	71.23	9	7265	70531
1 x 500N	120	3.5	2	29	510	64.07	16	66.89	10	7381	63588
1 x 600N	120	3.5	2	18	510	65.10	16	68.55	11	8675	68207
1 x 700N	120	3.5	2	61	480	61.77	16	71.59	11	8812	52418

Table 8.12: *Summary of the acoustic emission data for 8 strand Technora samples from all the test carried out*

Sample type	Applied Load (kg)	No. Of turns	Cycles to failure
Covered Dyneema	2	2	88653
Covered Dyneema	4	2	49997
Uncovered Dyneema	2	2	49441
Uncovered Dyneema	4	2	21103
Covered Technora	2	2	12216
Covered Technora	4	2	8320
Uncovered Technora	2	2	1785
Uncovered Technora	4	2	821

Table 8.13: *Rope on rope abrasion test results for the different rope samples*

Exposure periods (days)	Load (N)	STD	Extension (mm)	STD
0	922.70	48.57	47.88	2.30
7	896.48	6.9	63.8	2.07
14	890.70	7.9	73	5.3
28	842.60	16.1	58.8	4.8
56	887.23	10.8	70.6	6.7

Table 8.14: *Natural weathering results of the Dyneema rope samples*

Exposure periods (days)	Load (N)	STD	Extension (mm)	STD
1	870.3	13.7	52.2	3.6
2	850.3	11.8	61.1	4.6
3	832.3	13.22	65.3	5.38
8	799.3	15.06	63.4	7.8
16	782.9	12.36	62.5	7.3

Table 8.15: *Tensile test results for Dyneema ropes after sea water conditioning*

Exposure periods (days)	Load (N)	STD	Extension (mm)	STD
1	881.3	10.31	53.1	4.8
2	848.4	26.12	62.4	5.2
3	826.3	16.62	64.7	5.49
8	792.2	13.52	70.4	7.9
16	787.4	14.9	73.2	8.3

Table 8.16: *Tensile test results for Dyneema ropes after exposure to water at 54°C*

Exposure periods (days)	Load (N)	STD	Extension (mm)	STD
1	832	11.33	58.3	5.7
2	830.1	14.13	61.8	8.7
3	823	15.21	68	7.69
8	800.3	12.68	70.4	9.4
16	788.3	13.57	72.6	9.76

Table 8.17: *Tensile test results of Dyneema ropes after Dry heat (54°C) conditioning*

Exposure periods (days)	Load (N)	STD	Extension (mm)	STD
1	865.4	12.95	52.3	8.5
2	853	10.41	58.2	8.9
3	848.3	11.63	64.7	5.49
8	846.3	13.81	65.3	8.9
16	830.2	12.68	69.1	10.3

Table 8.18: *Tensile test results of Dyneema ropes after Subzero temperature (-22 ℃) conditioning*

Figure 2.1: *A Paraglider in flight*

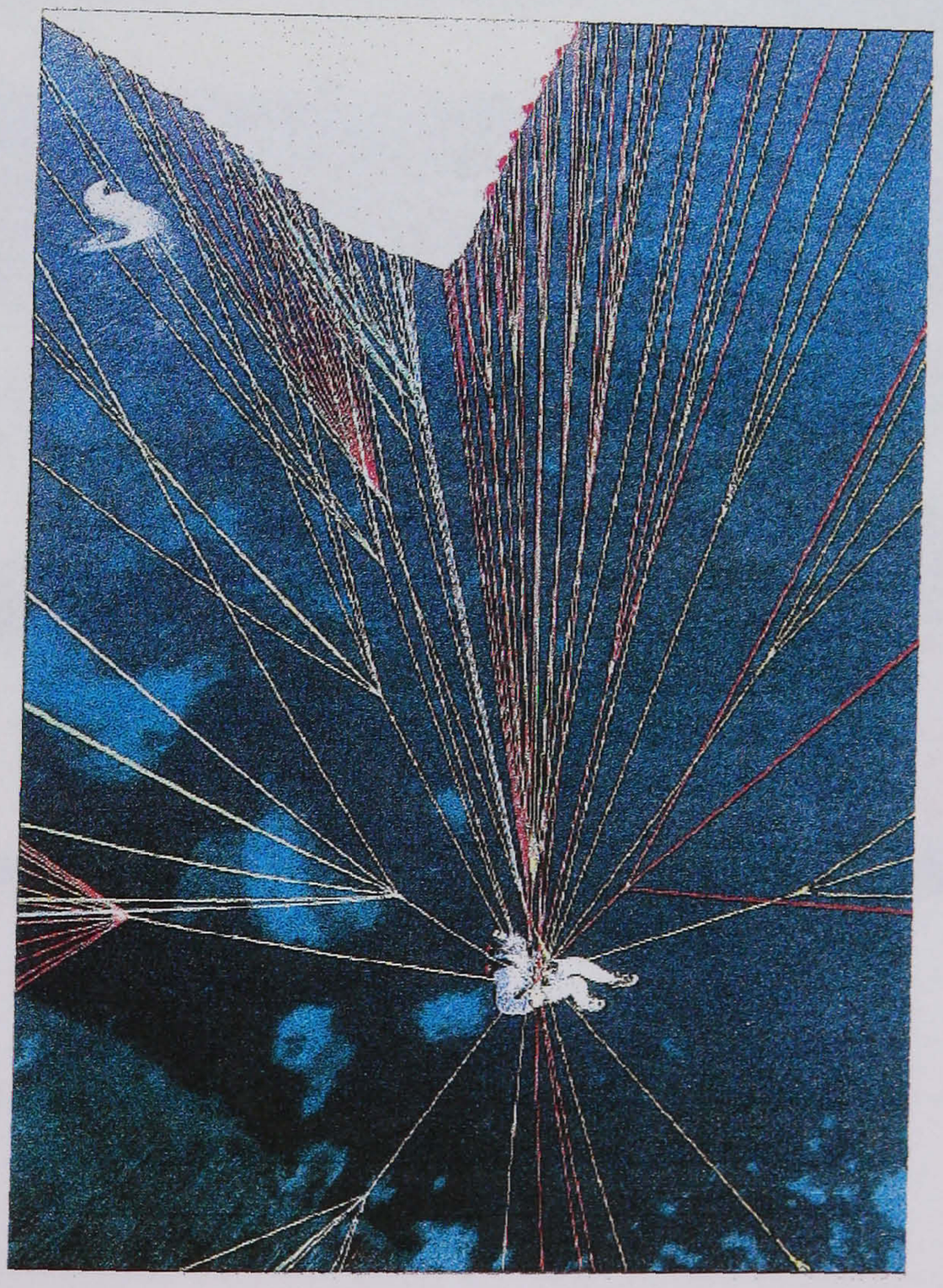

Figure 2.2: *Picture showing different parts of a paraglider*

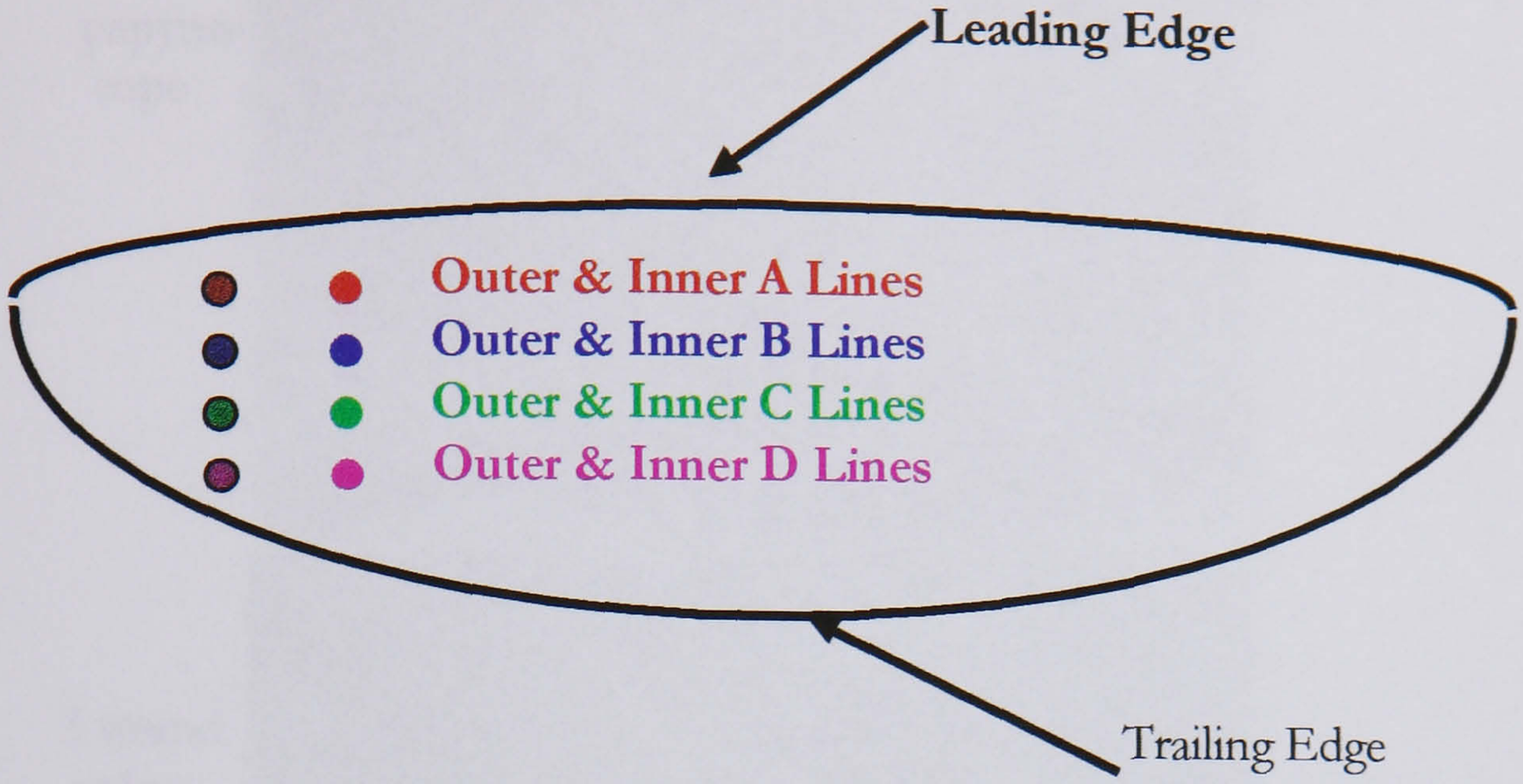

Figure 2.3: *Paraglider canopy showing line layout positions*

Braided

Plaited

Twisted

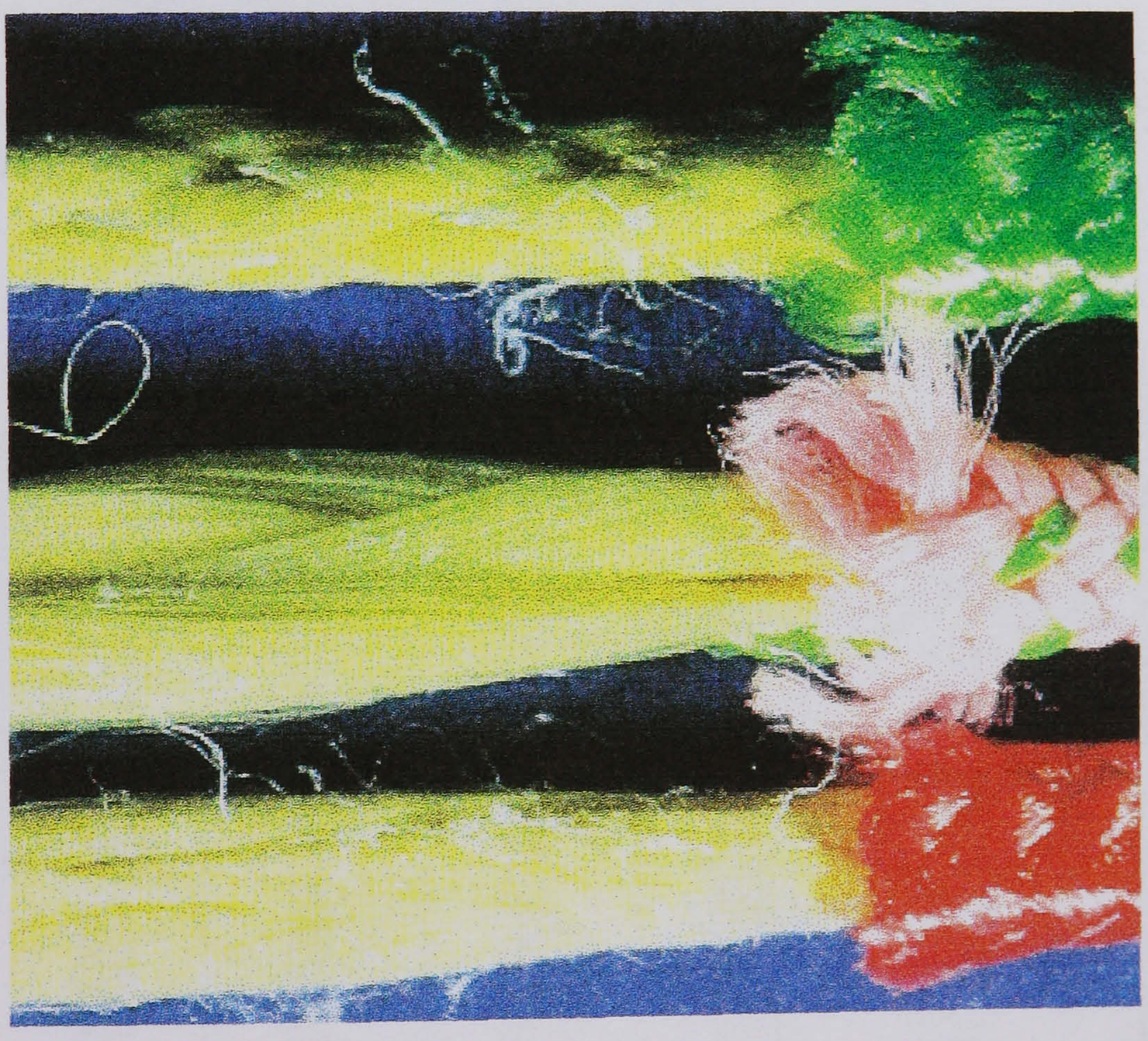

Figure 2.4: *Different Paraglider Lines Constructions*

3 strand papyrus rope

3 strand nylon rope

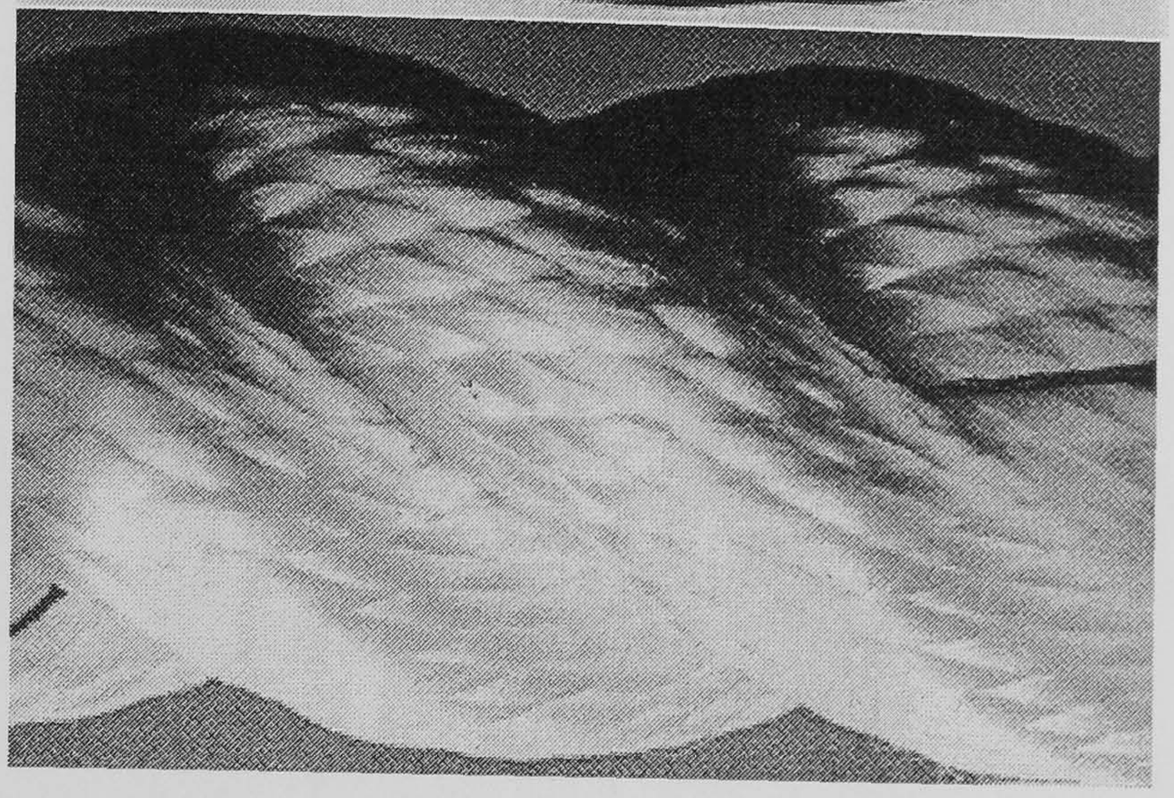

Figure 3.1: *Comparison of the constructions of a 5000 year old papyrus rope with a nylon rope of the same construction*

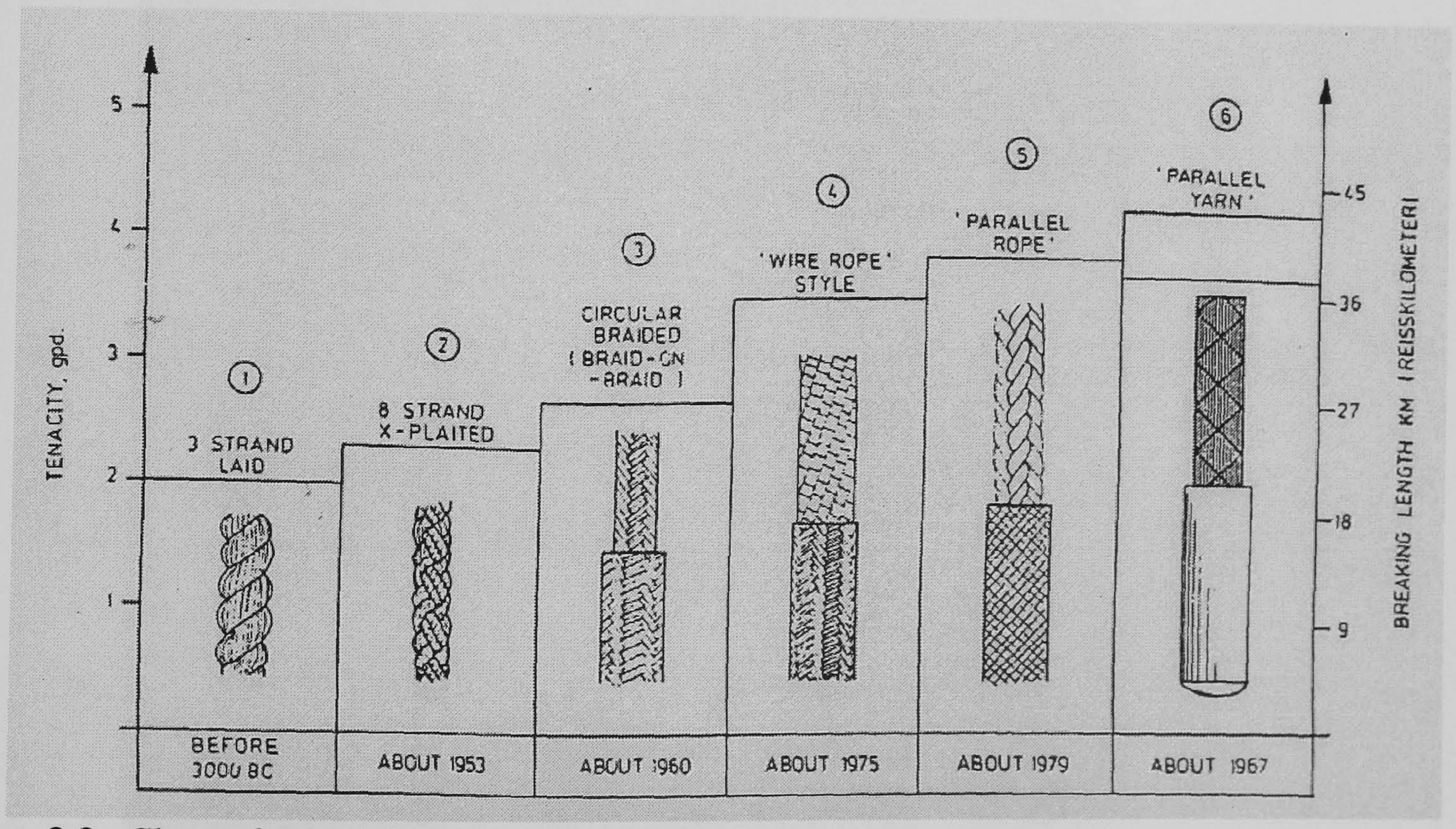

Figure 3.2: *Chronological development of rope design*

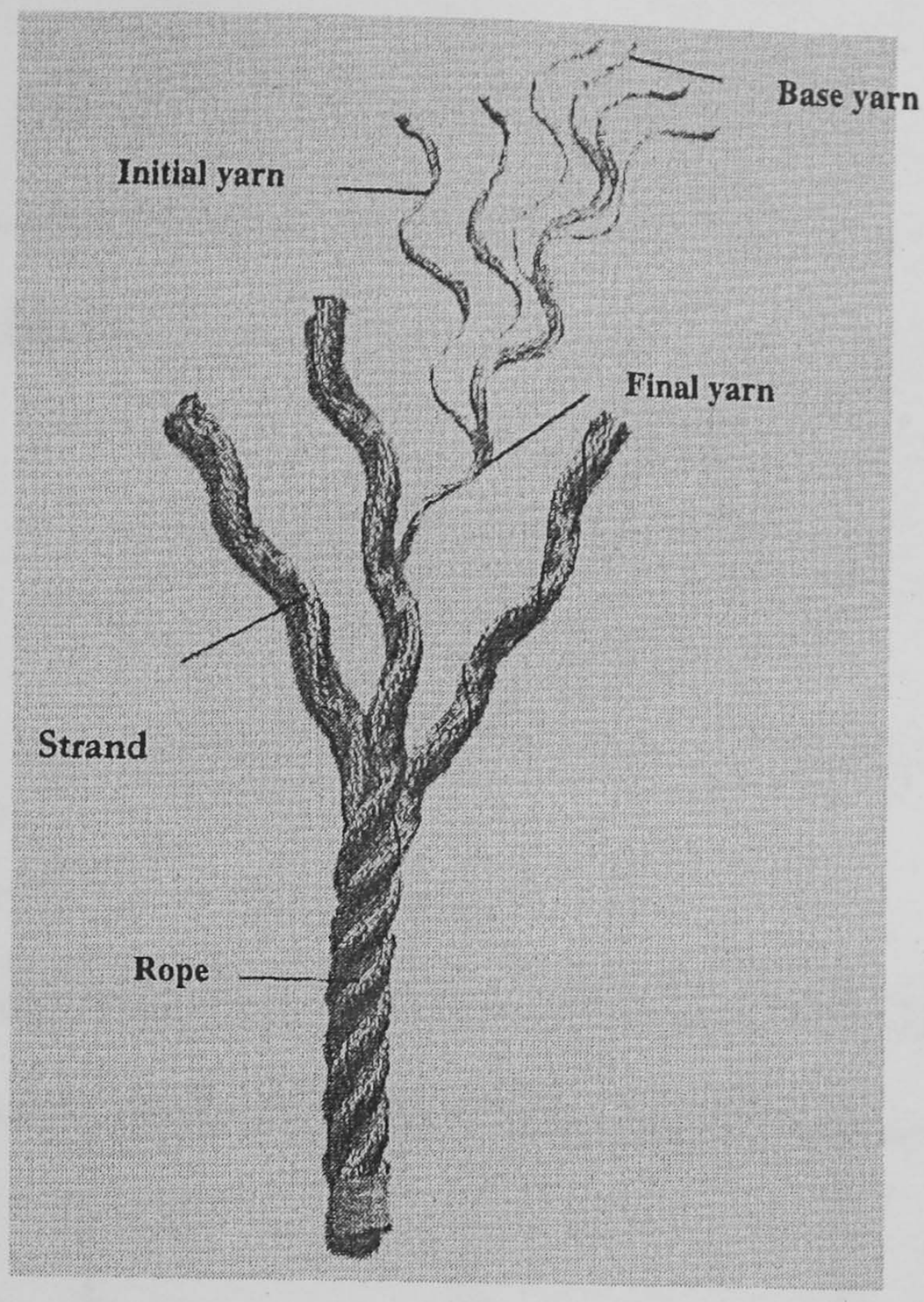

Figure 3.3: Components of a rope

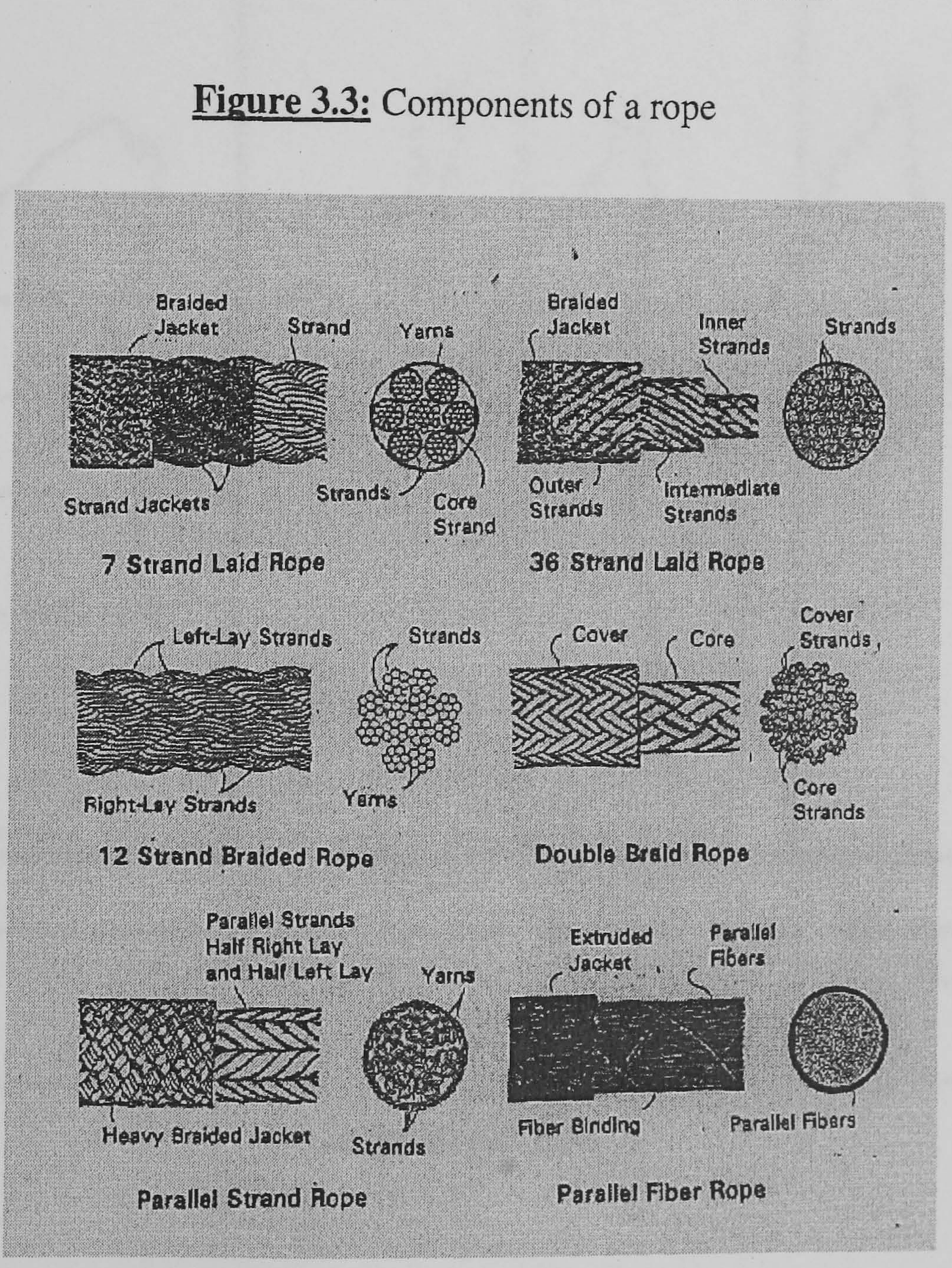

Figure 3.4: *Various rope designs that are being used by the marine industry*

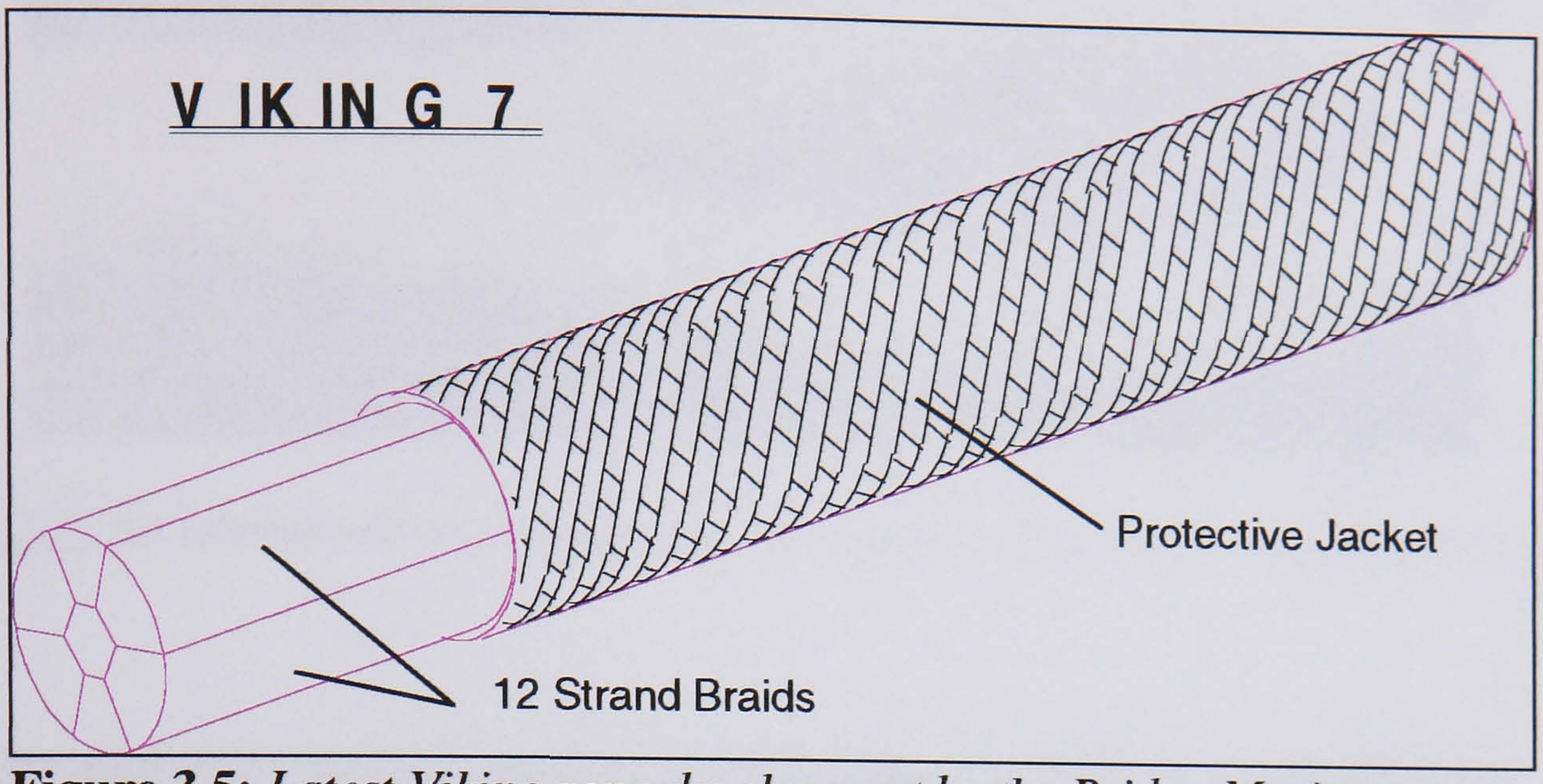

Figure 3.5: *Latest Viking rope development by the Bridon Marine*

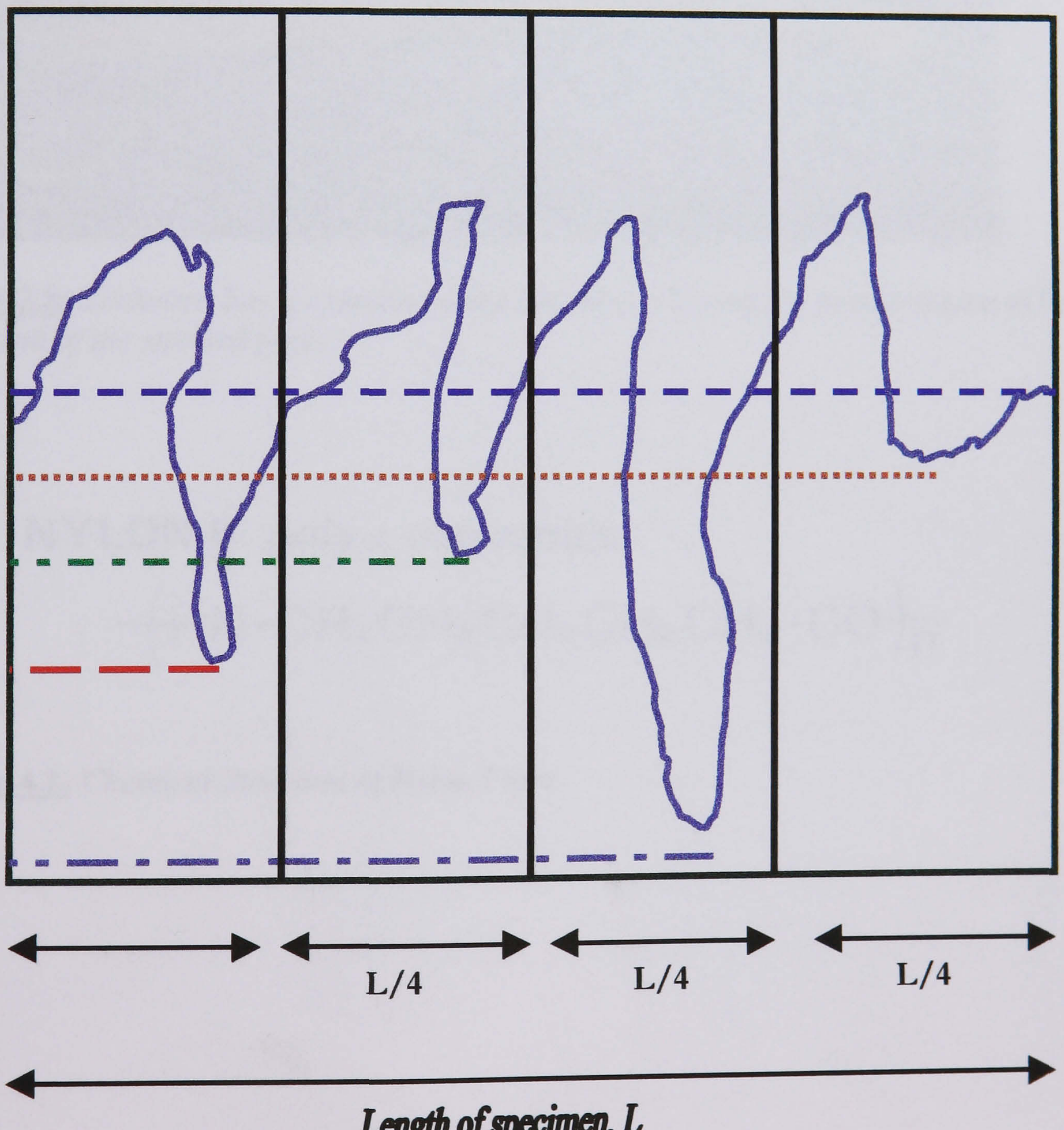

Figure3.6: *Graphical representation of the weakest link theory*

Figure 3.7: *An example of an Aramid line terminated using finger-trapping technique*

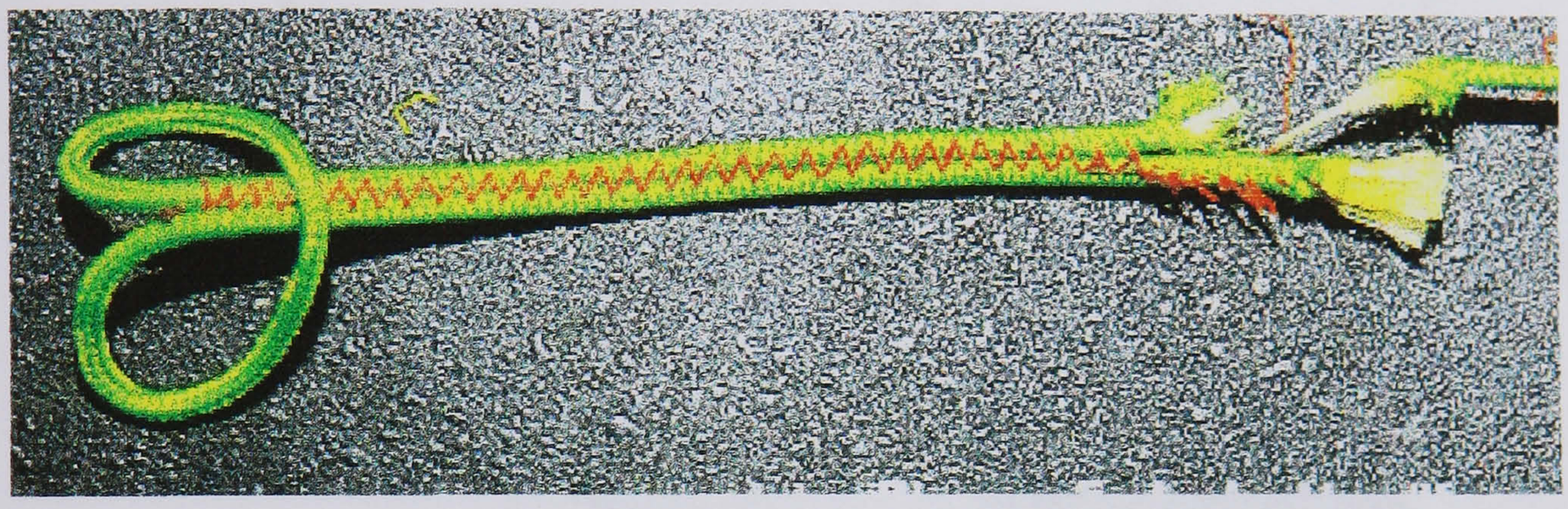

Figure 3.8: *Technora line terminated using stitching, showing the failure region to be at the end of the stitched part.*

NYLON 6: poly-ϵ-capramide

$$-\left(HN\cdot CH_2CH_2CH_2CH_2CH_2\cdot CO\right)_n-$$

Figure 4.1: *Chemical Structure of Nylon Fibre*

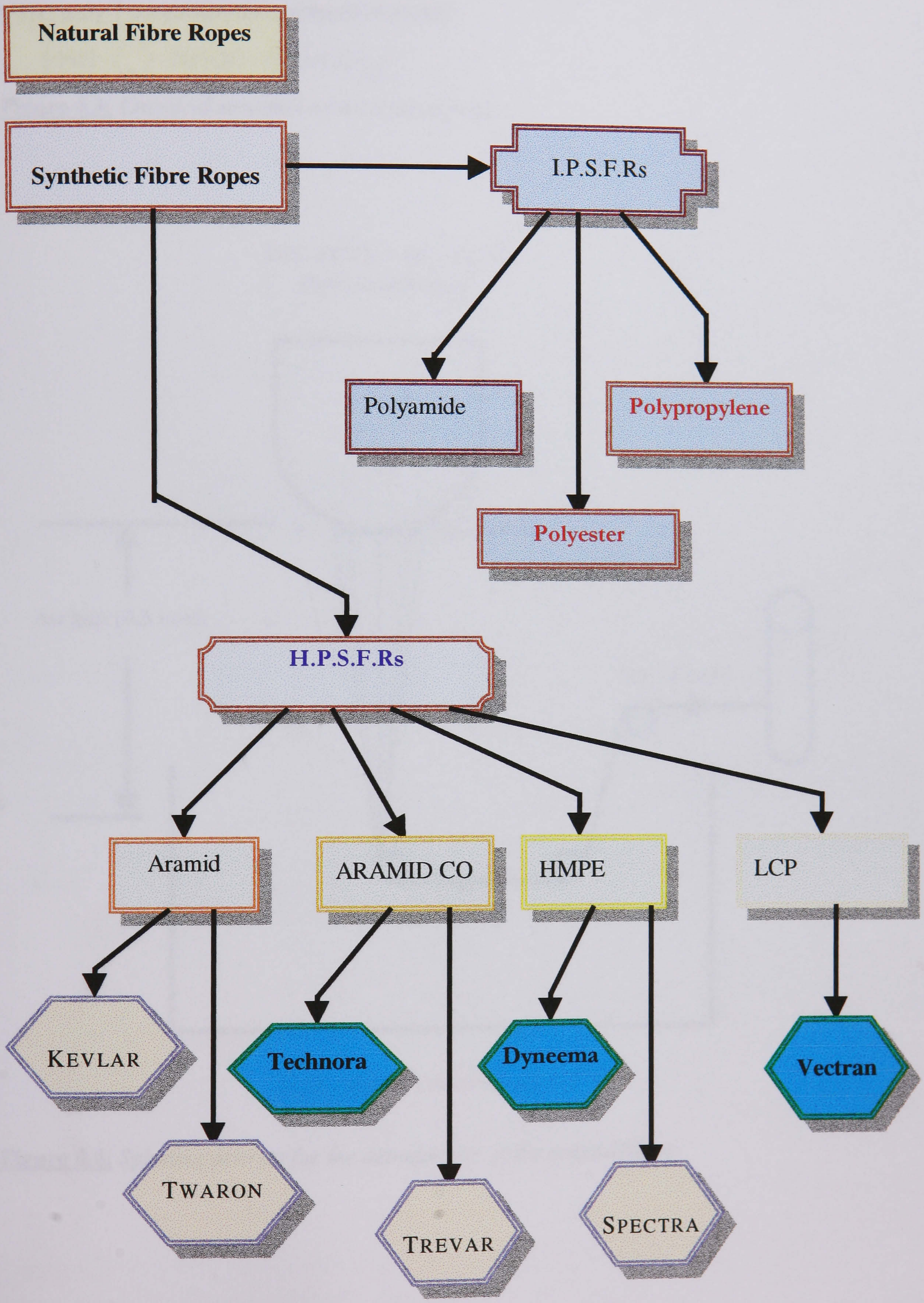

Figure 4.2: *Flow chart showing the different fibres available for rope manufacture*

Technora®: co-poly-(paraphenylene/3,4'-oxydiphenylene terephthalamide)

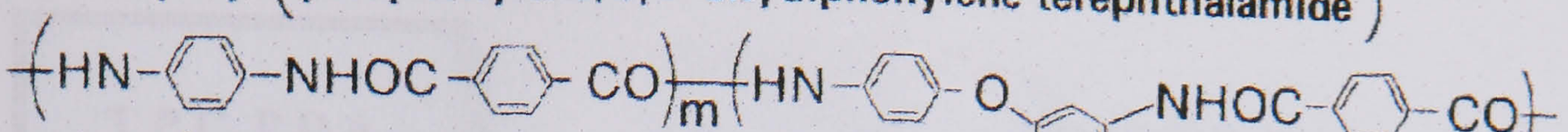

PPTA: poly-(paraphenylene terephthalamide)

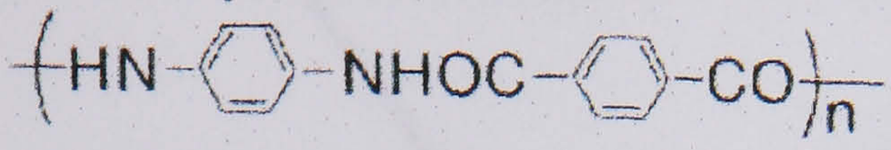

Figure 4.3: *Chemical structure of the aramid family*

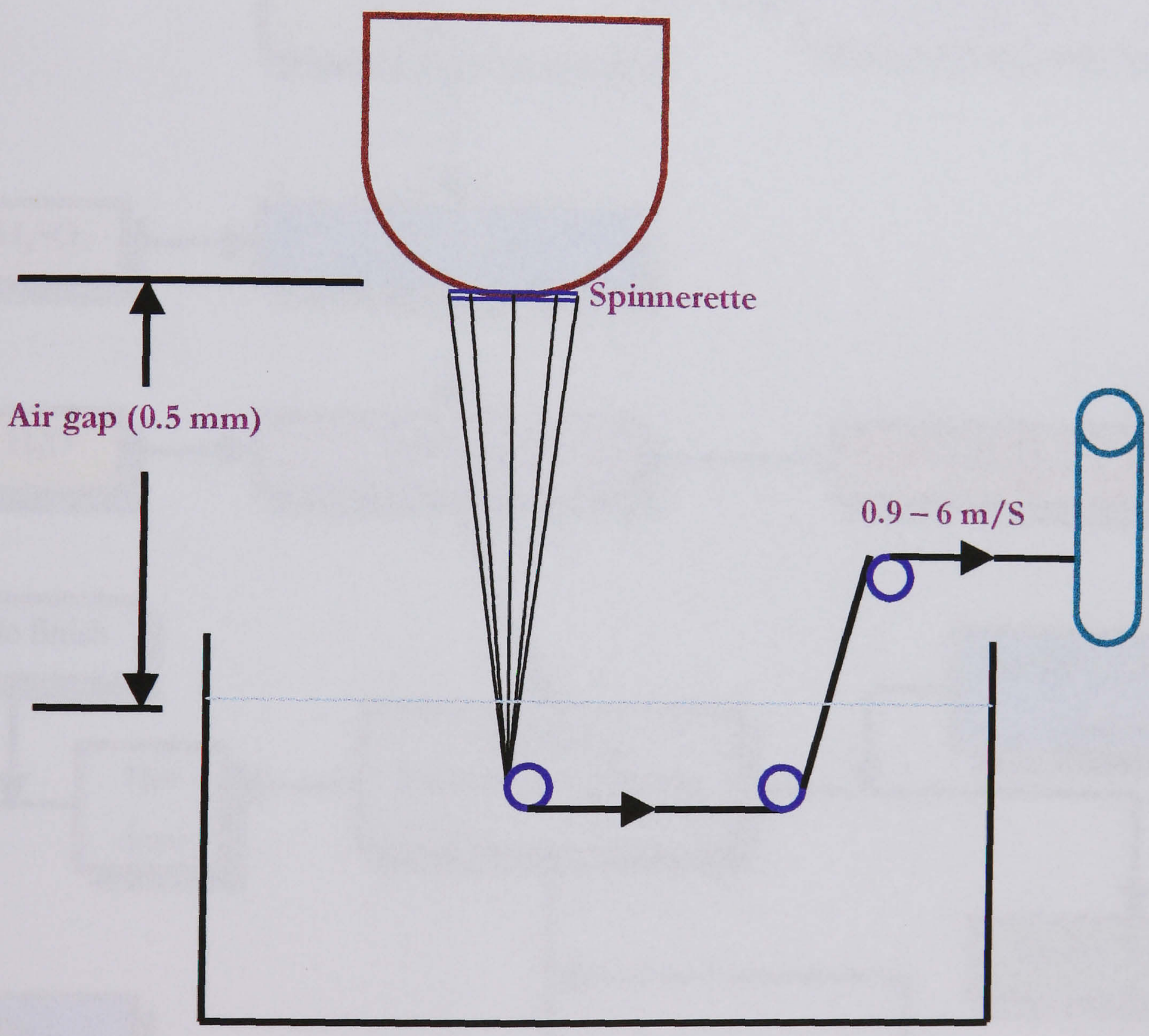

Figure 4.4: *Spinning process for the manufacture of the aramid fibres*

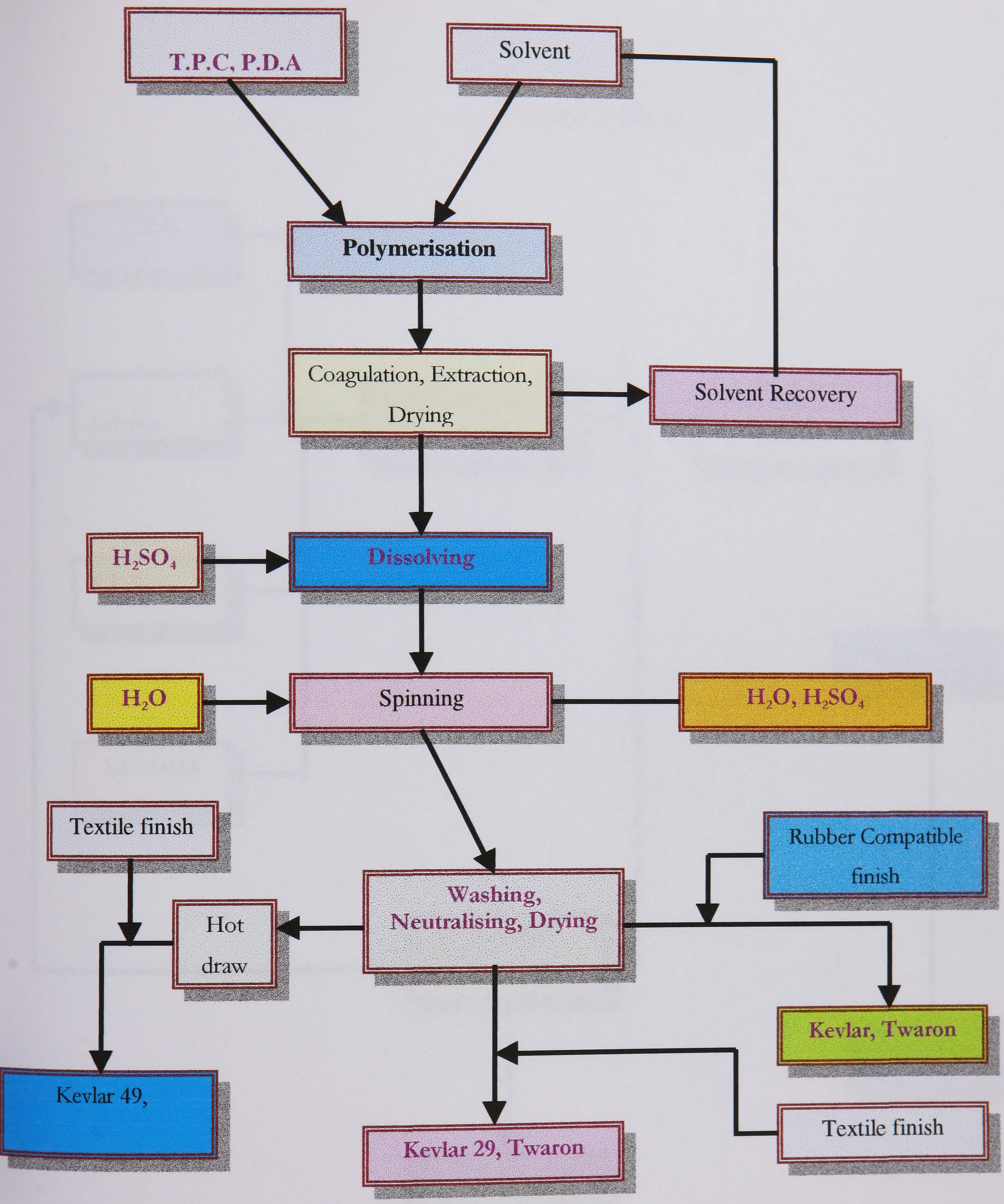

Figure 4.5: *Graphical representation of the aramid production process*

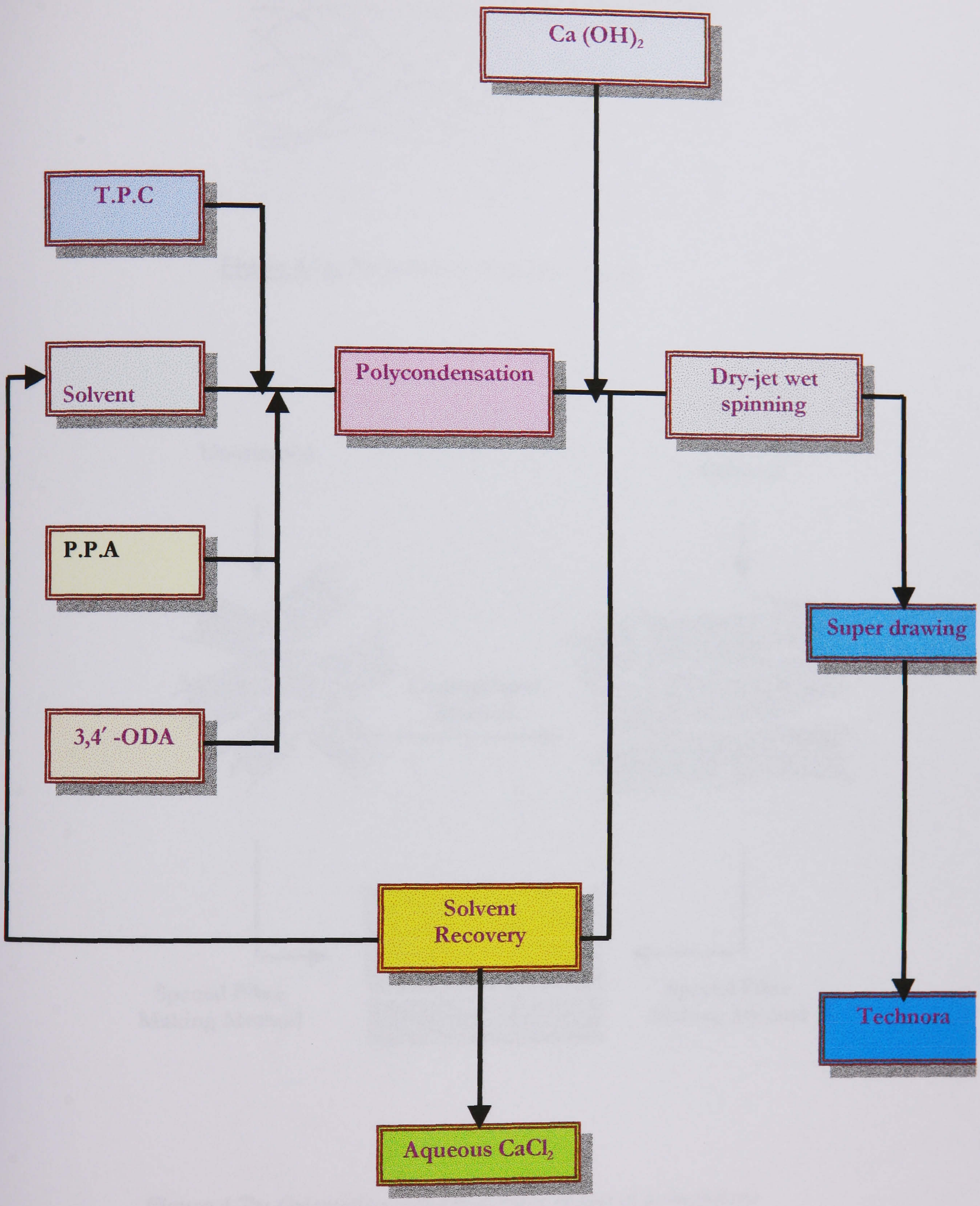

Figure 4.6: *Graphical representation of the Technora production process*

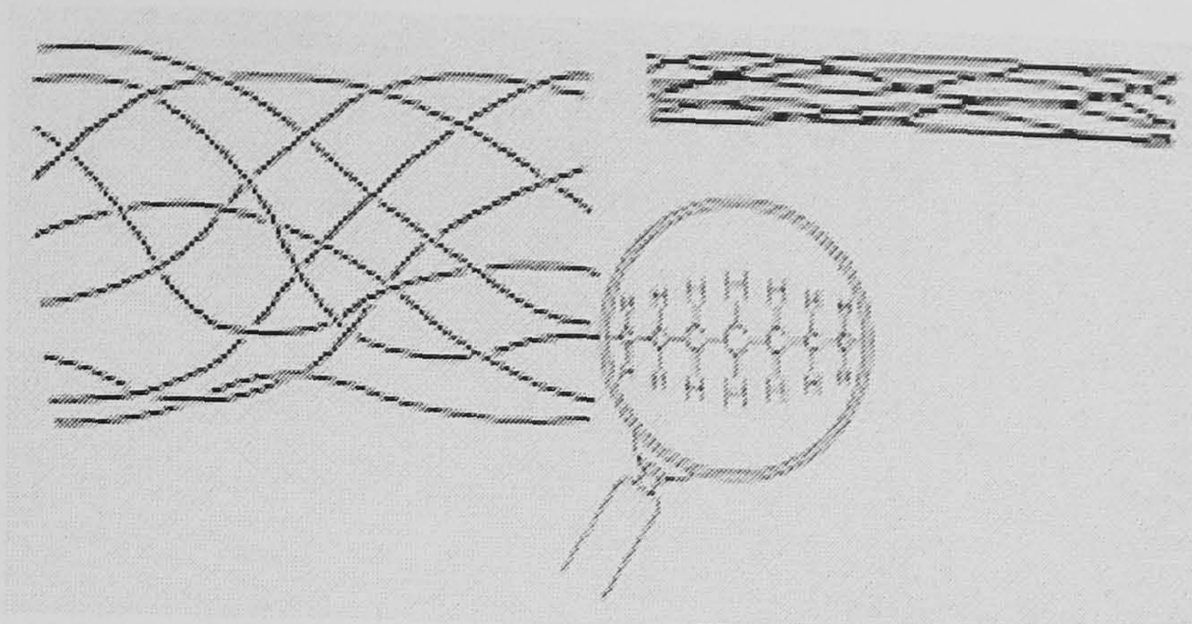

Figure 4.7a: *Polyethylene molecular chains*

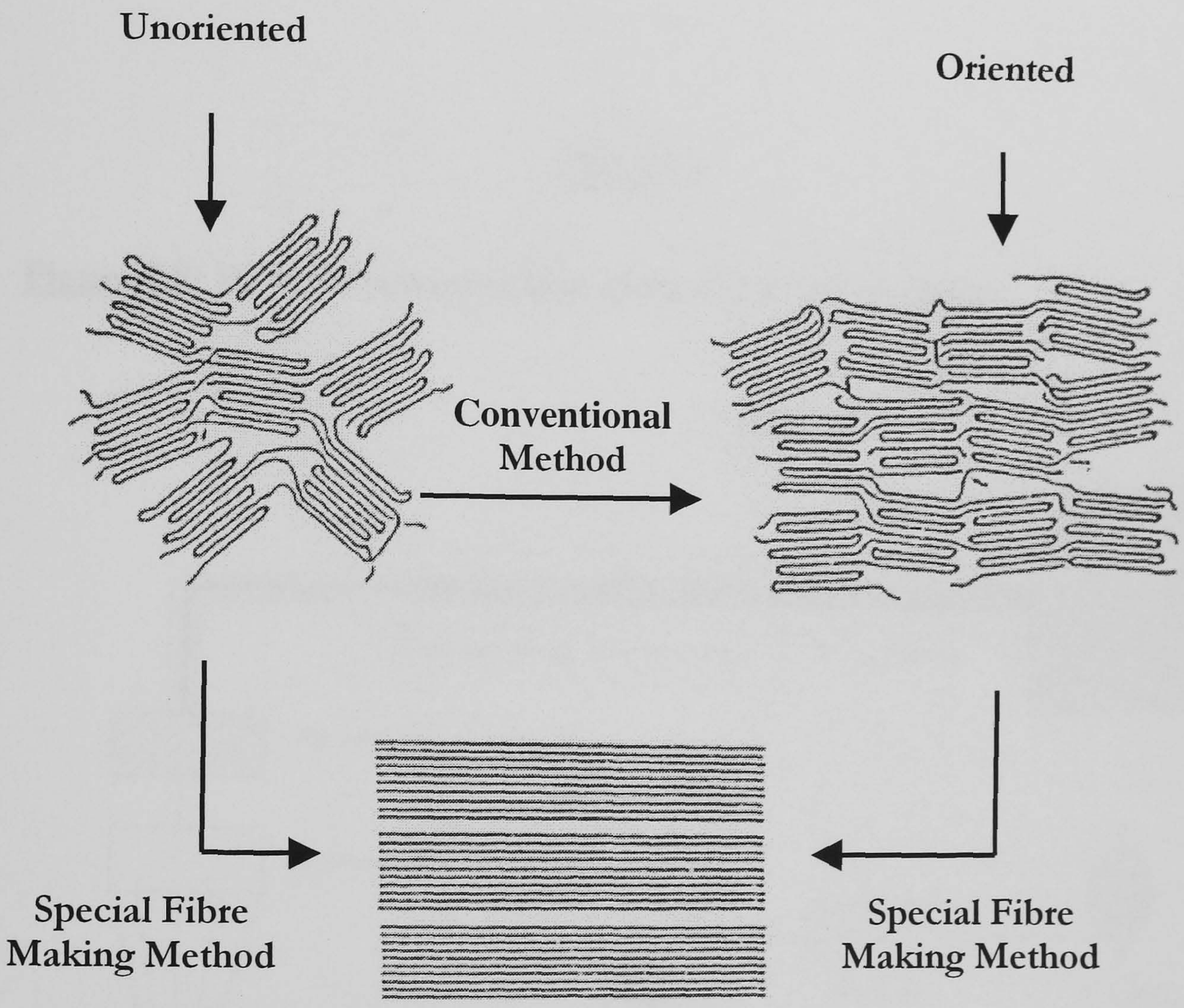

Figure 4.7b: *Orientation of the molecular chains of polyethylene*

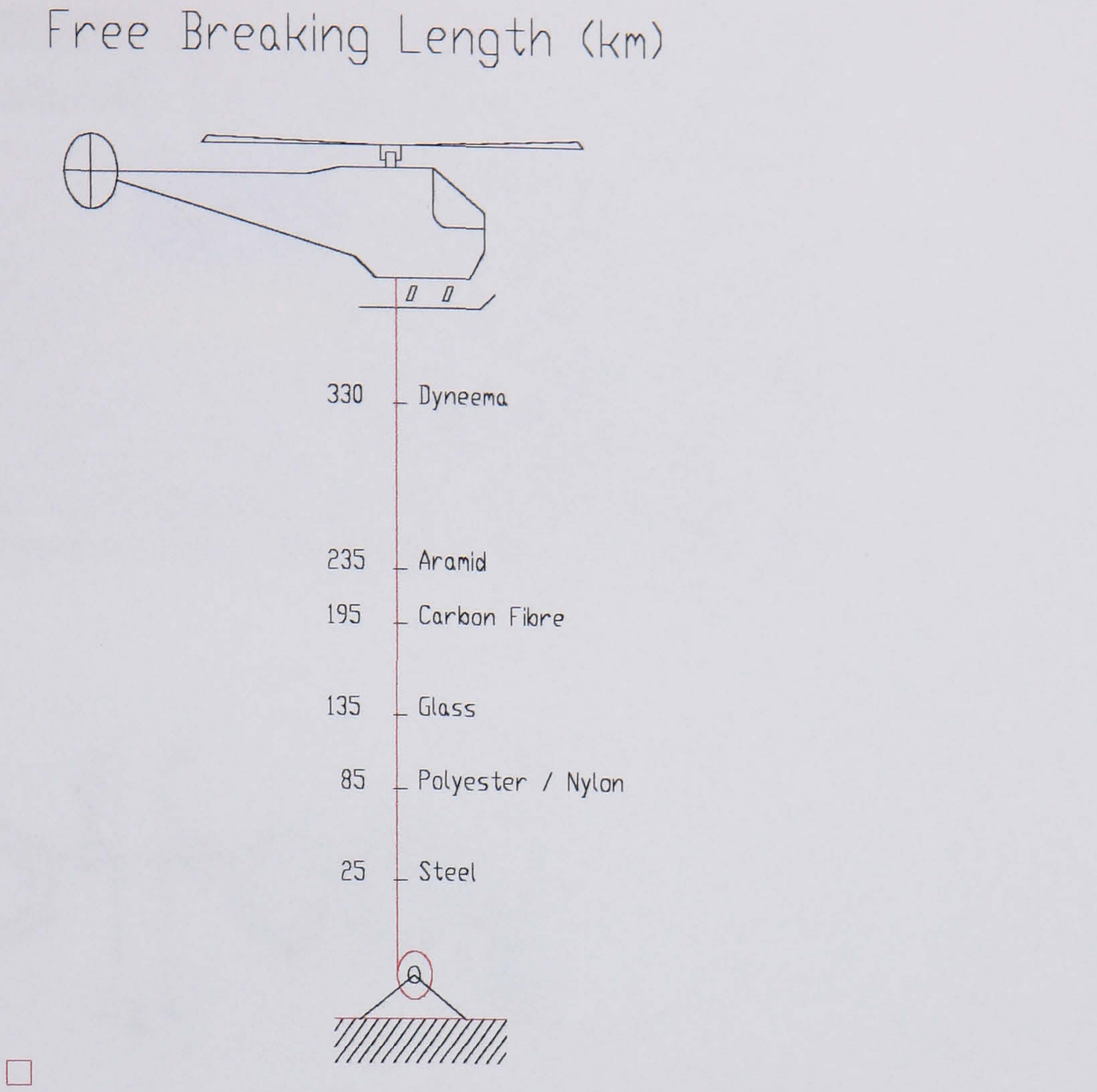

Figure 4.8: *Pictorial representation of the free breaking length*

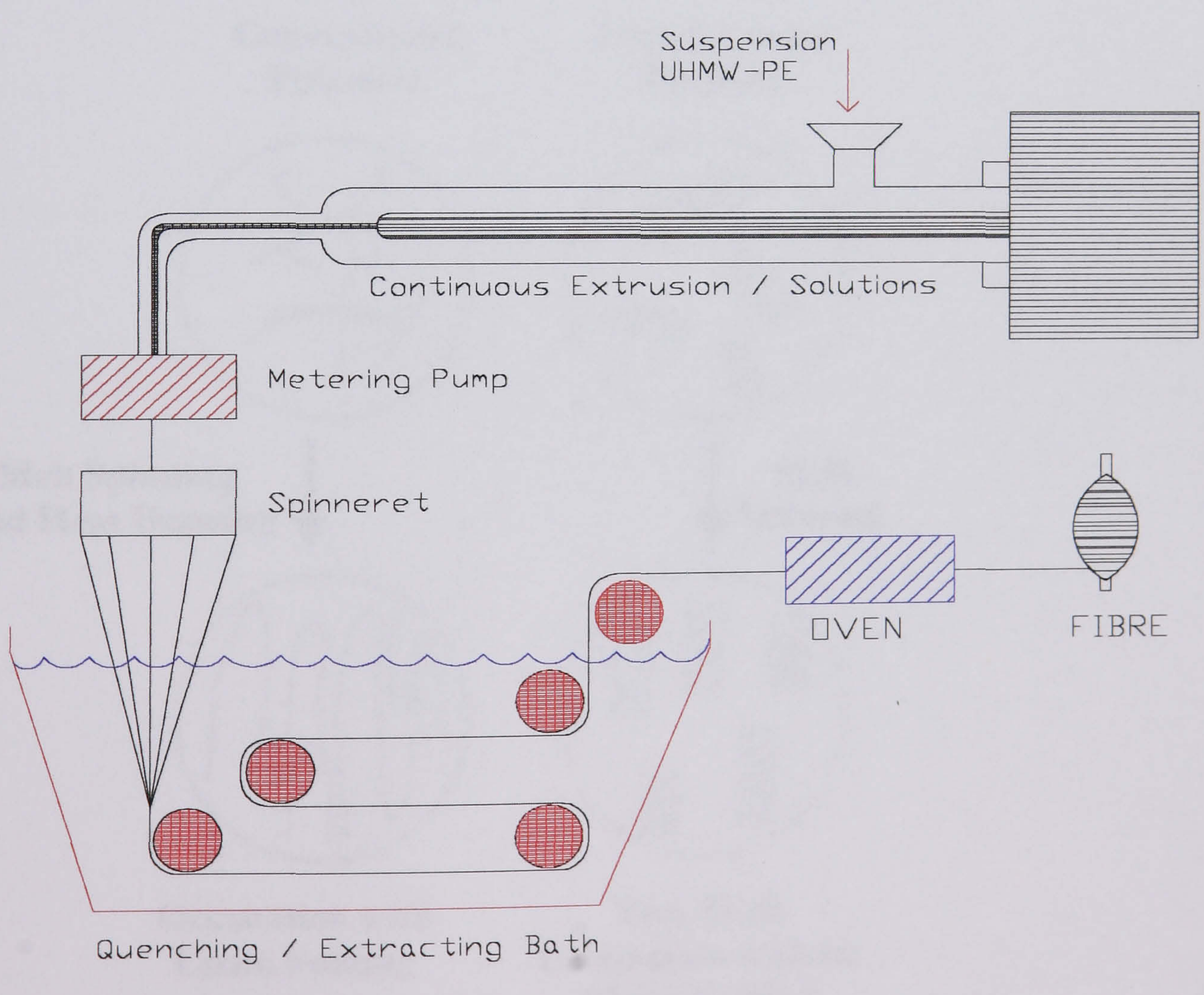

Figure 4.9: *Gel Spinning technique for processing of Dyneema*

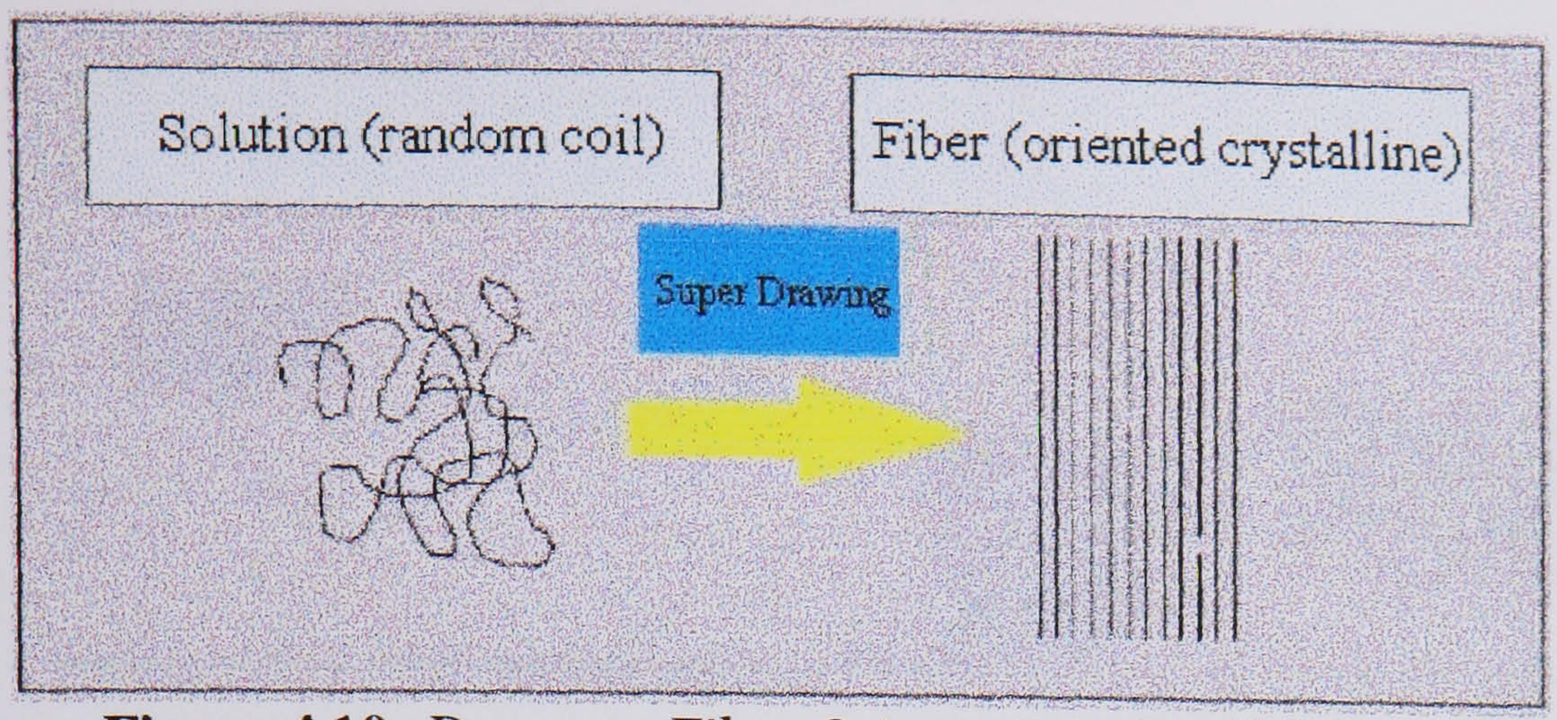

Figure 4.10: *Dyneema Fibre Orientation after Gel spinning*

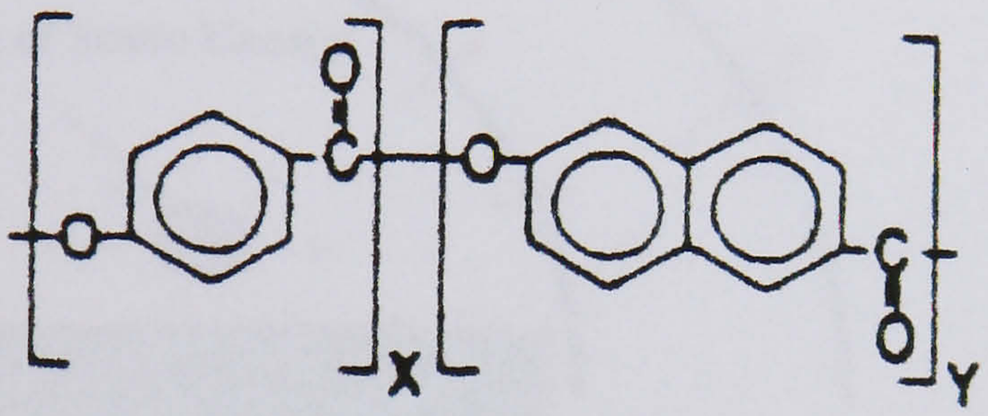

Figure 4.11: *Chemical structure of Vectran fibres*

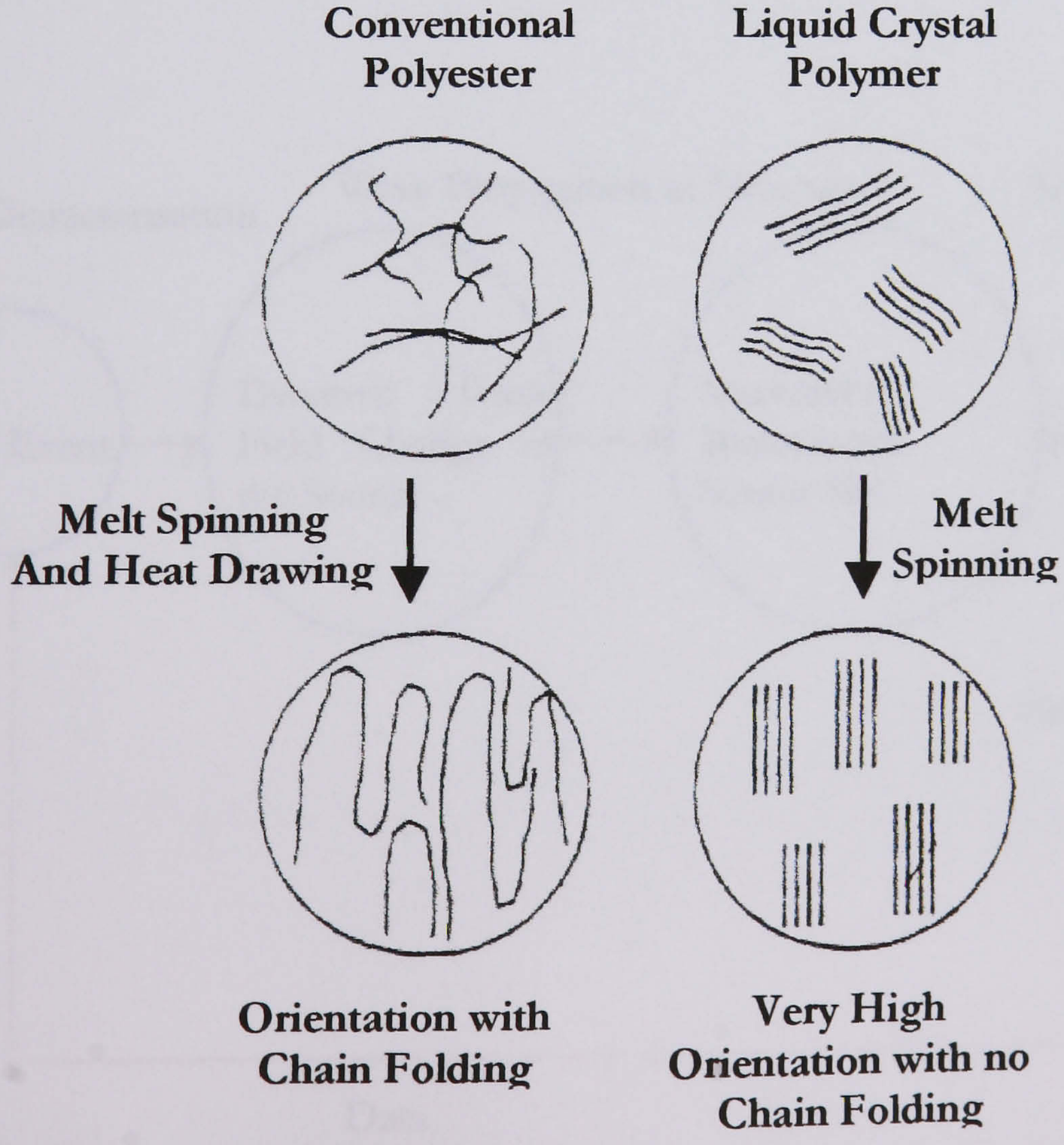

Figure 4.12: *Schematic diagram of molecular chain structure of Vectran*

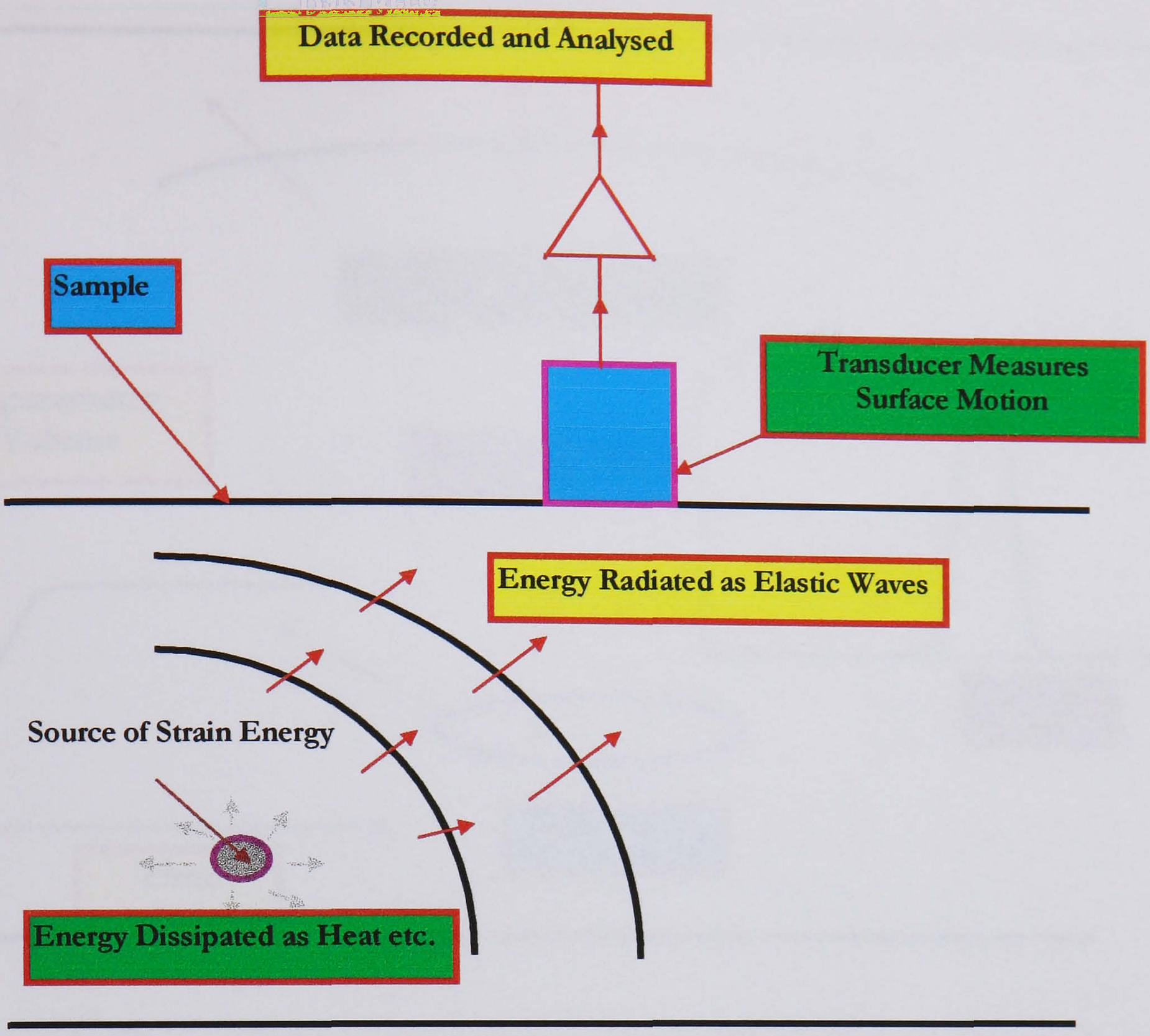

Figure 6.1: *Sudden localised changes in stress or strain within a body radiate some energy as elastic waves (acoustic emission) whilst some is dissipated as heat.*

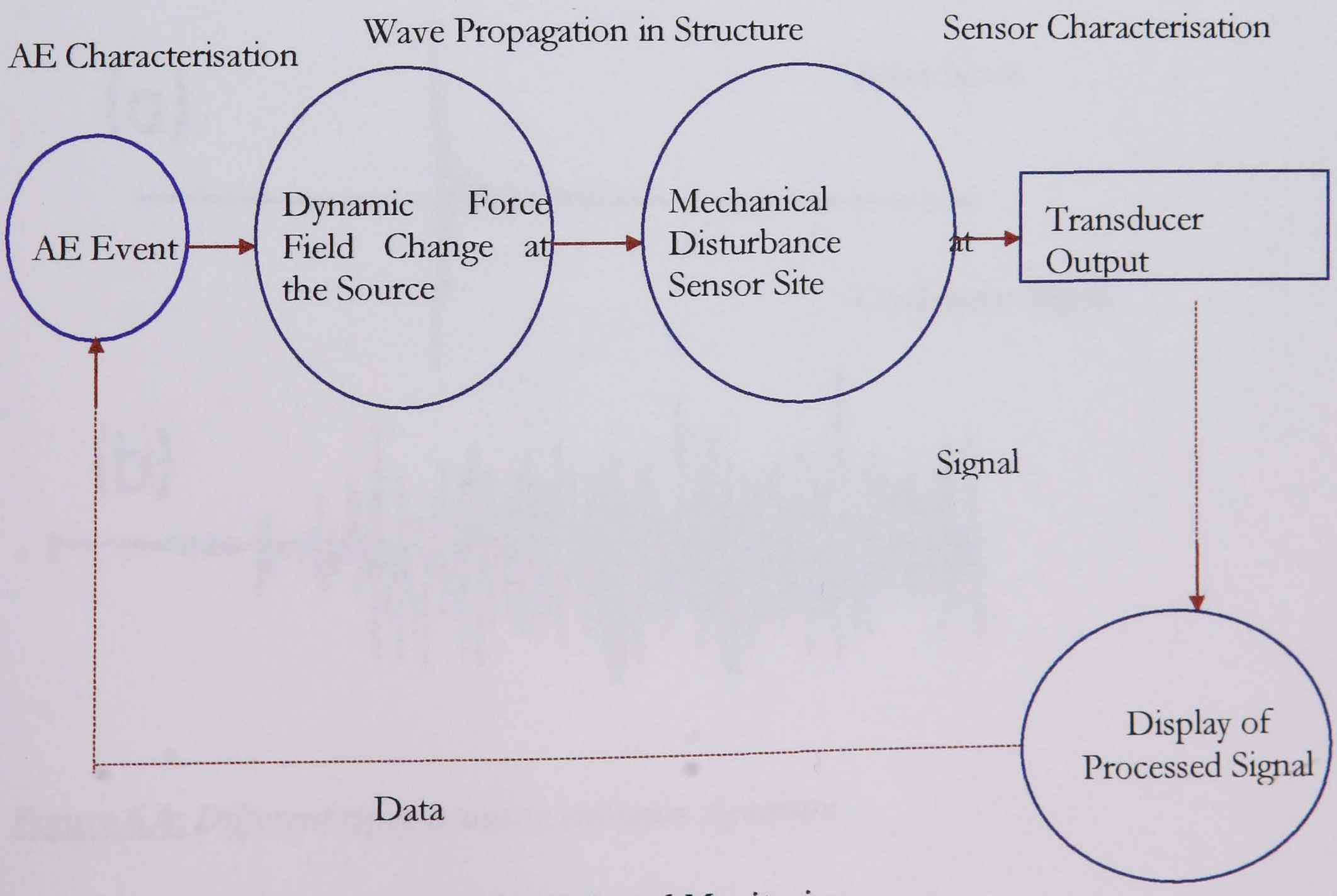

Figure 6.2: *Simplified Process of AE Signal Monitoring*

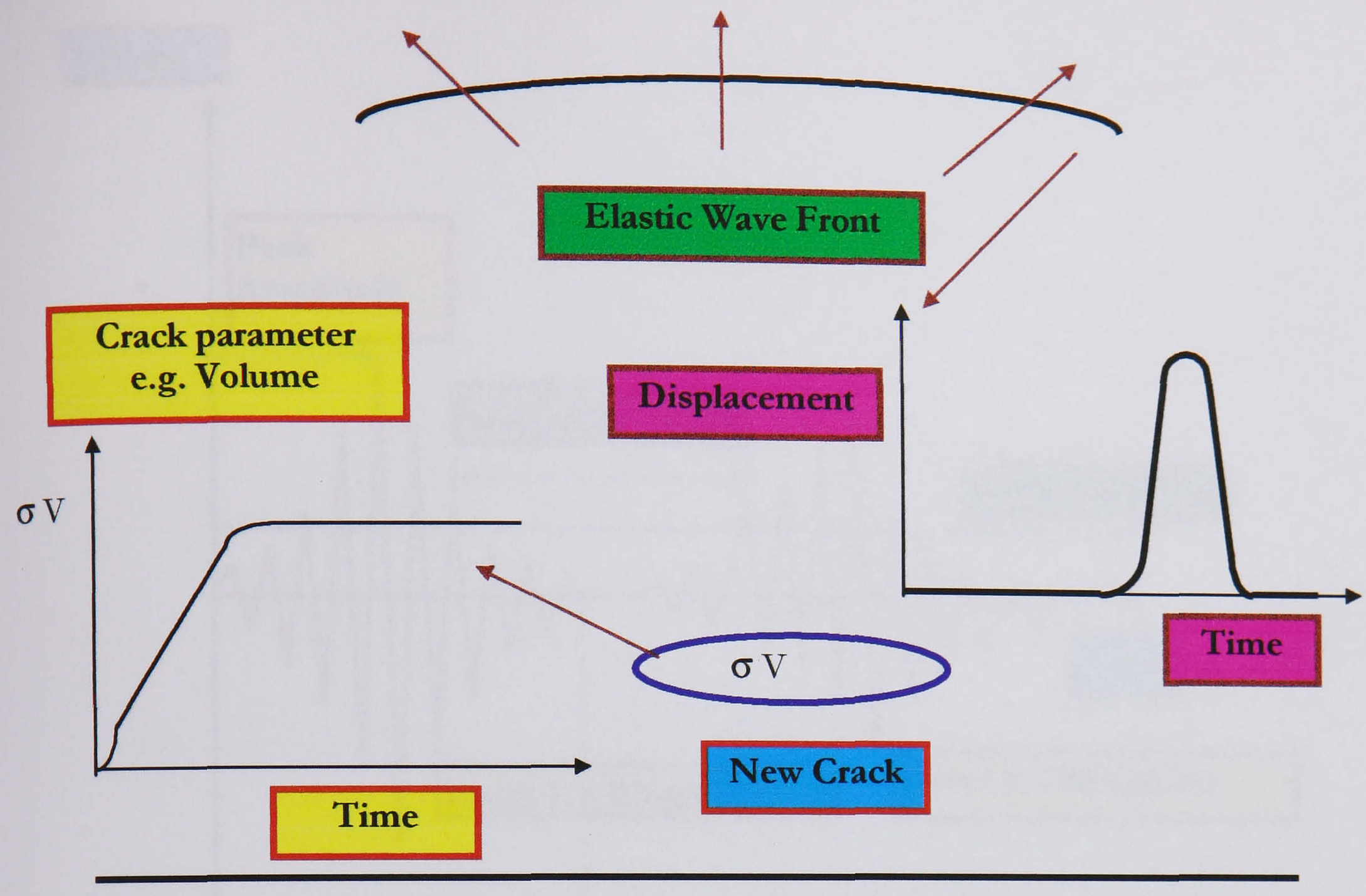

Figure 6.3: *When a crack is formed, its dimensions suddenly increase from zero, accompanied by a local change in stress, which acts as a source of ultrasonic waves. The compression wave is a pulse of displacement.*

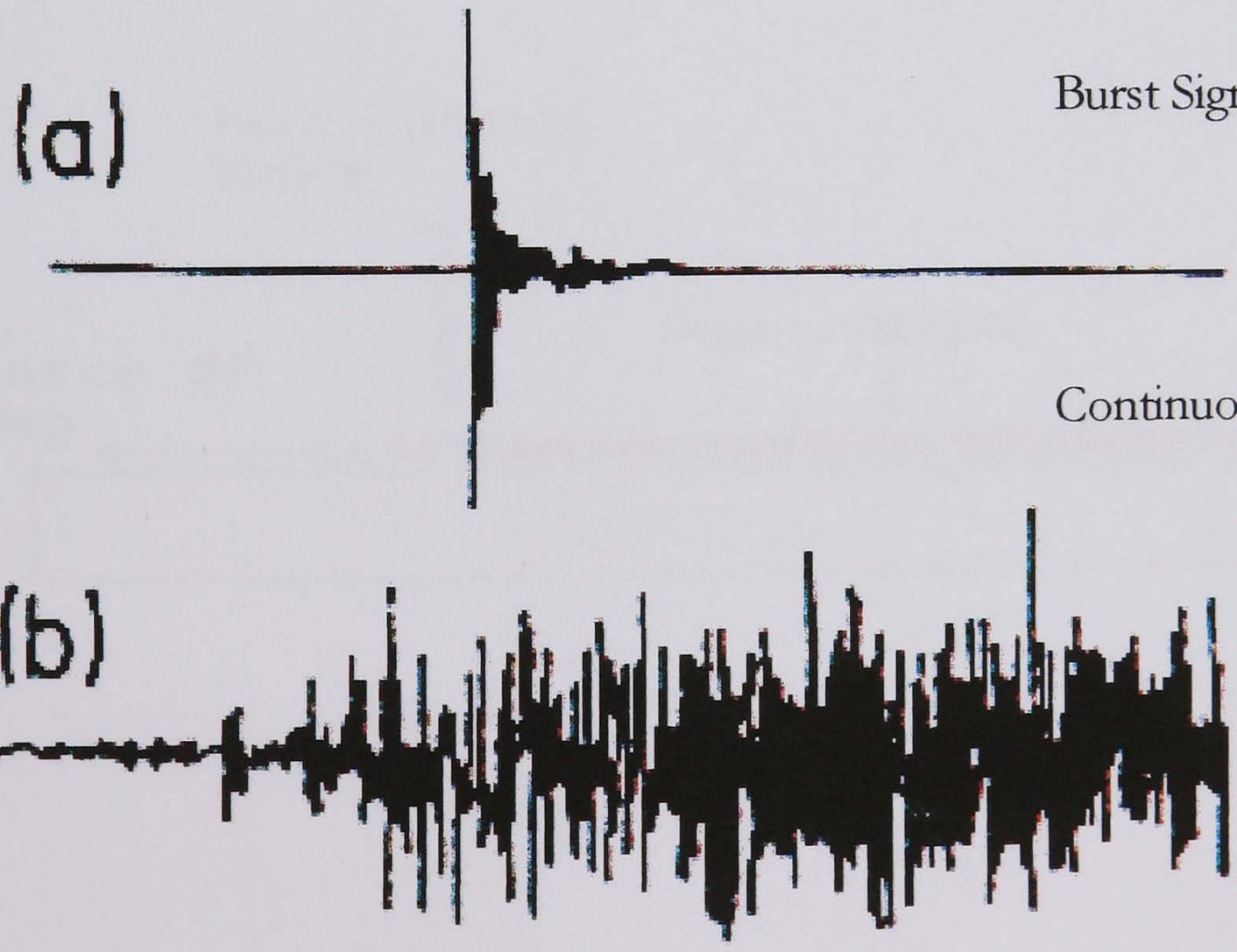

Figure 6.4: *Different types acoustic emission signature*

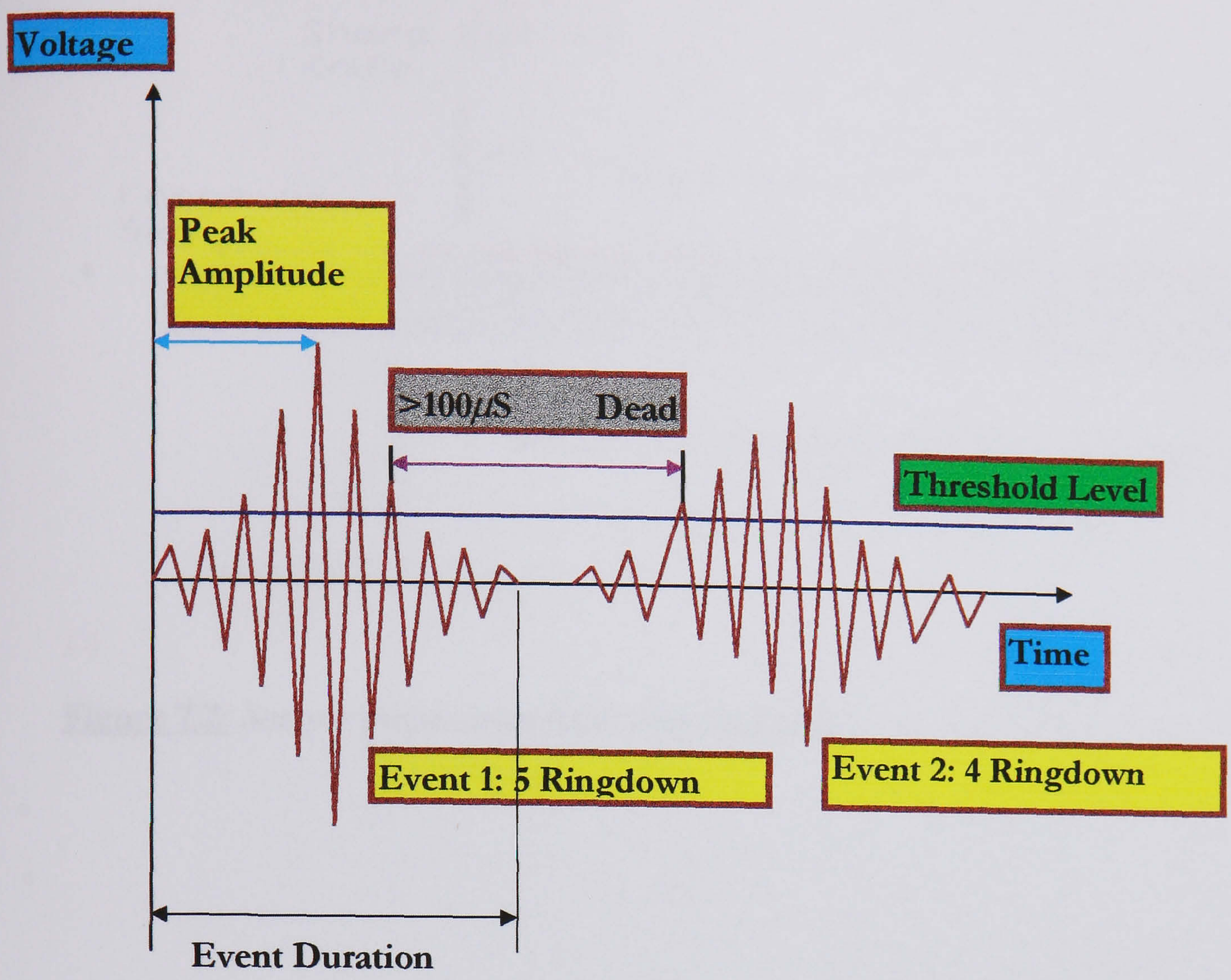

Figure 6.5: *The AE signal processing methods, showing the difference between event counting and ring down count.*

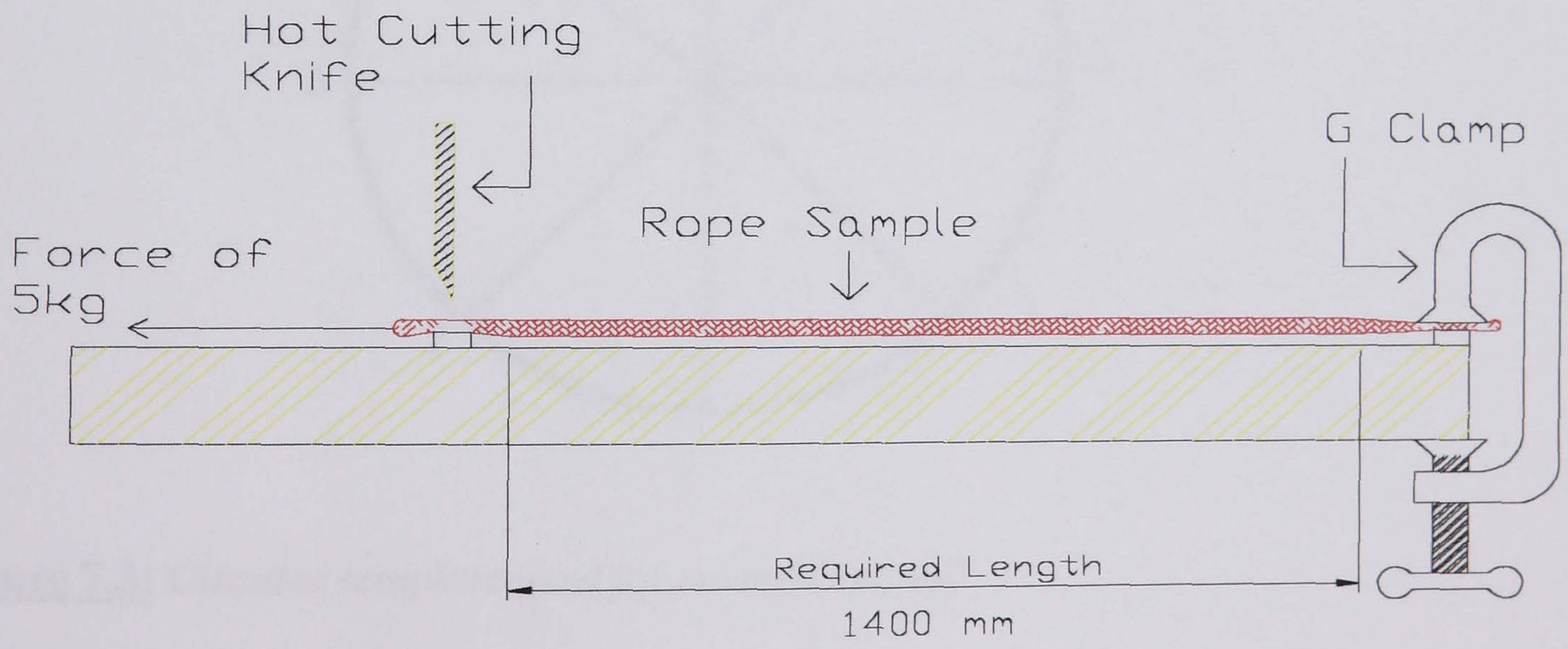

Figure 7.1: *Sample preparation fixture for Dyneema and Vectran samples*

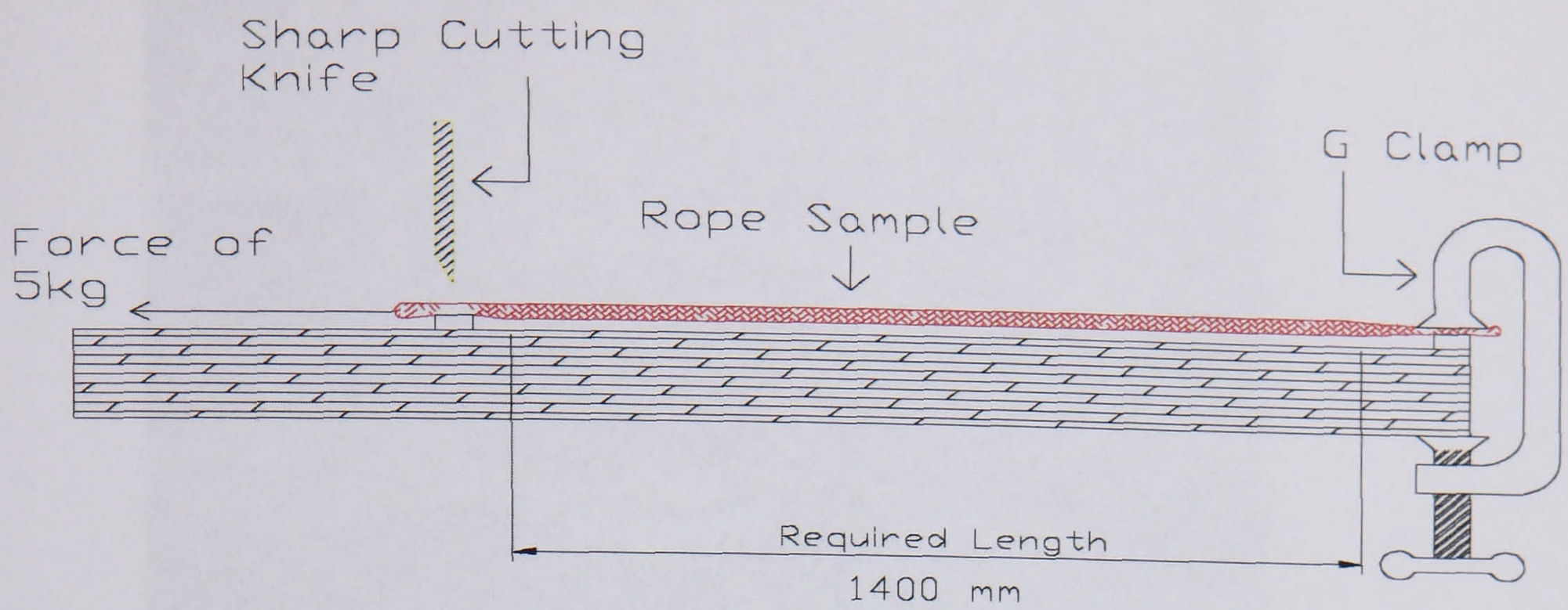

Figure 7.2: *Sample preparation fixture for Technora*

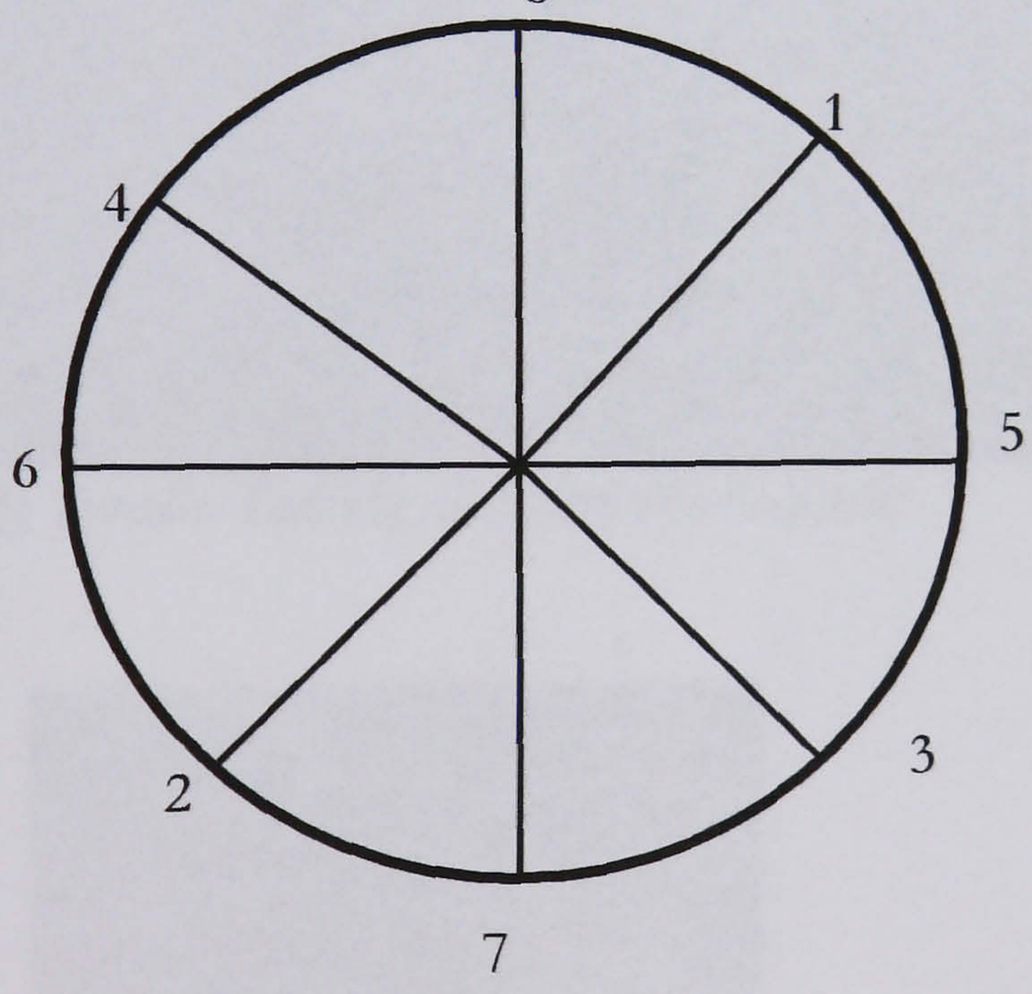

Figure 7.3: *Circular template used for strand removal*

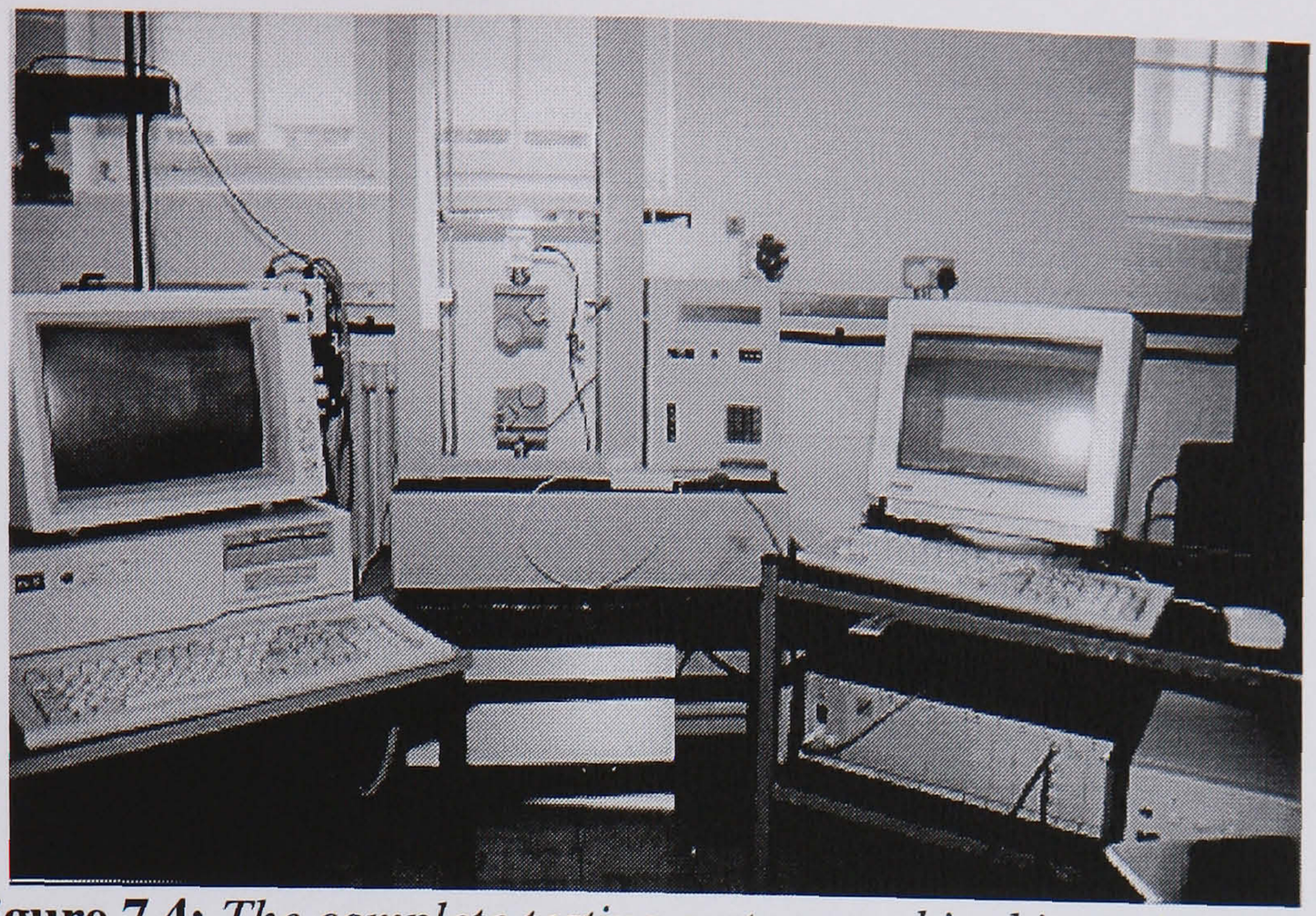

Figure 7.4: *The complete testing system used in this project*

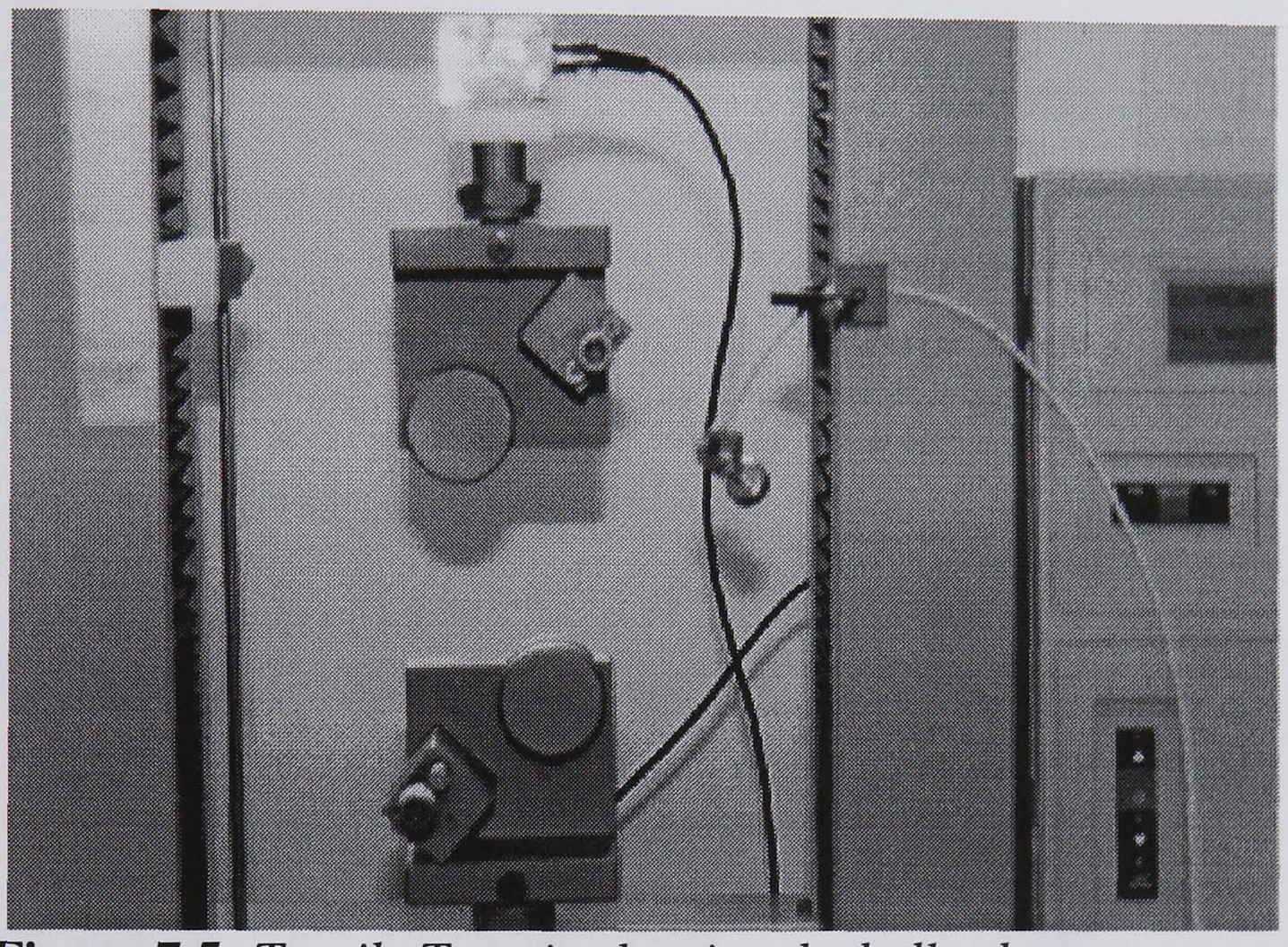

Figure 7.5: *Tensile Test rig showing the bollards*

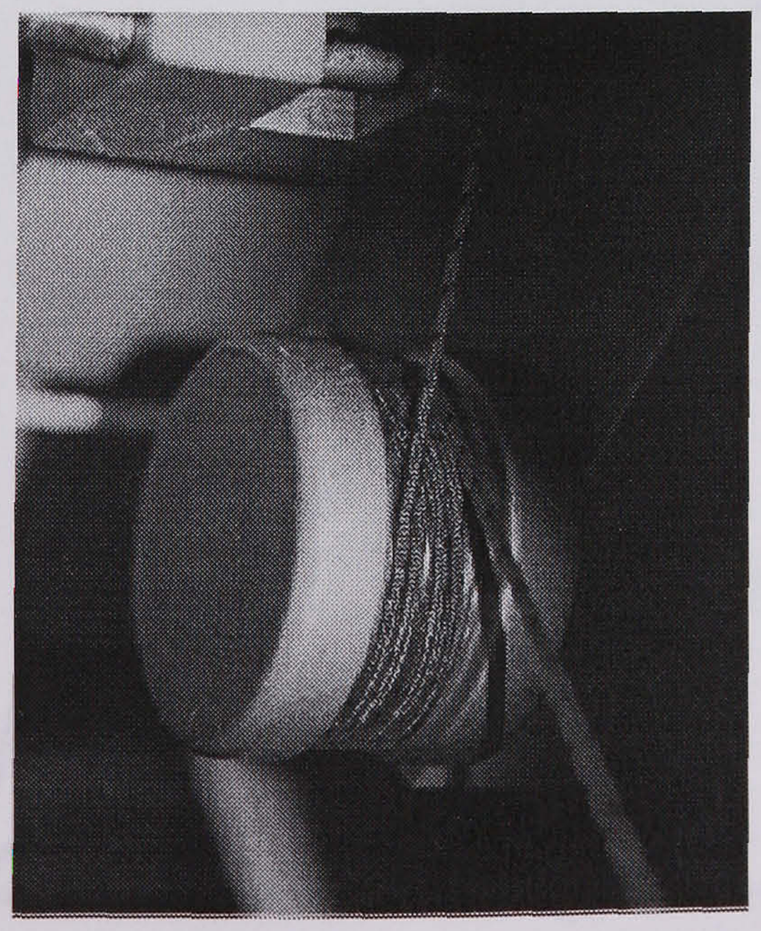

Figure 7.6: *Rope test rig showing the rope going round the bollard four times*

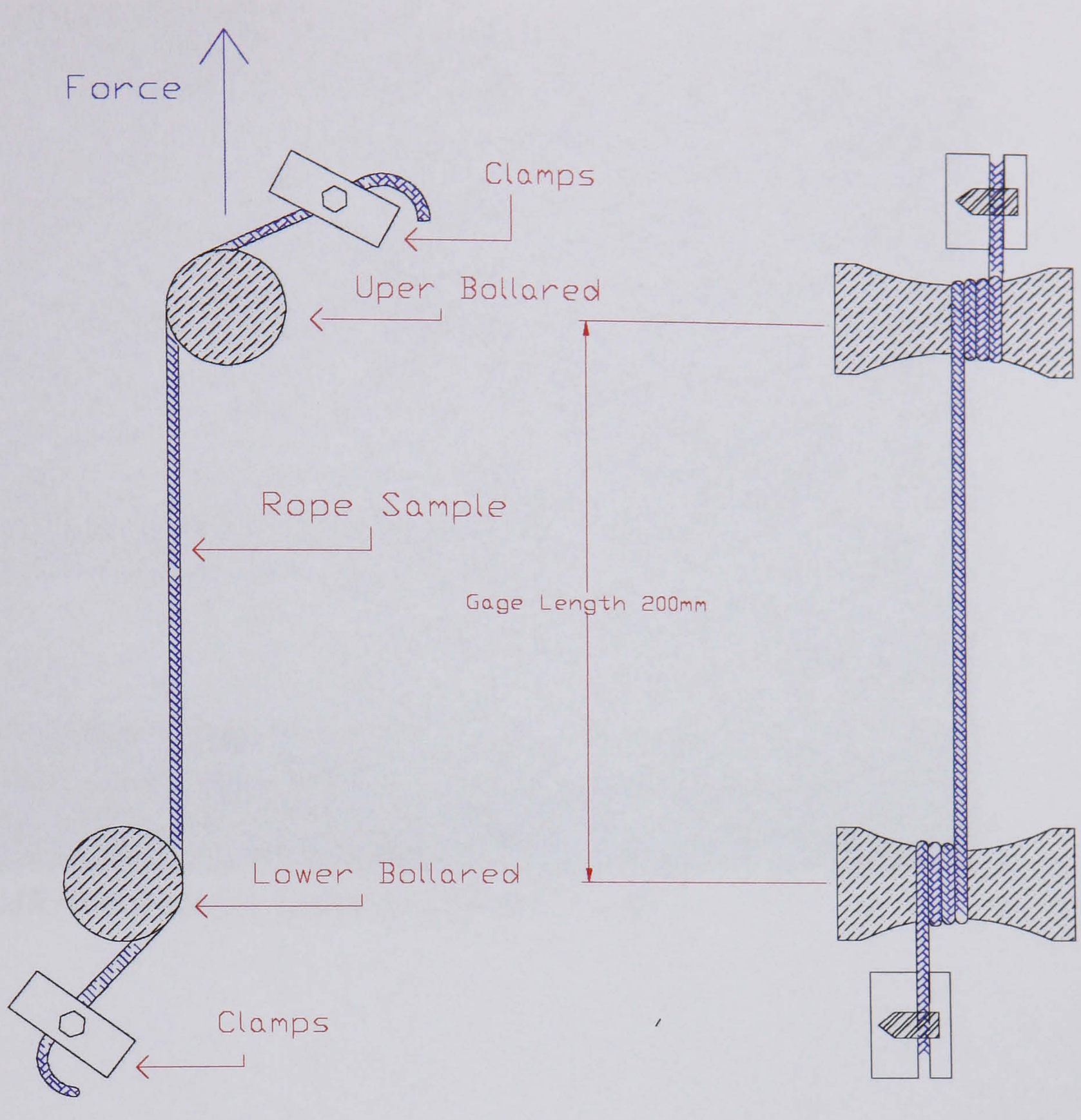

Figure 7.7: *Schematic diagram of the test rig*

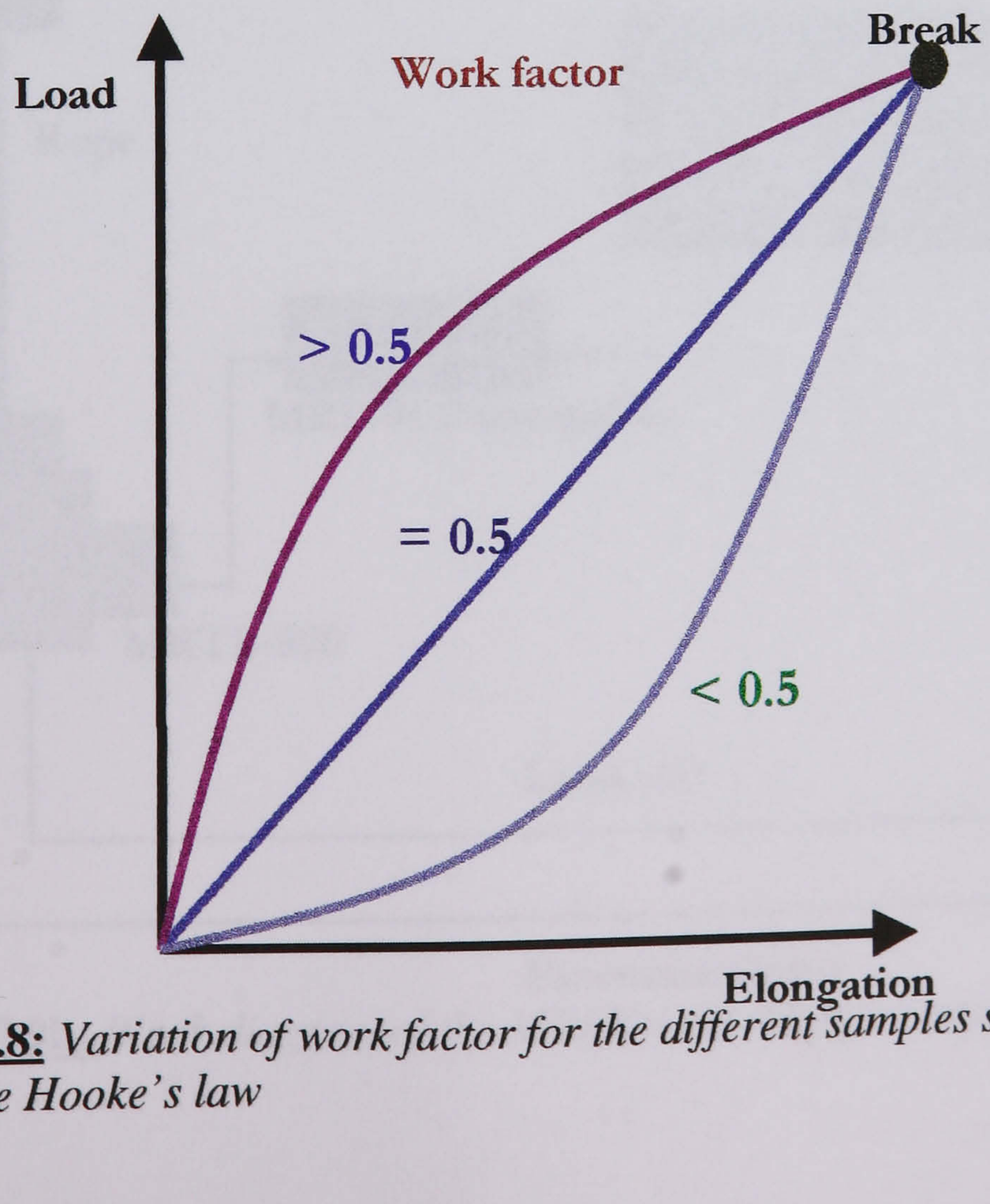

Figure 7.8: *Variation of work factor for the different samples showing how closely they follow the Hooke's law*

Figure 7.9a: *MR1004 Acoustic Emission equipment used*

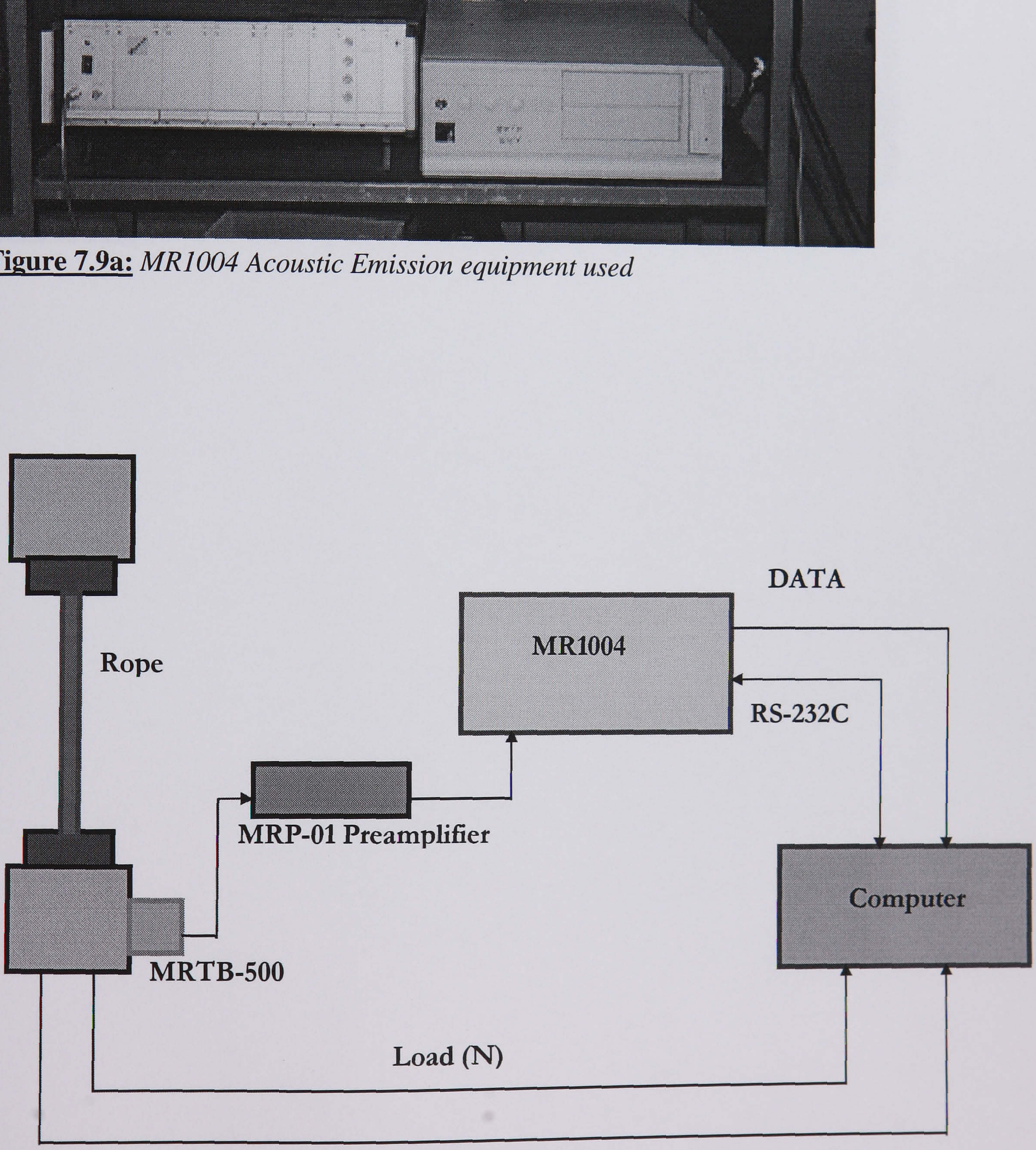

Figure 7.9b: *Block diagram of the MR1004 AE Analyser set-up used in this project.*

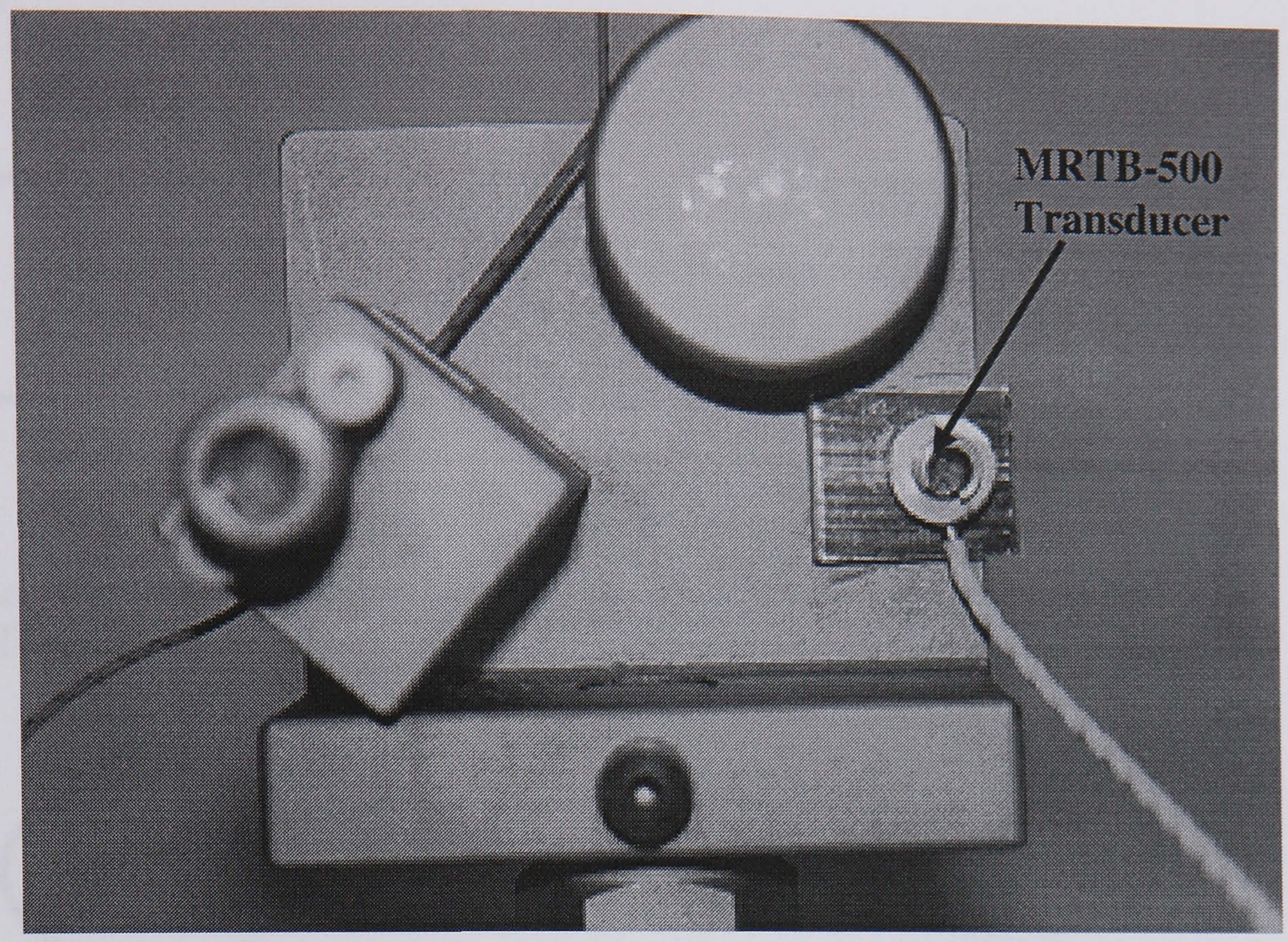

Figure 7.10: *Lower bollard of the test rig showing the position of the transducer.*

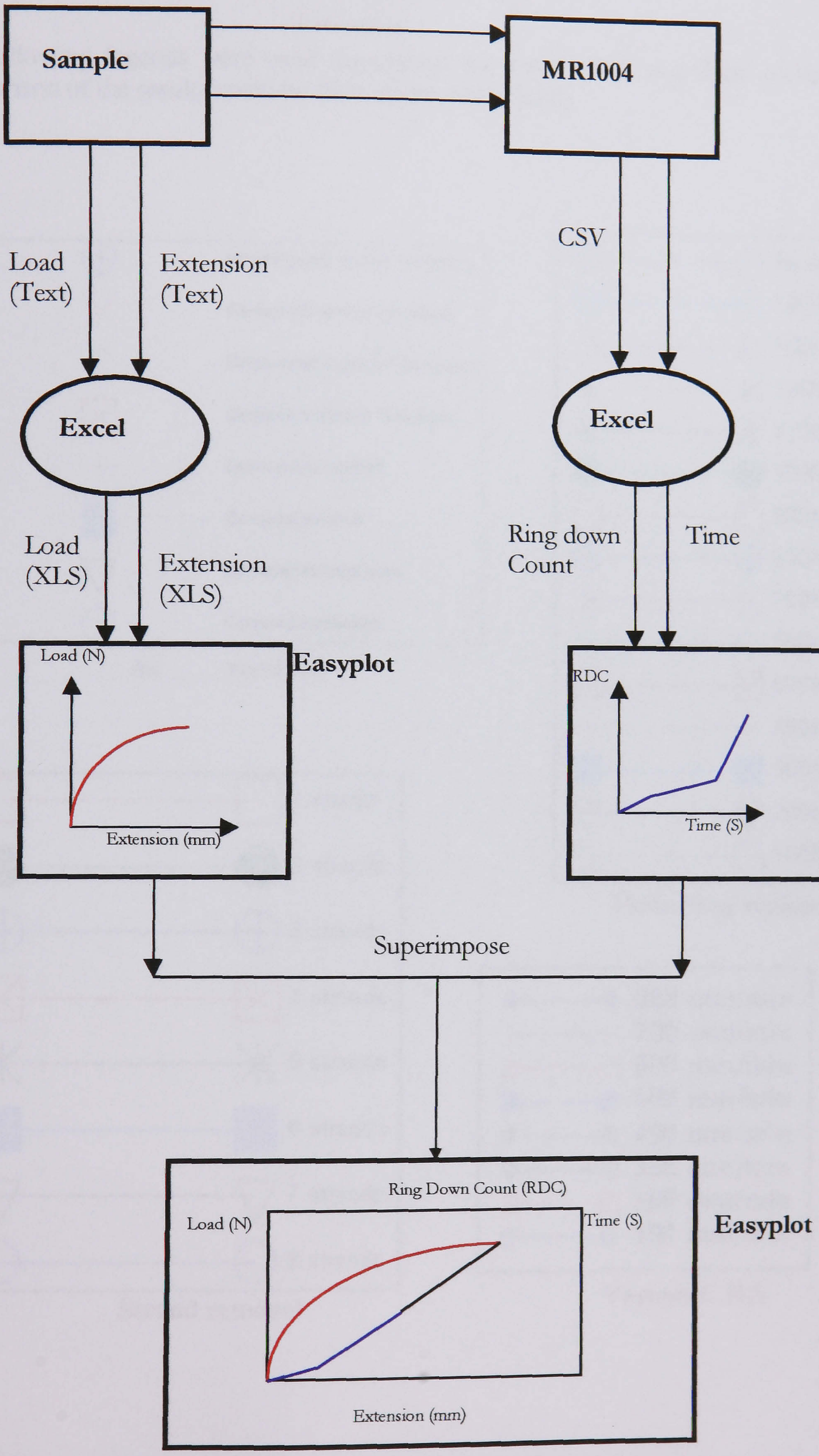

Figure 7.11: *Block diagram showing the steps in presenting the results graphically*

Legends used

The following legends were used throughout the report. This was done so that the comparison of the results could be undertaken more clearly.

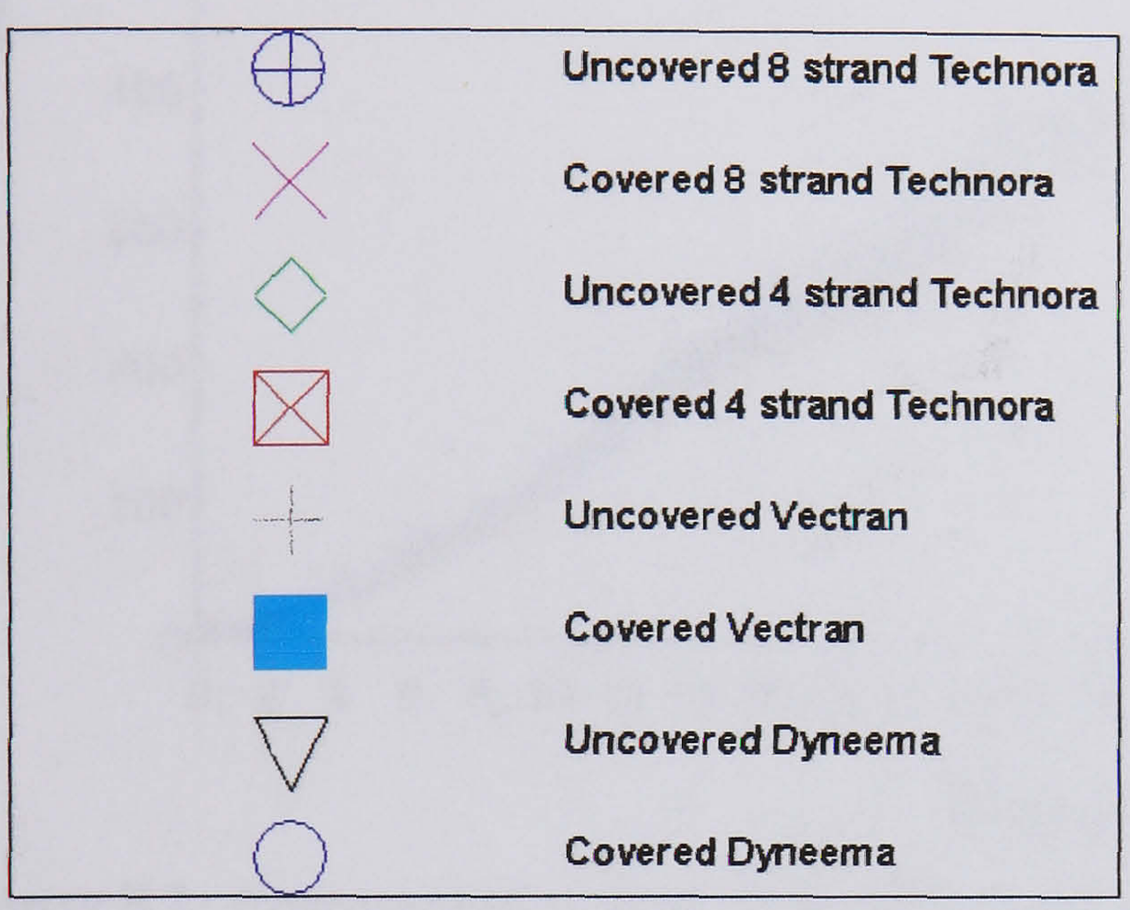

As received

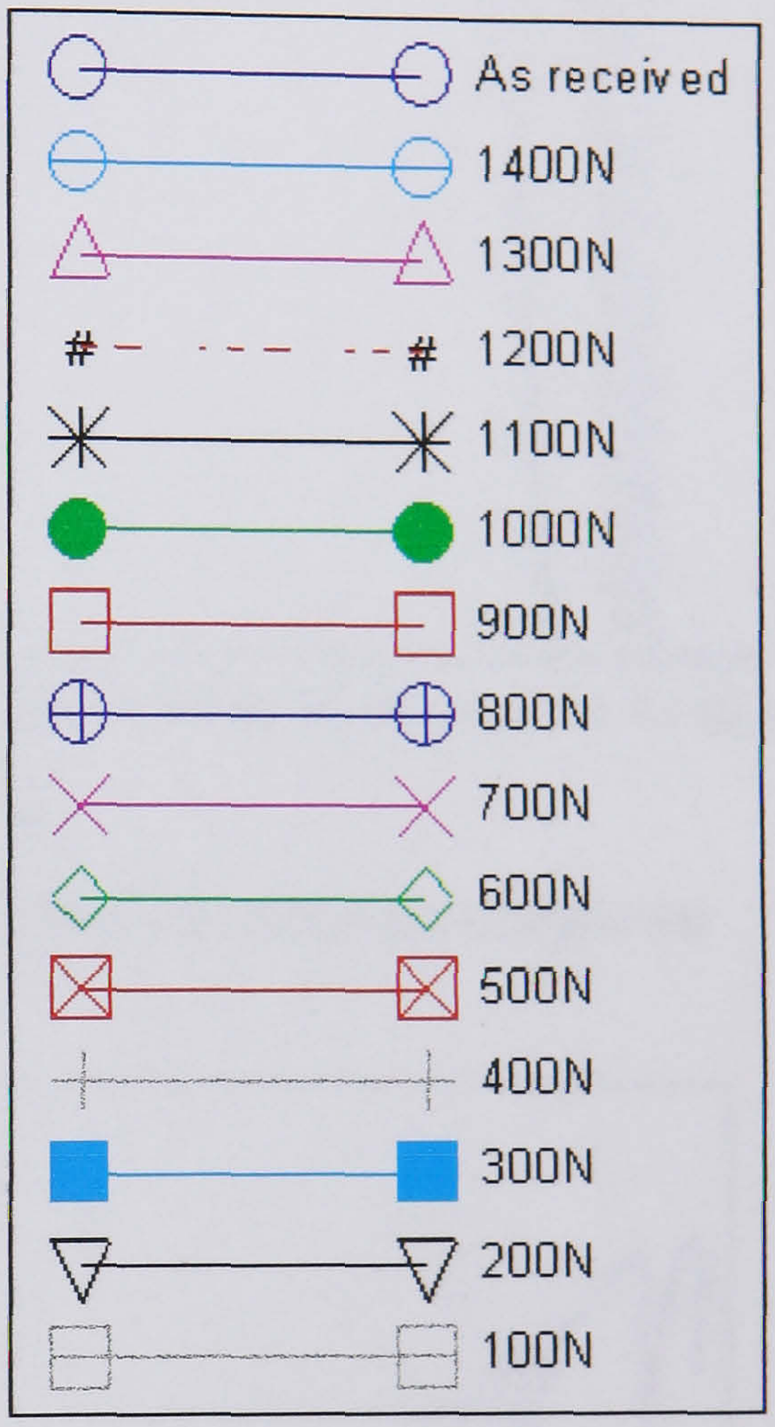

Preloading regimes

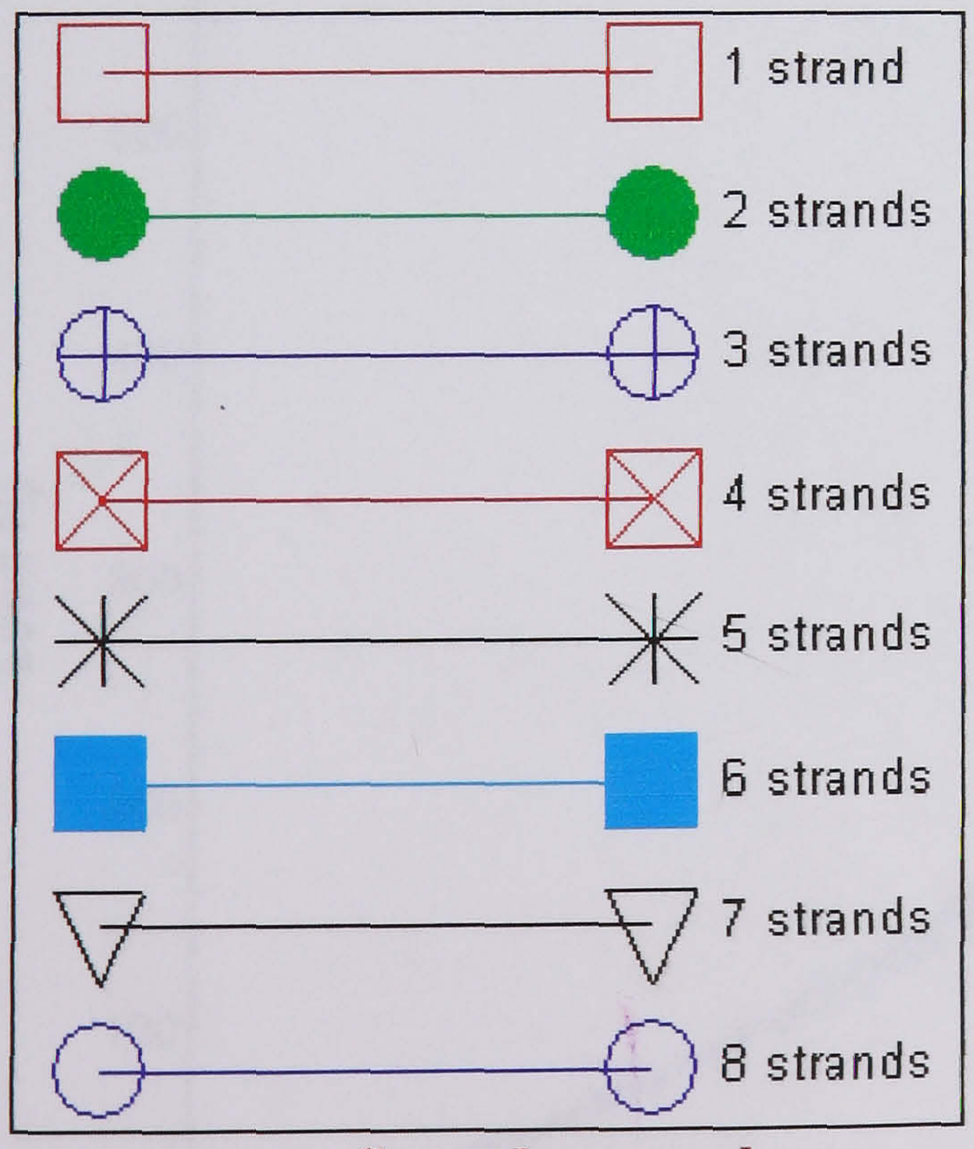

Strand removal

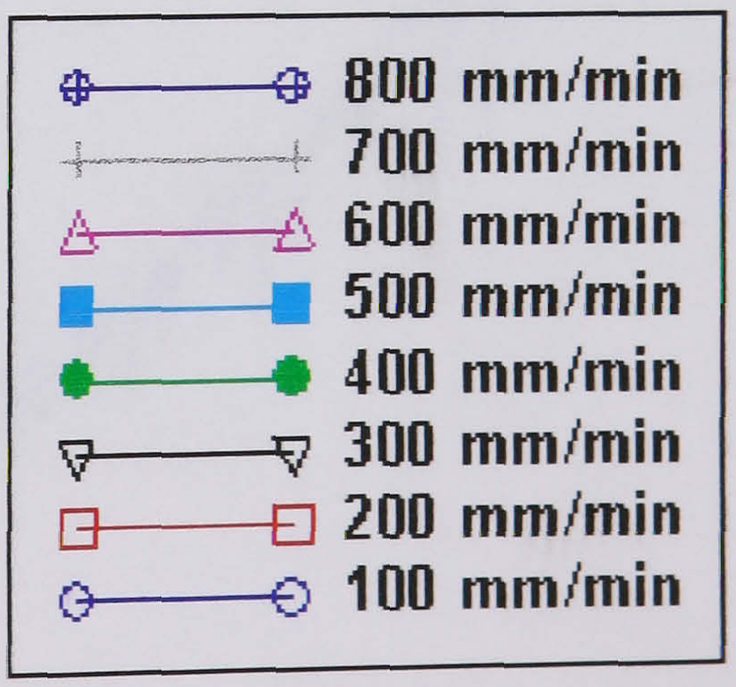

Various C.H.S

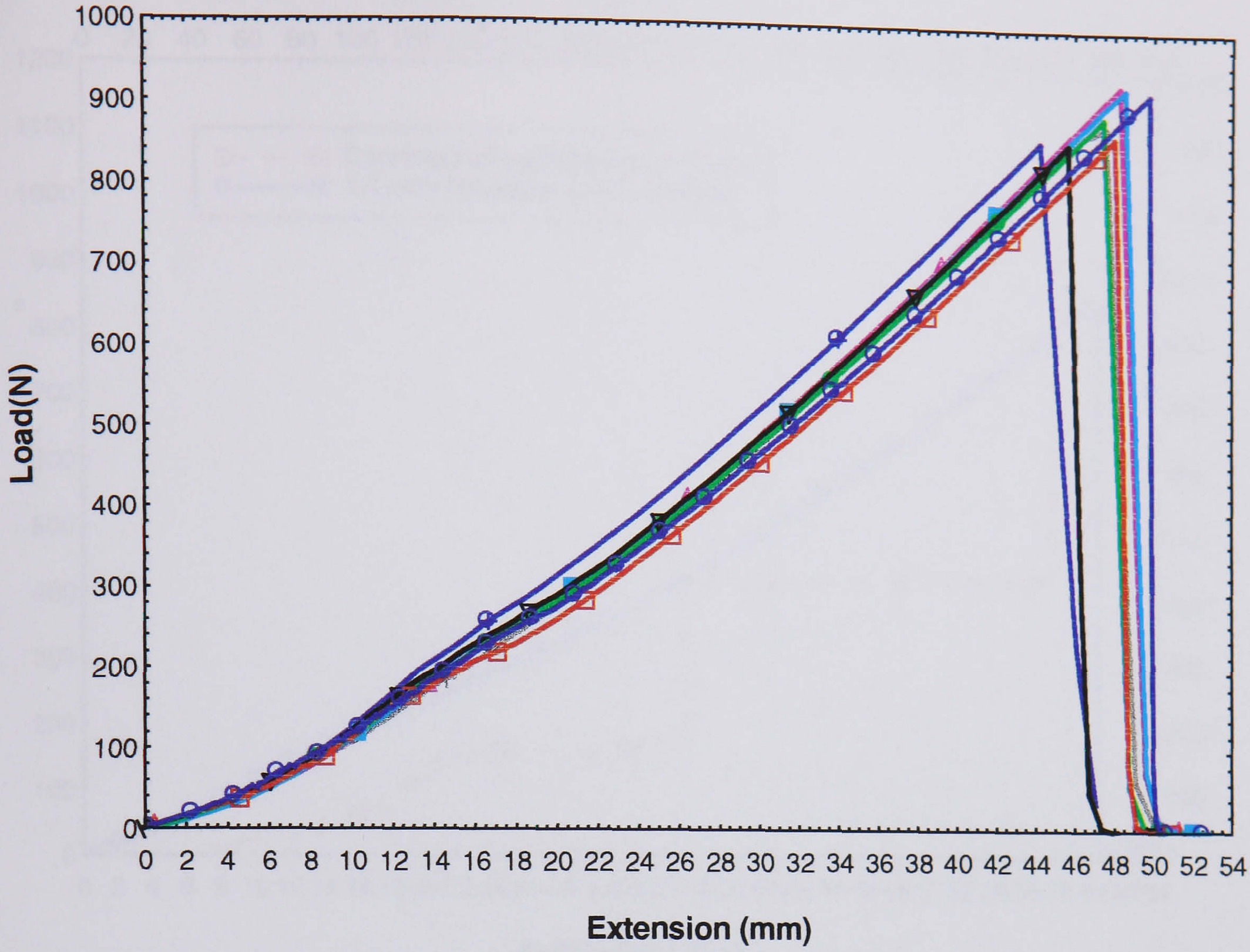

Figure 8.1: *Representative load - extension profiles for Dyneema subjected to different cross head speeds (see legends on page 252).*

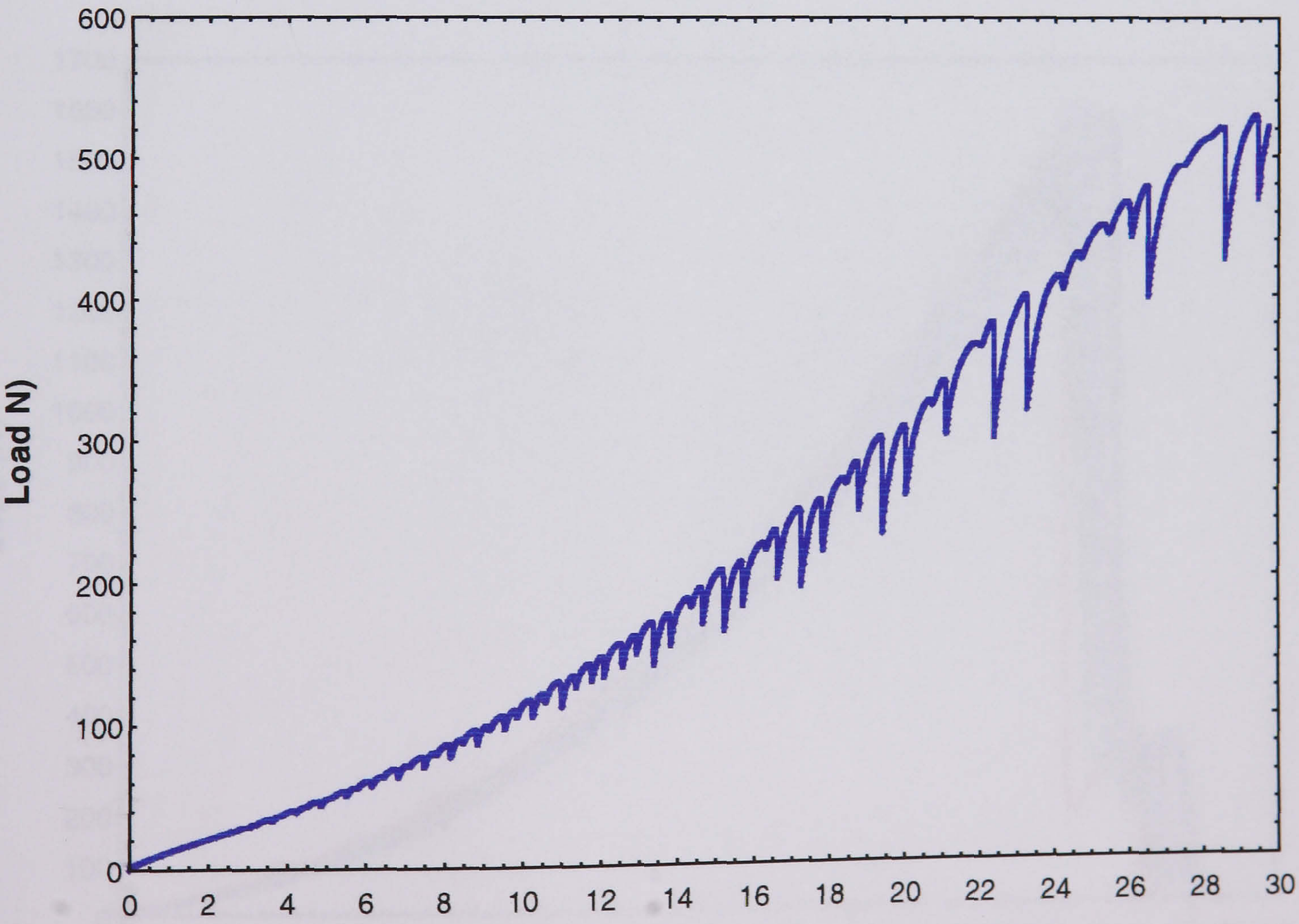

Figure 8.2: *Variation of load and extension of Dyneema at1 mm/min cross head speed (see legends on page 252).*

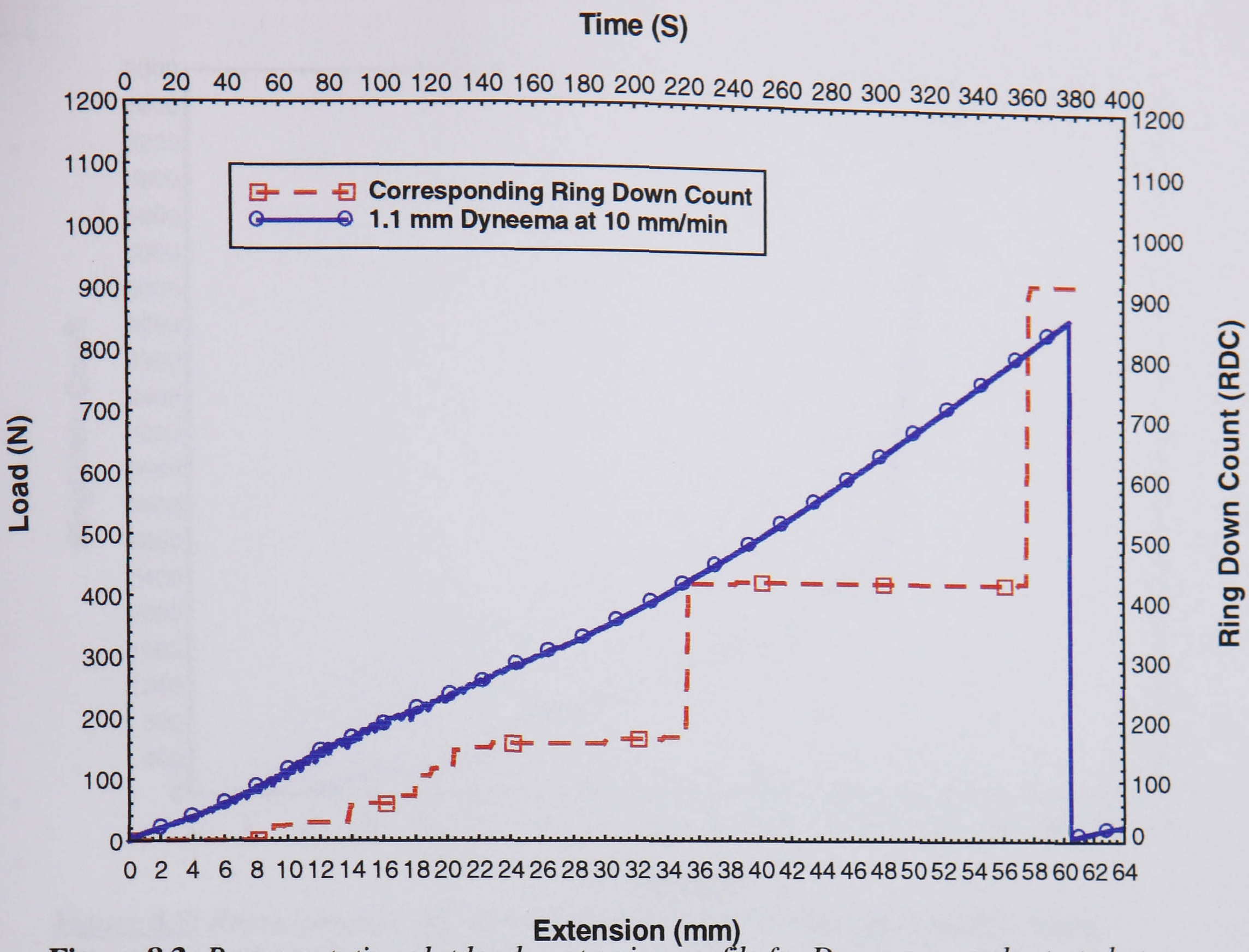

Figure 8.3: *Representative plot load - extension profile for Dyneema samples tested at 10 mm/min with corresponding acoustic emission (see legends on page 252).*

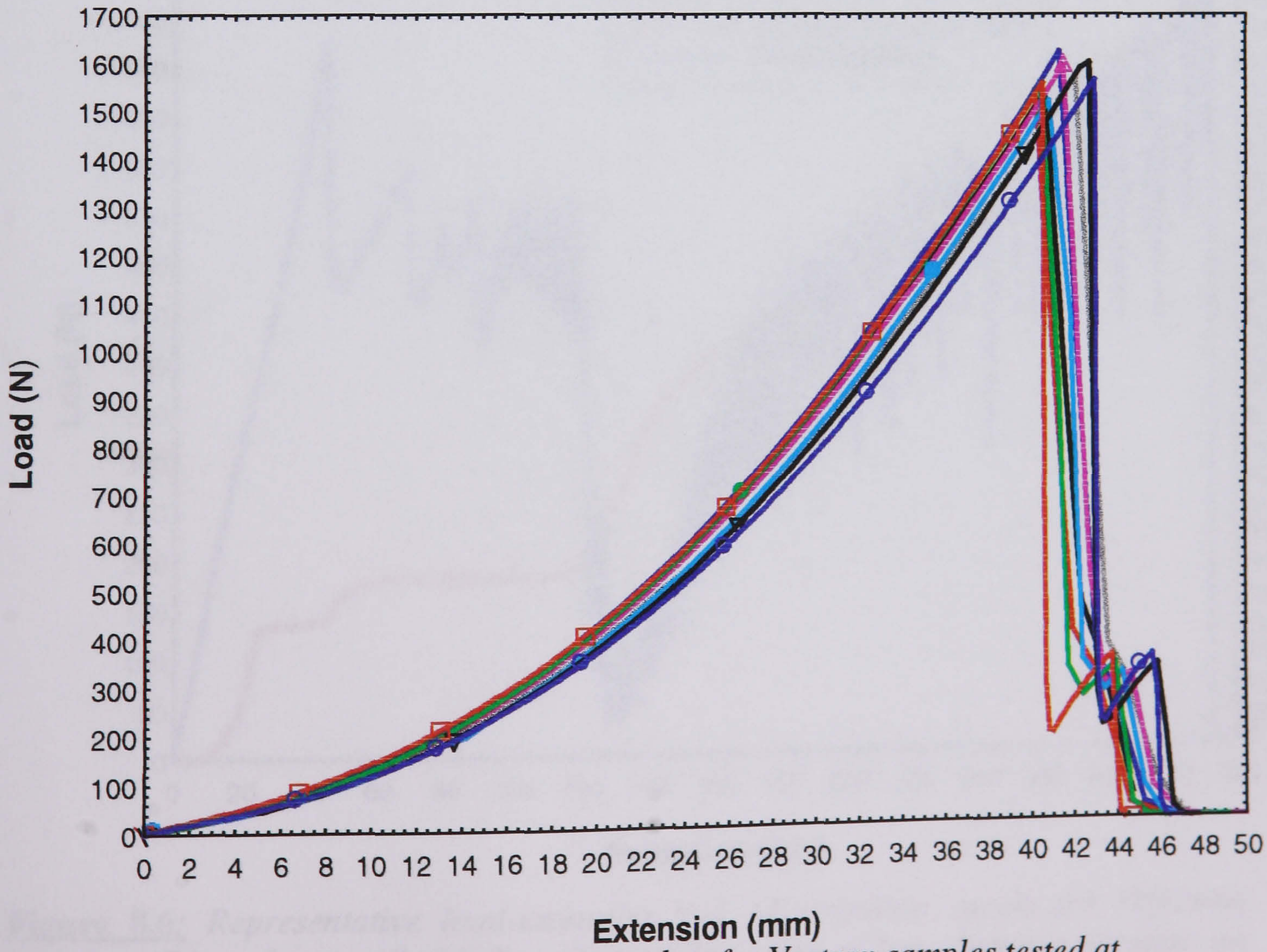

Figure 8.4: *Representative load - extension plots for Vectran samples tested at different cross head speeds (see legends on page 252).*

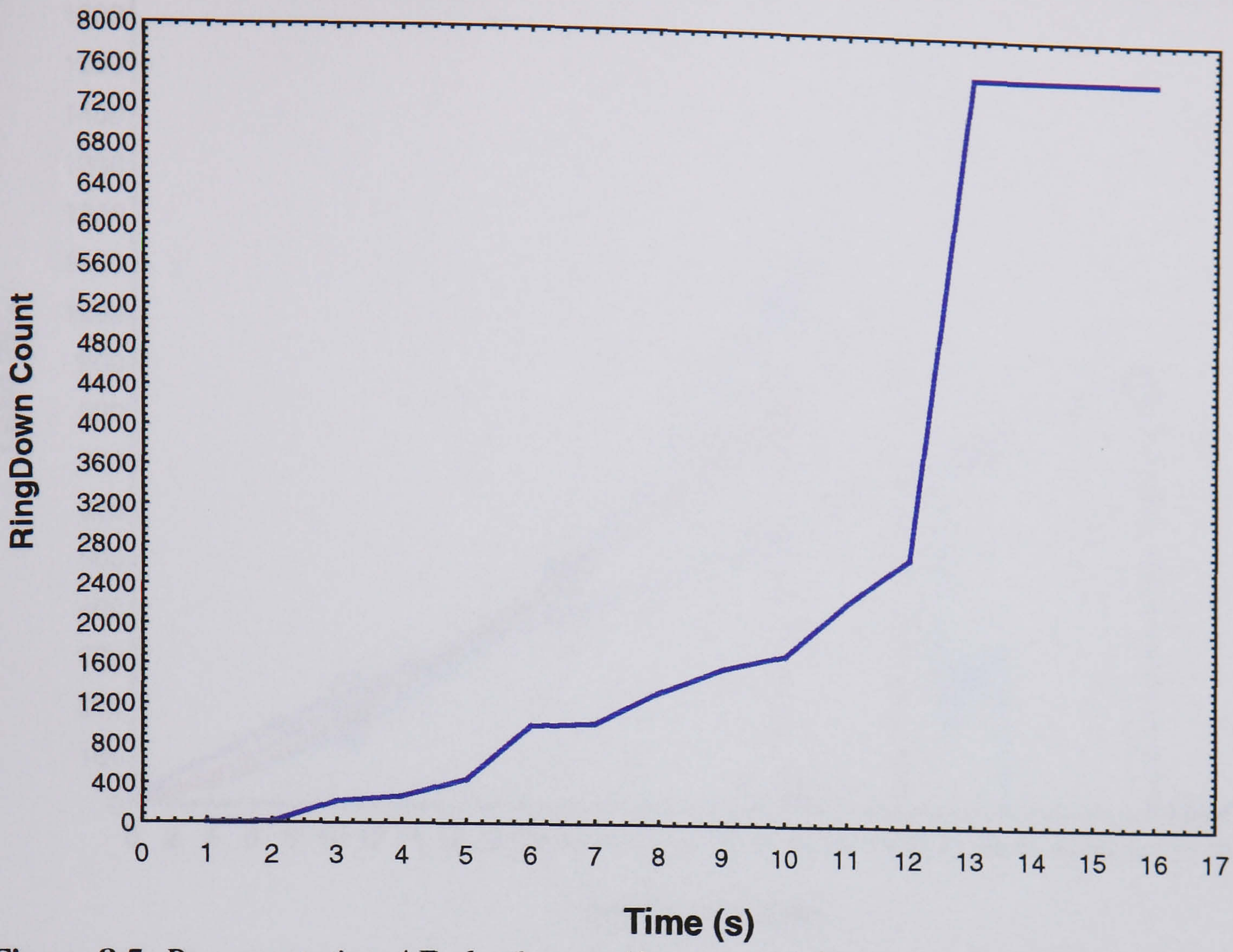

Figure 8.5: *Representative AE plot for a uniform rate of damage caused by clamp tightening (see legends on page 252).*

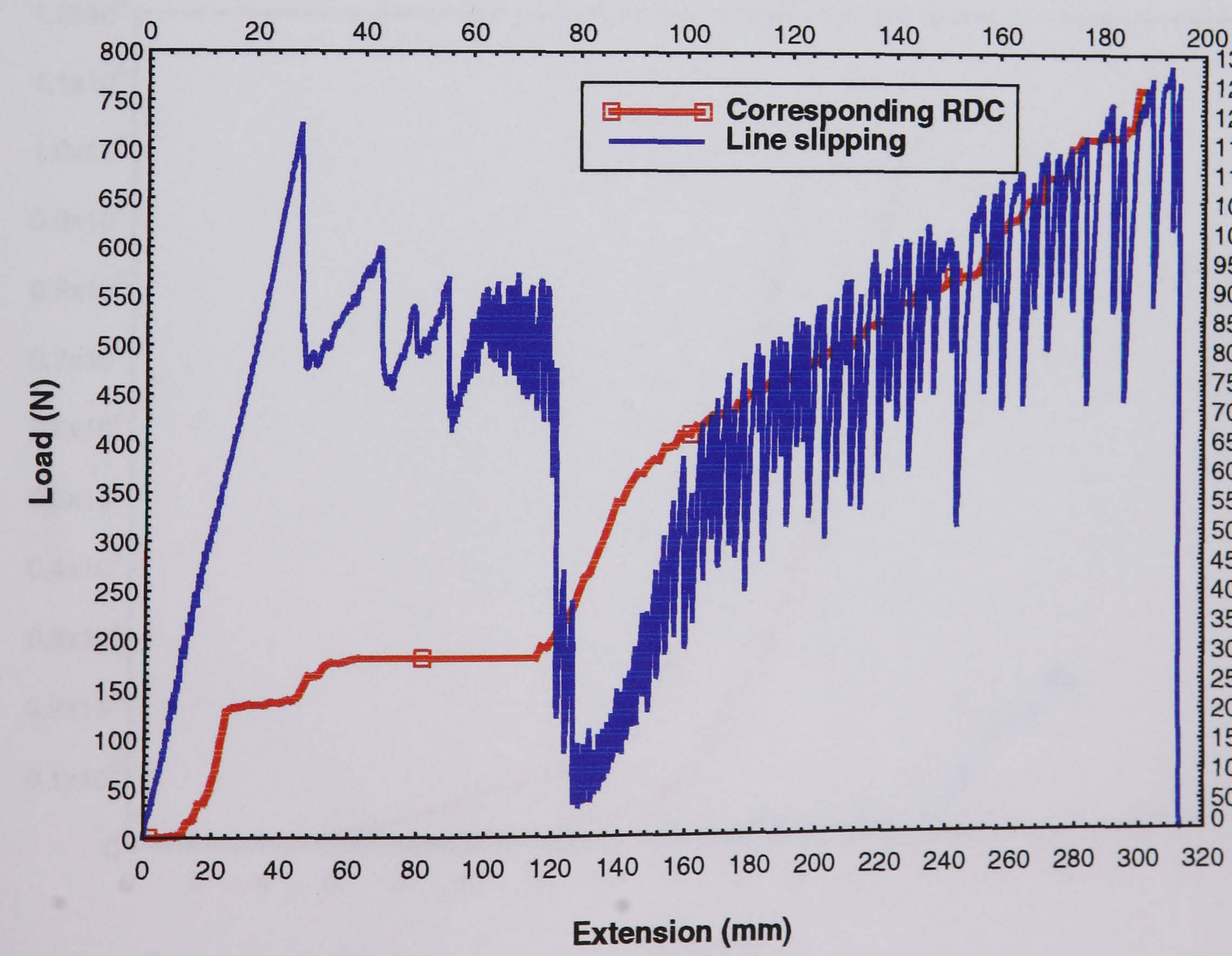

Figure 8.6: *Representative load-extension and AE-extension curves for Dyneema samples subjected to tensile loading showing the effect of low clamping pressure on rope slippage (see legends on page 252).*

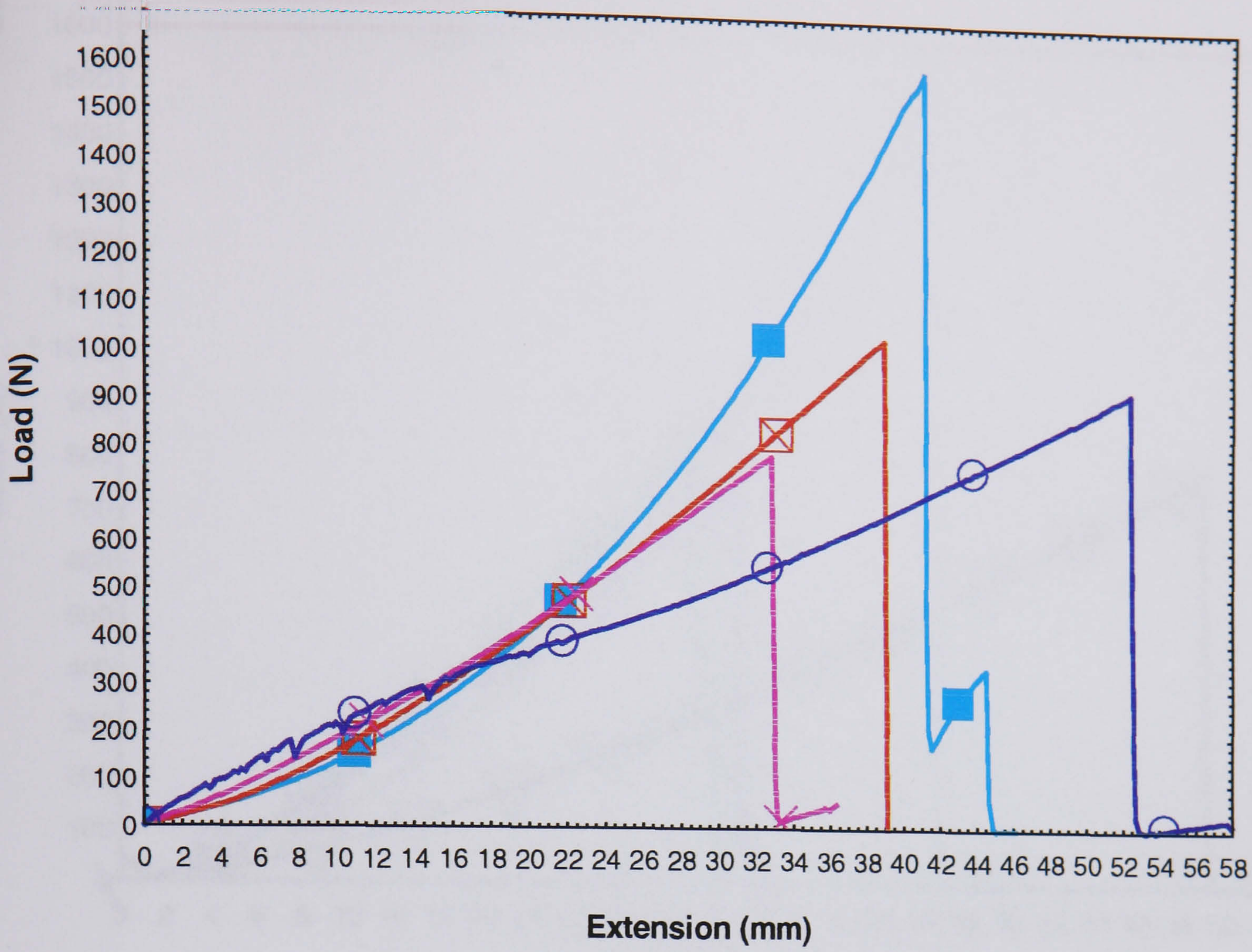

Figure 8.7a:*Representative load – extension curves for all the covered ropes tested (see legends on page 252).*

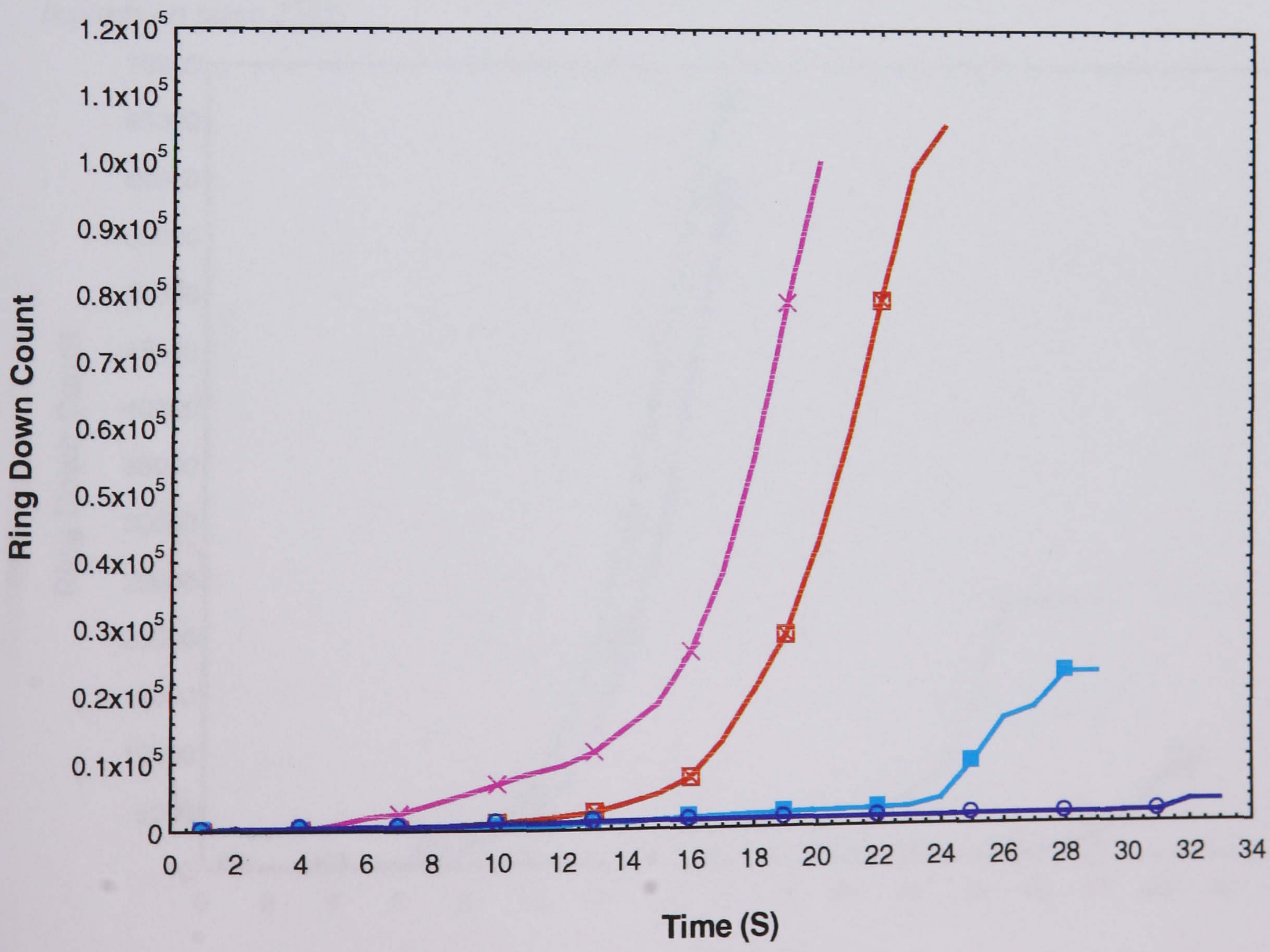

Figure 8.7b: Reresentative acoustic emission plots for the covered ropes relating to Figure 8.7a (see legends on page 252).

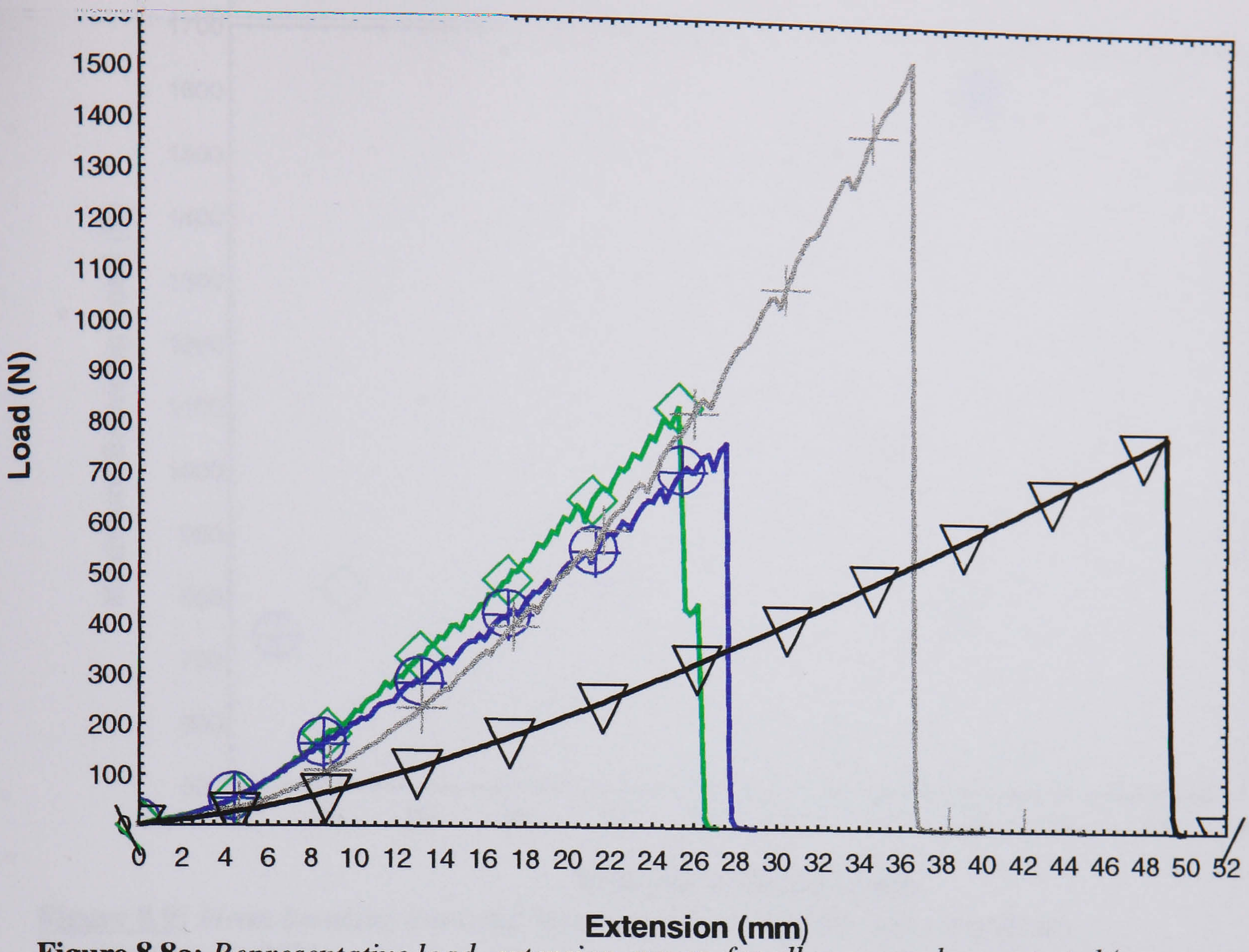

Figure 8.8a: *Representative load- extension curves for all uncovered ropes tested (see legends on page 252).*

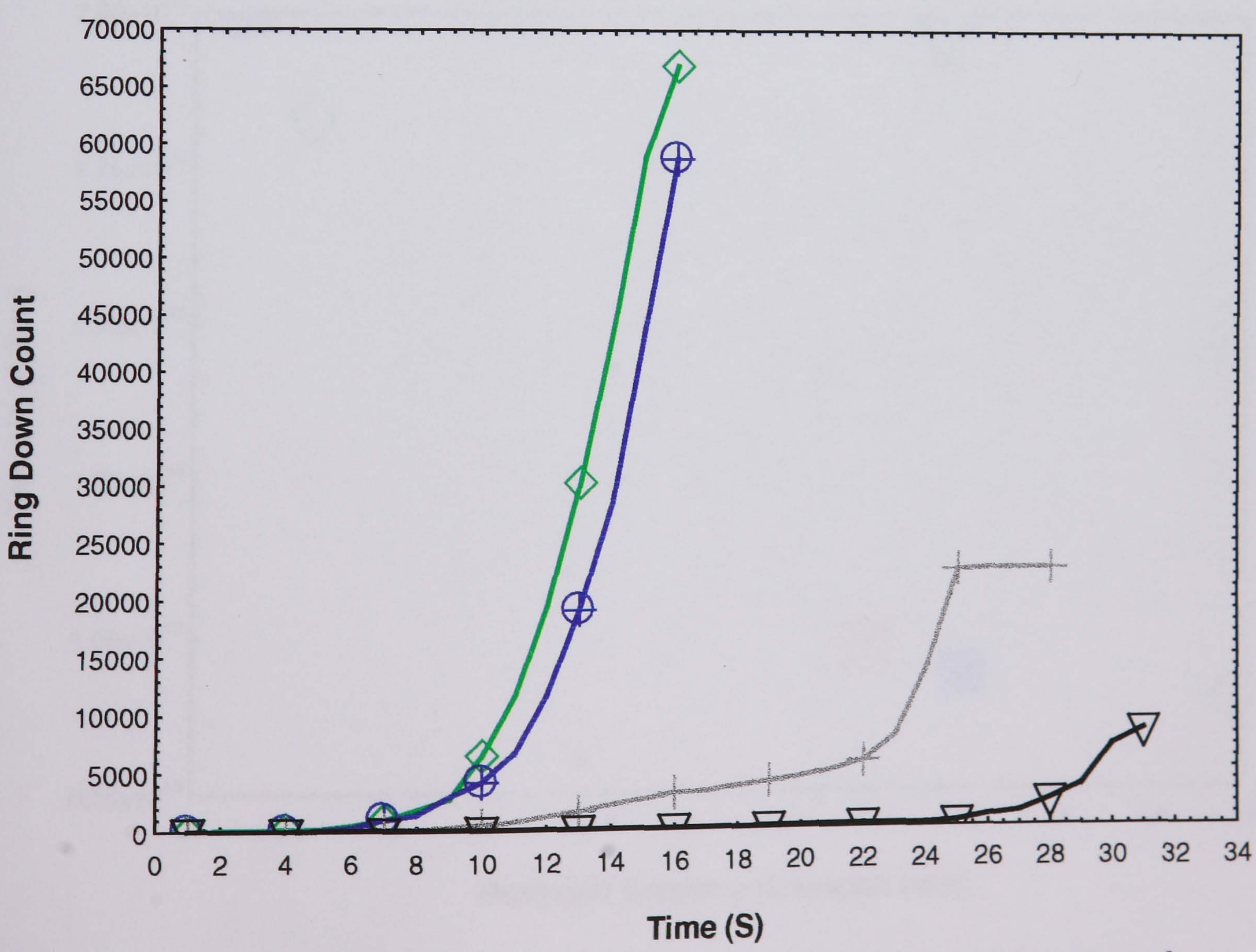

Figure 8.8b: *Representative acoustic emission plots for all the uncovered ropes tested in Figure 8.8a. (see legends on page 252).*

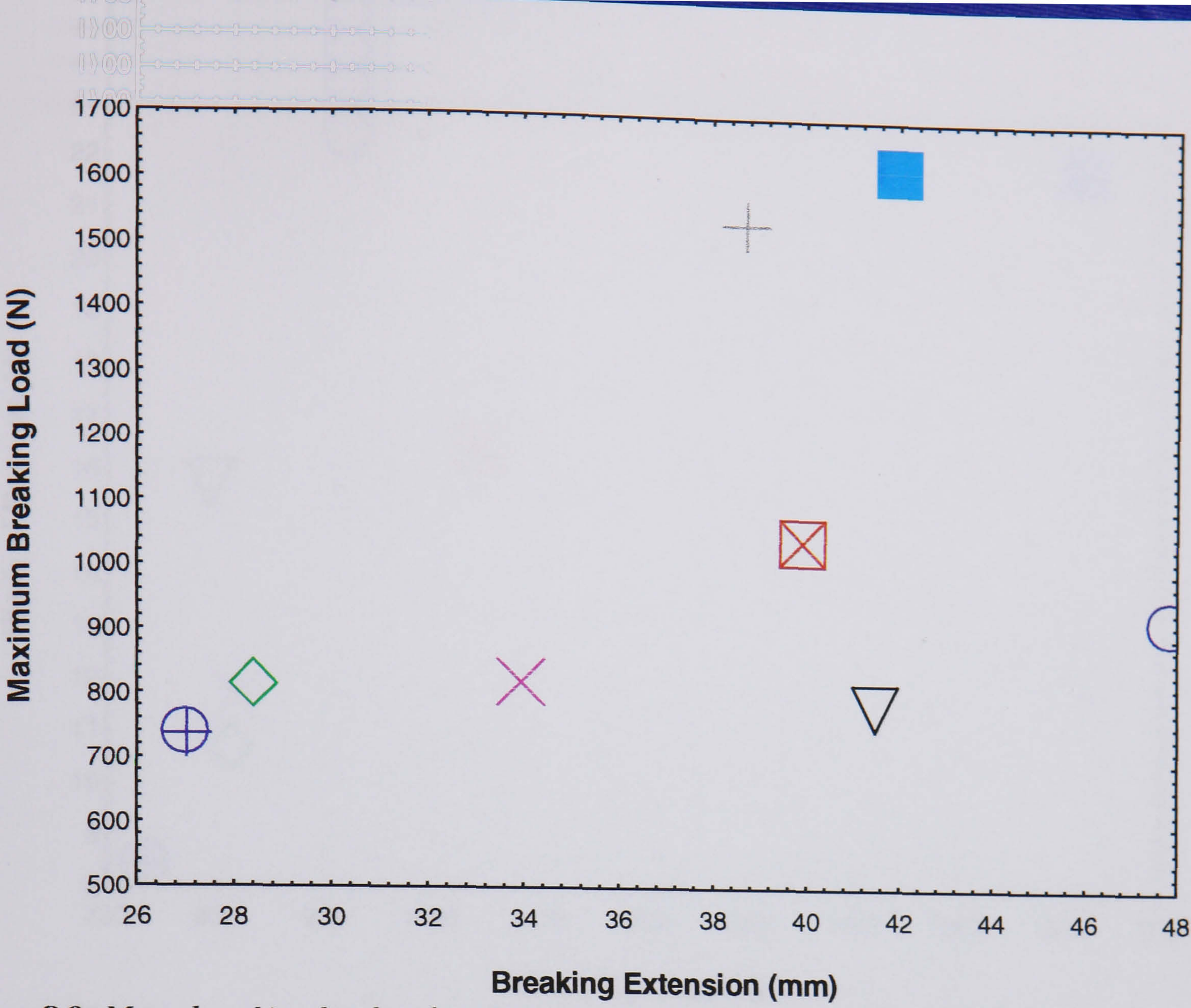

Figure 8.9: *Mean breaking load and max. extension for all the ropes tested (see legends on page 252).*

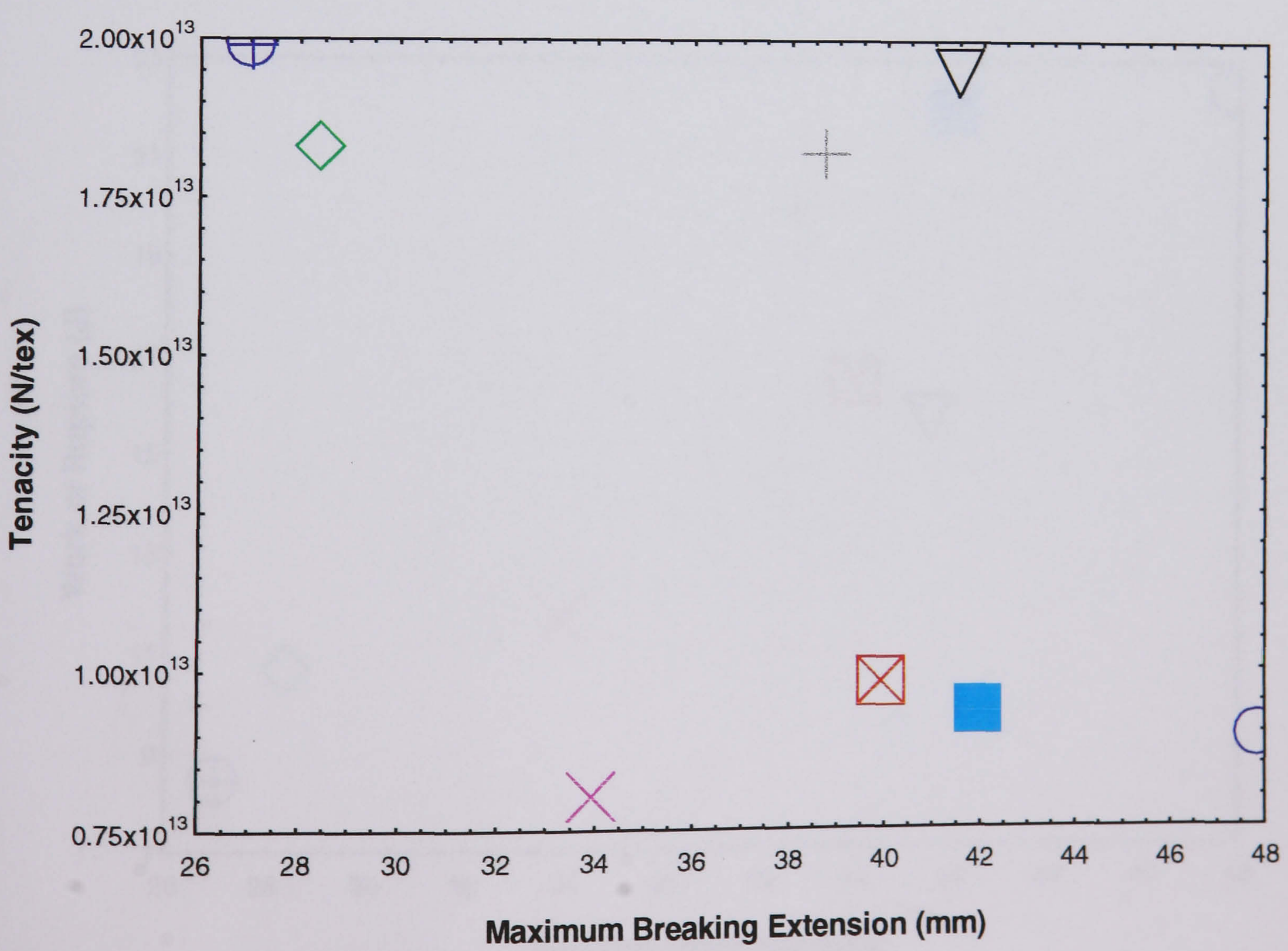

Figure 8.10: *Mean tenacity and max. extension for all the different ropes tested (see legends on page 252).*

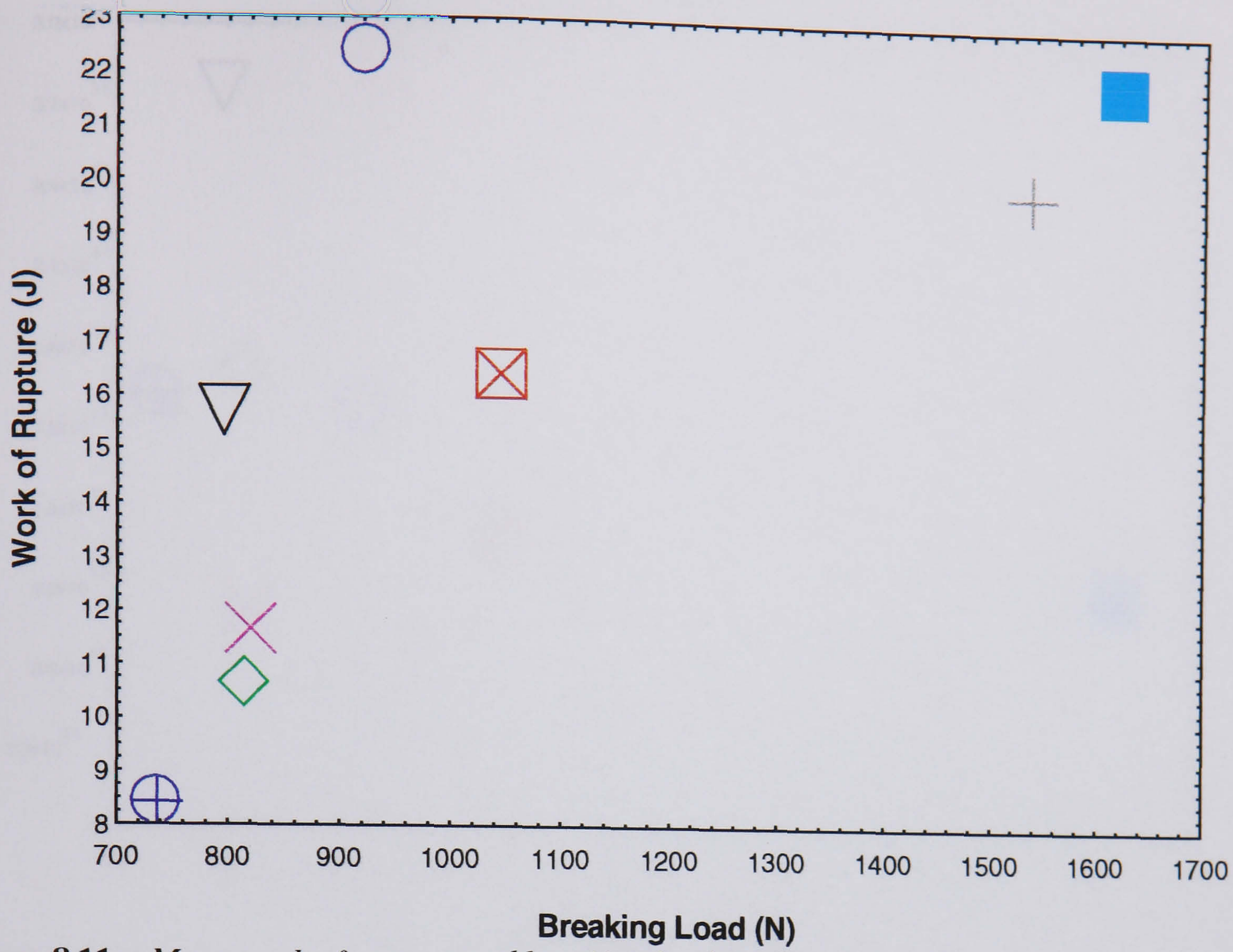

Figure 8.11a: *Mean work of rupture and breaking load for different ropes tested (see legends on page 252).*

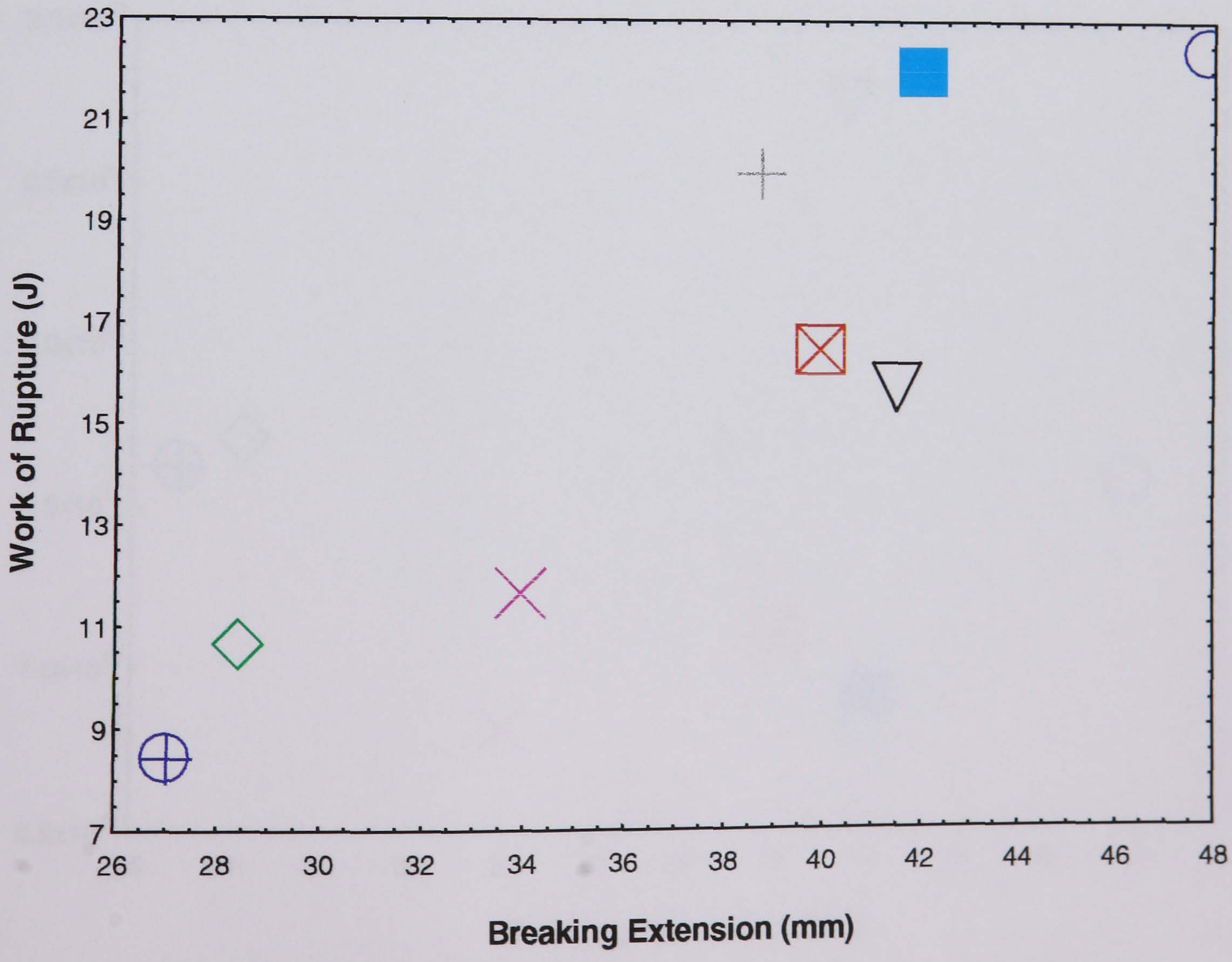

Figure 8.11b: *Mean work of rupture and max. extension for different ropes tested (see legends on page 252).*

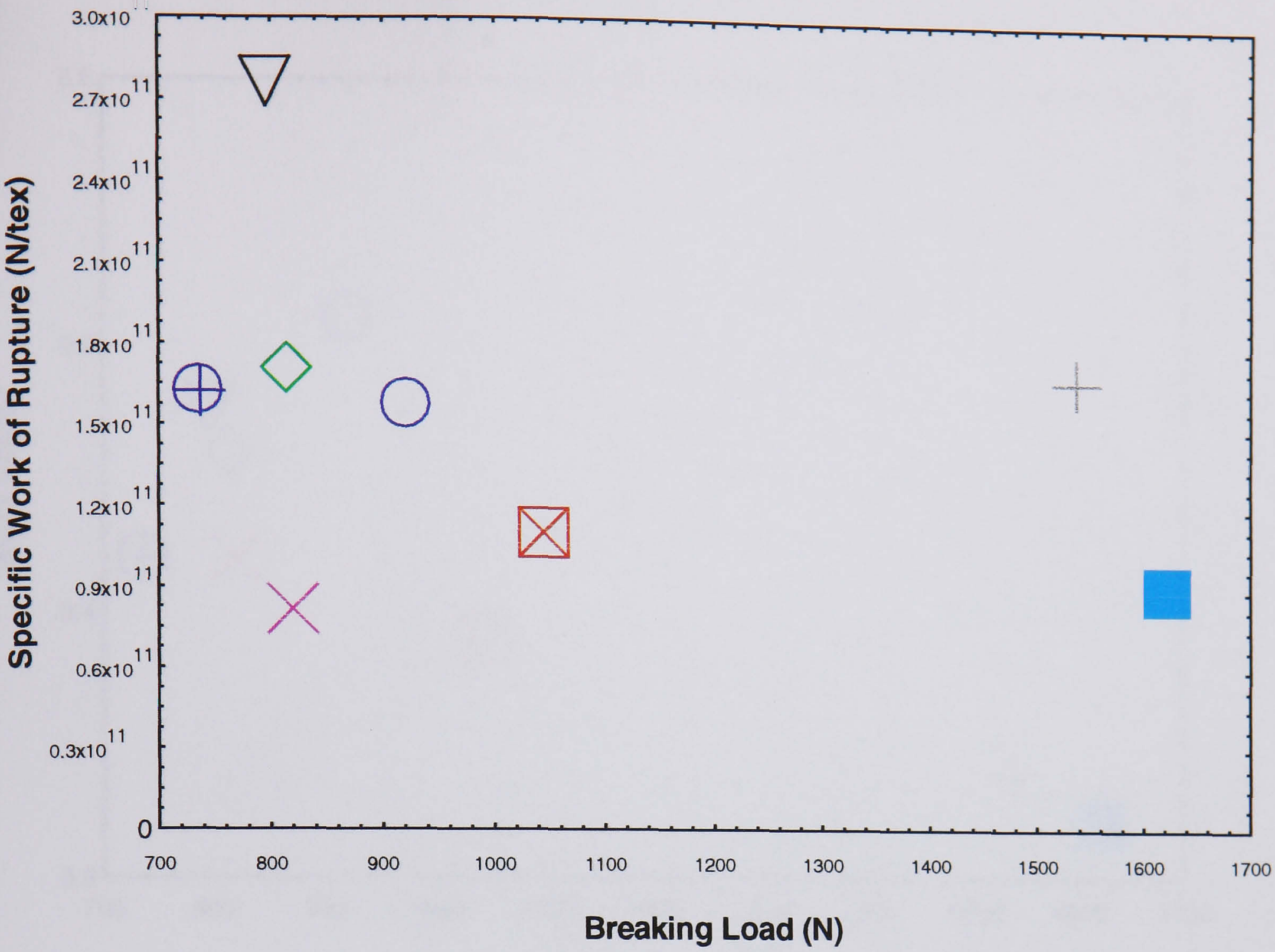

Figure 8.12a: *Mean specific work of rupture and breaking load for different ropes tested (see legends on page 252).*

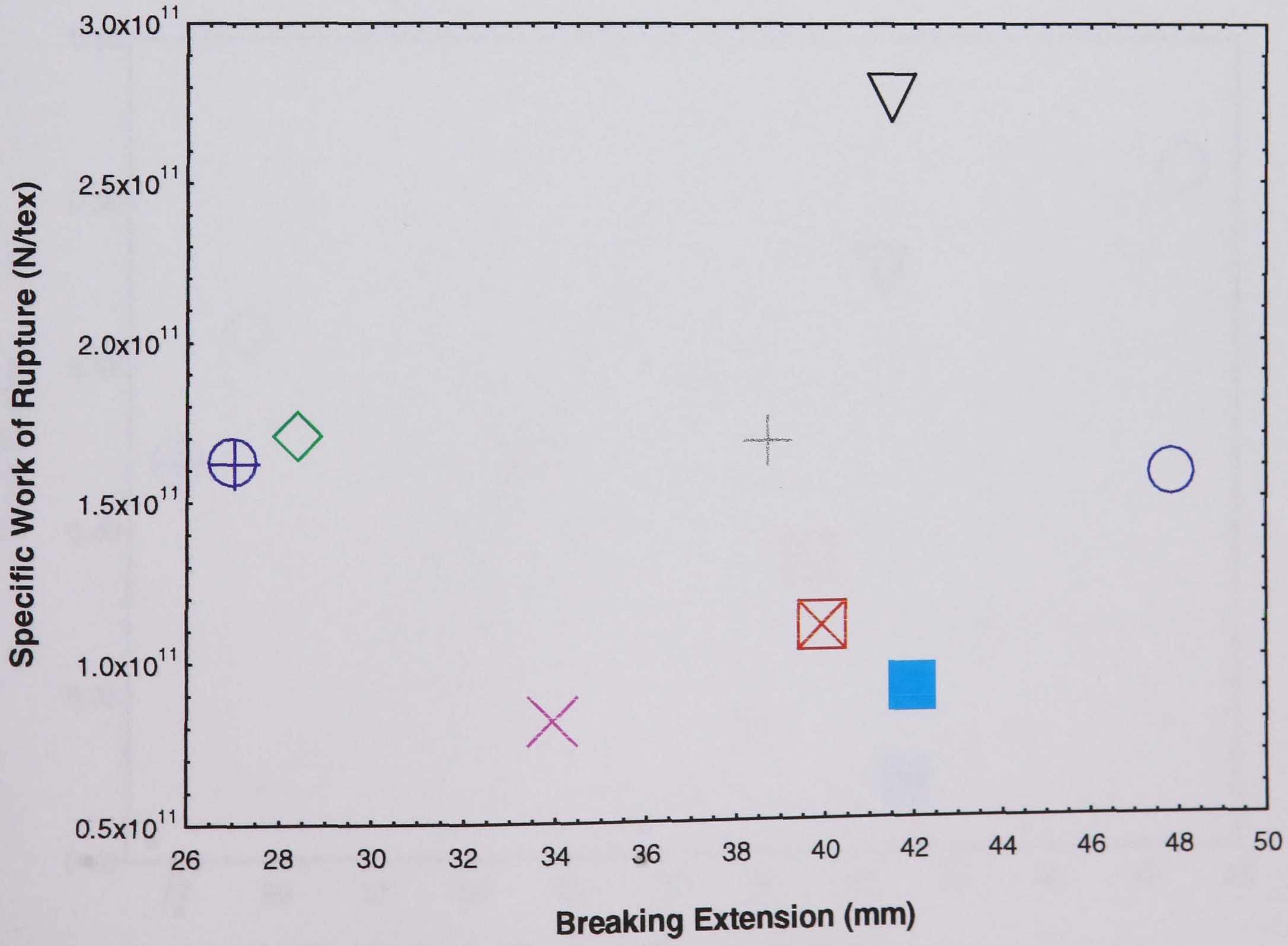

Figure 8.12b: *Mean specific work of rupture and max. extension for different ropes tested (see legends on page 252).*

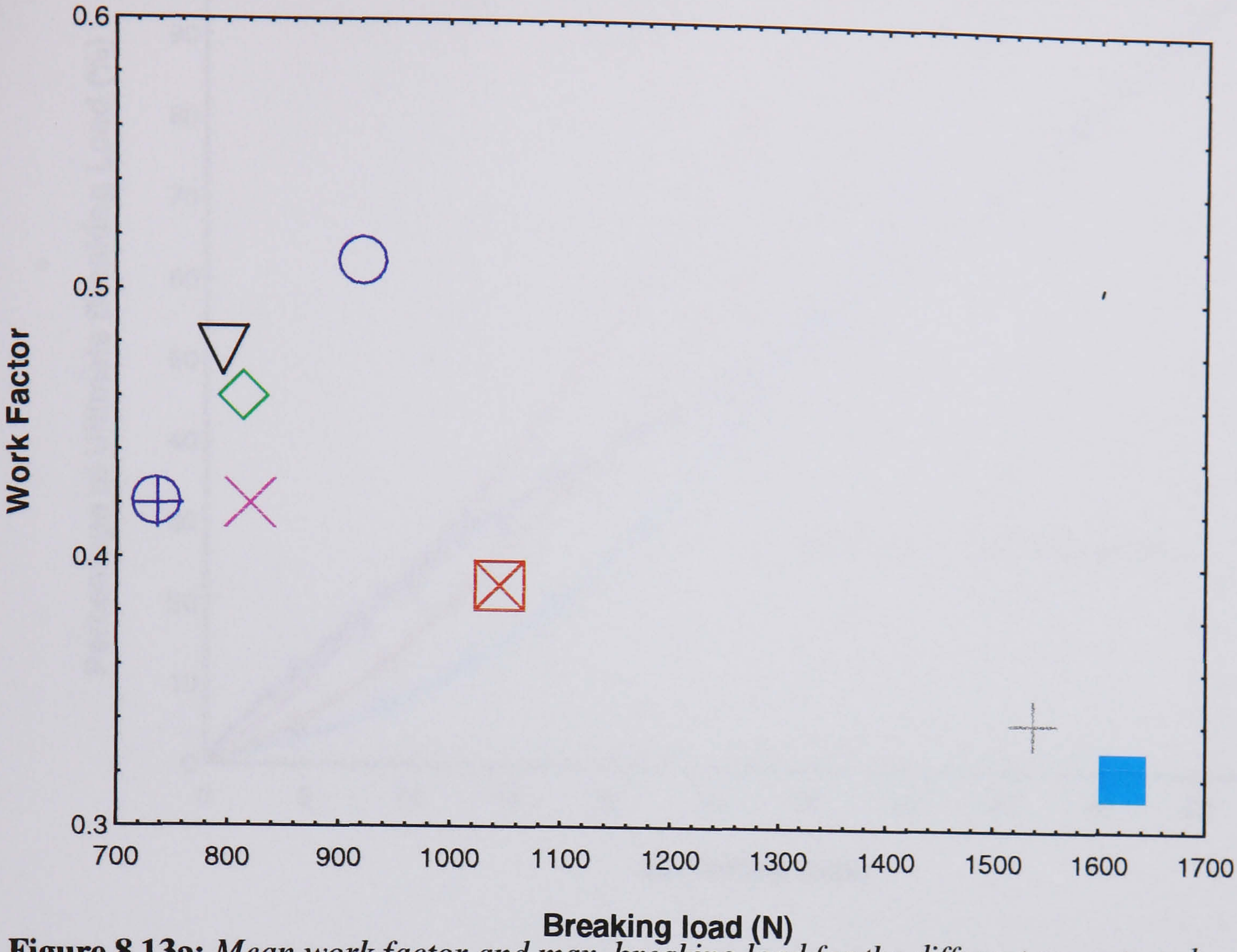

Figure 8.13a: *Mean work factor and max. breaking load for the different ropes tested (see legends on page 252).*

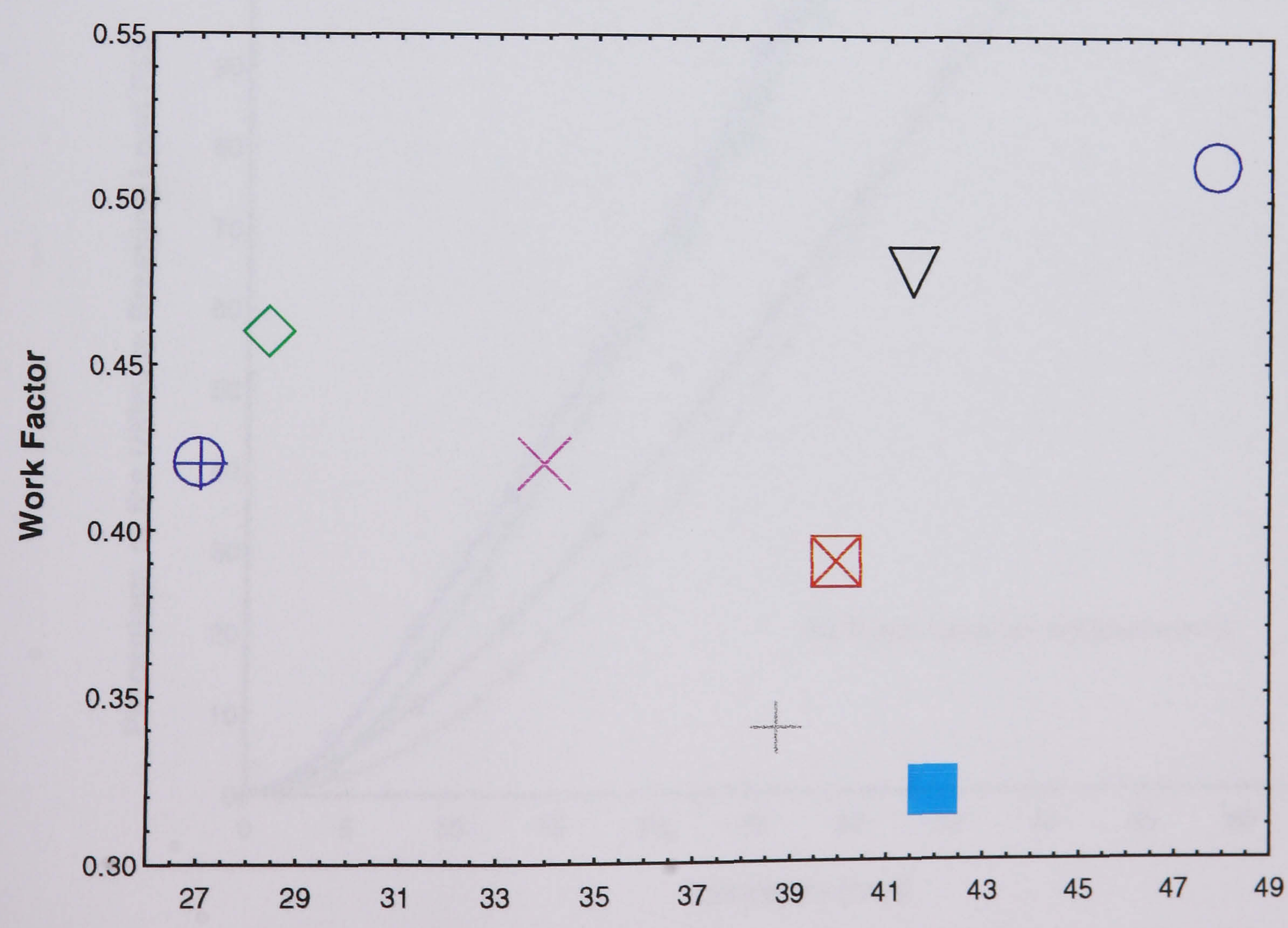

Figure 8.13b: *Mean work factor and max. extension for different ropes tested (see legends on page 252).*

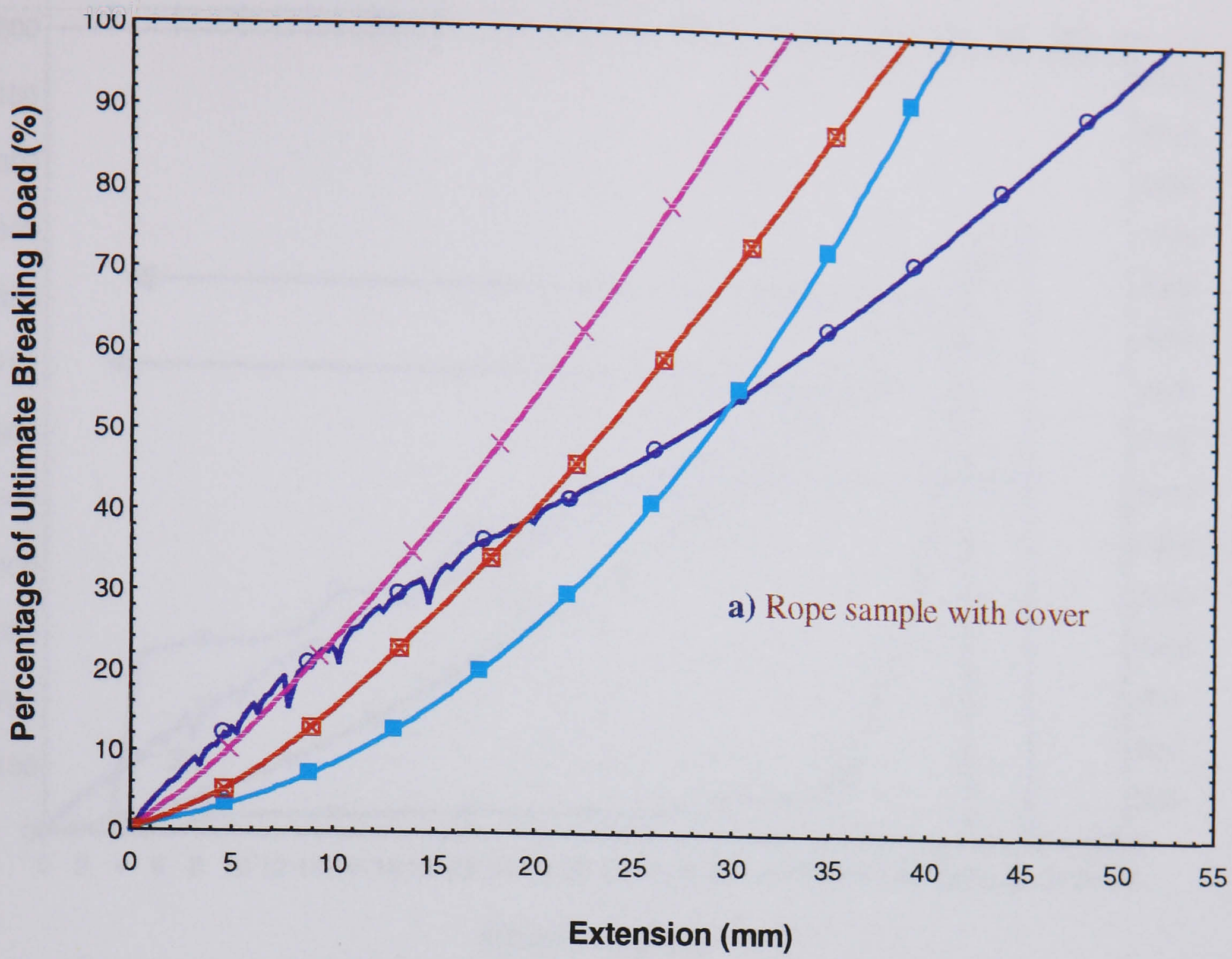

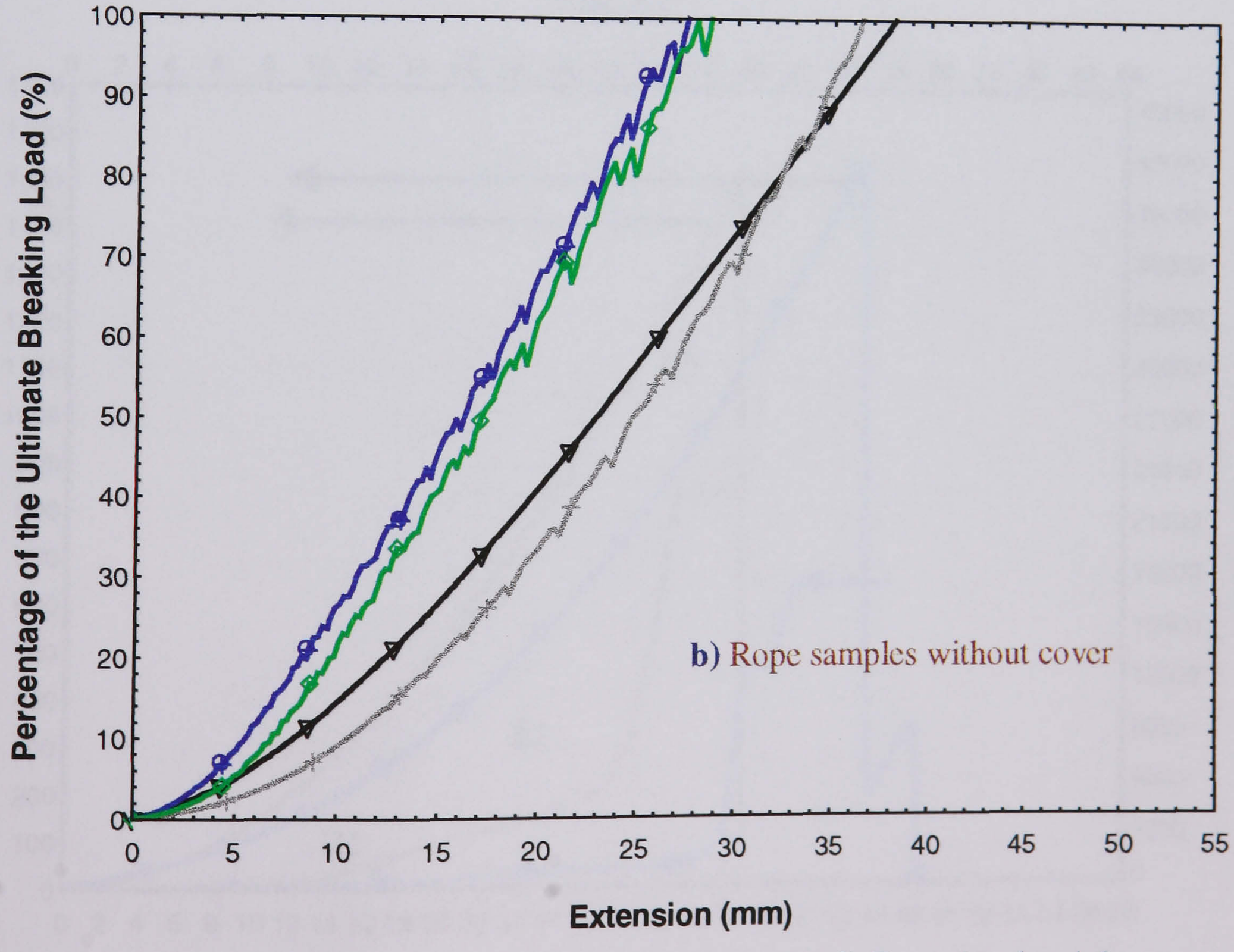

Figure 8.14b: *Representative curves of Load (% of ultimate load)-Extension (mm) for all the rope samples tested (see legends on page 252).*

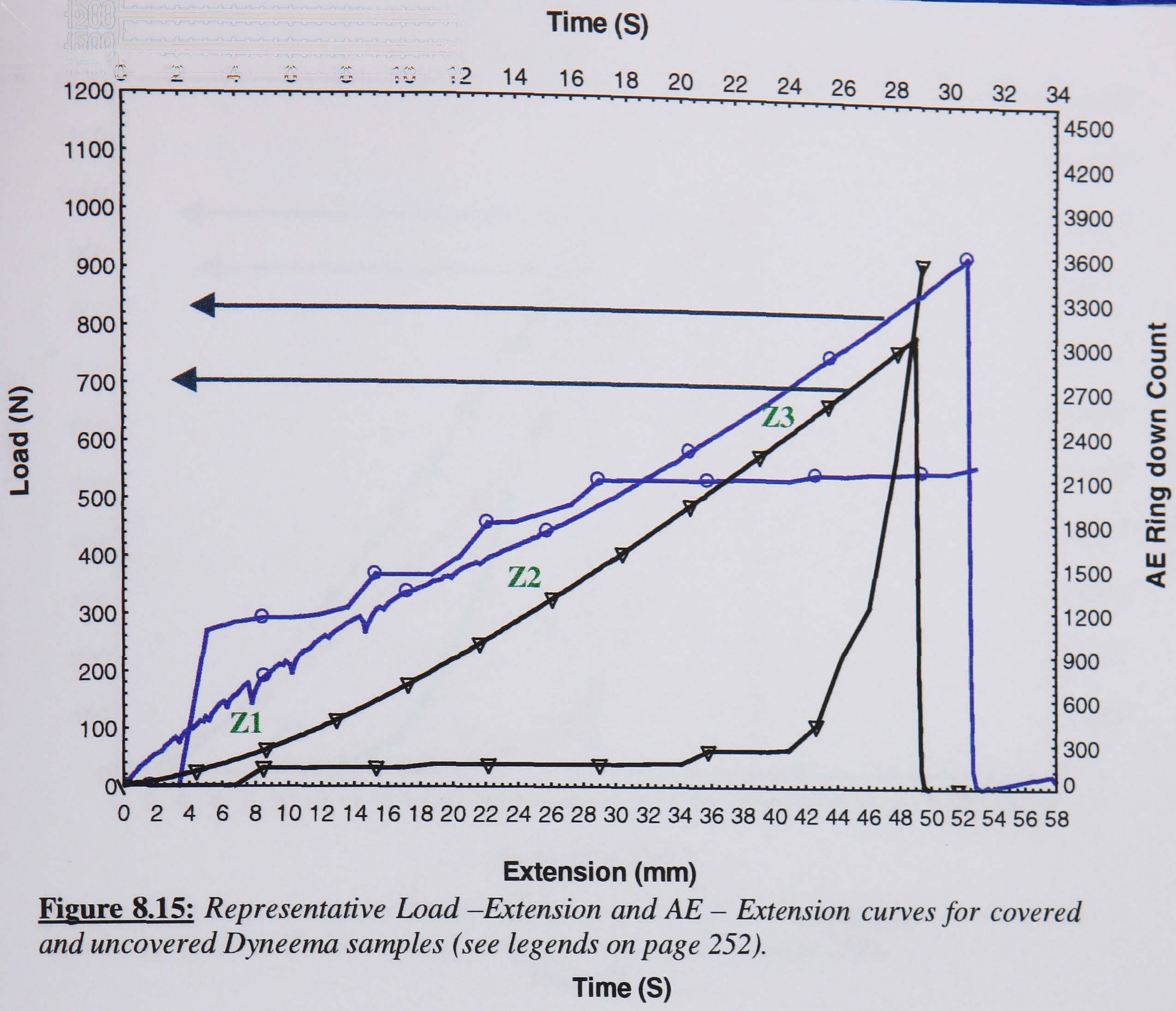

Figure 8.15: *Representative Load –Extension and AE – Extension curves for covered and uncovered Dyneema samples (see legends on page 252).*

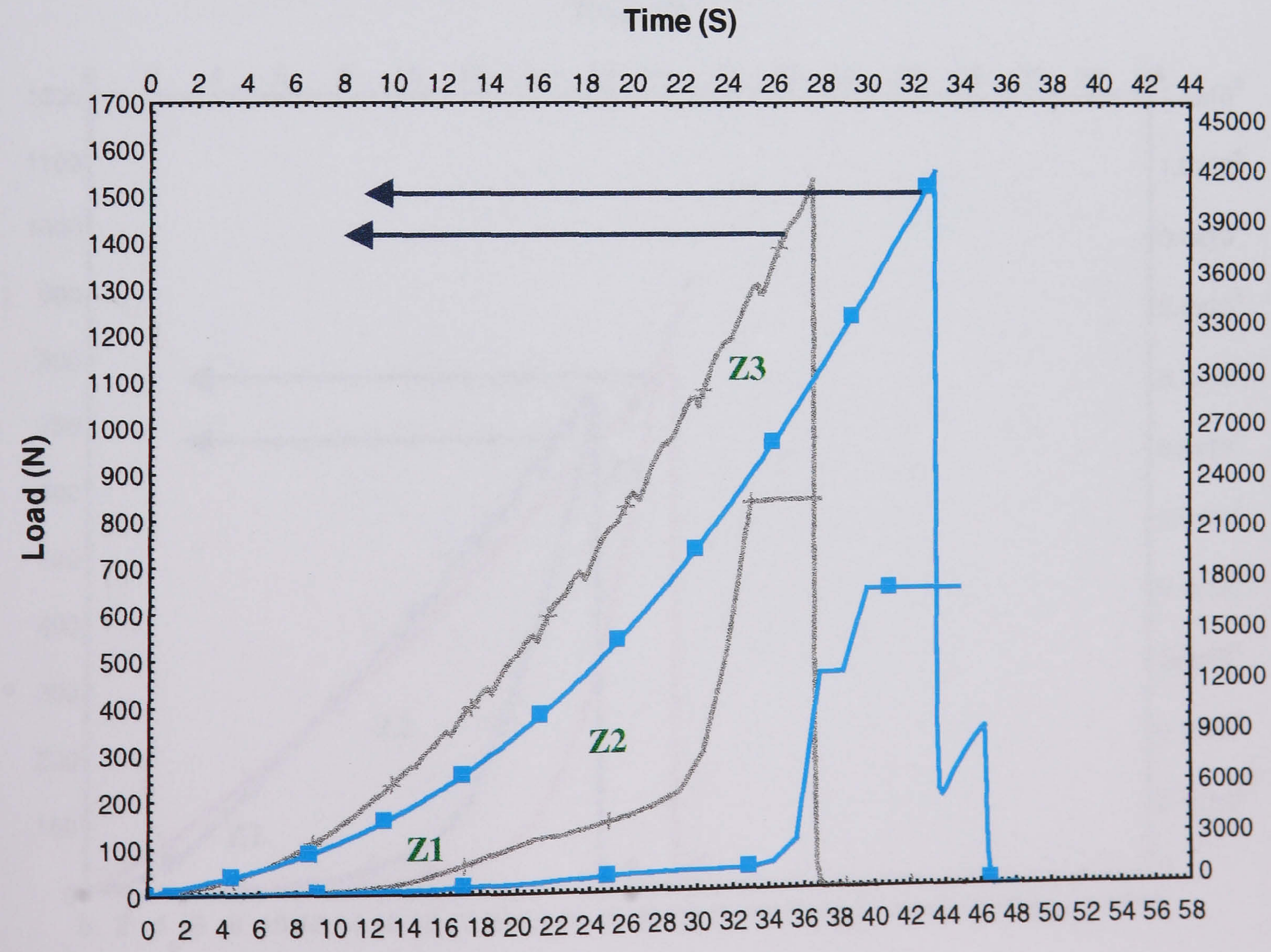

Figure 8.16: *Representative Load – Extension and AE – Extension curves for covered and uncovered Vectran rope samples (see legends on page 252).*

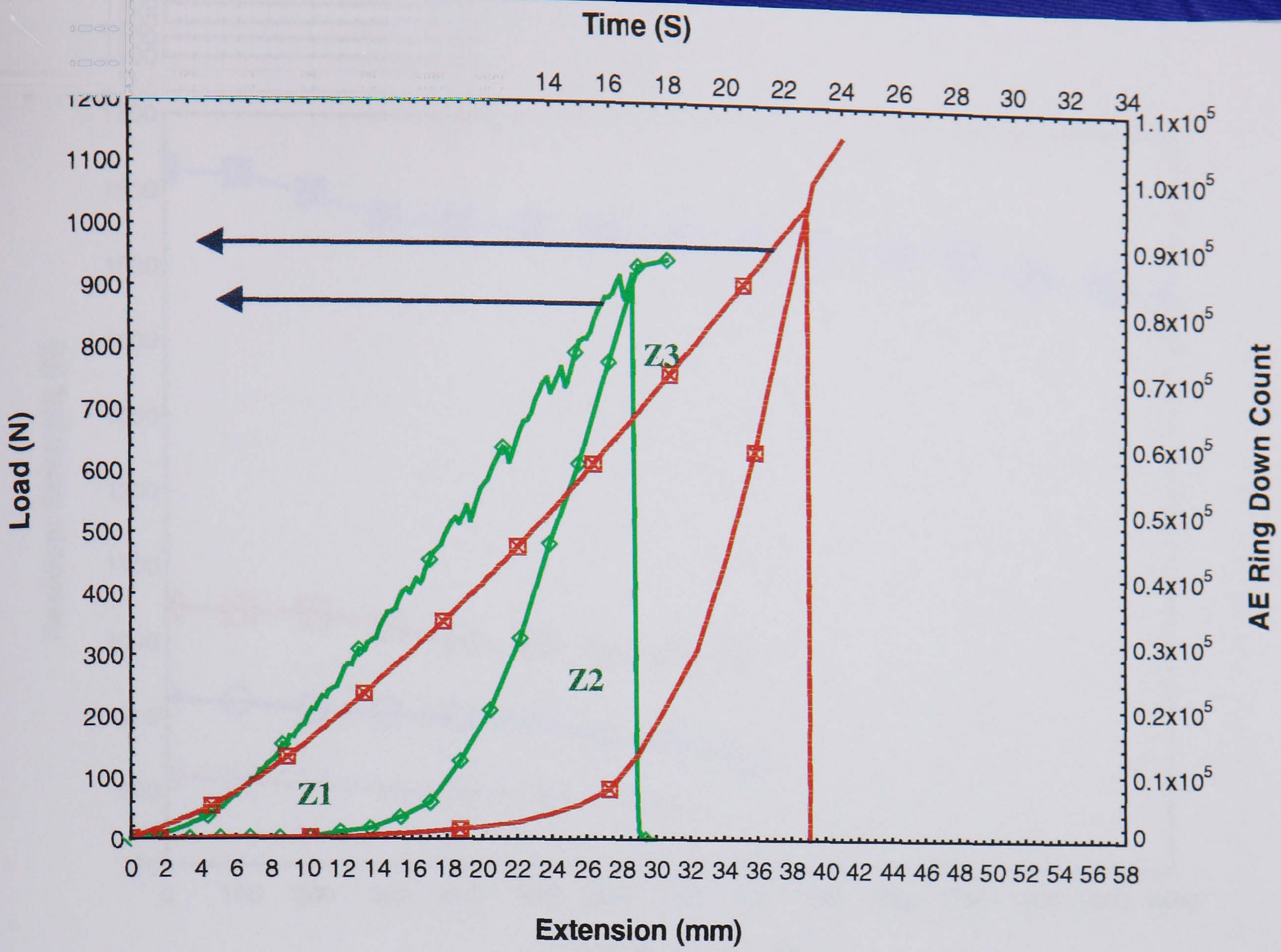

Figure 8.17: *Representative Load – Extension and AE – Extension for covered and uncovered 4 strand Technora rope samples (see legends on page 252).*

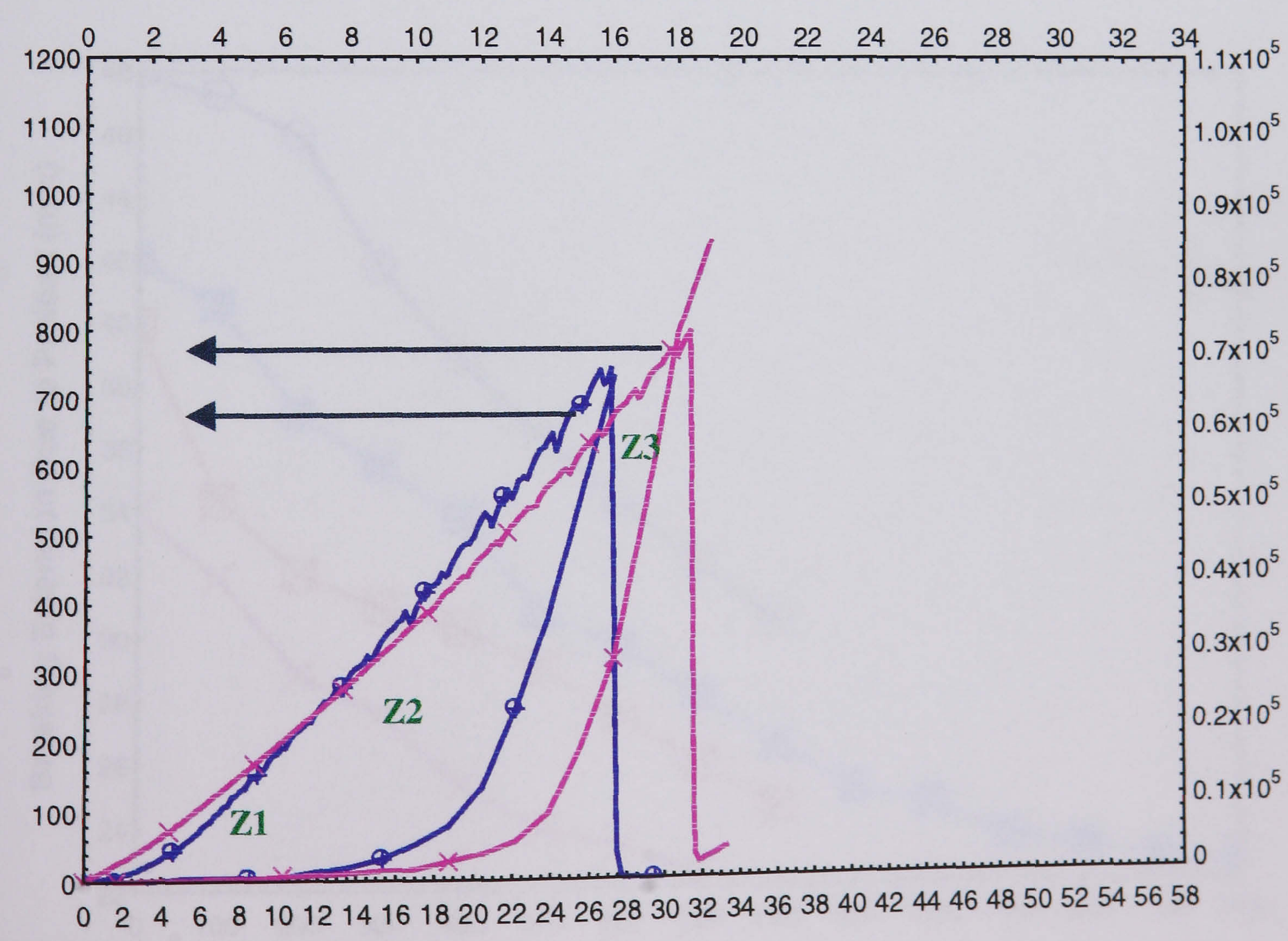

Figure 8.18: *Representative Load – Extension and AE – Extension for covered and uncovered 8 strands Technora samples (see legends on page 252).*

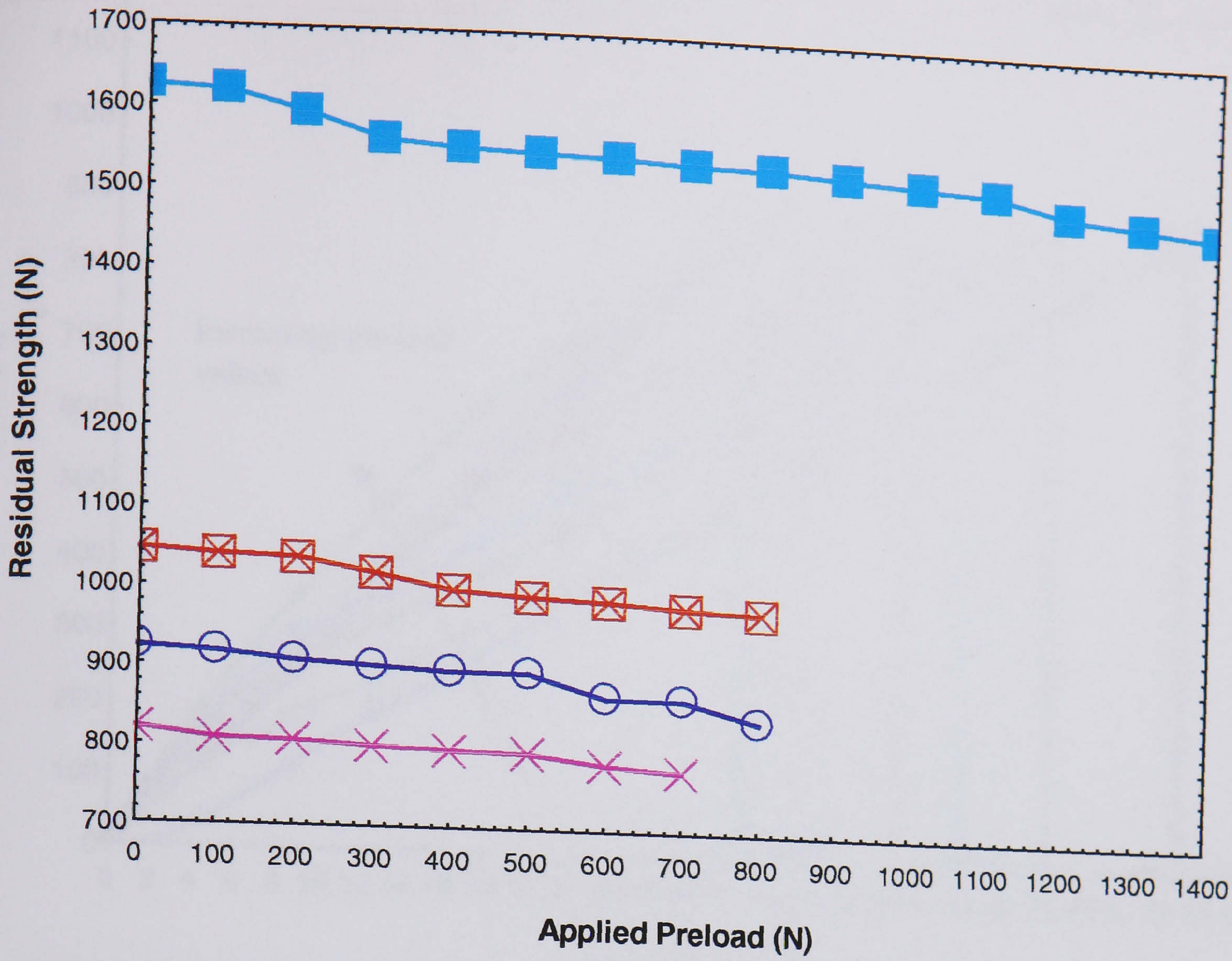

Figure 8.19a: *Mean residual strength against applied preload curves for all the ropes tested (see legends on page 252).*

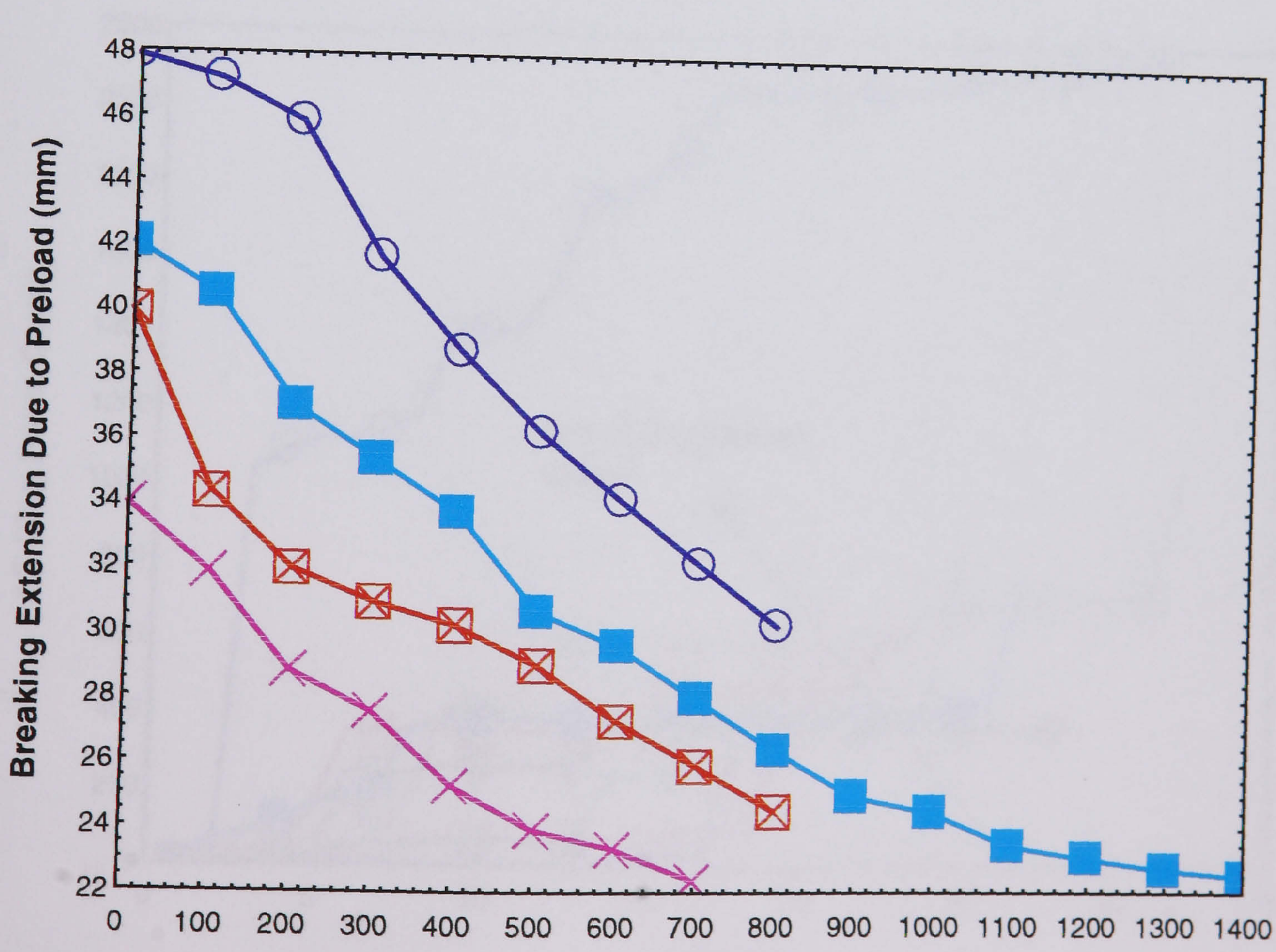

Figure 8.19b: *Mean breaking extension against the applied preload curves for all the ropes tested (see legends on page 252).*

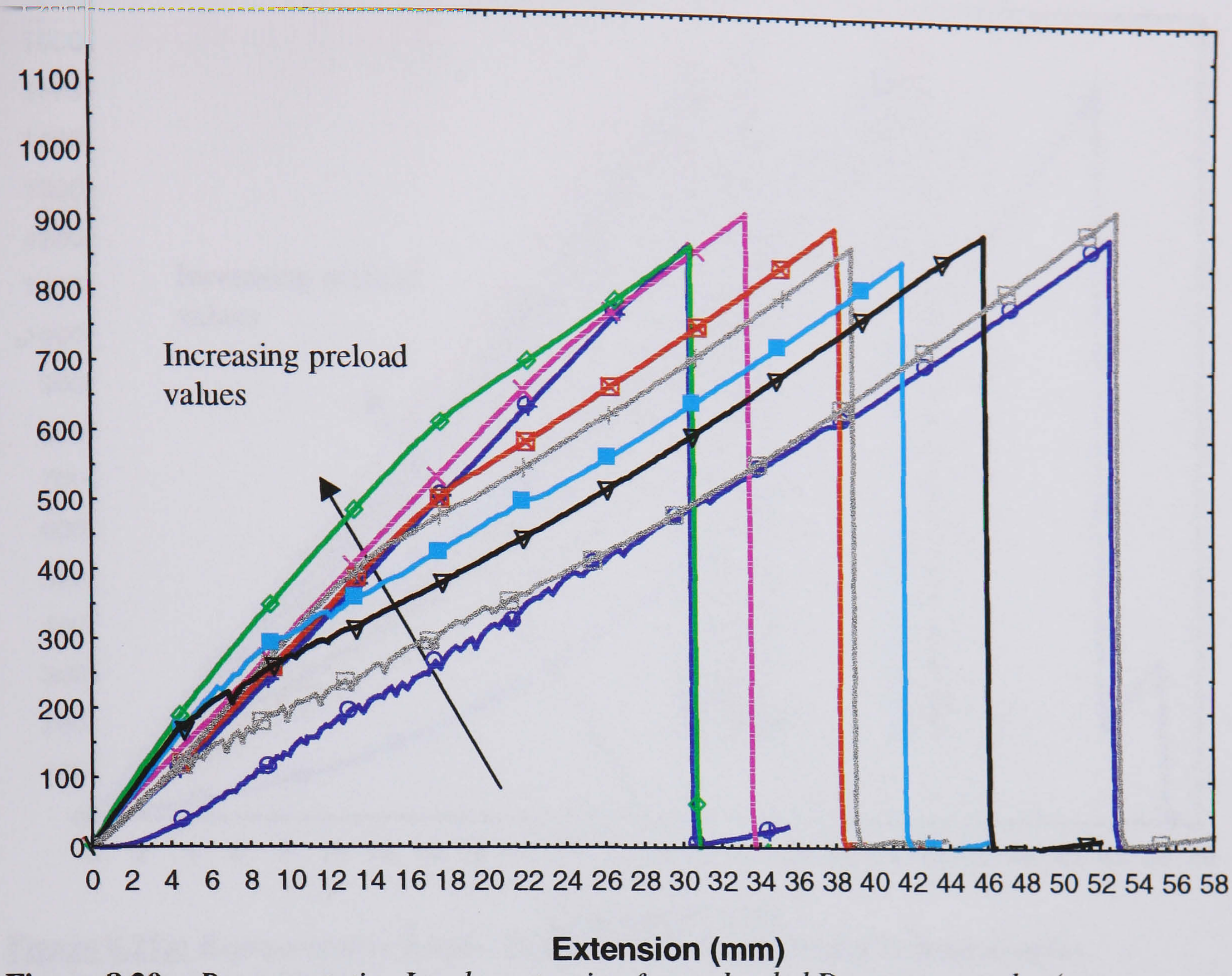

Figure 8.20a: *Representative Load – extension for preloaded Dyneema samples (see legends on page 252).*

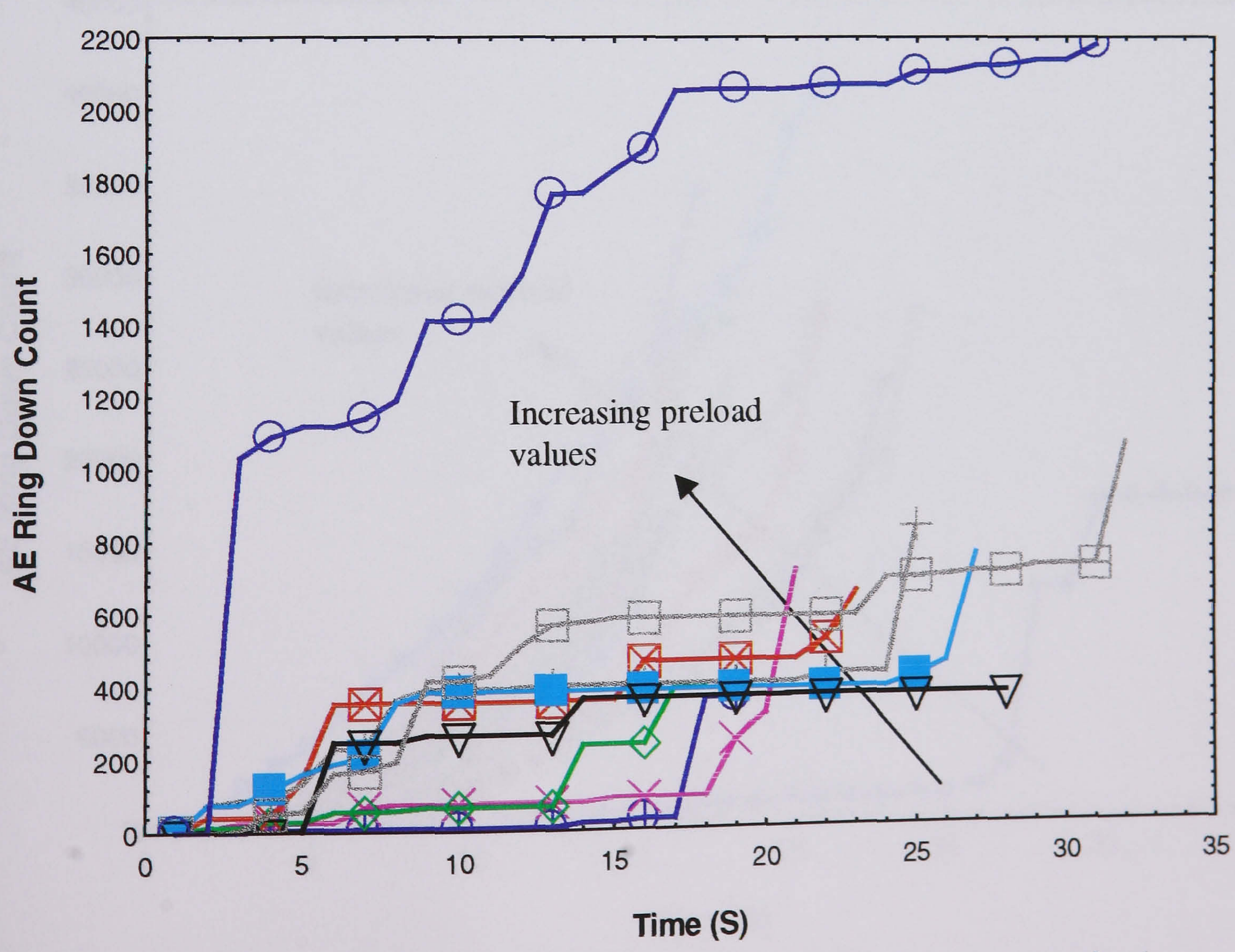

Figure 8.20b: *Representative AE _extension for the preloaded Dyneema samples (see legends on page 252).*

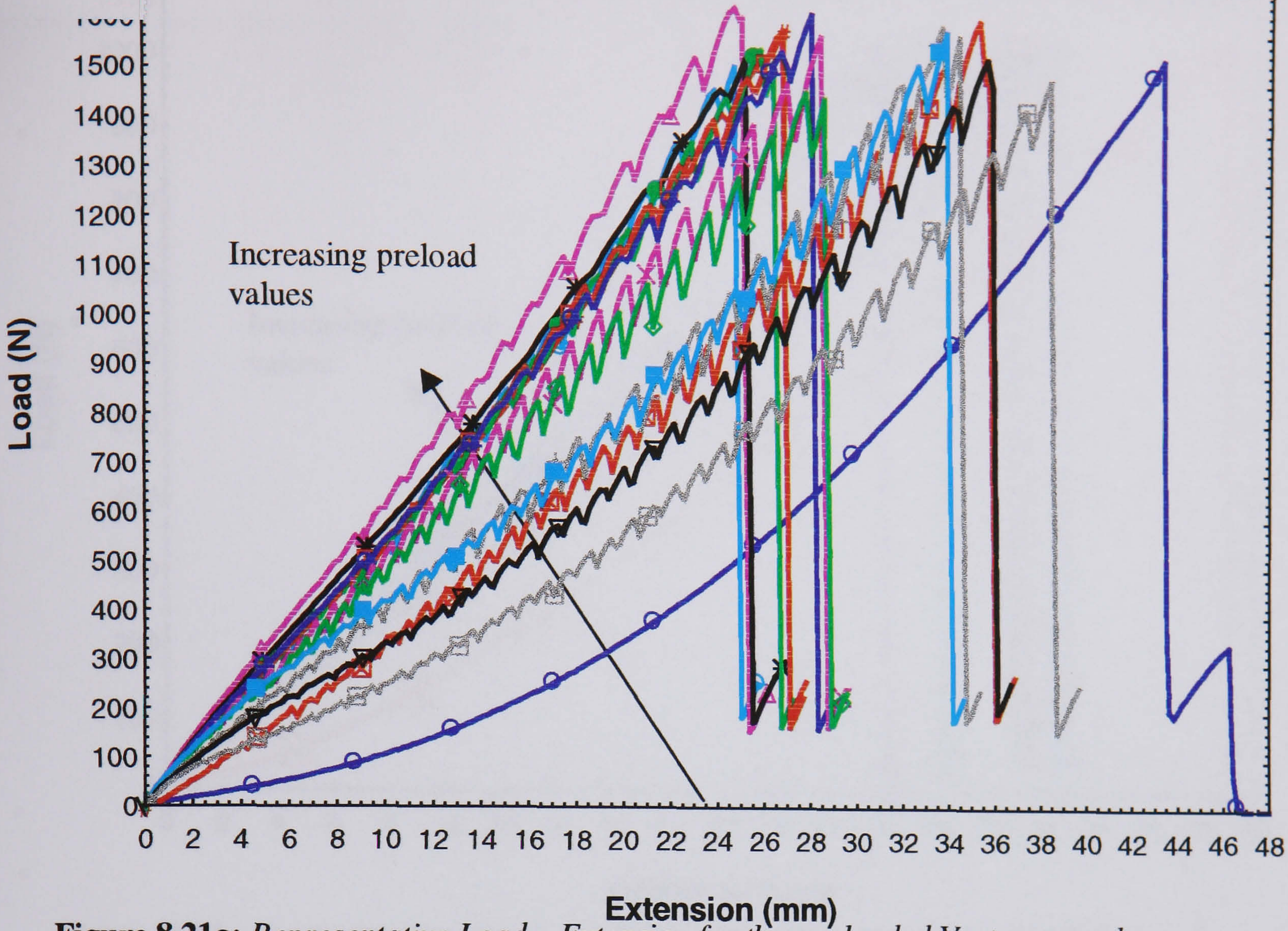

Figure 8.21a: *Representative Load – Extension for the preloaded Vectran samples (see legends on page 252).*

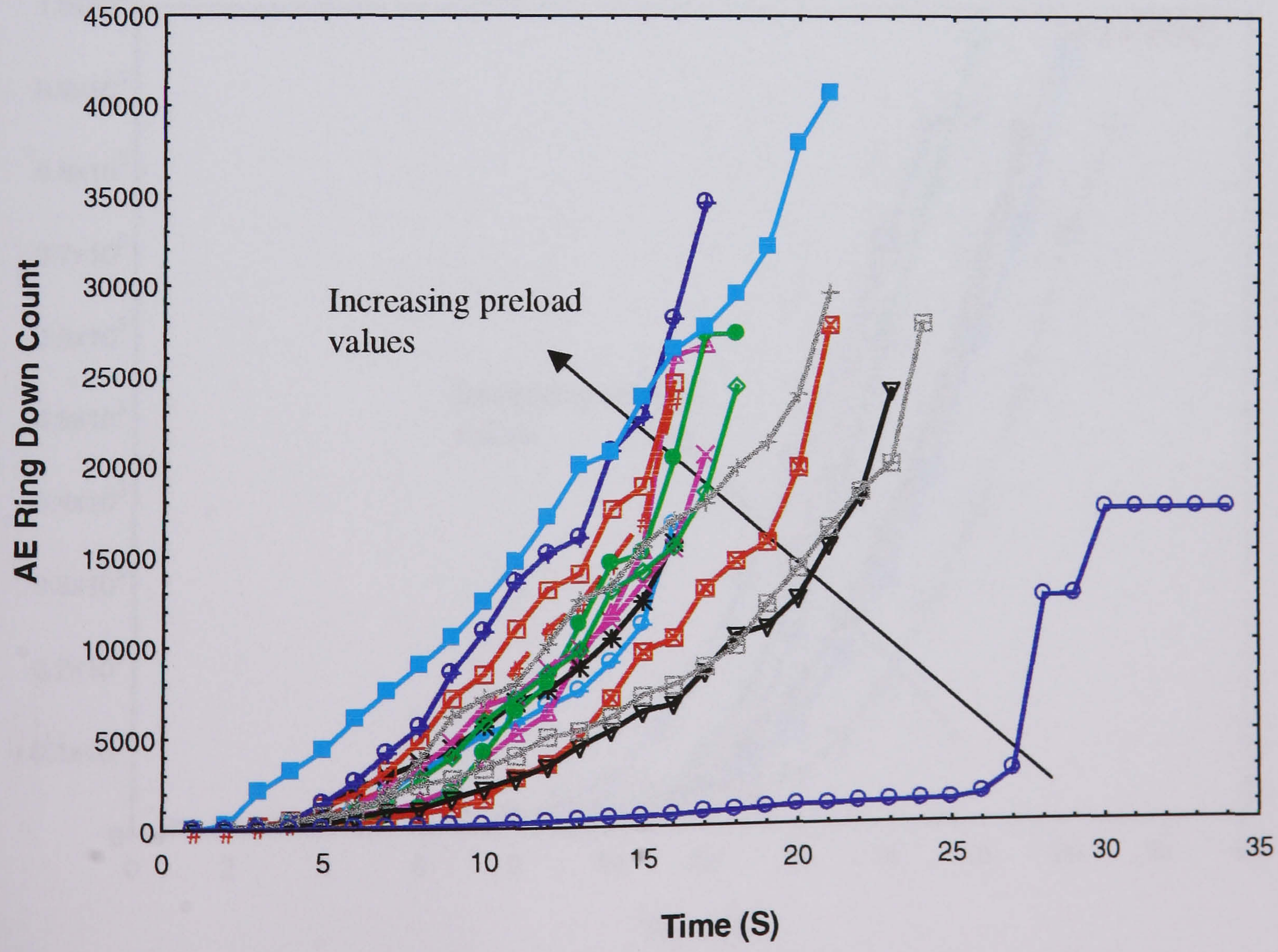

Figure 8.21b: *Representative AE - Extension for preloaded Vectran samples (see legends on page 252).*

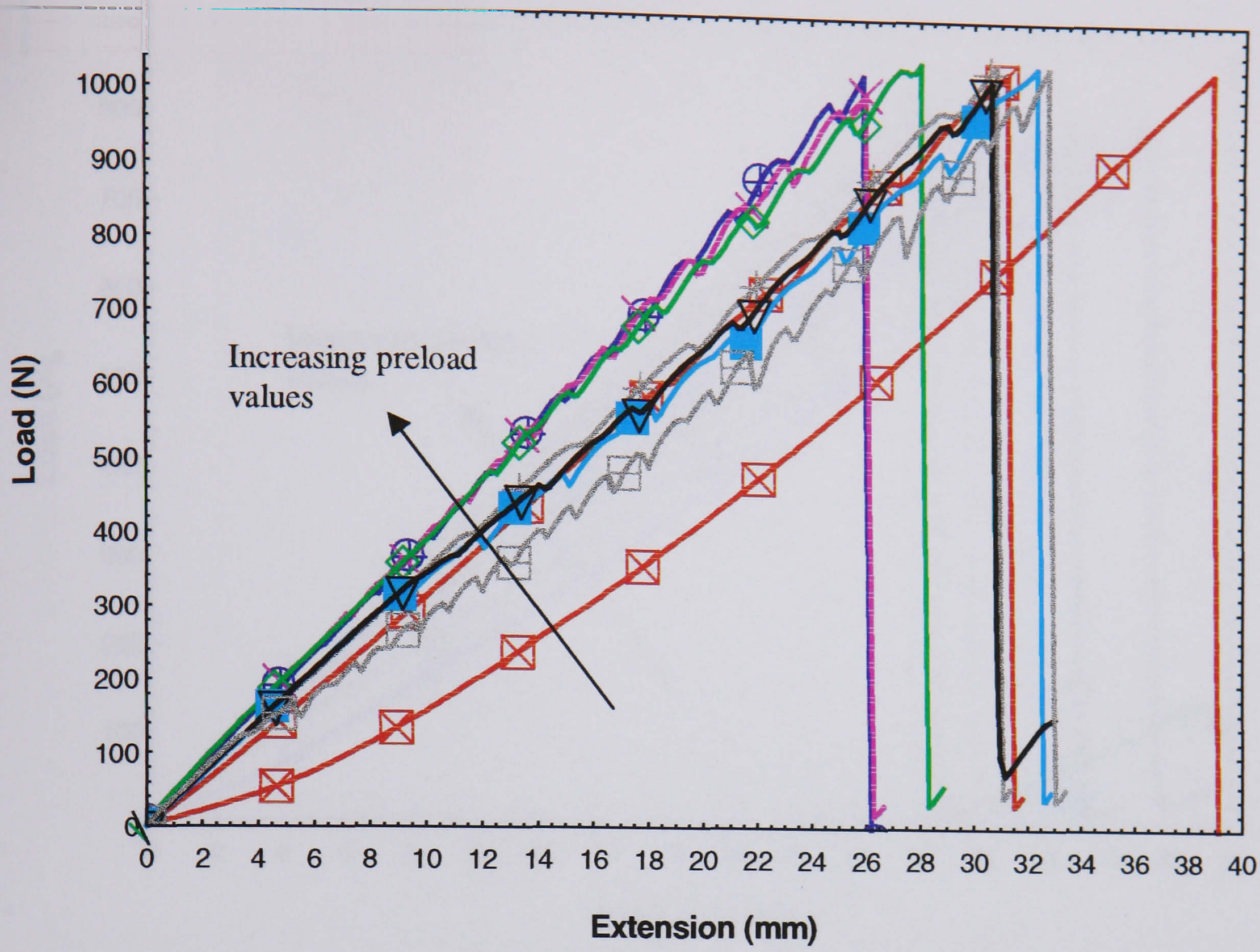

Figure 8.22a: *Representative Load – Extension for the preloaded 4 strand Technora samples (see legends on page 252).*

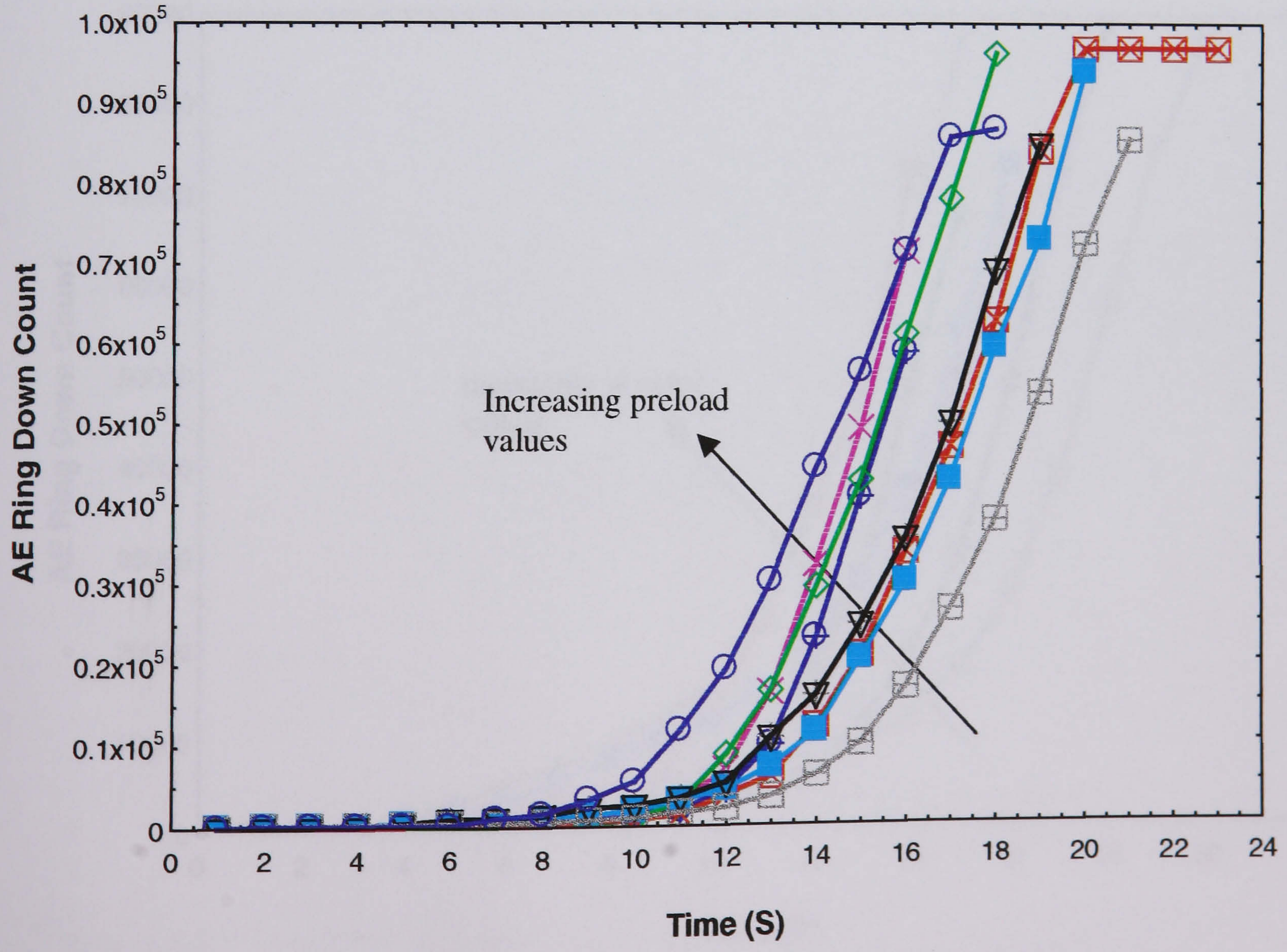

Figure 8.22b: *Representative AE – Extension for preloaded 4 strand Technora samples (see legends on page 252).*

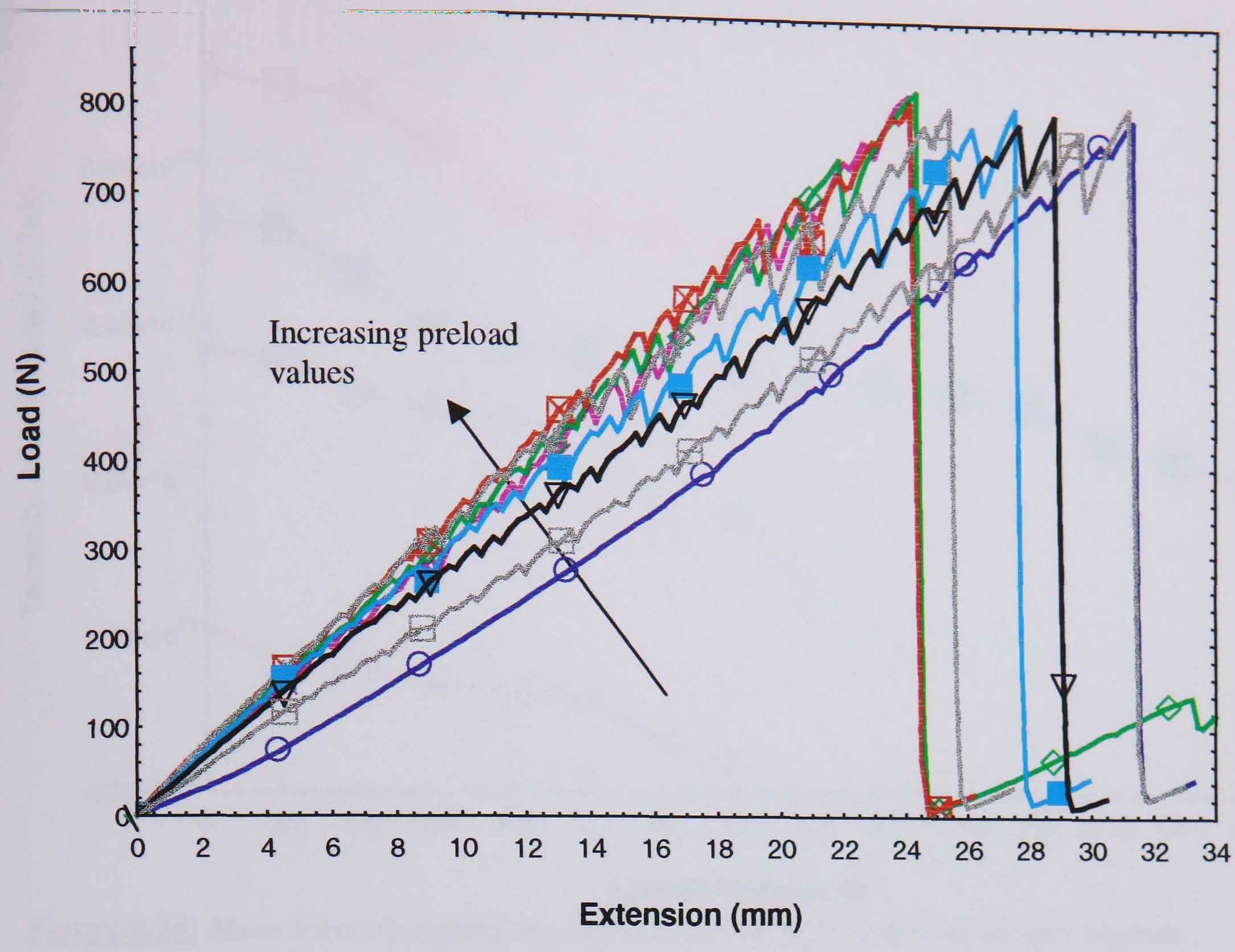

Figure 8.23a: *Representative Load – Extension for preloaded 8 strand Technora samples (see legends on page 252).*

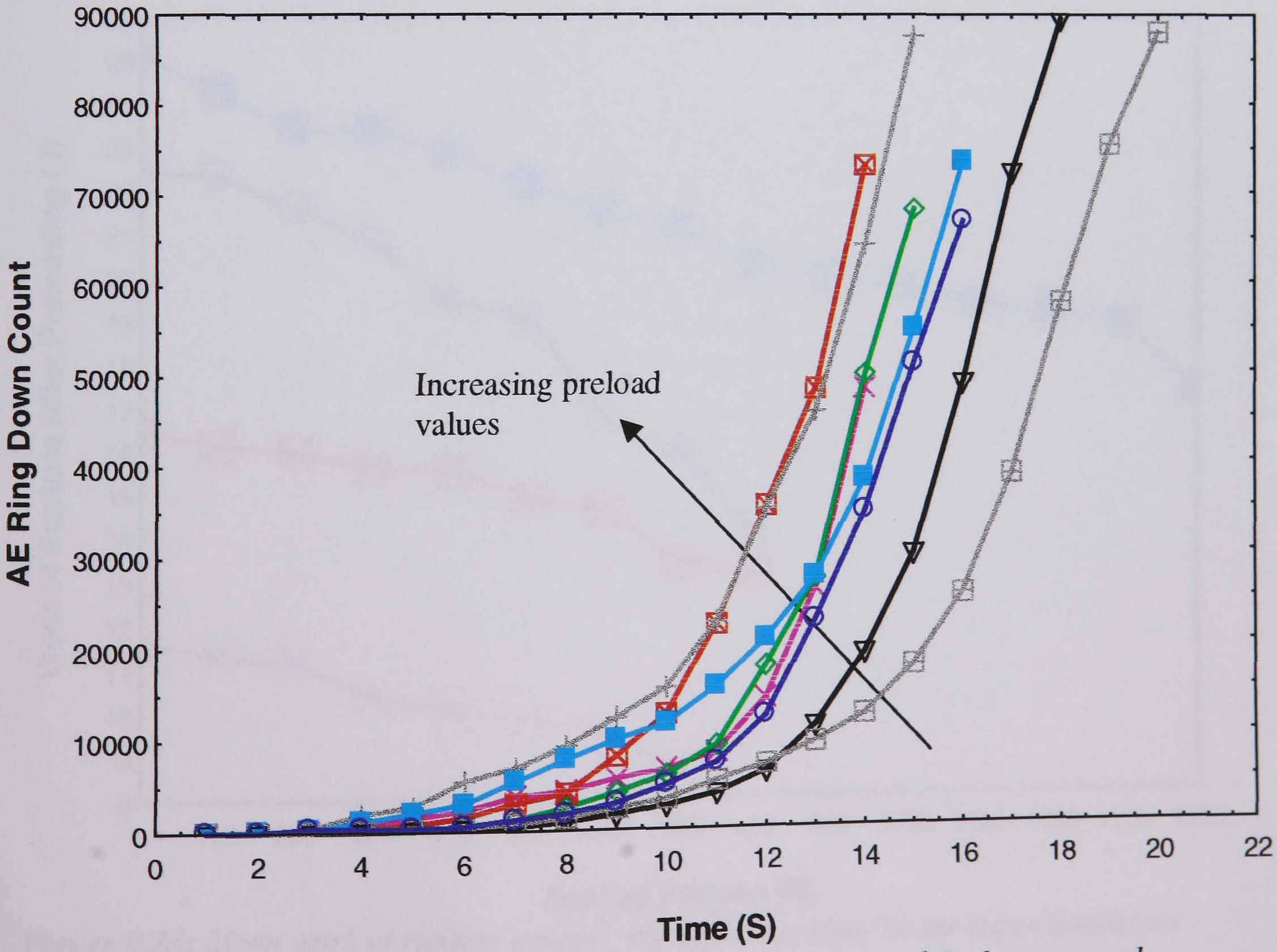

Figure 8.23b: *Representative AE-Extension for preloaded 8 strand Technora samples (see legends on page 252).*

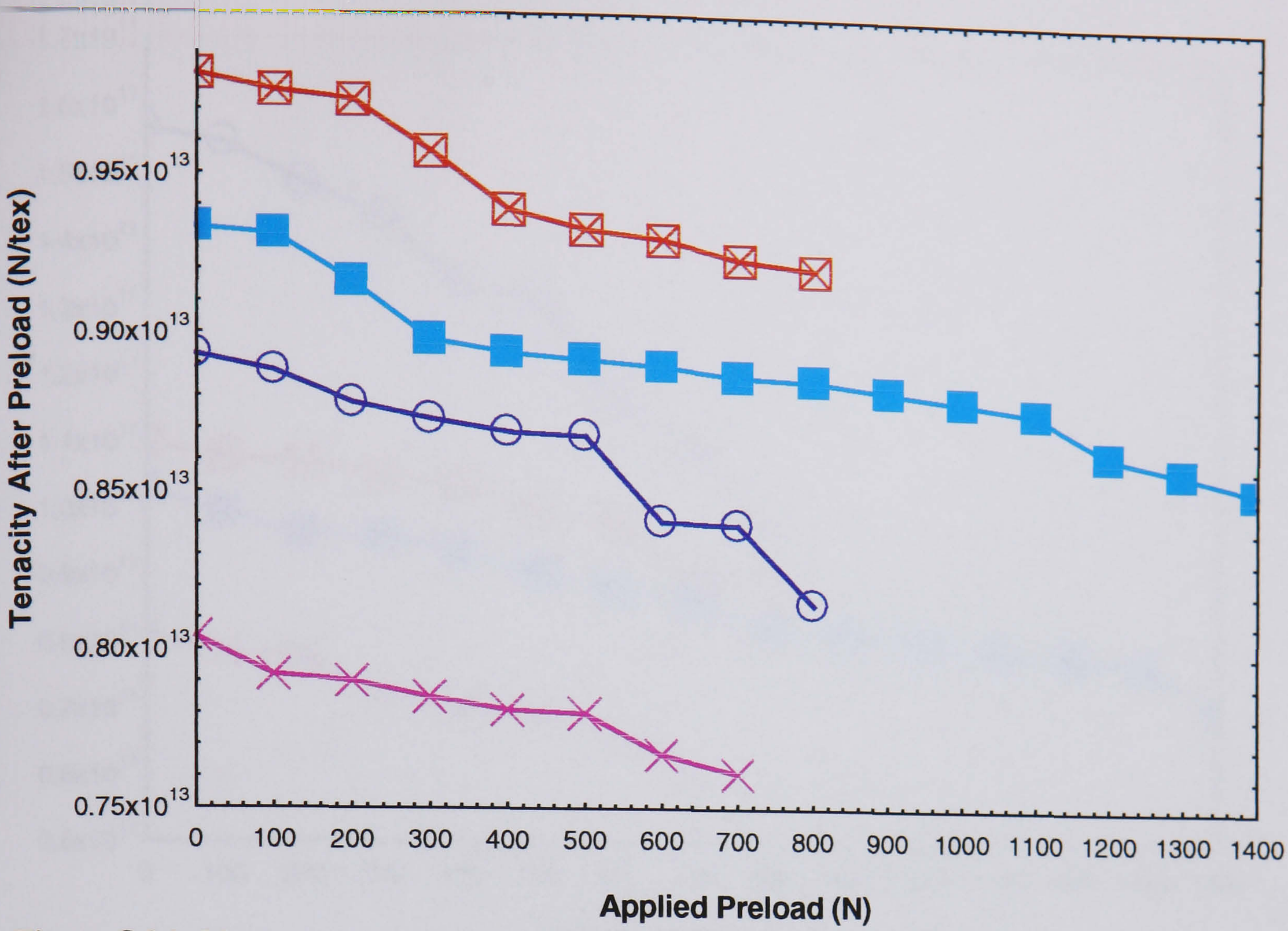

Figure 8.24: *Mean tenacity against the applied preload in the ropes tested (see legends on page 252).*

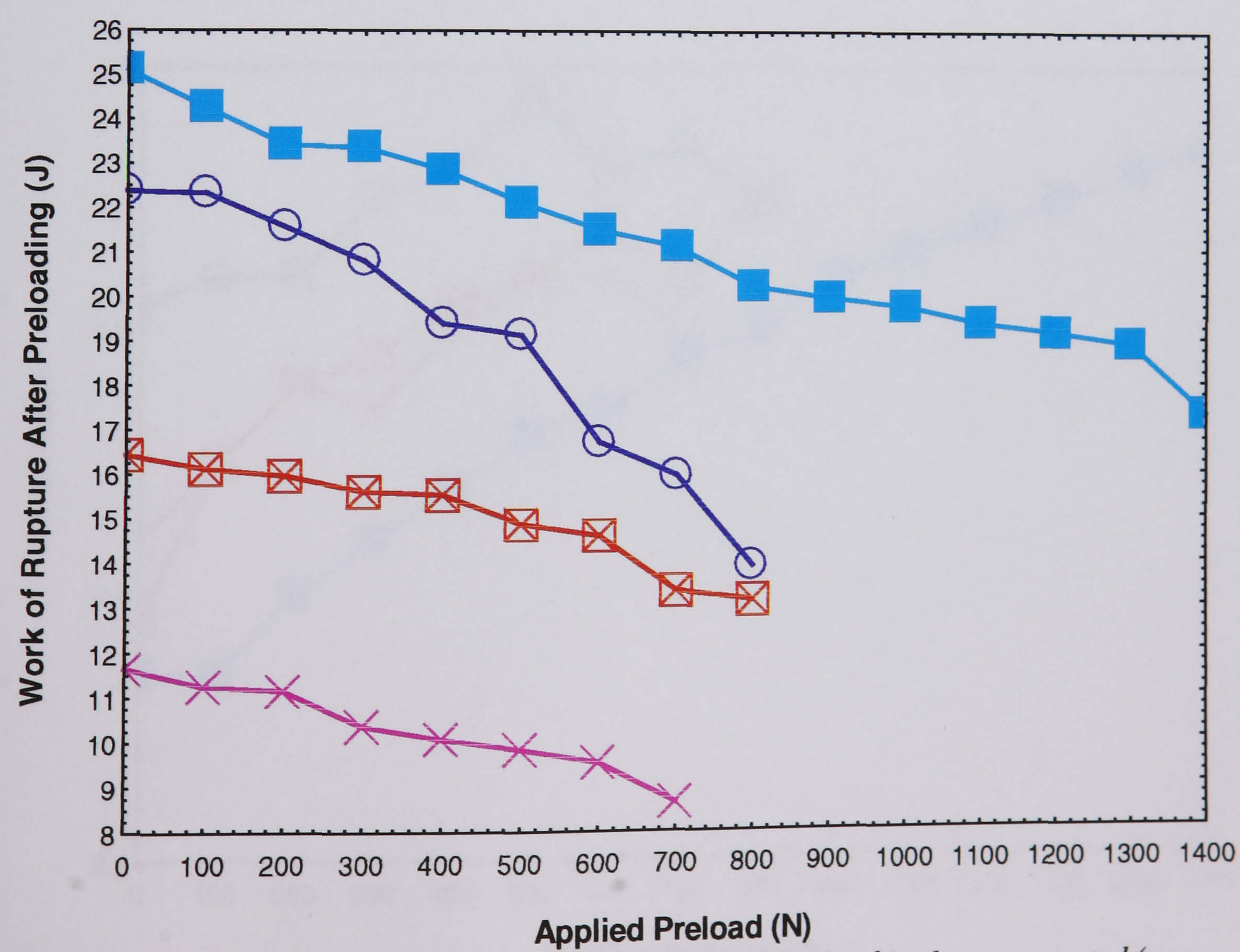

Figure 8.25: *Mean work of rupture against the applied preload in the ropes tested (see legends on page 252).*

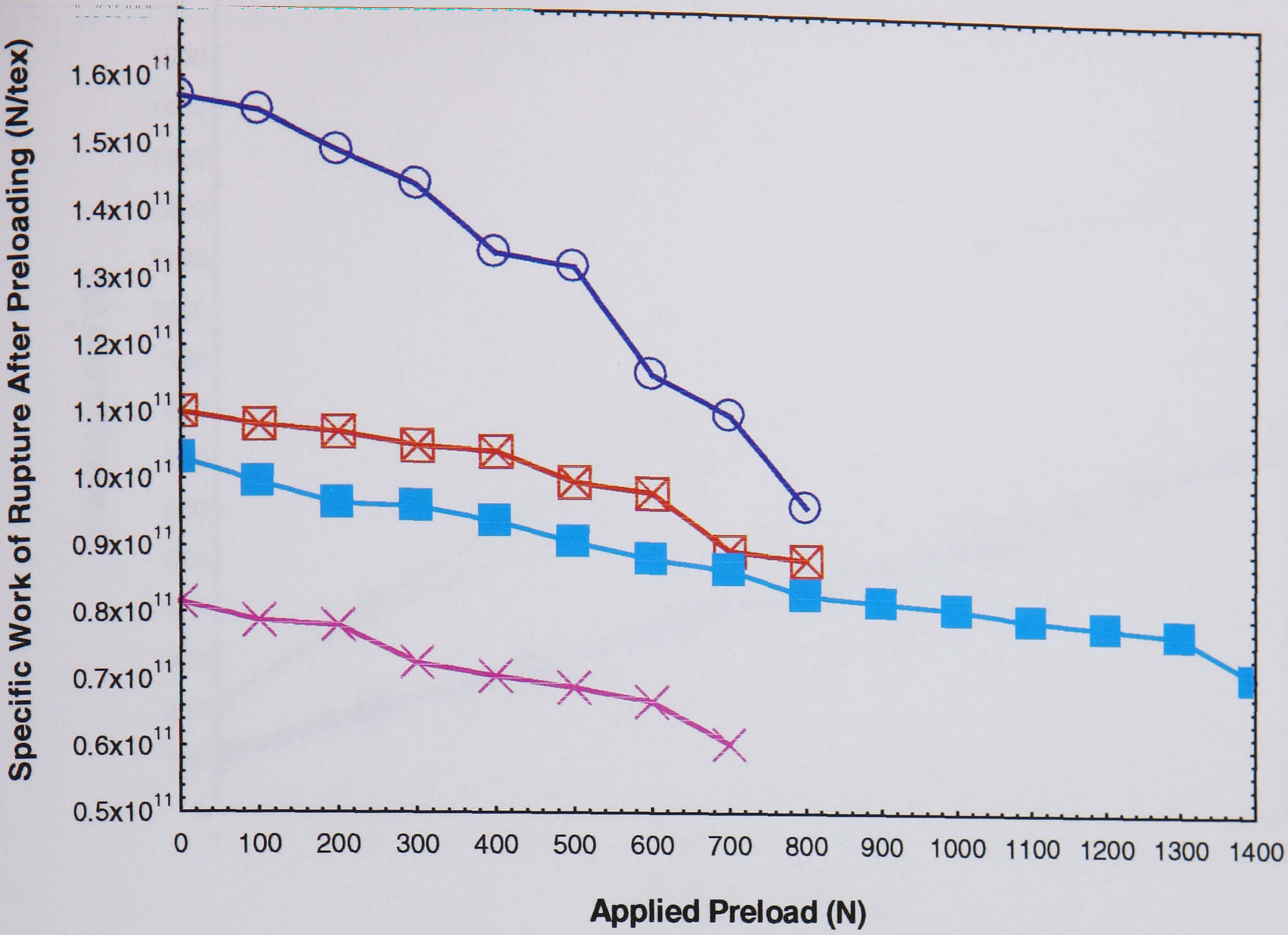

Figure 8.26: *Mean specific work of rupture against applied preload for the ropes tested (see legends on page 252).*

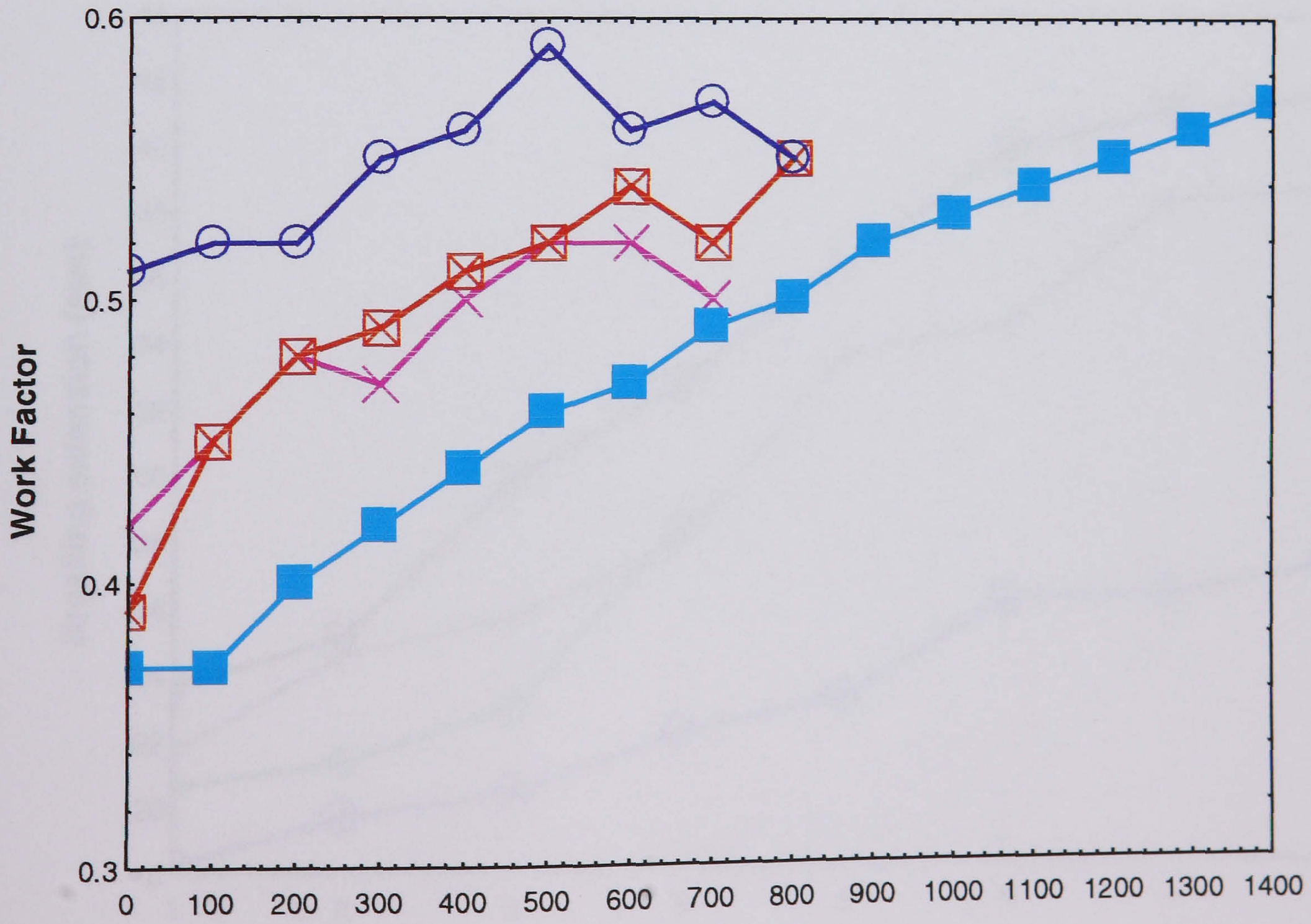

Figure 8.27: *Mean work factor with against applied preload for the ropes tested (see legends on page 252).*

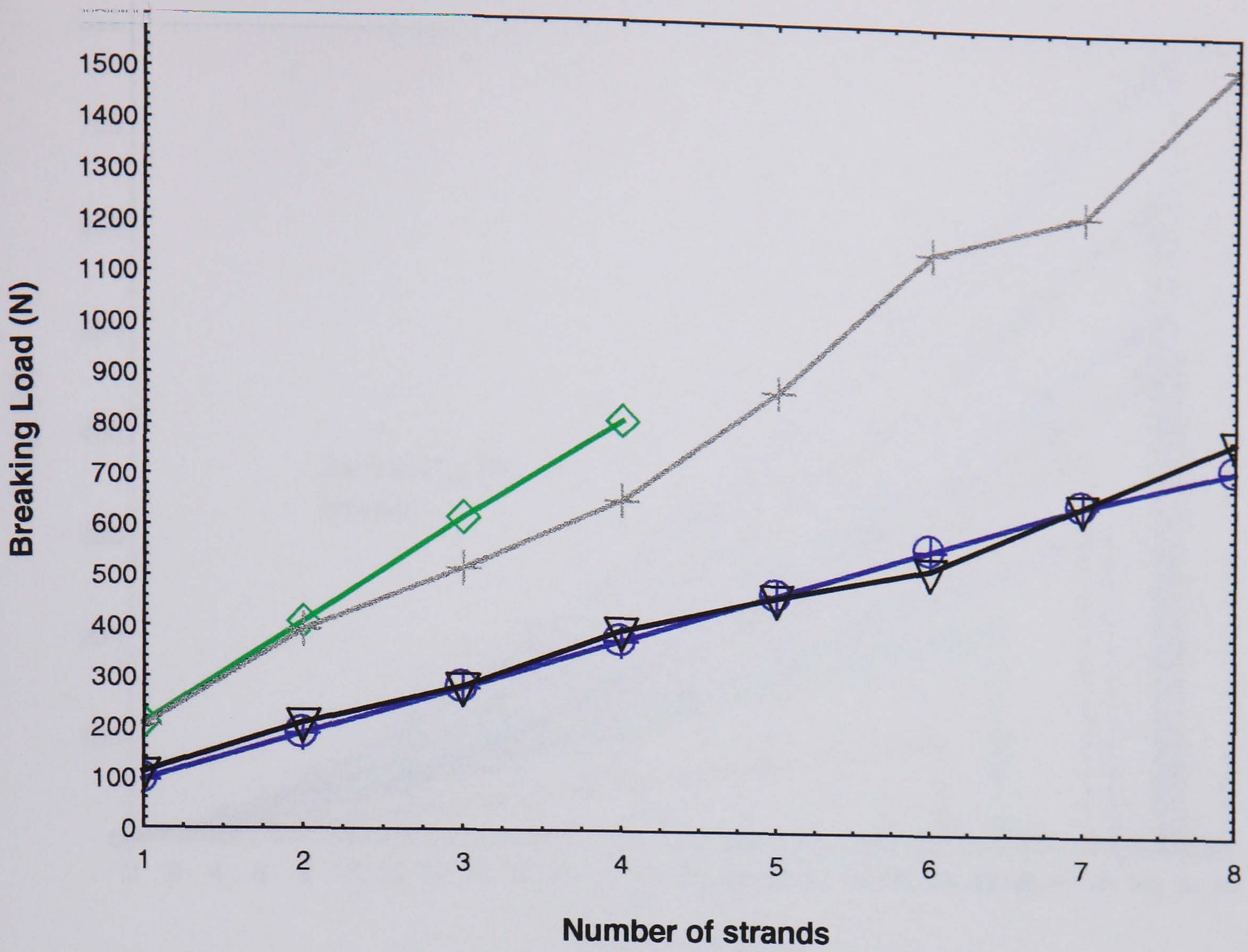

Figure 8.28a: *Mean breaking load against No. of strands for different samples tested (see legends on page 252).*

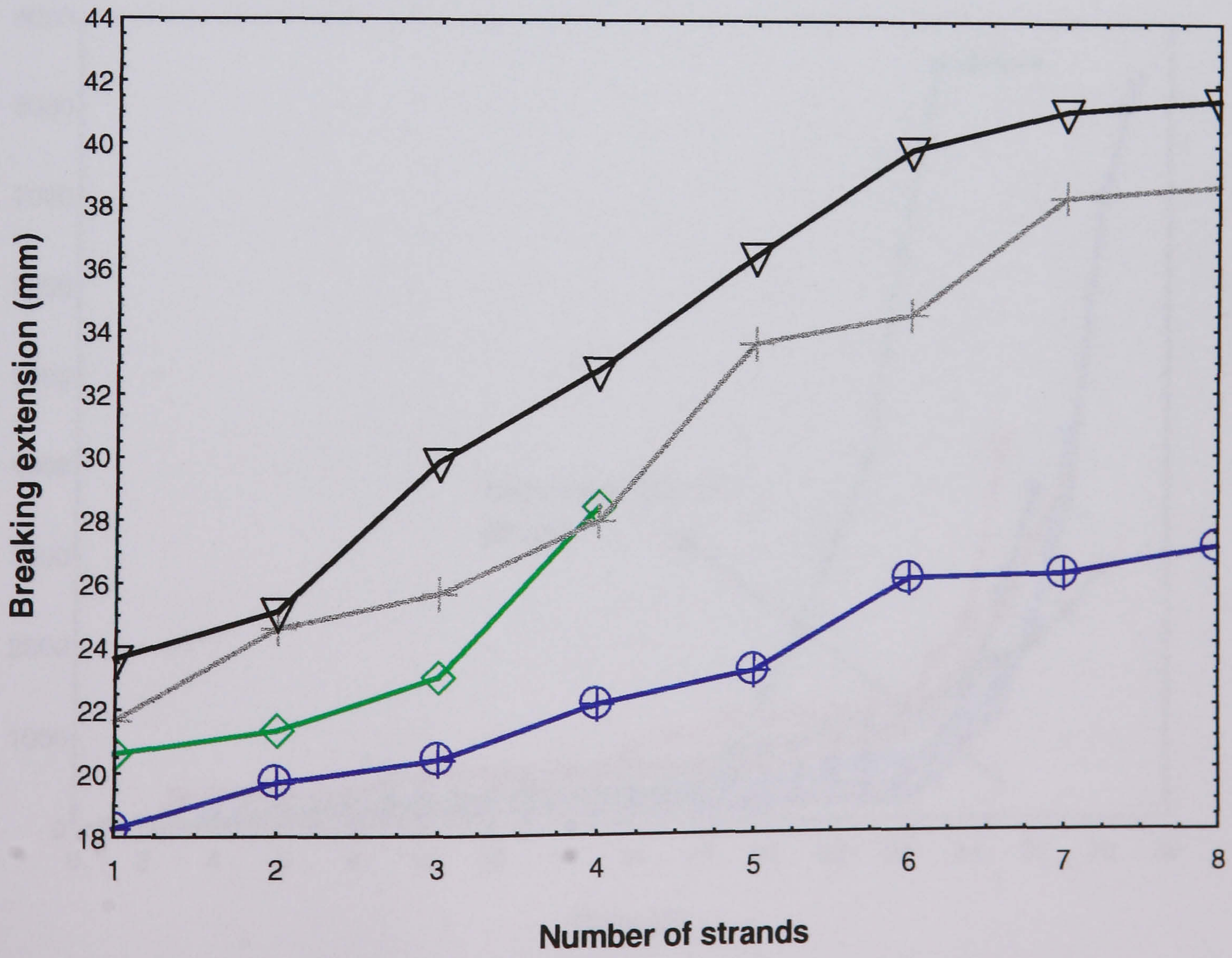

Figure 8.28b: *Mean breaking extension against No. of strands for different samples tested (see legends on page 252).*

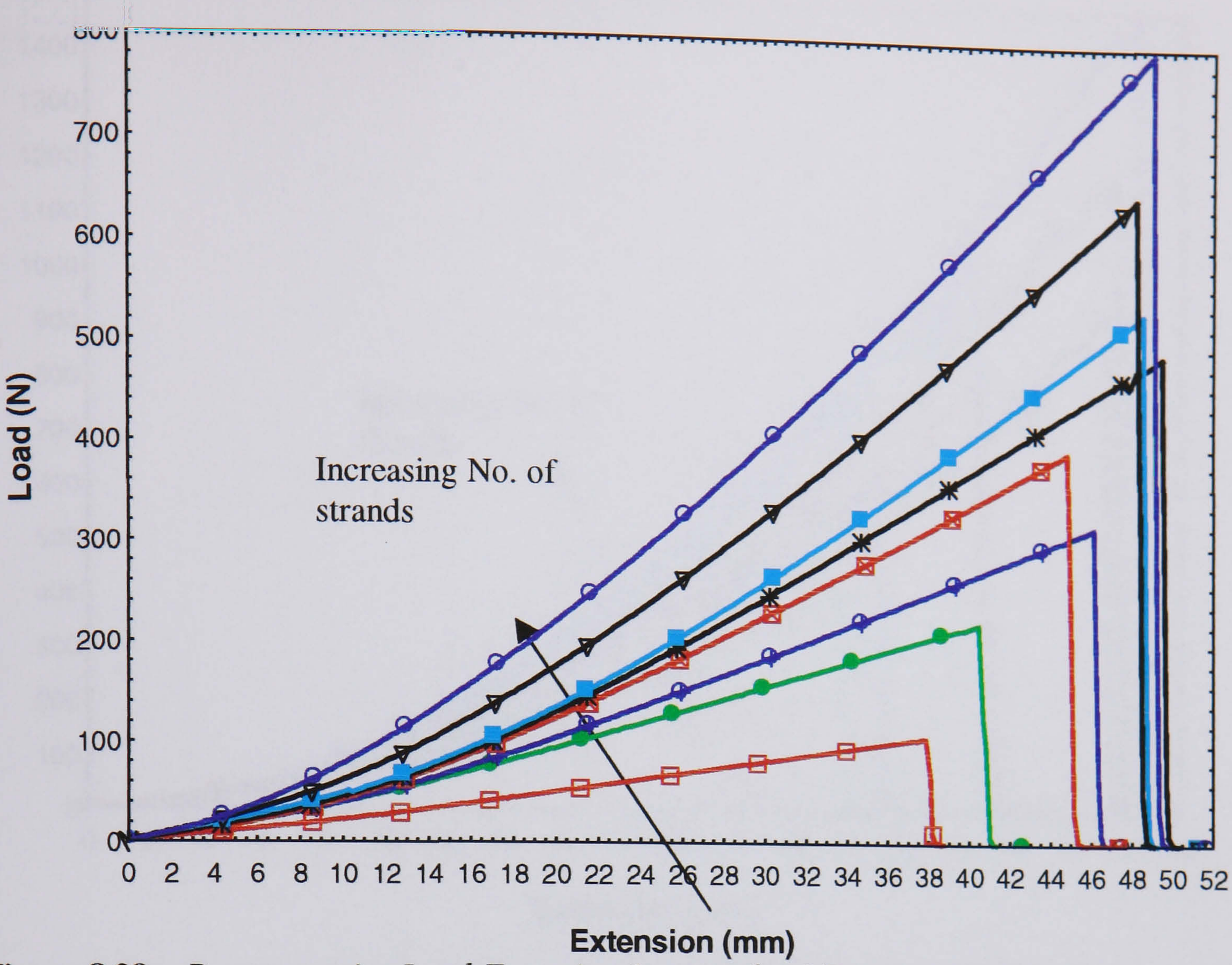

Figure 8.29a: *Representative Load-Extension for strands of Dyneema samples (see legends on page 252).*

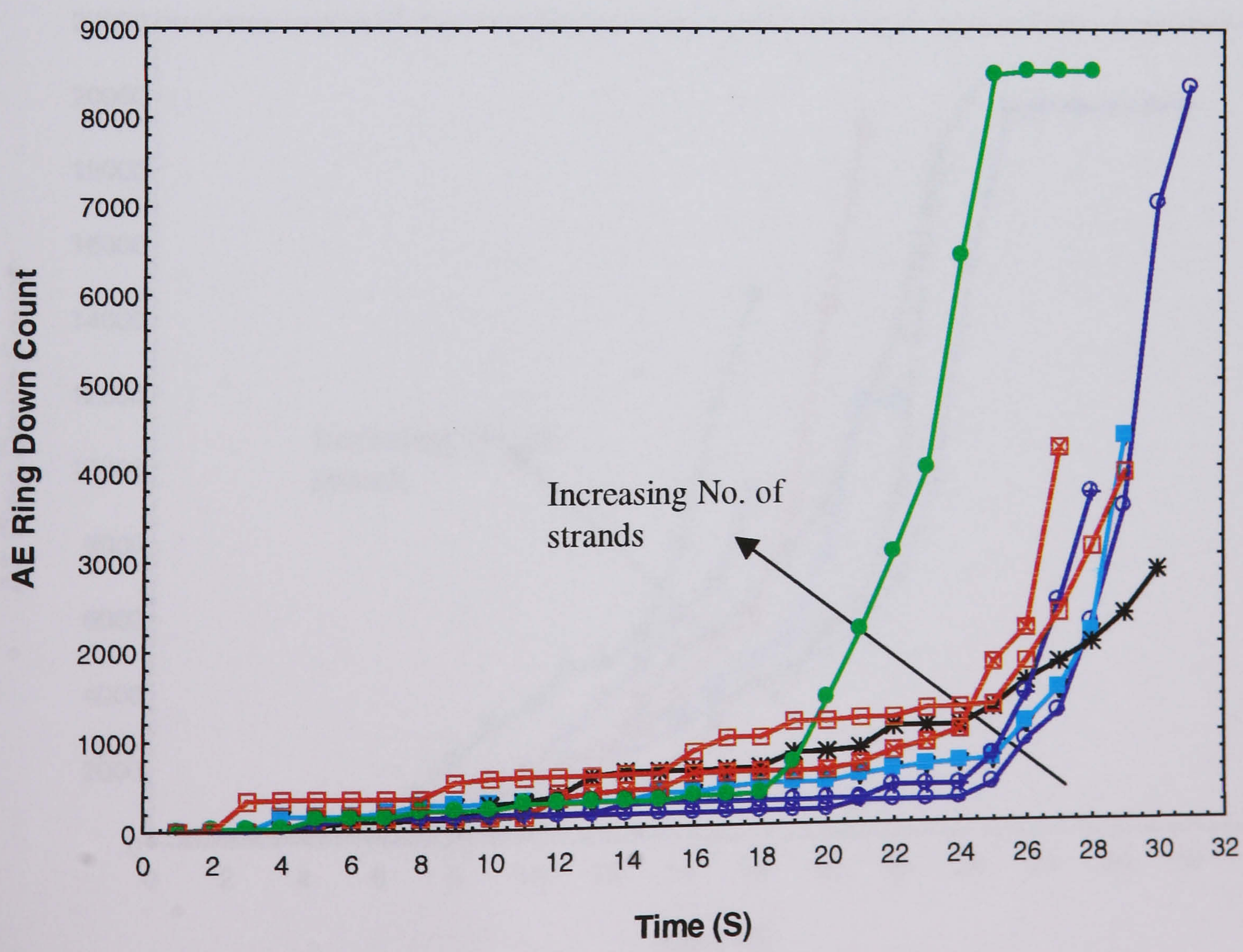

Figure 8.29b: *Representative AE-Extension for strands of Dyneema samples (see legends on page 252).*

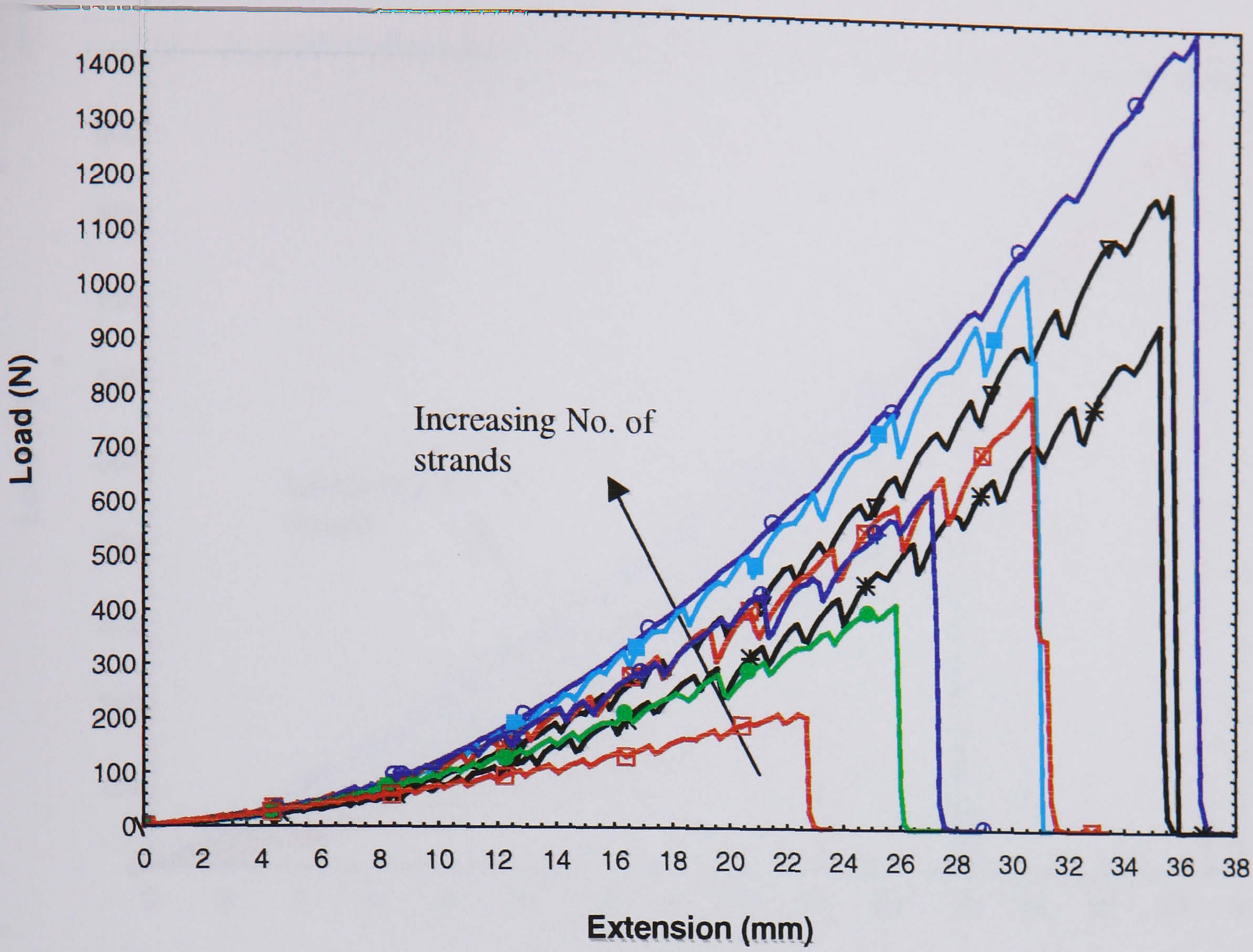

Figure 8.30a: *Representative Load-Extension for strands of Vectran samples (see legends on page 252).*

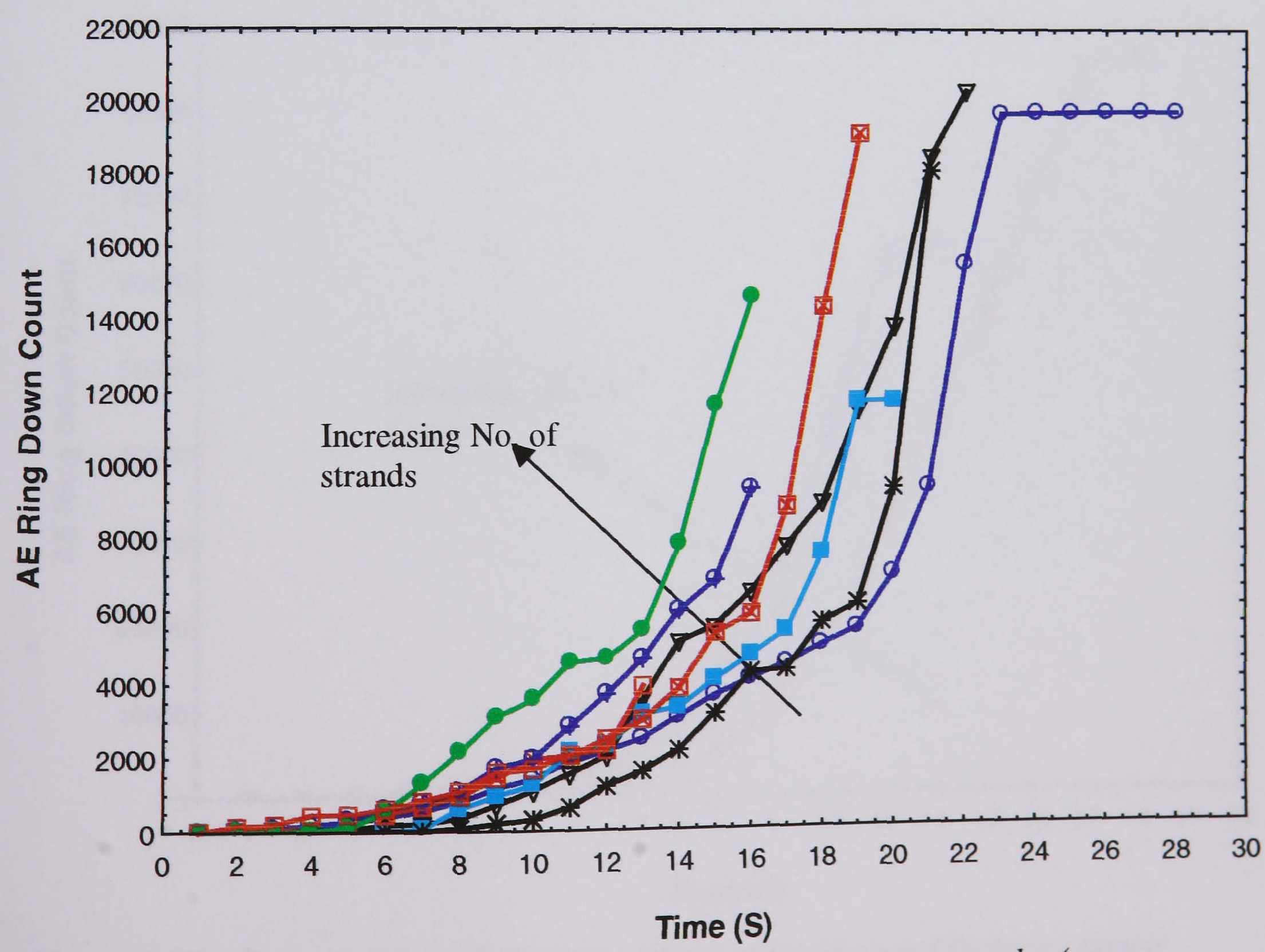

Figure 30b: *Representative of AE-Extension for strands of Vectran samples (see legends on page 252).*

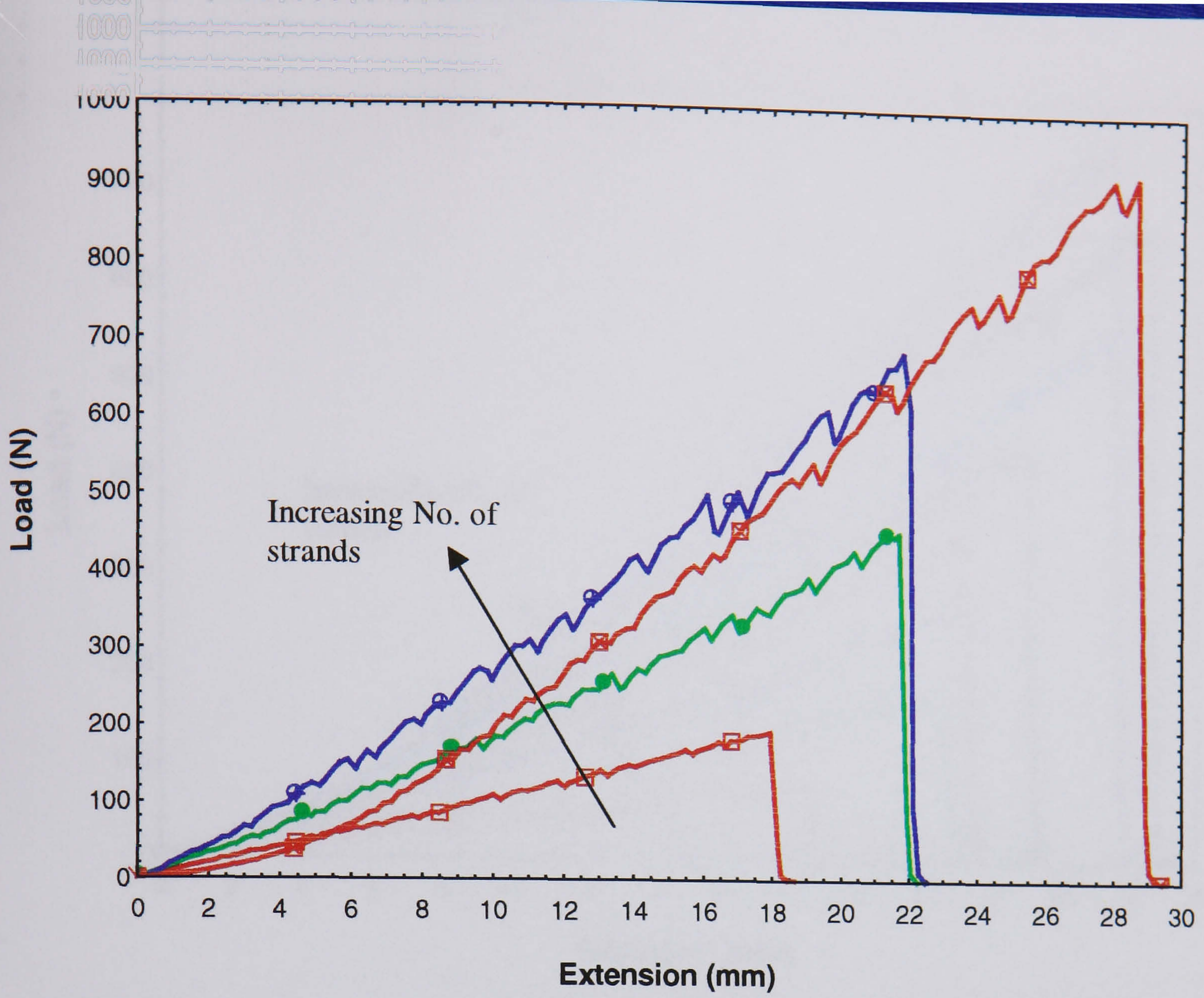

Figure 8.31a: *Representative of Load-Extension for strands of 4 strand Technora samples (see legends on page 252).*

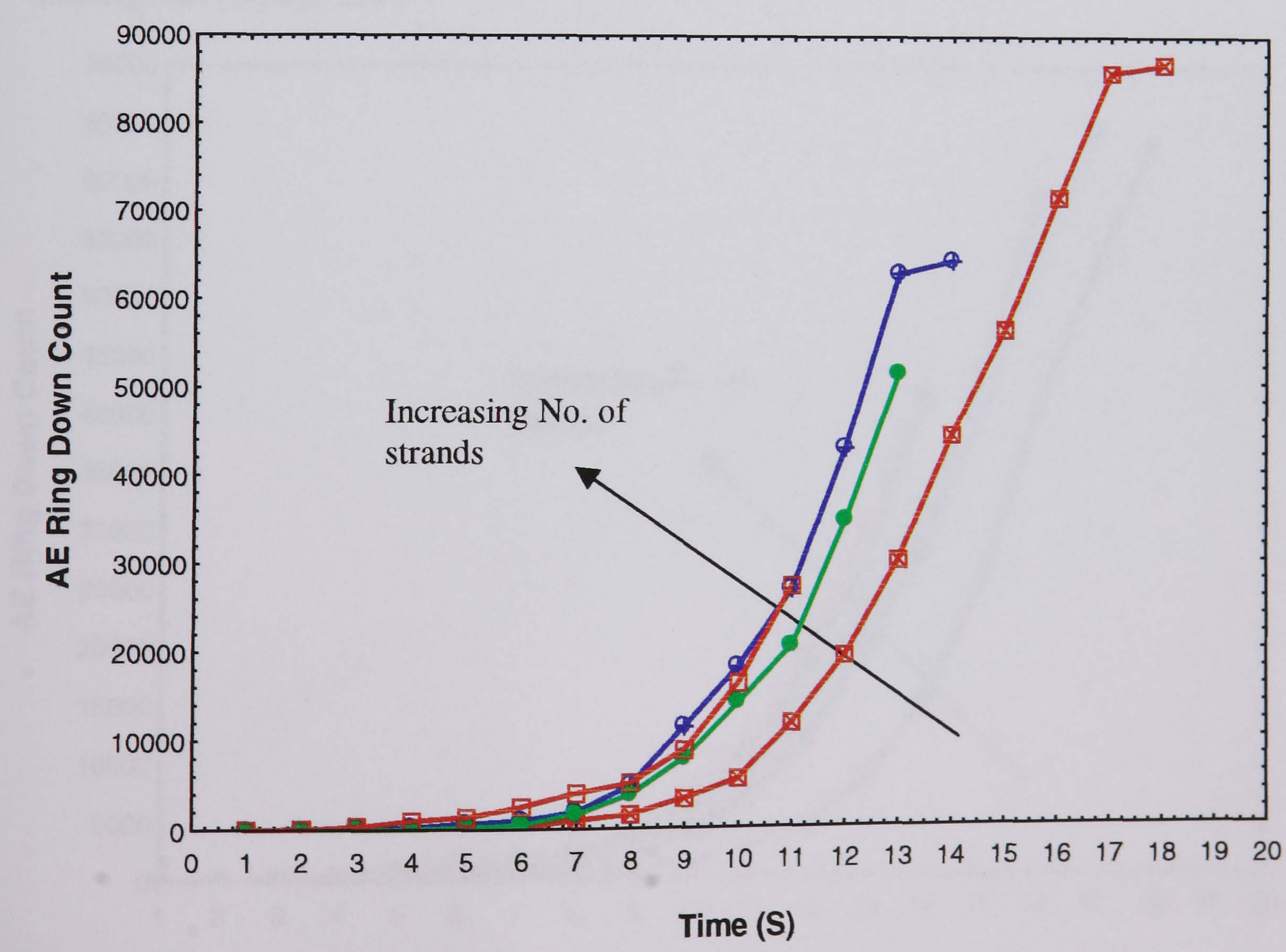

Figure 8.31b: *Representative AE-Extension for strands of 4 strand Technora sample (see legends on page 252).*

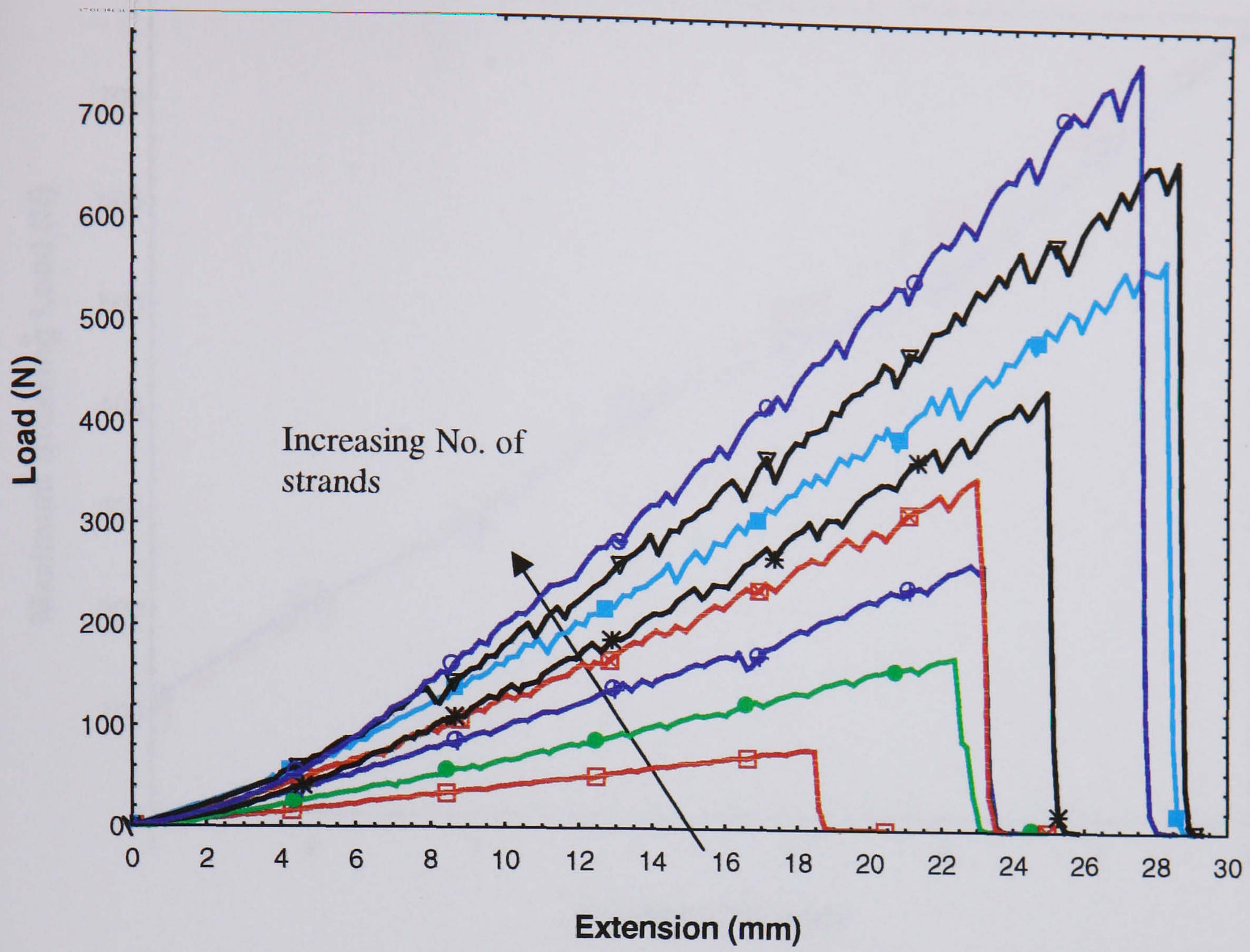

Figure 8.32a: *Representative Load-Extension for strands of 8 strand Technora samples (see legends on page 252).*

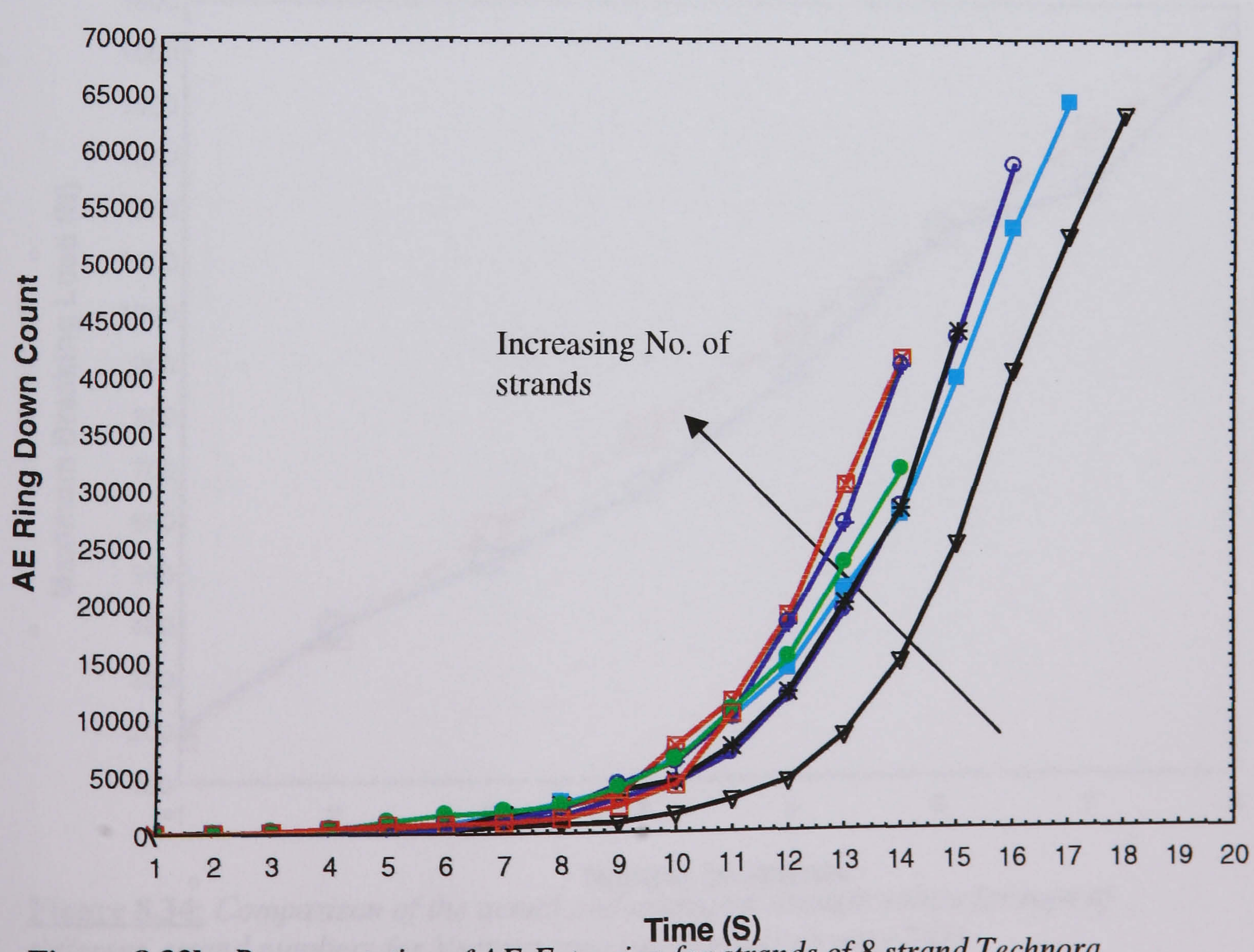

Figure 8.32b: *Representative of AE-Extension for strands of 8 strand Technora samples (see legends on page 252).*

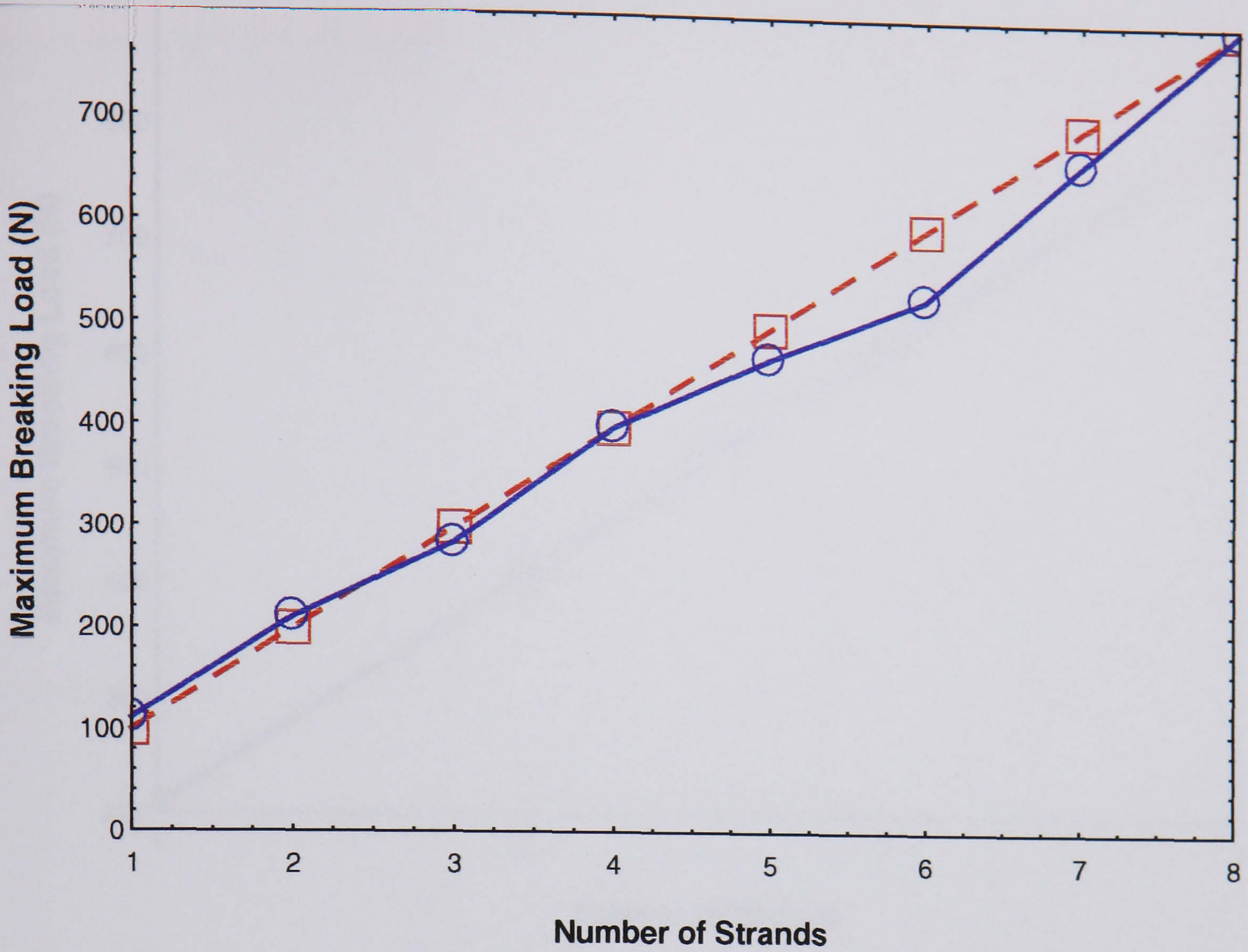

Figure 8.33: *Comparison of the actual and estimated strength values for rope of different strand numbers for Dyneema rope (see legends on page 252).*

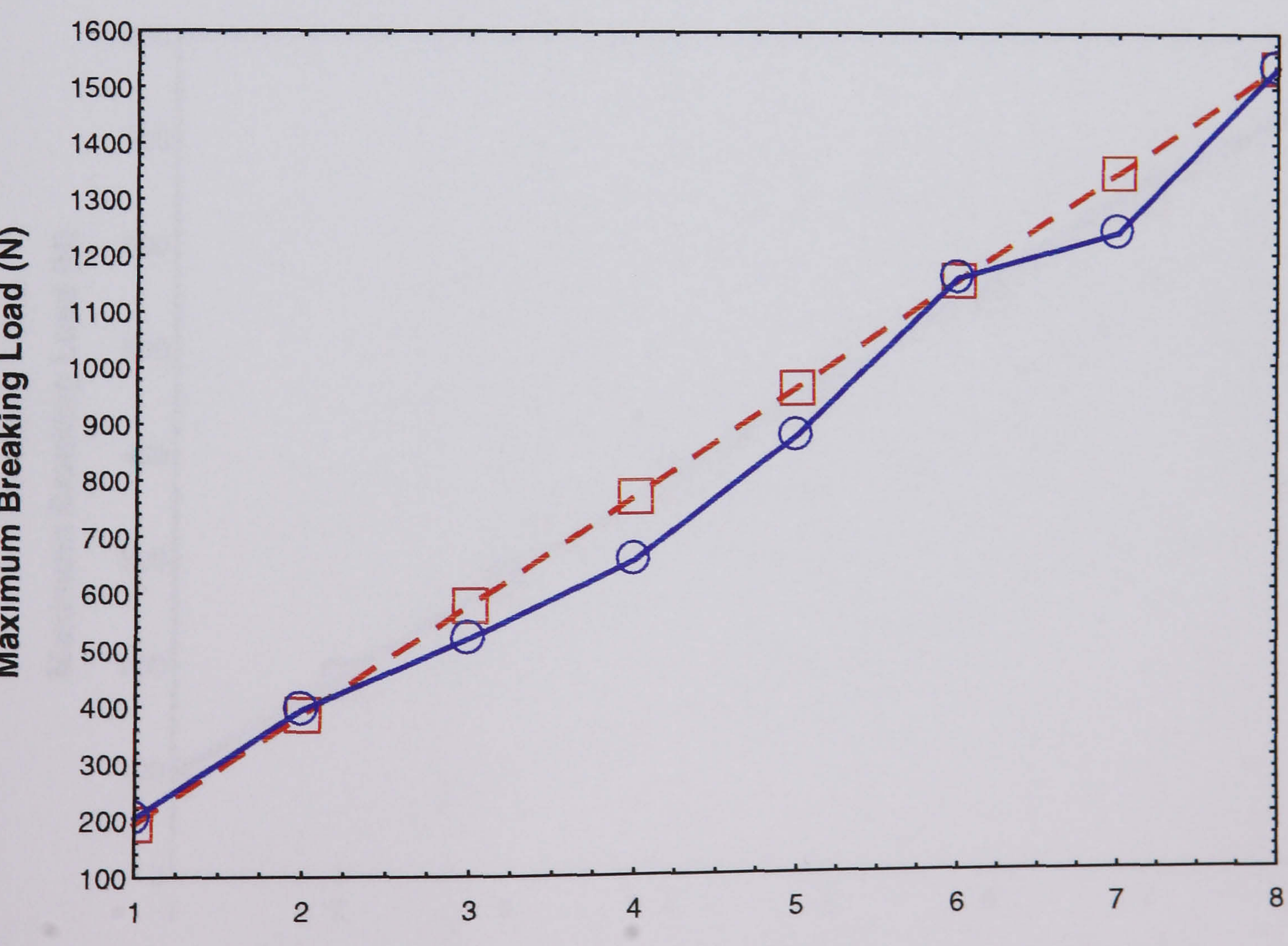

Figure 8.34: *Comparison of the actual and estimated strength values for rope of different strand numbers for Vectran rope (see legends on page 252).*

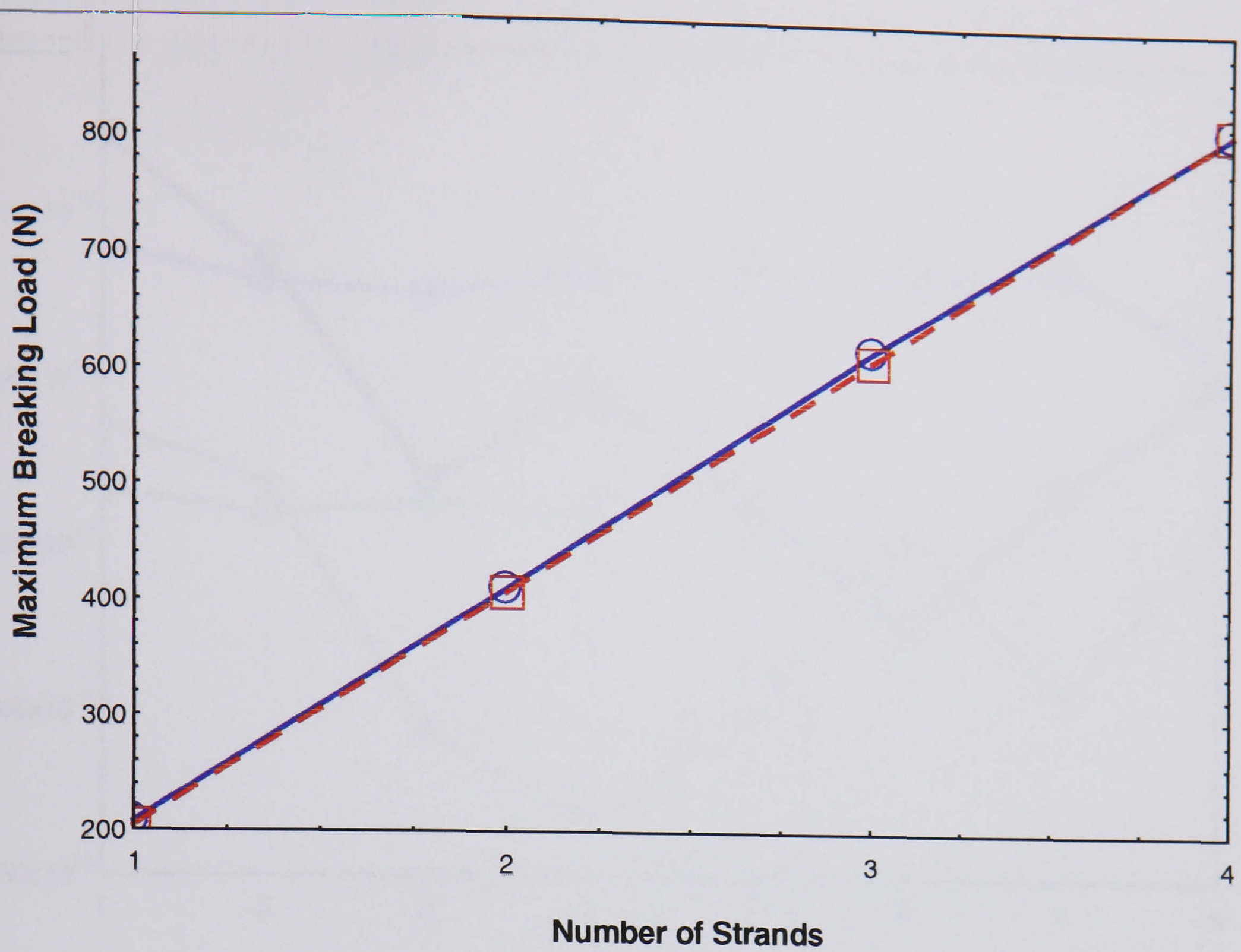

Figure 8.35: *Comparison of the actual and estimated strength for rope of different strand number for 4 strand Technora (see legends on page 252).*

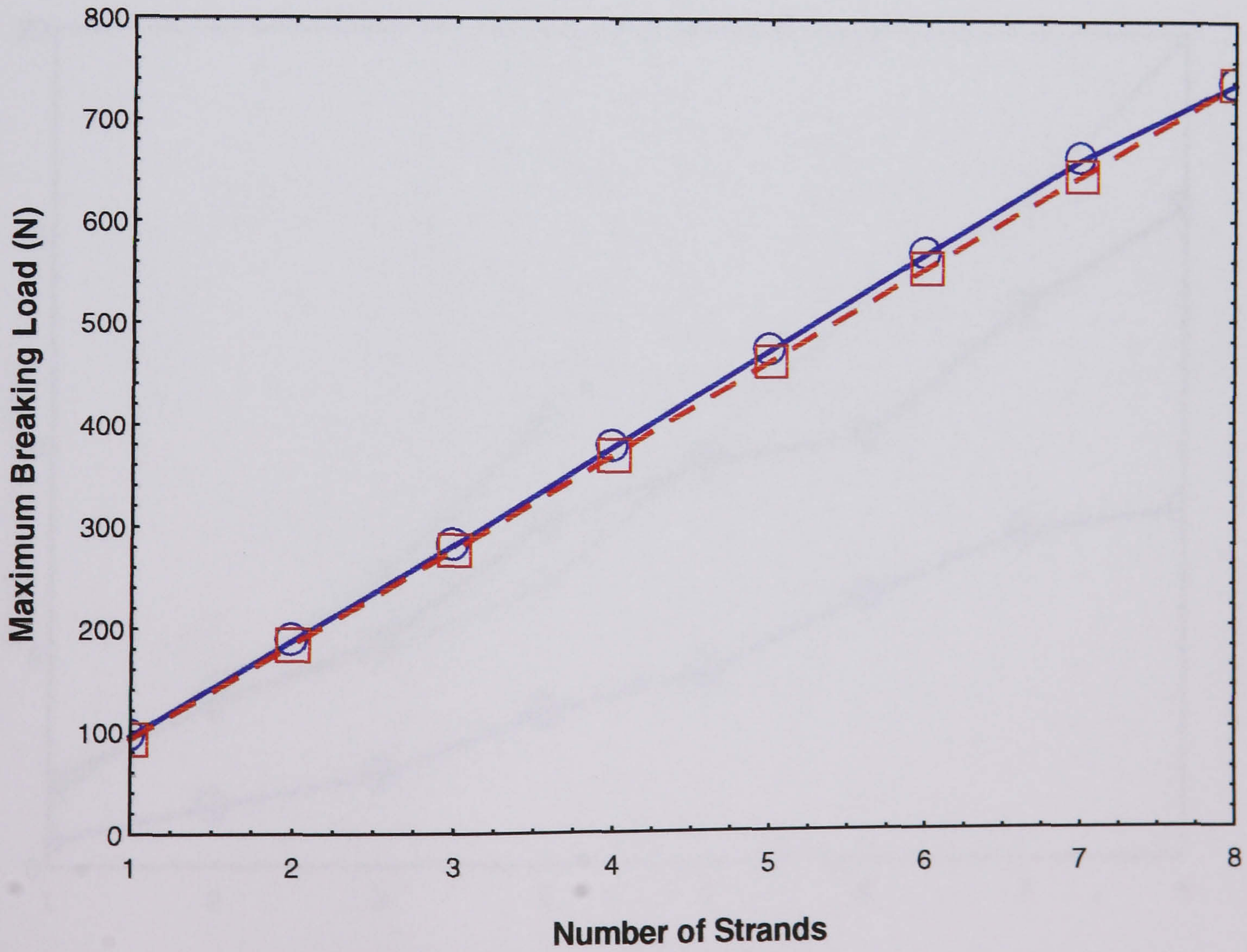

Figure 8.36: *Comparison of actual and estimated strength for rope of different strand numbers for 8 strand Technora rope (see legends on page 252).*

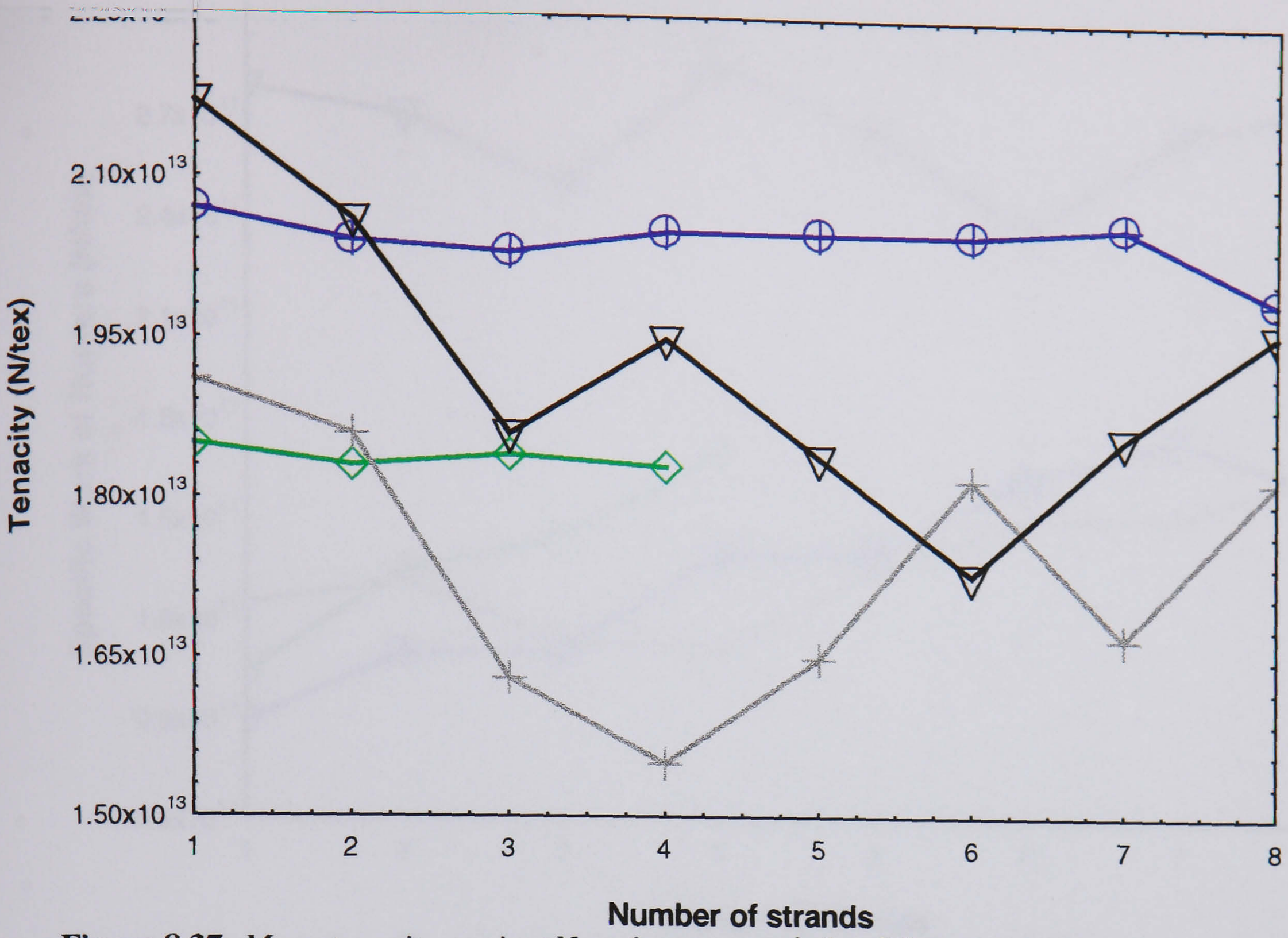

Figure 8.37: *Mean tenacity against No. of rope strands for different samples tested (see legends on page 252).*

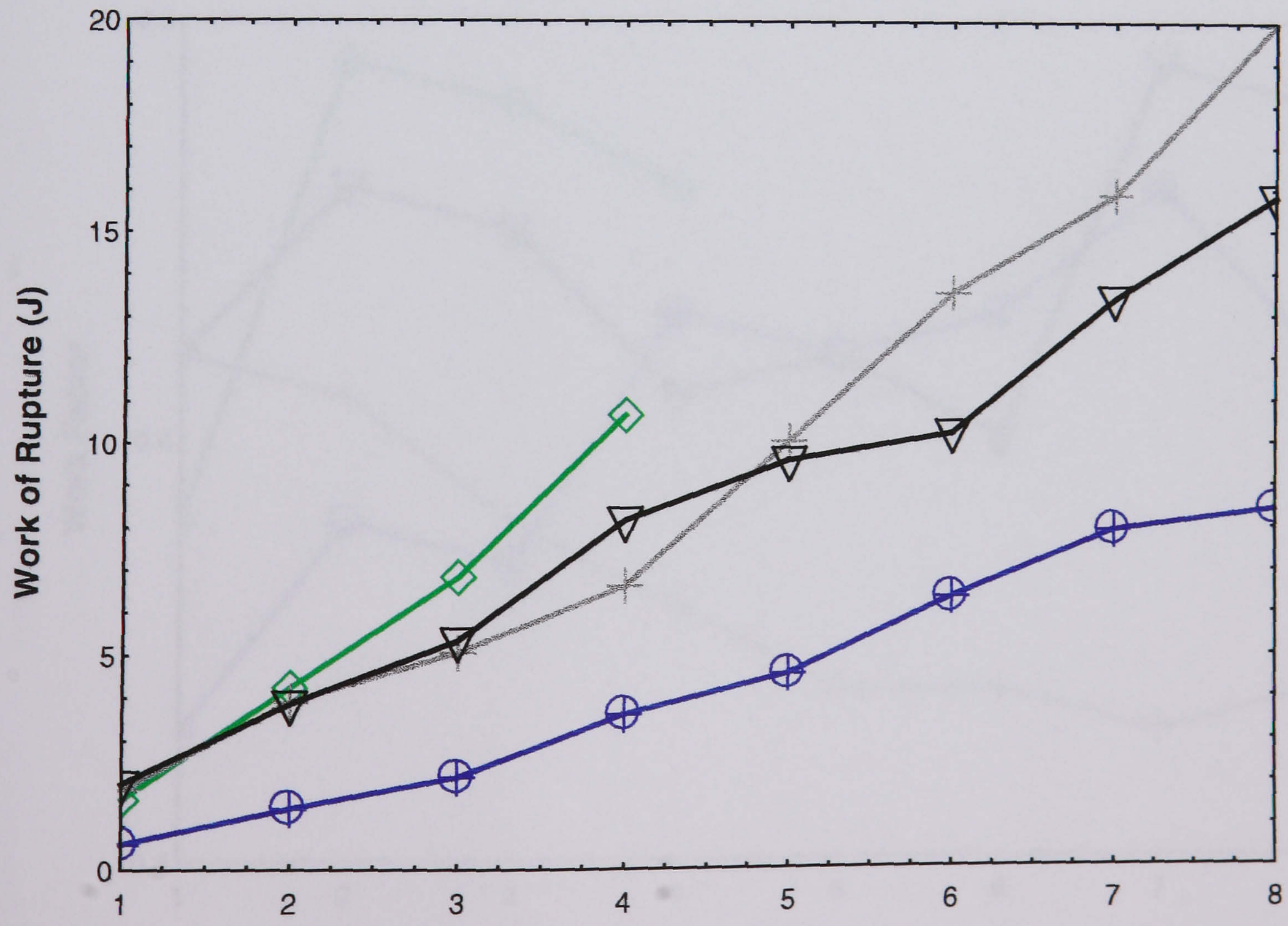

Figure 8.38: *Mean work of rupture against No. of strands for different samples tested (see legends on page 252).*

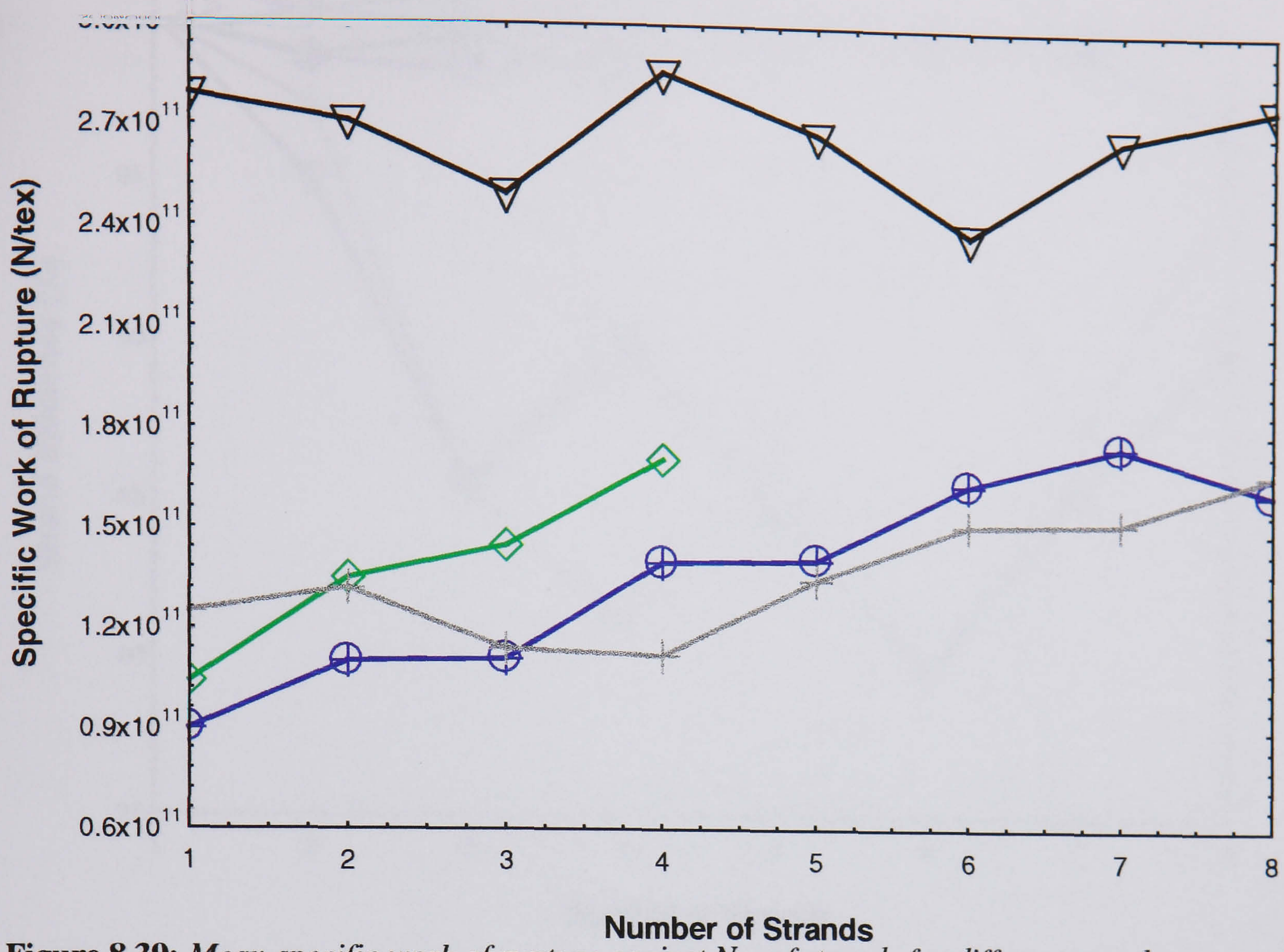

Figure 8.39: *Mean specific work of rupture against No. of strands for different samples tested (see legends on page 252).*

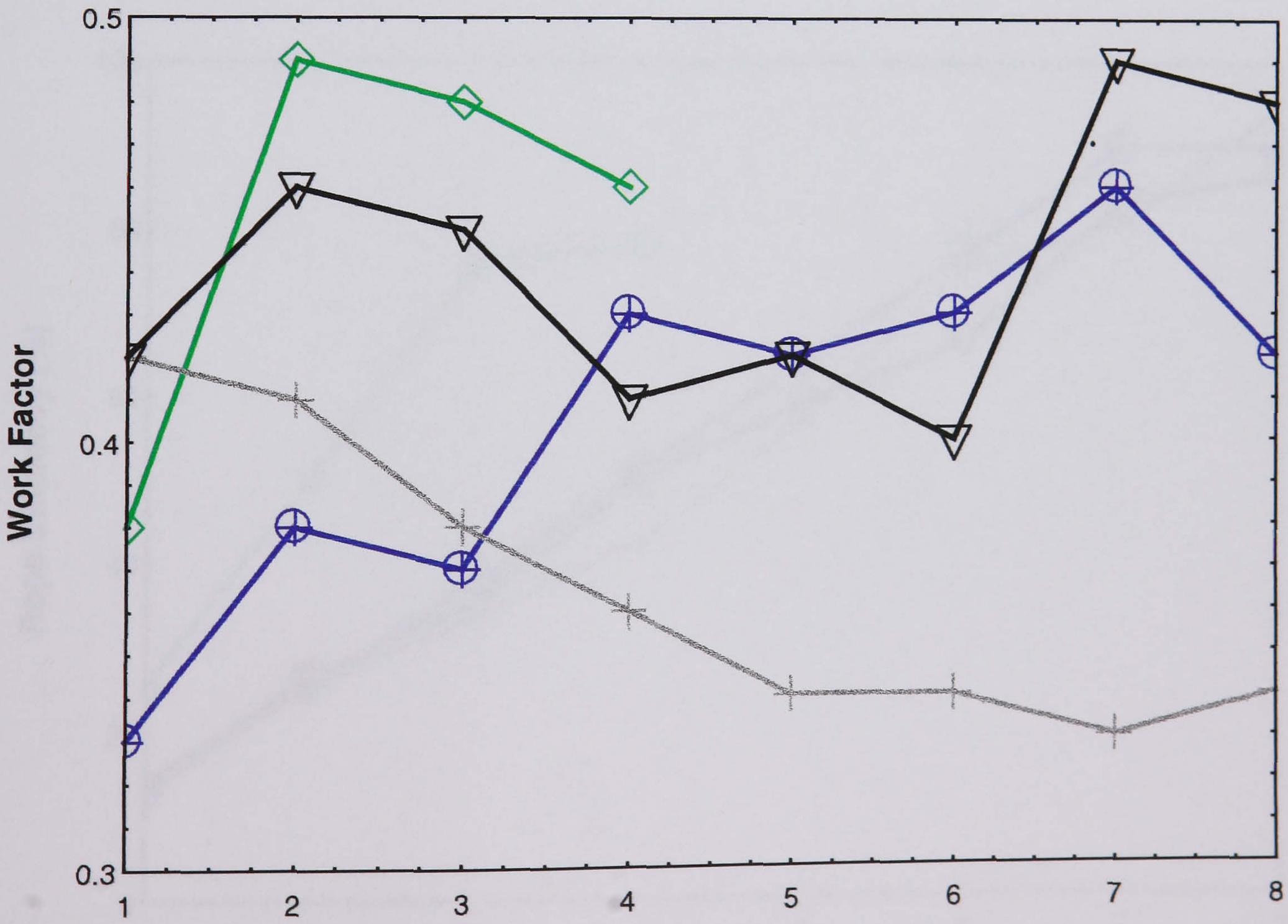

Figure 8.40: *Mean work factor against No. of strands for different samples tested (see legends on page 252).*

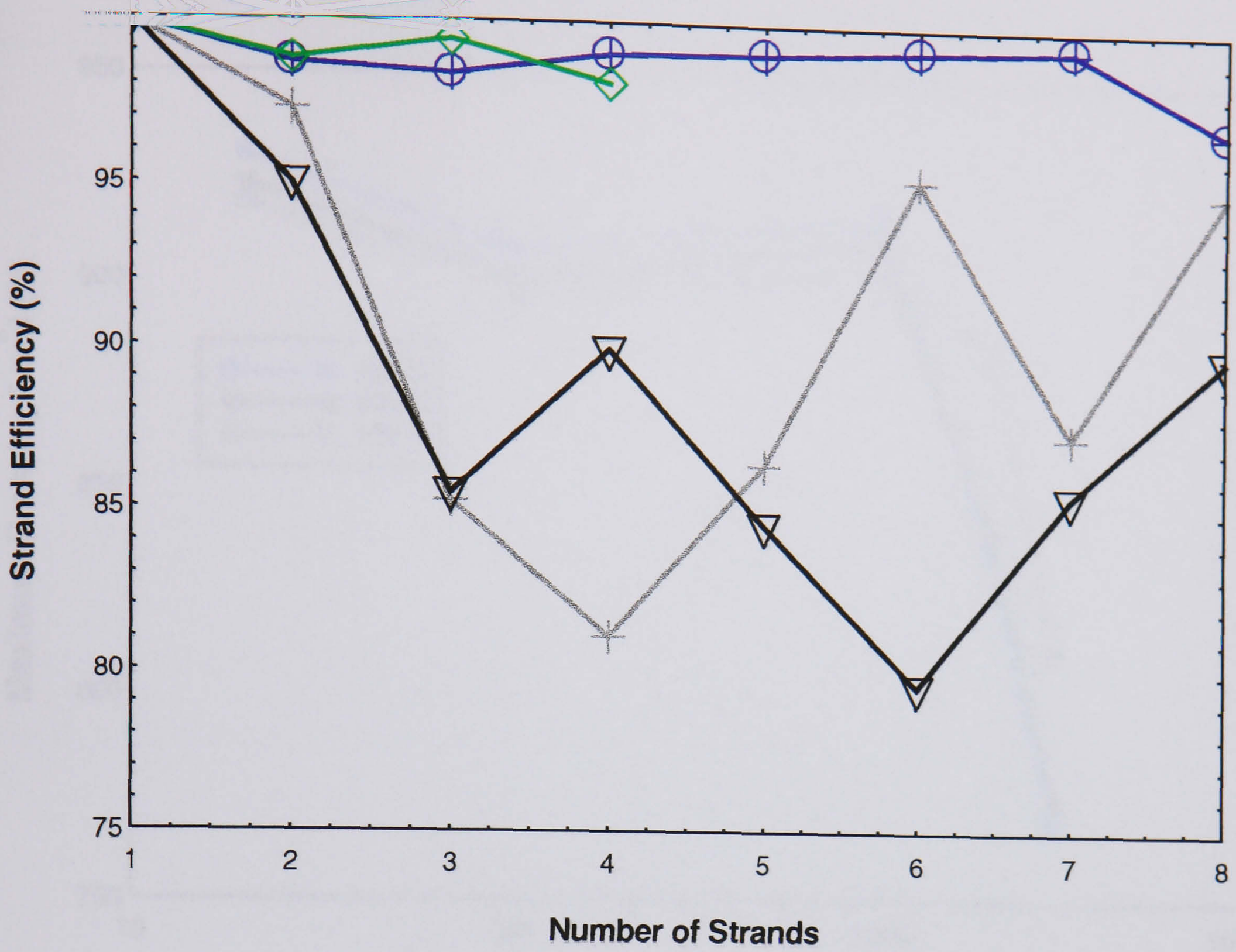

Figure 8.41: *Mean strand efficiency against No. of strands for different samples tested (see legends on page 252).*

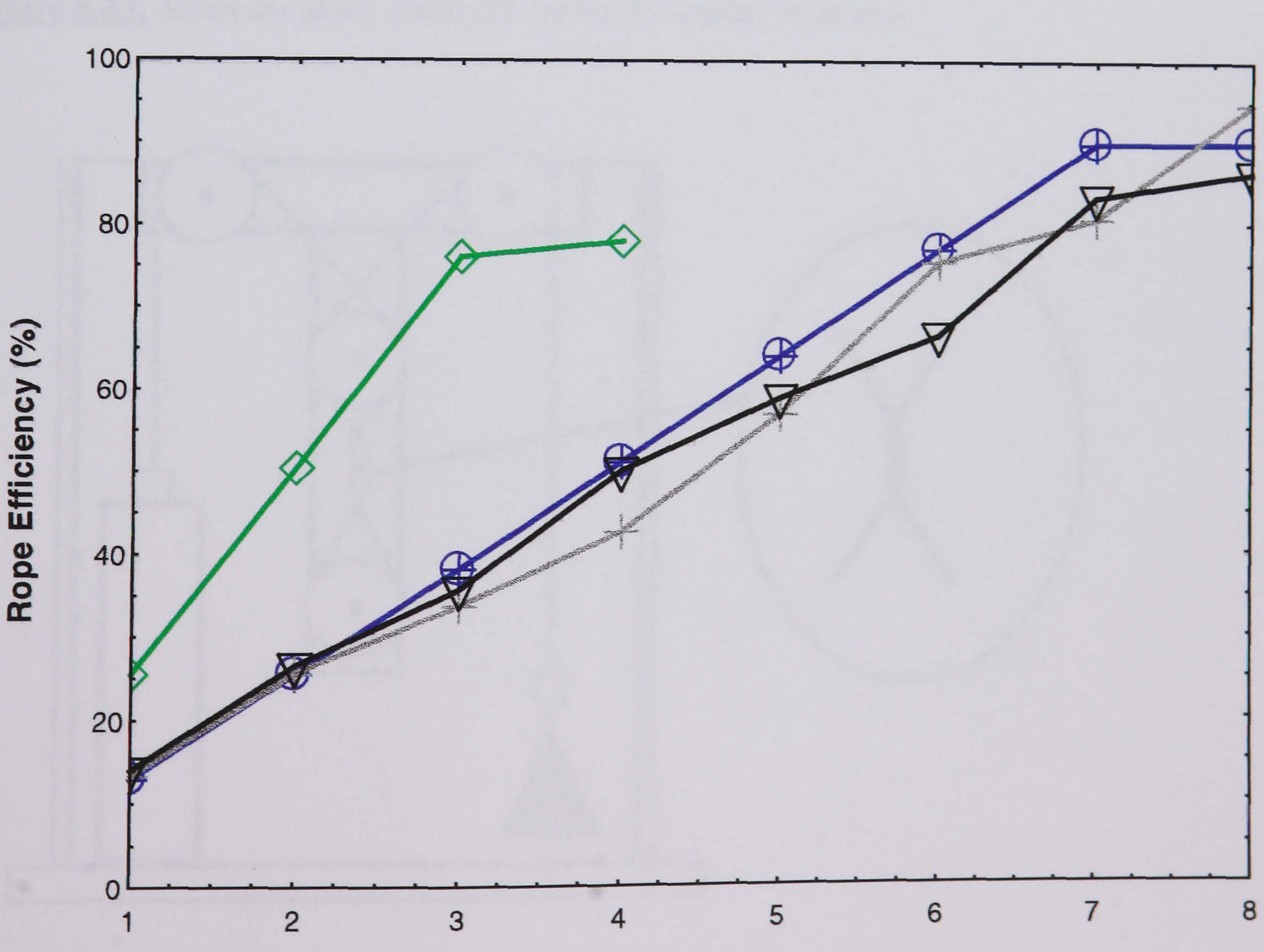

Figure 8.42: *Mean rope efficiency against No. of strands for different samples tested (see legends on page 252).*

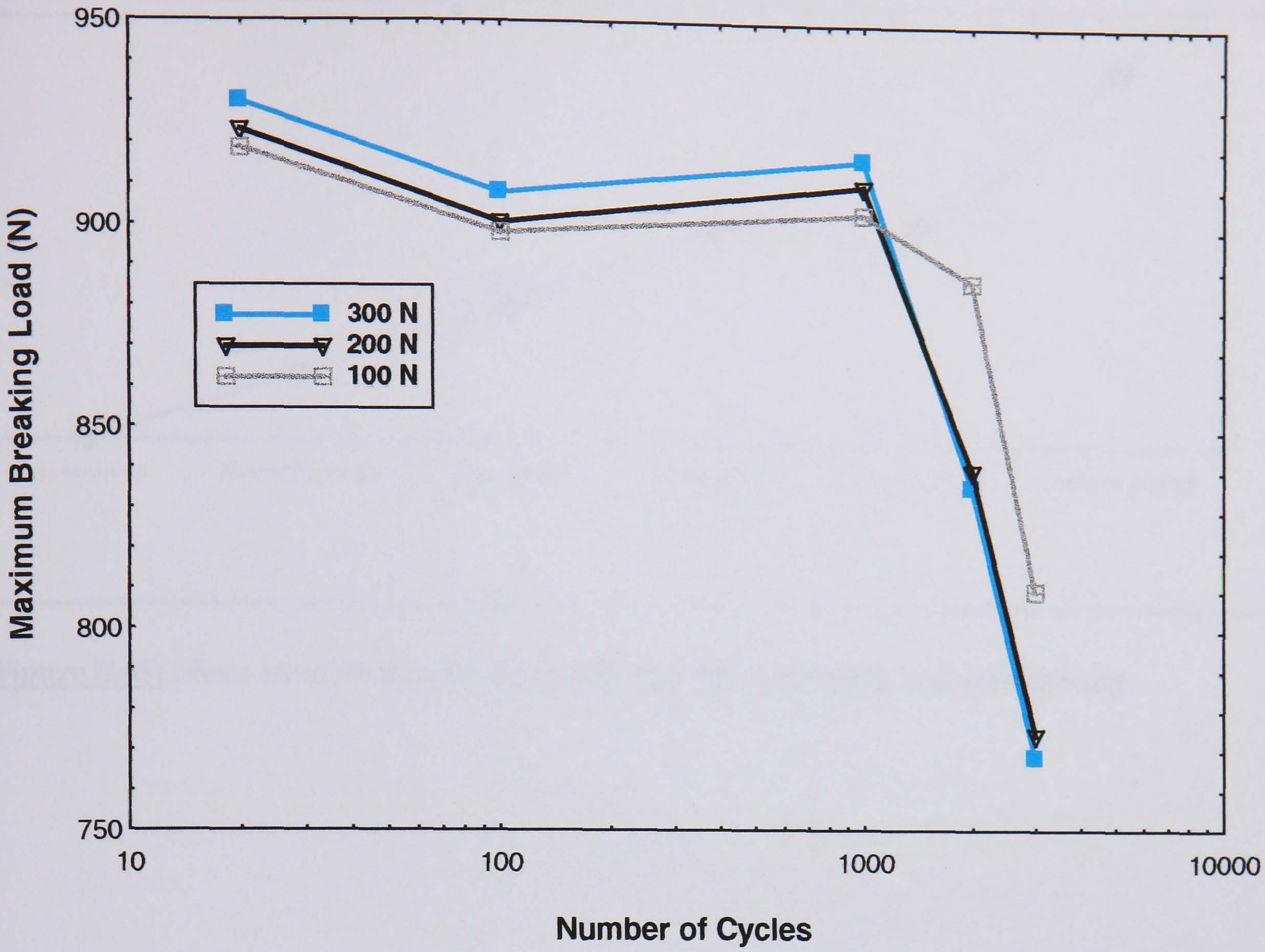

Figure 8.43: *Mean breaking loads for cyclically loaded Dyneema*

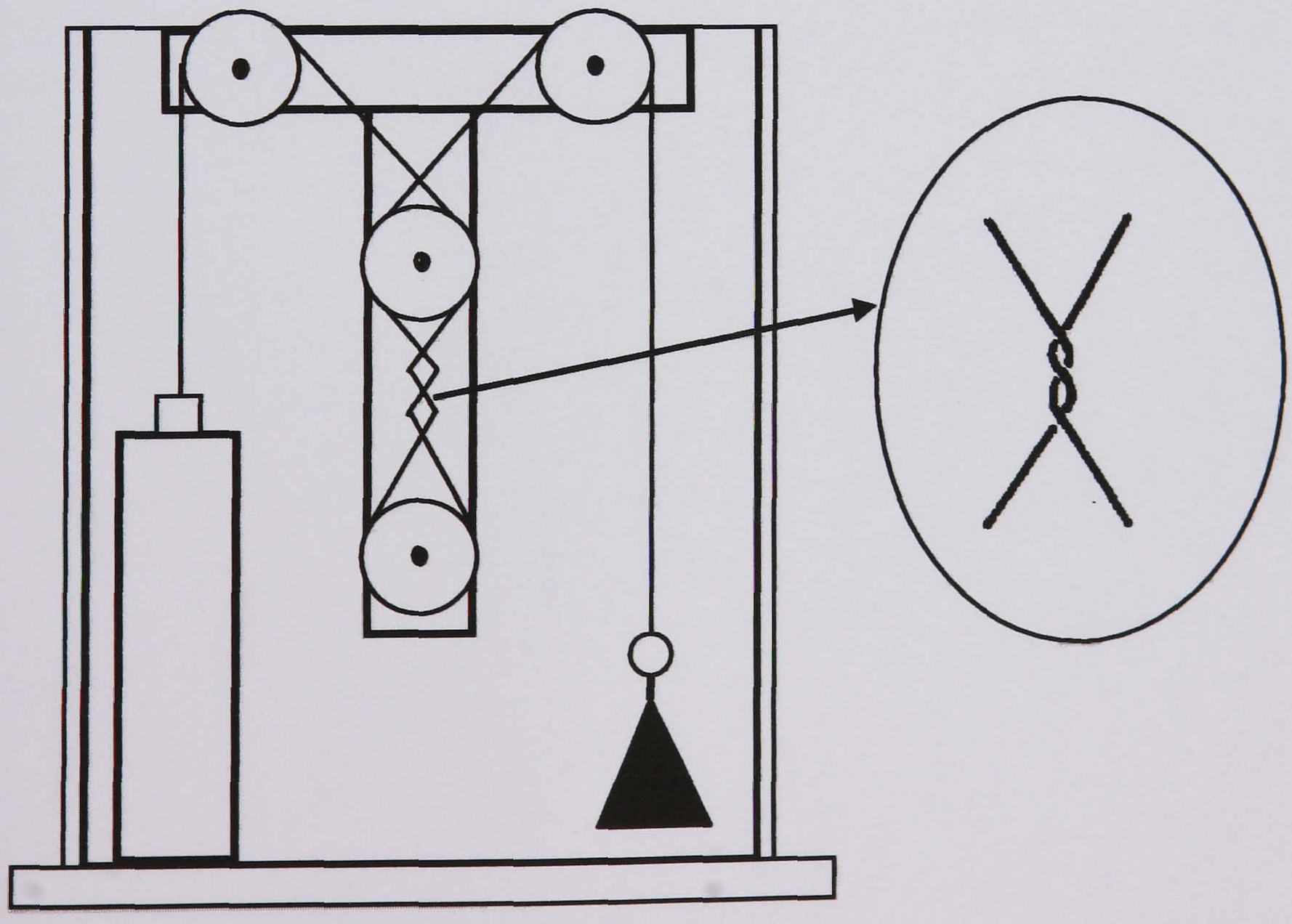

Figure 8.44: *Rope abrasion testing rig used in this study*

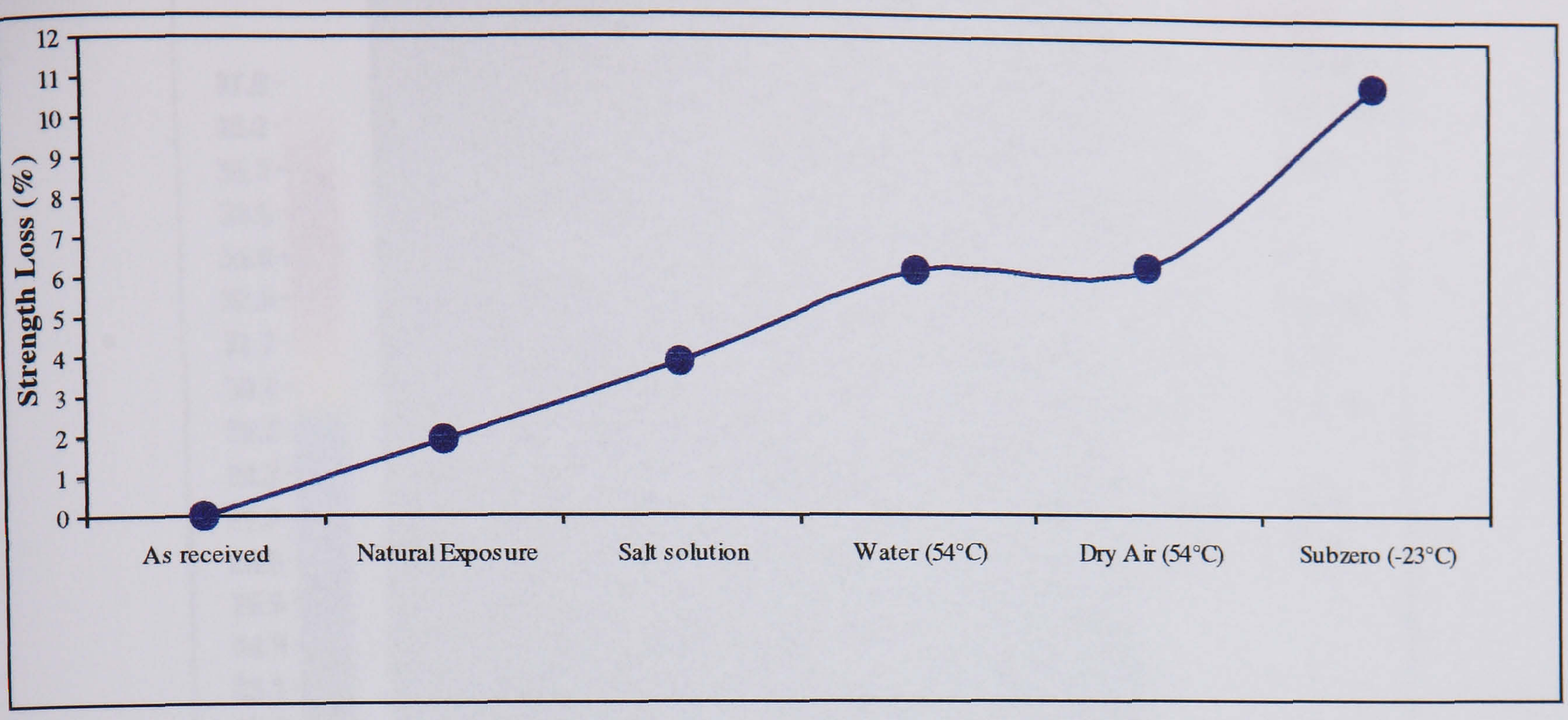

Figure 8.45: *Mean strength loss for Dyneema rope after environmental conditioning*

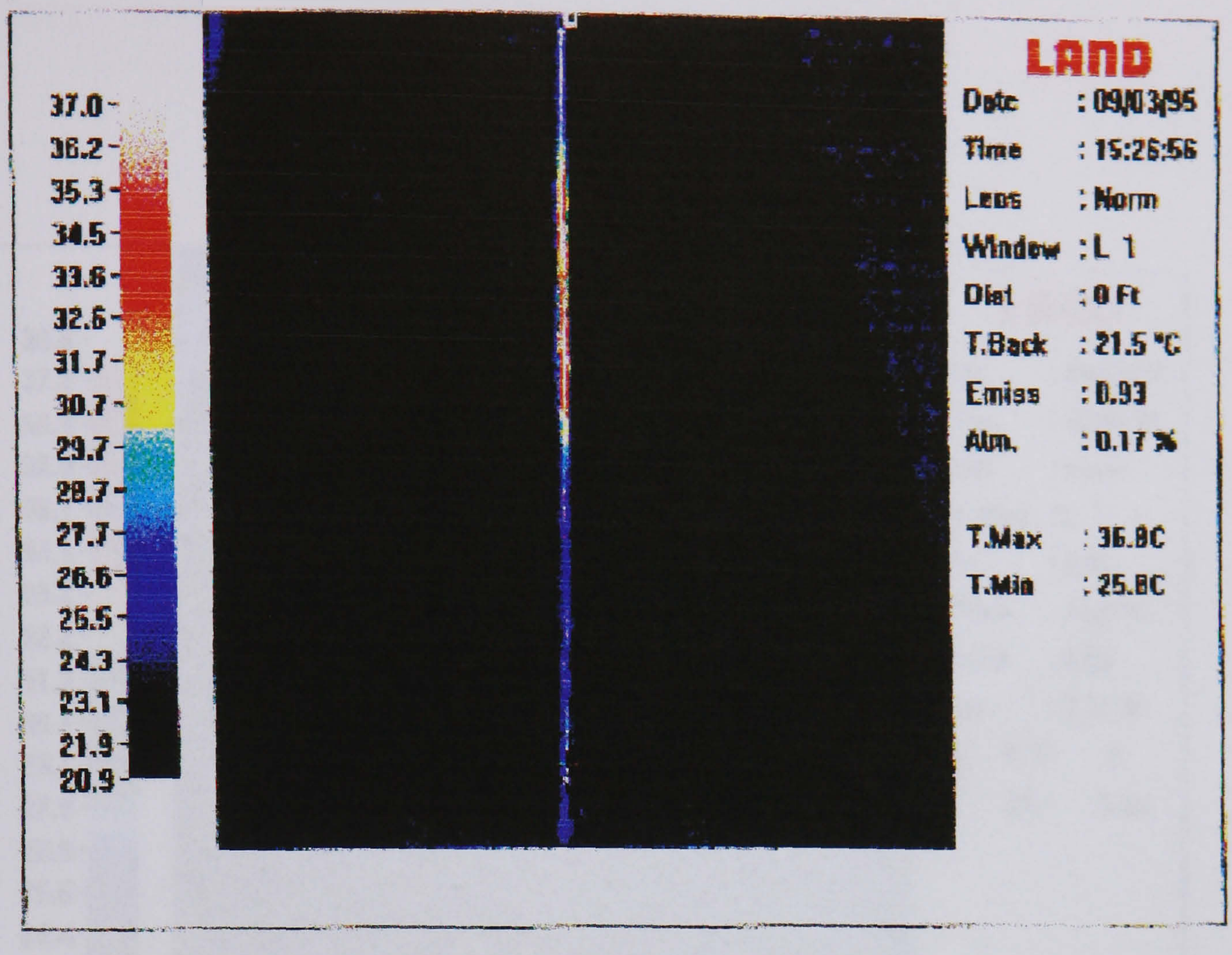

Figure 8.46: *Thermograph of covered Dyneema ropes showing the increase in temperature on the surface of the rope*

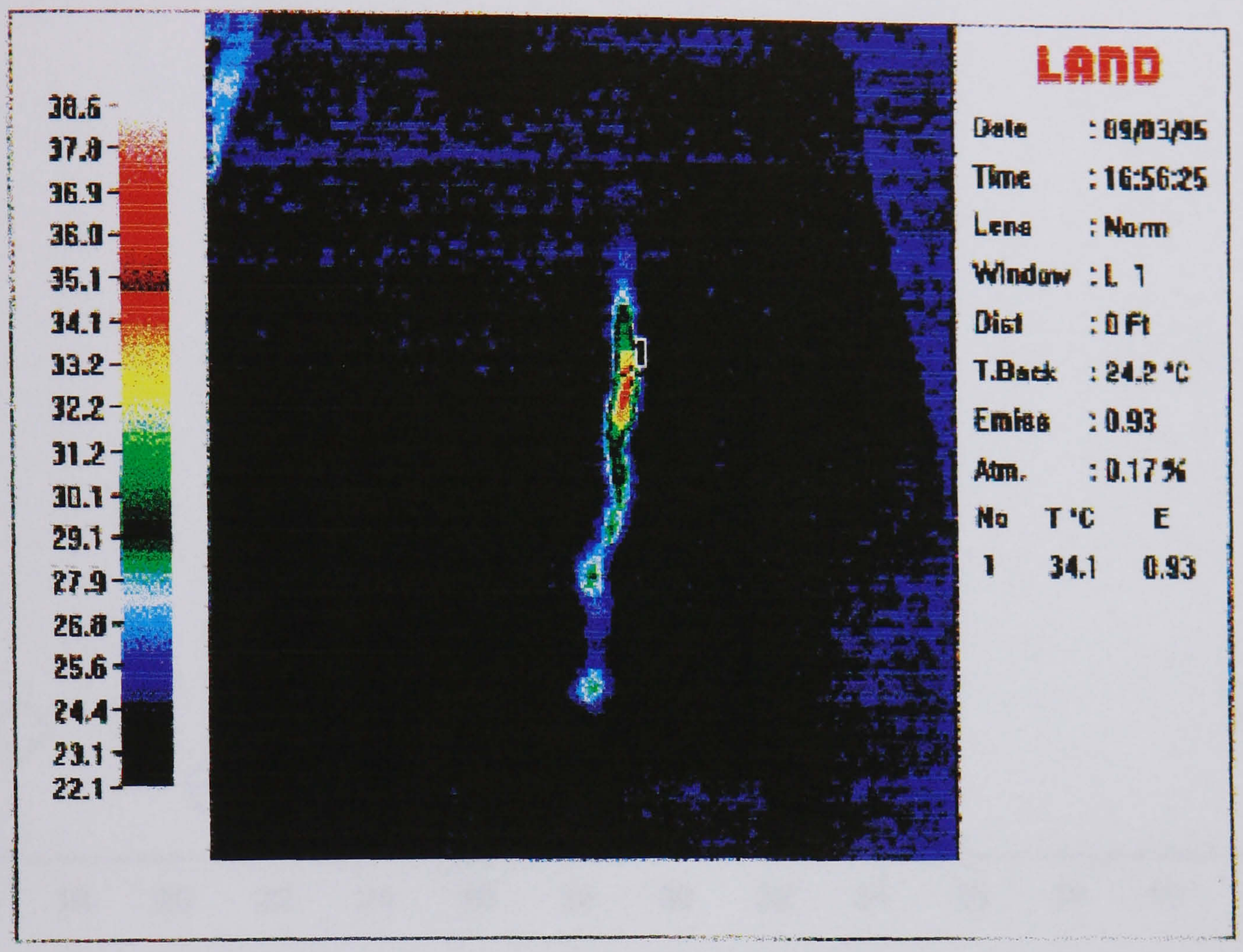

Figure 8.47: *Thermograph of the fractured zone of covered Dyneema ropes*

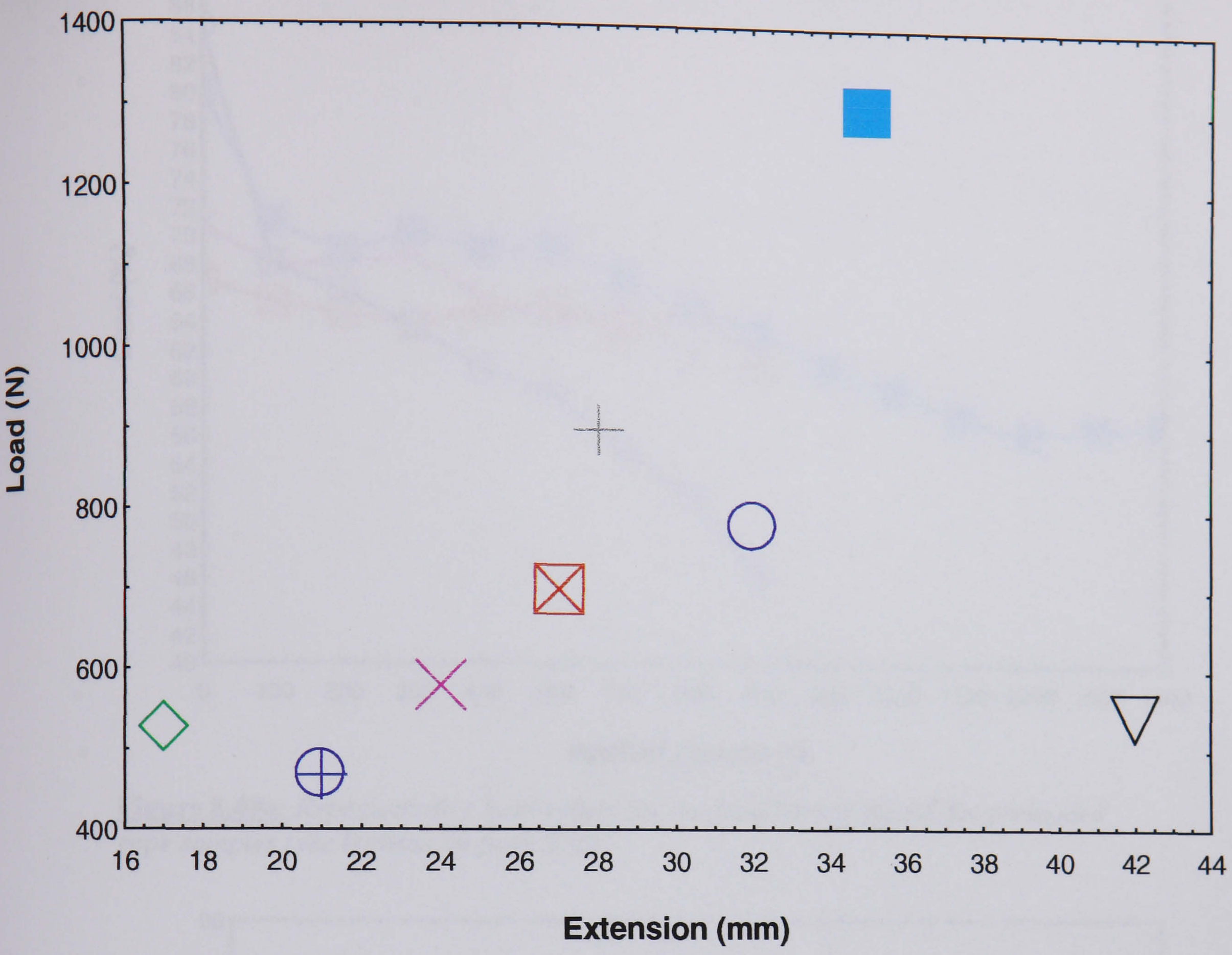

Figure 8.48: *Representative values of the final part of the AE for the as received rope samples (see legends on page 252).*

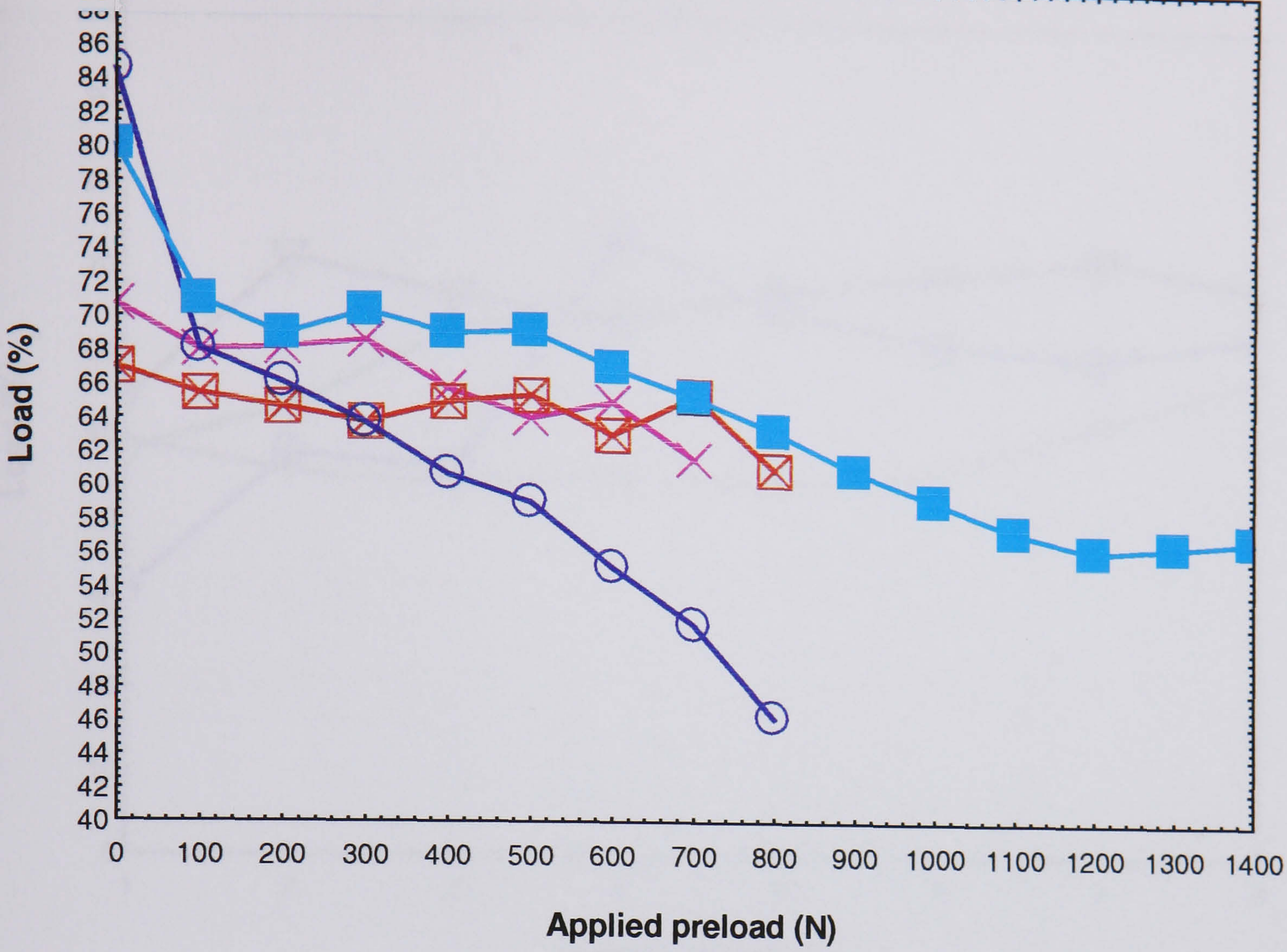

Figure 8.49a: *Representative load values for the final part of the AE for preloaded rope samples (see legends on page 252).*

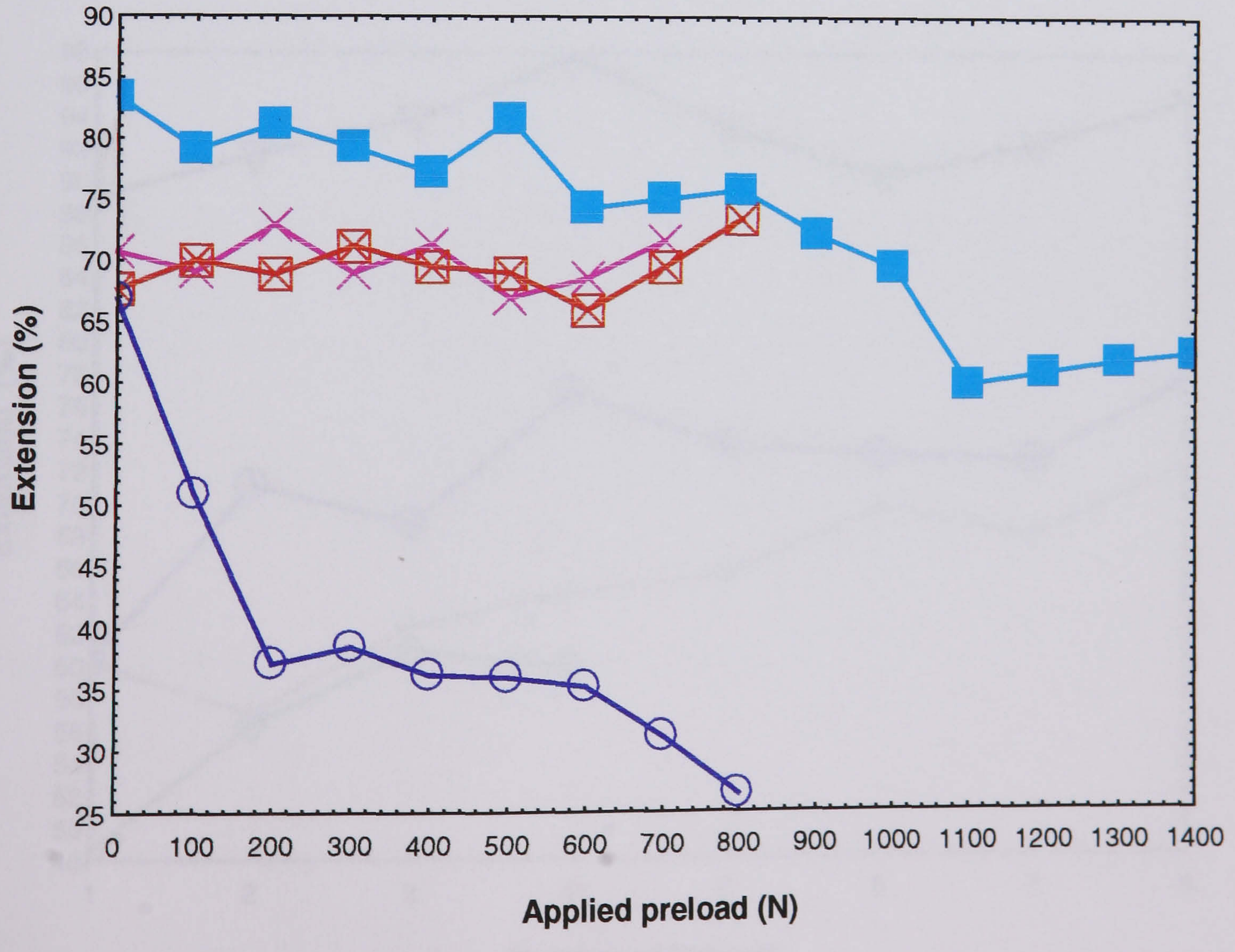

Figure 8.49b: *Representative extension values of the final part of the AE of preloaded rope samples (see legends on page 252).*

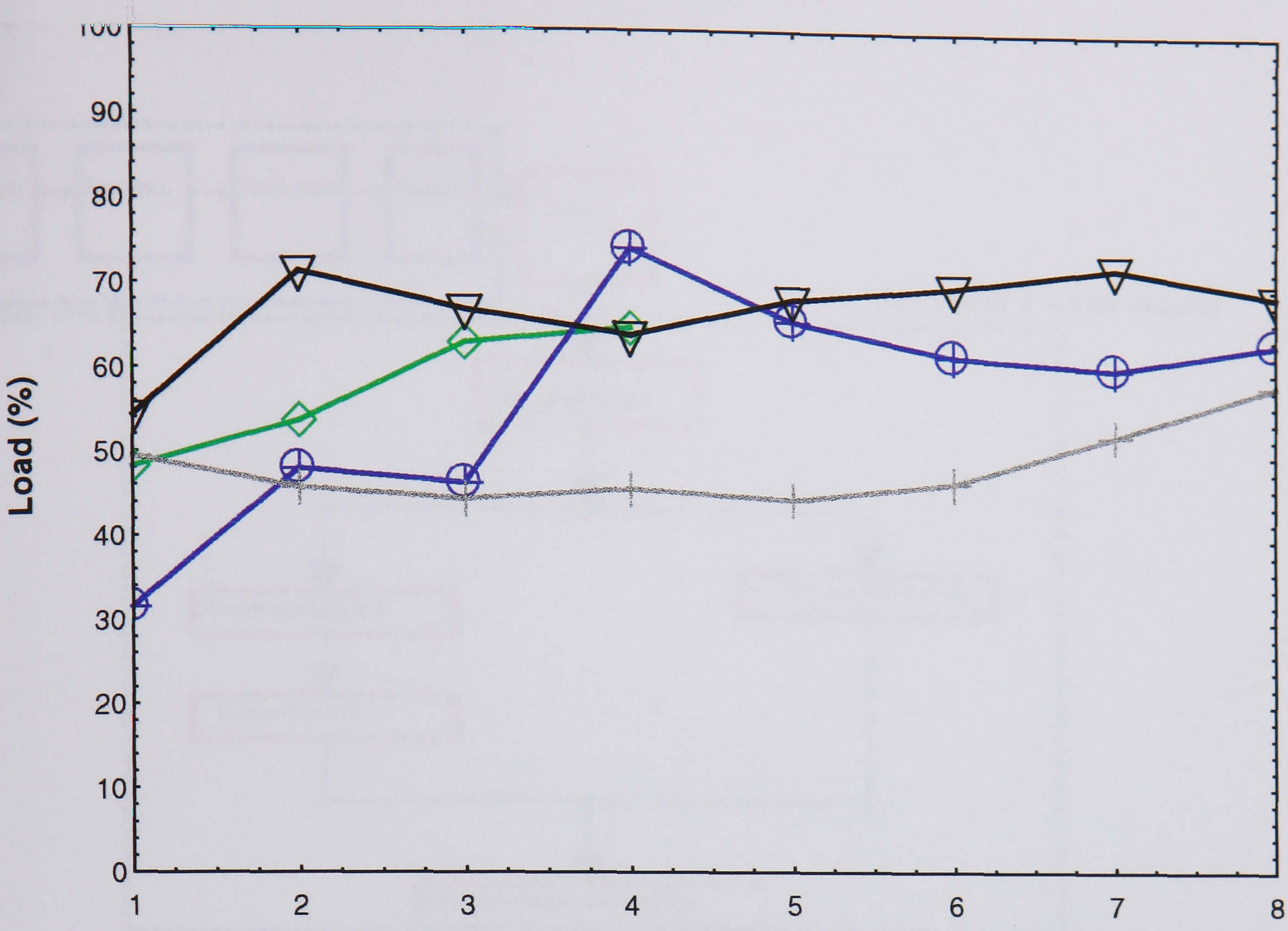

Figure 8.50a: *Representative strength values for the final part of AE with strand removal (see legends on page 252).*

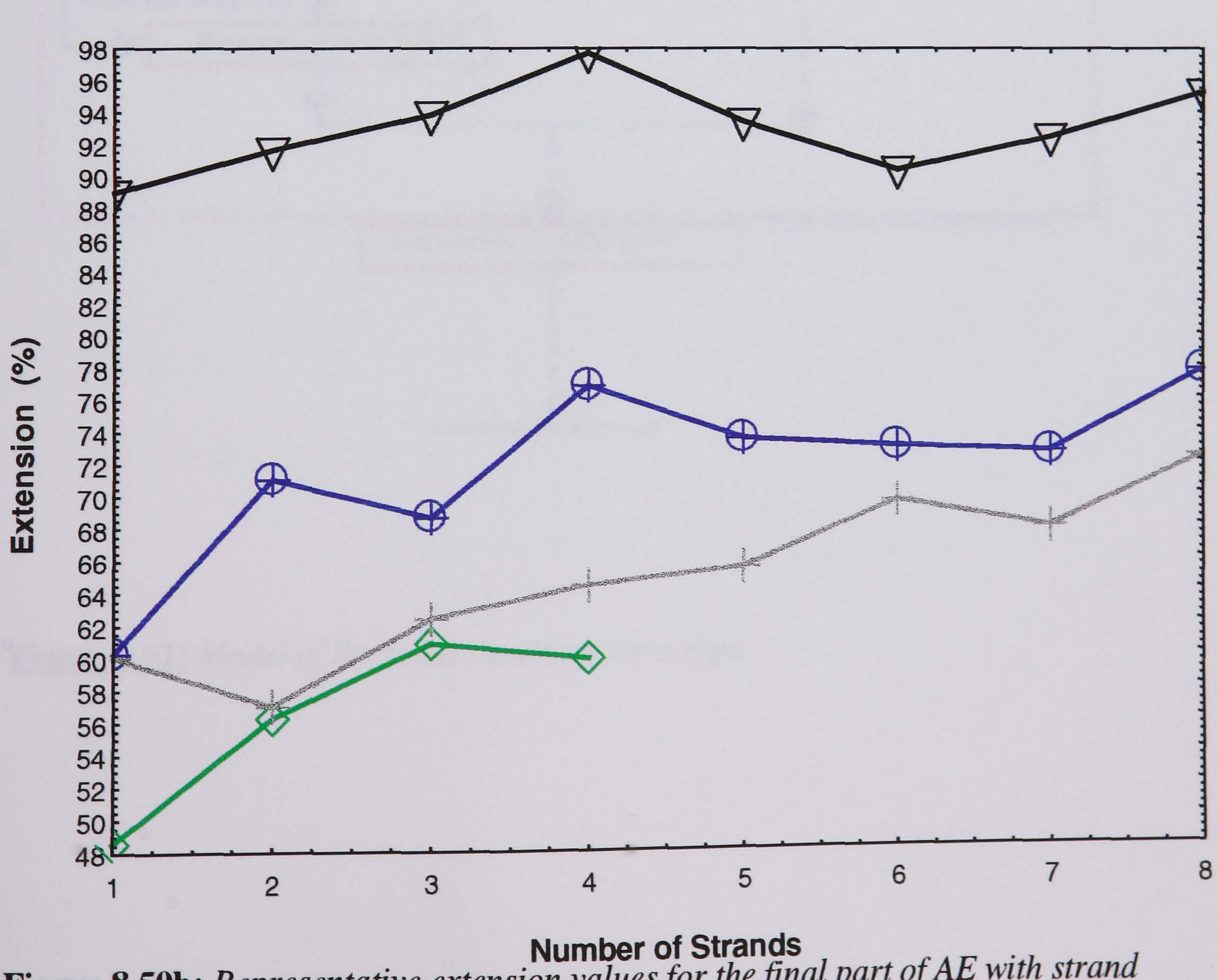

Figure 8.50b: *Representative extension values for the final part of AE with strand removal (see legends on page 252).*

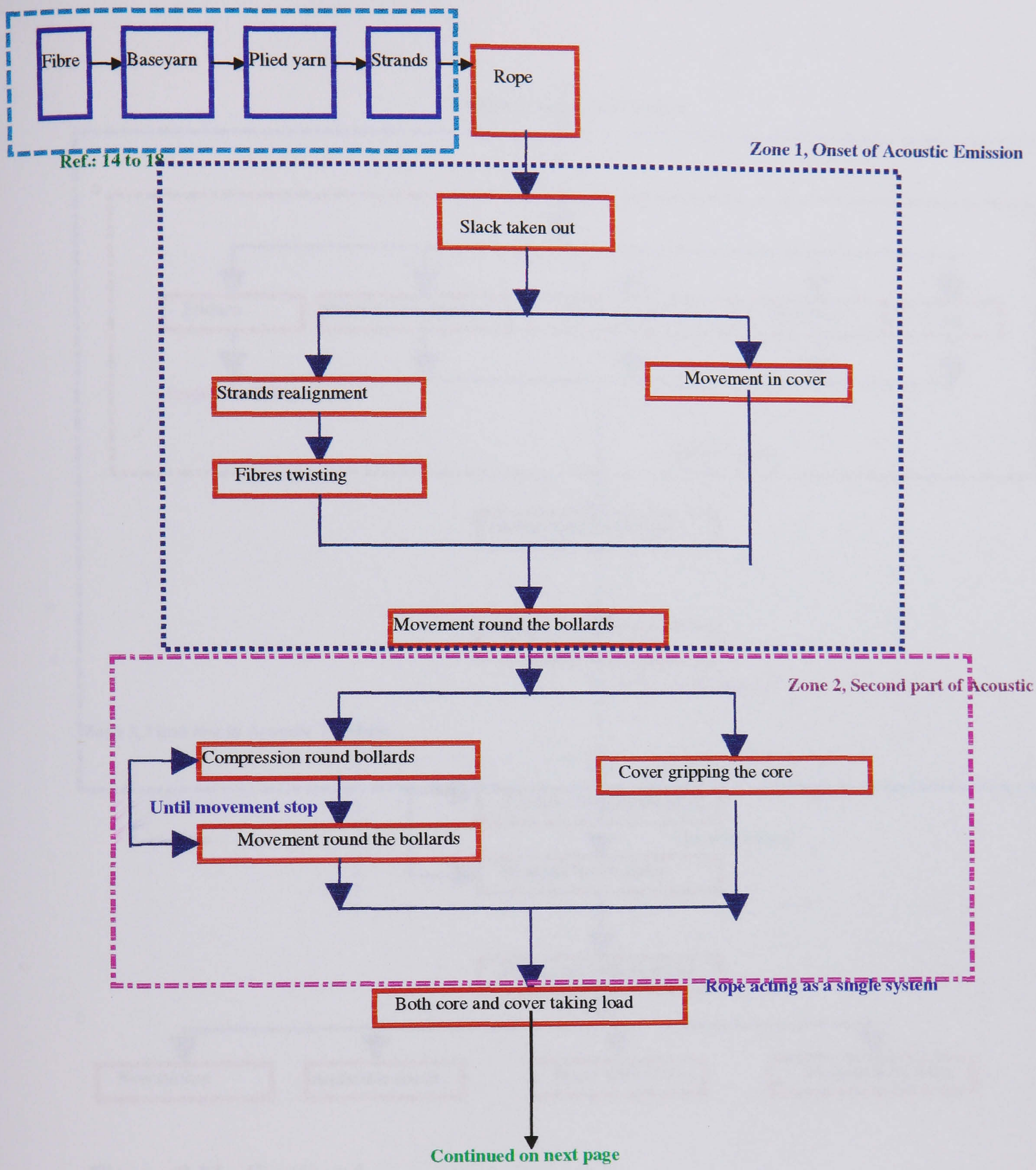

Figure 8.51: *Model of the failure analysis for a rope*

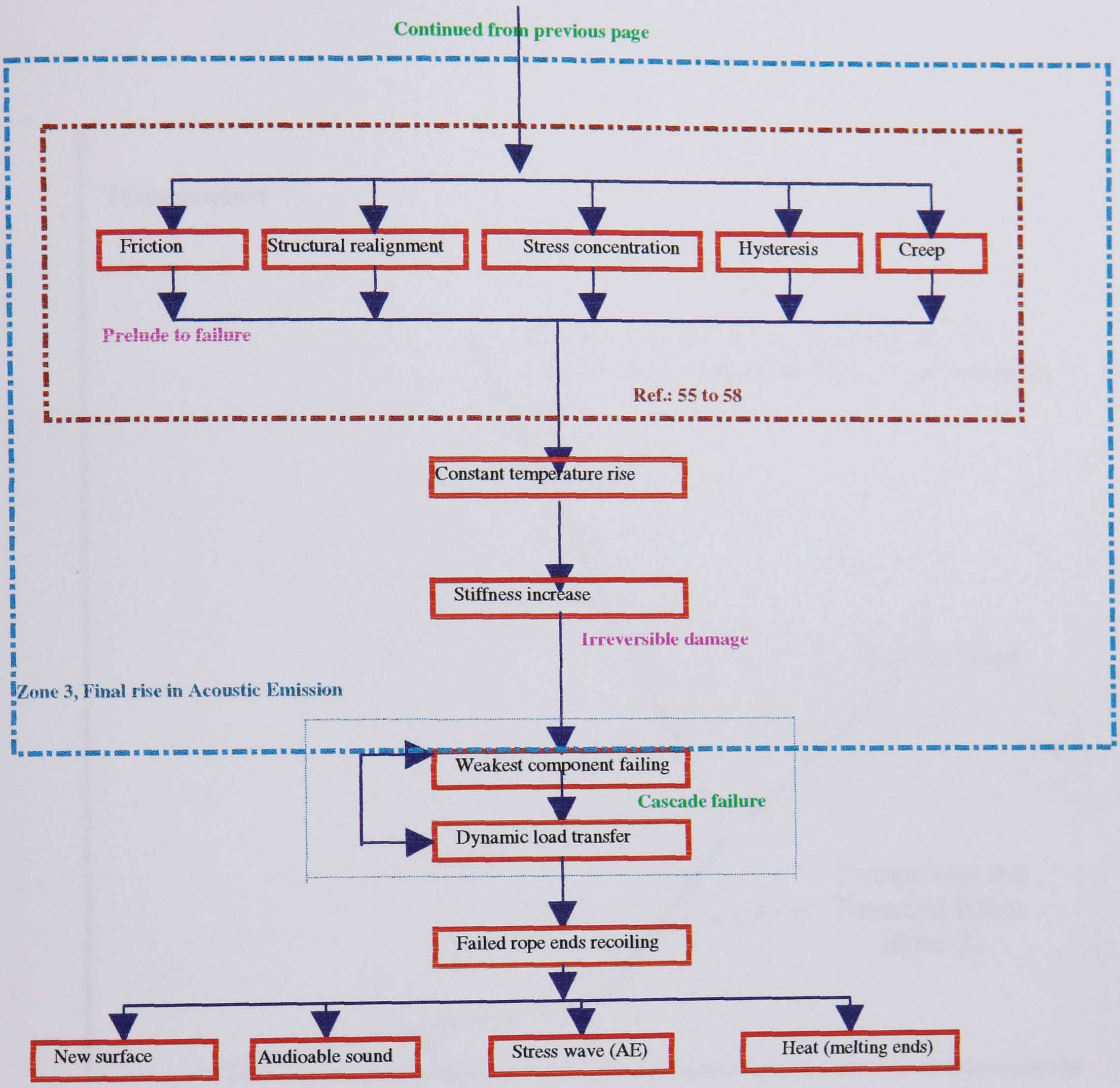

Figure 8.51: *Continued*

Figure 8.52: *Model of the failure analysis for the thermal imaging*

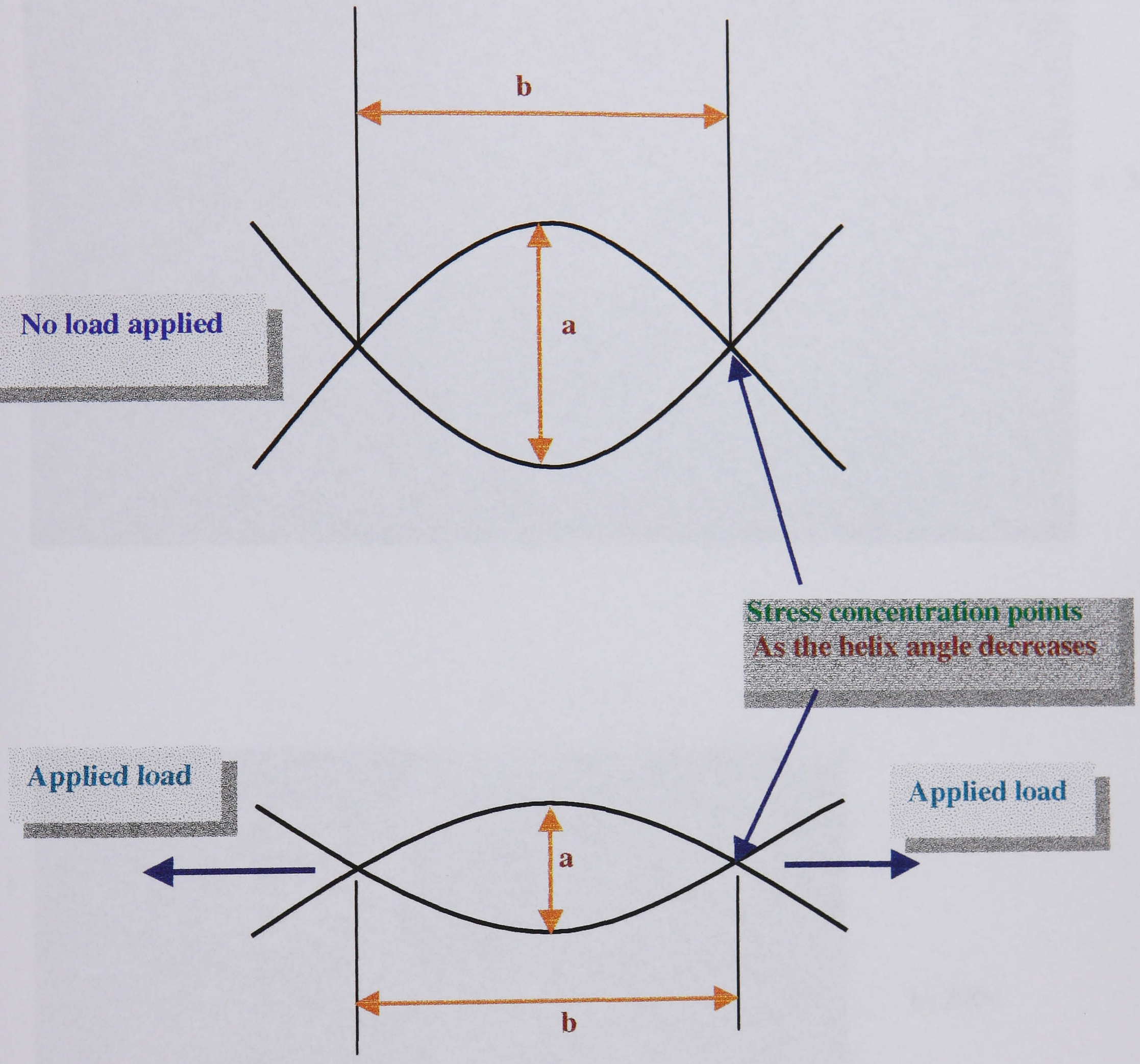

Figure 8.53: *Stress concentration representation*

a) 30×

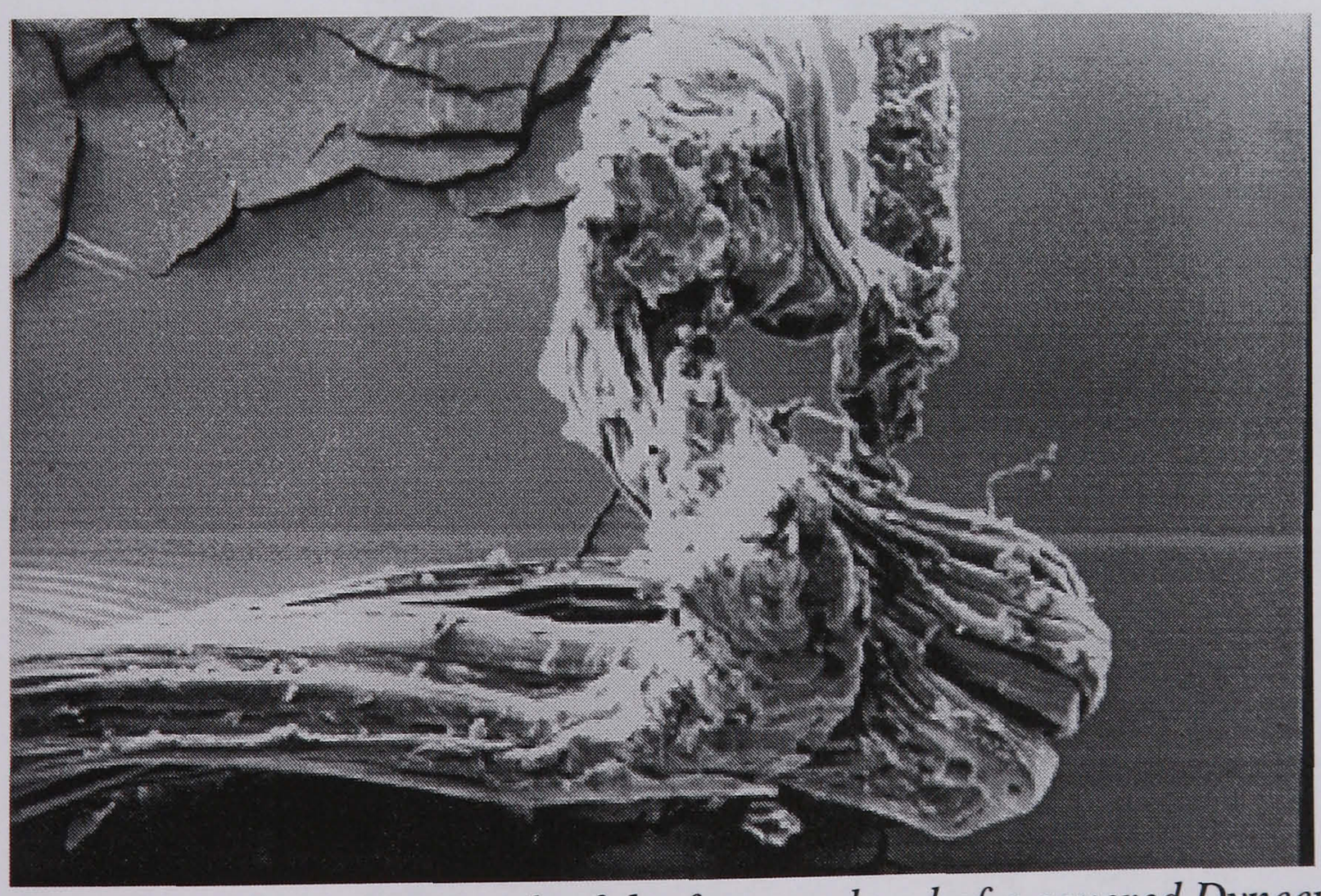

b) 200×

Plate 8.1: *SEM micrograph of the fractured end of a covered Dyneema rope Showing the melted region*

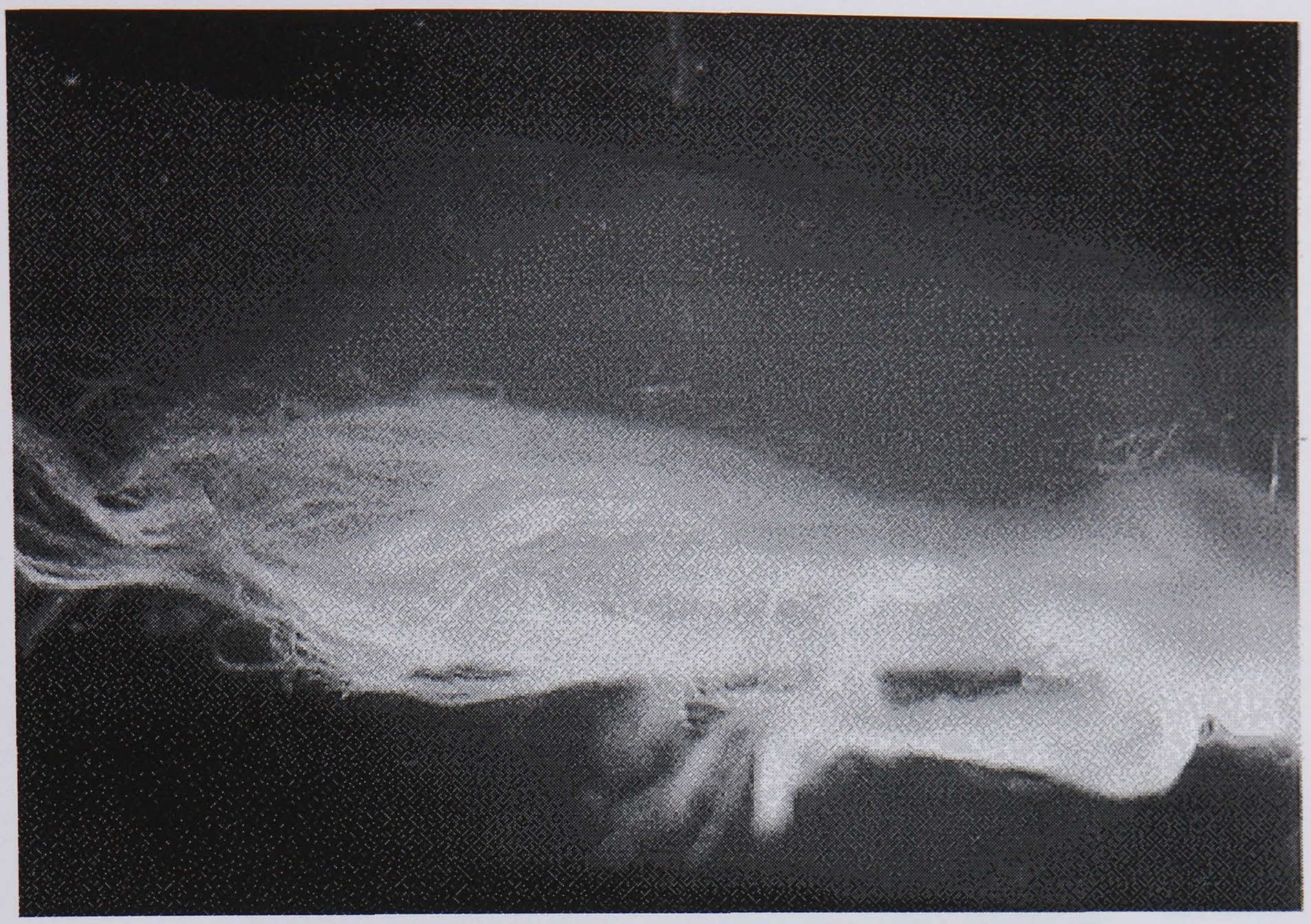

Plate 8.2a: *Failed end of an uncovered Dyneema line after tensile loading.*

Plate 8.2b: *SEM micrographs of the fractured end of uncovered Dyneema showing the collapse of fibres (30×)*

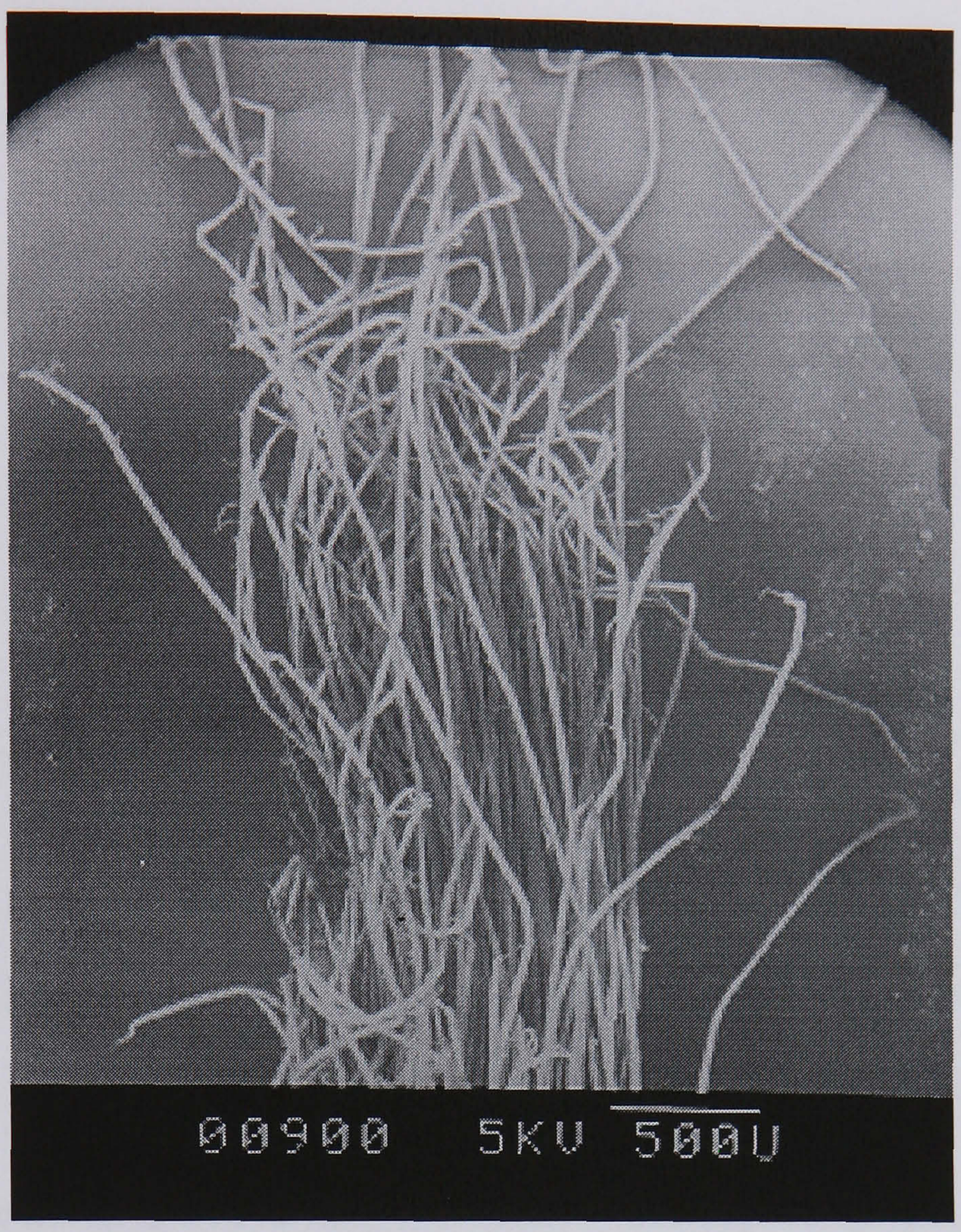

a) 30×

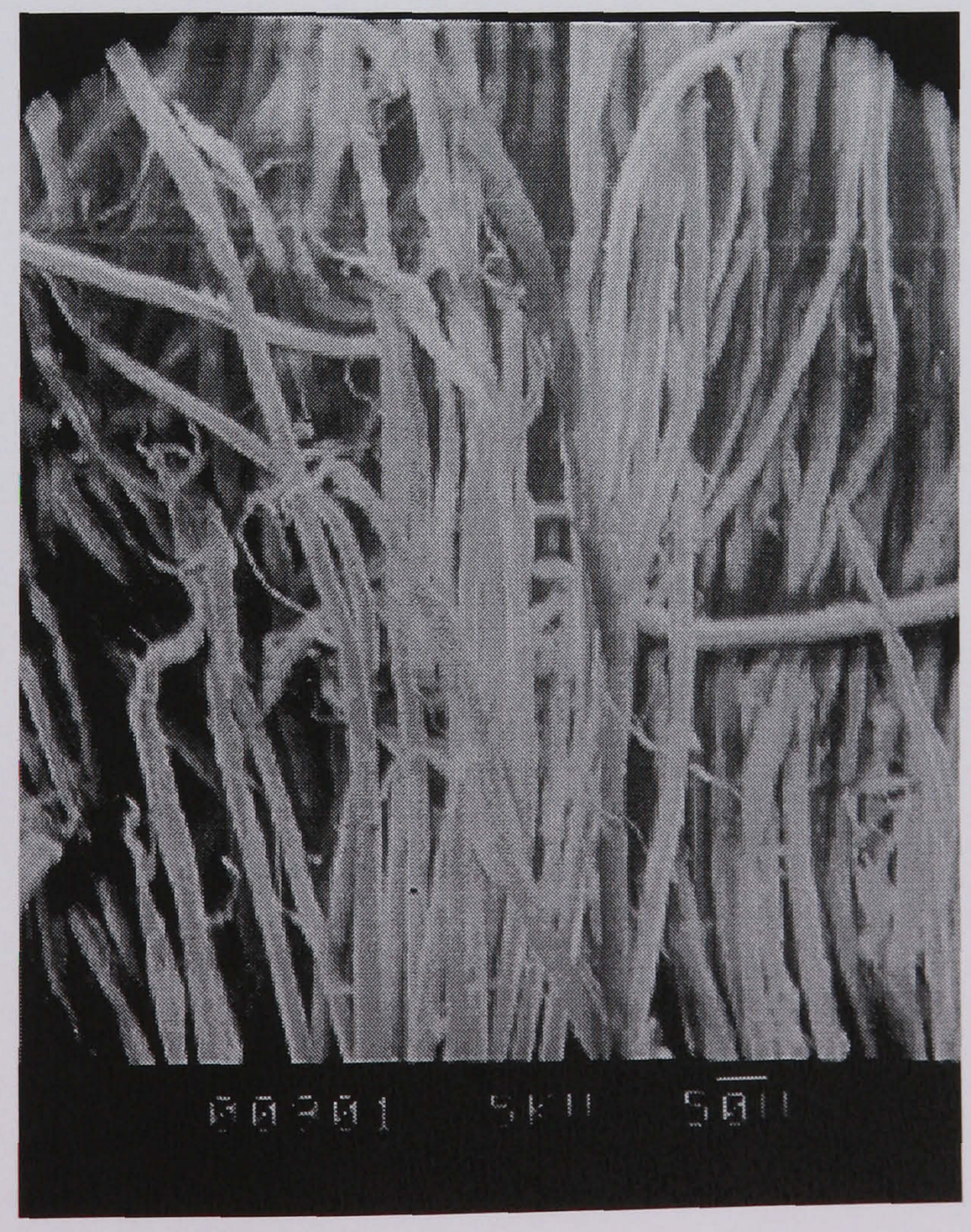

b) 100×

Plate 8.3: *SEM micrographs of a failed end of as received Vectran*

Plate 8.4: *SEM micrograph of as received Vectran showing fusion of the fibres and strands leading increased stiffness (30×)*

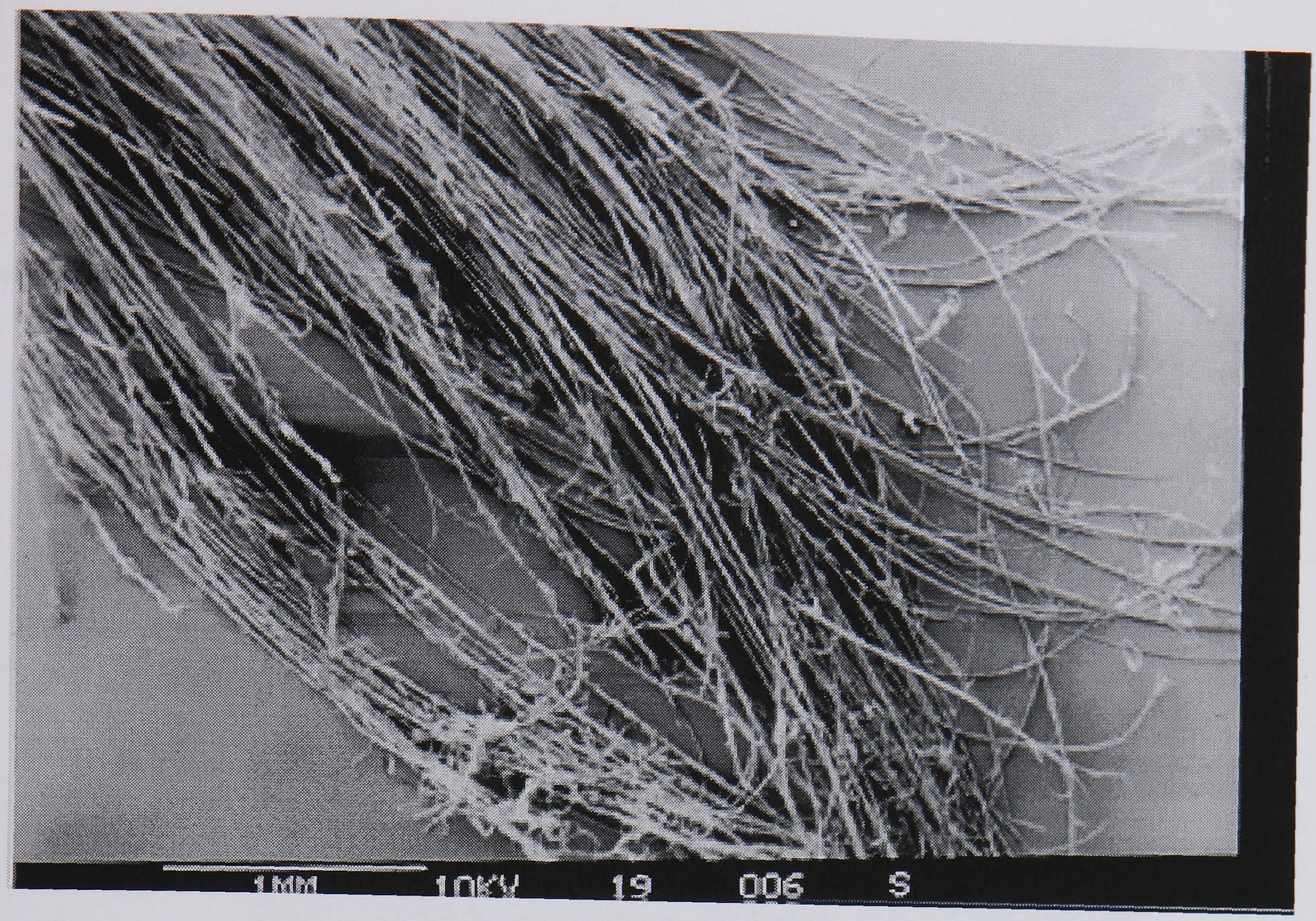

a) 100×

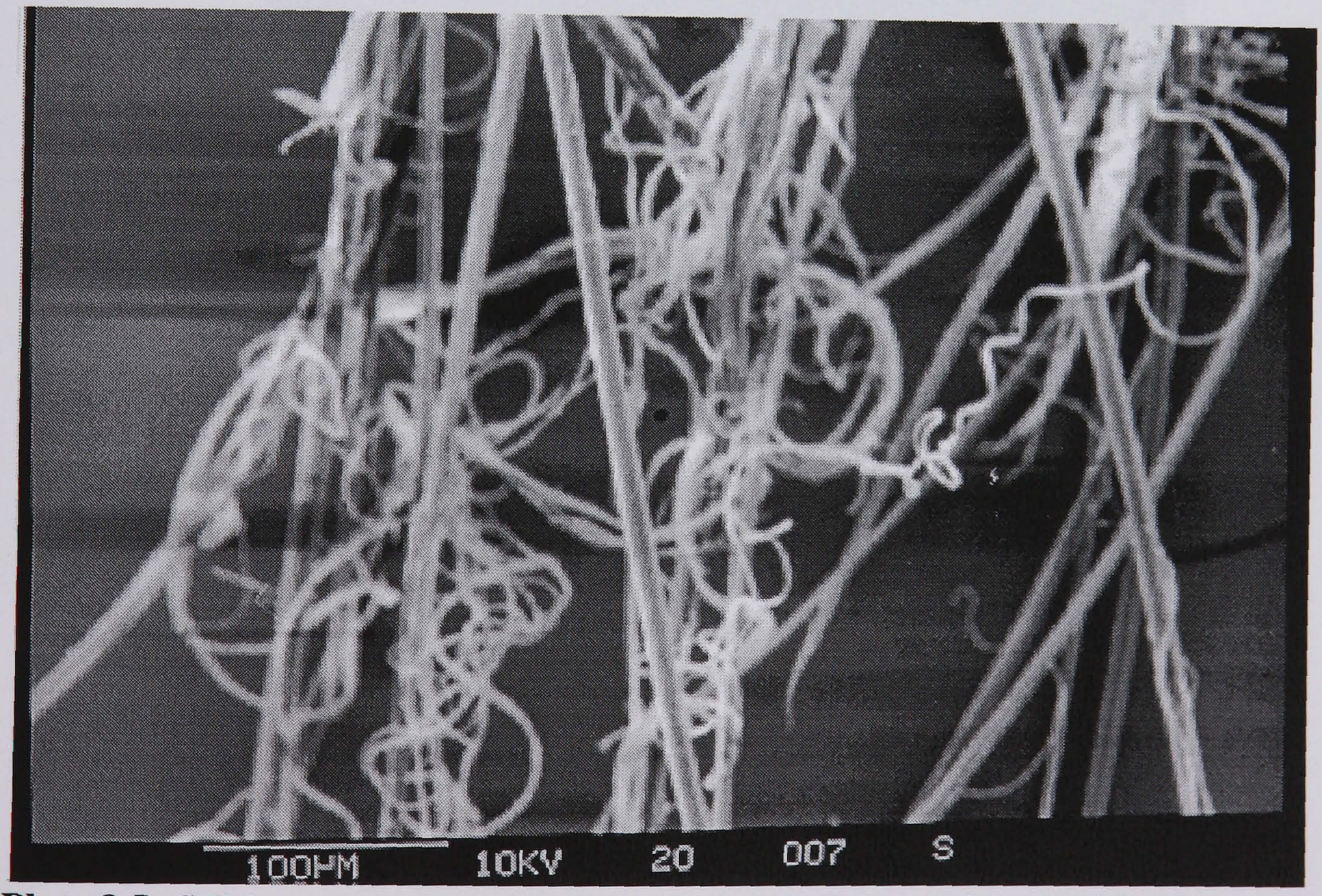

b) 1000×

Plate 8.5: *SEM micrographs of the fractured end of 4 strand covered Technora rope showing the fuzzing effect of fibres after failure (1000X)*

Plate 8.6: *SEM micrograph of the fractured end of an 8 strand covered Technora rope after tensile loading (30×)*

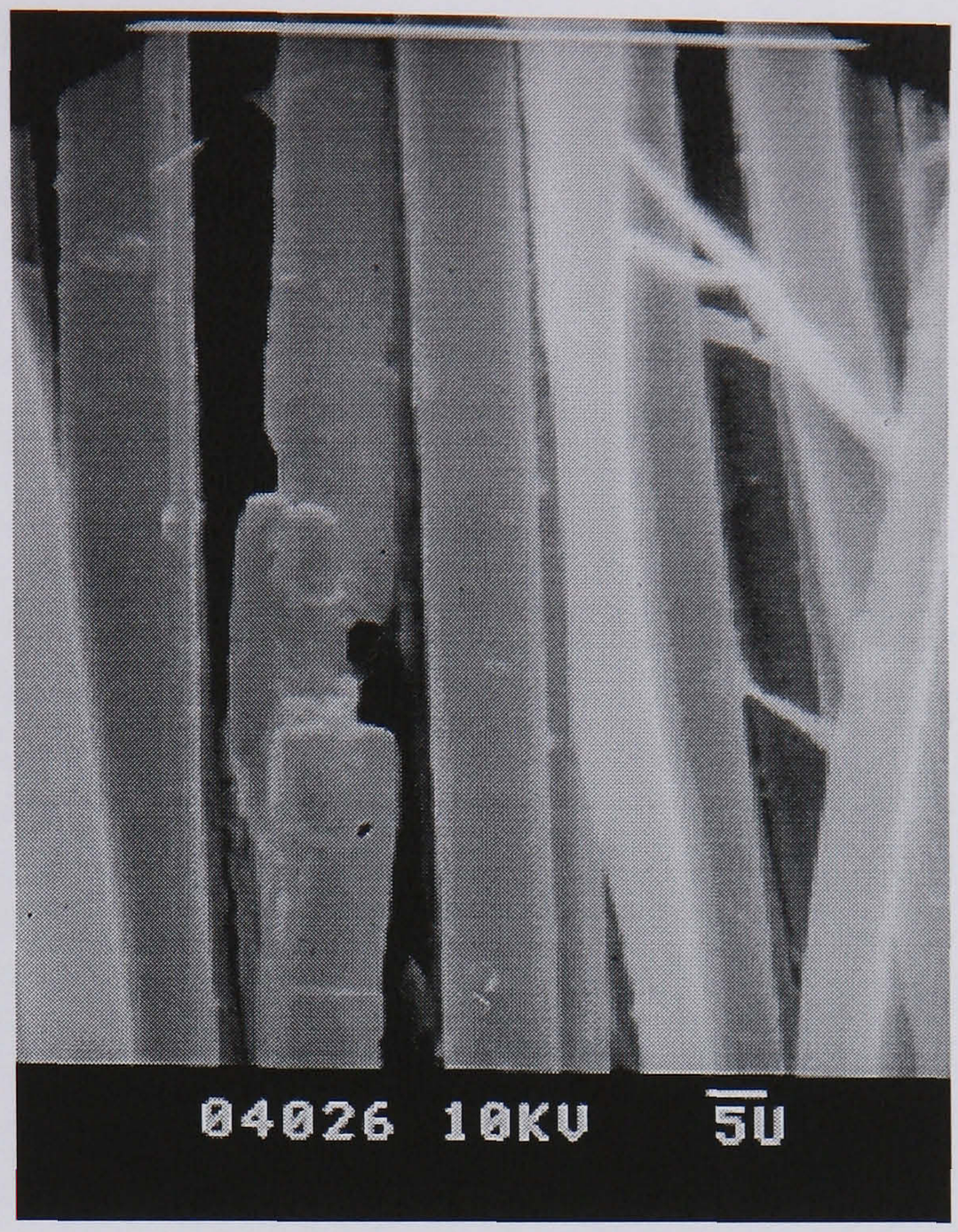

Plate 8.7a: *SEM micrographs of 8 strand covered Technora Rope fibres showing fibre fracture due to recoiling effects (1000×)*

Plate 8.7b: *SEM micrographs of failed 8 strand covered Technora fibres showing signs of kinkbanding and twisting (1000X)*

a) 100×

b) 500×

Plate 8.8: *SEM micrographs of fibres of an uncovered 8 strand Technora deforming & twisting*

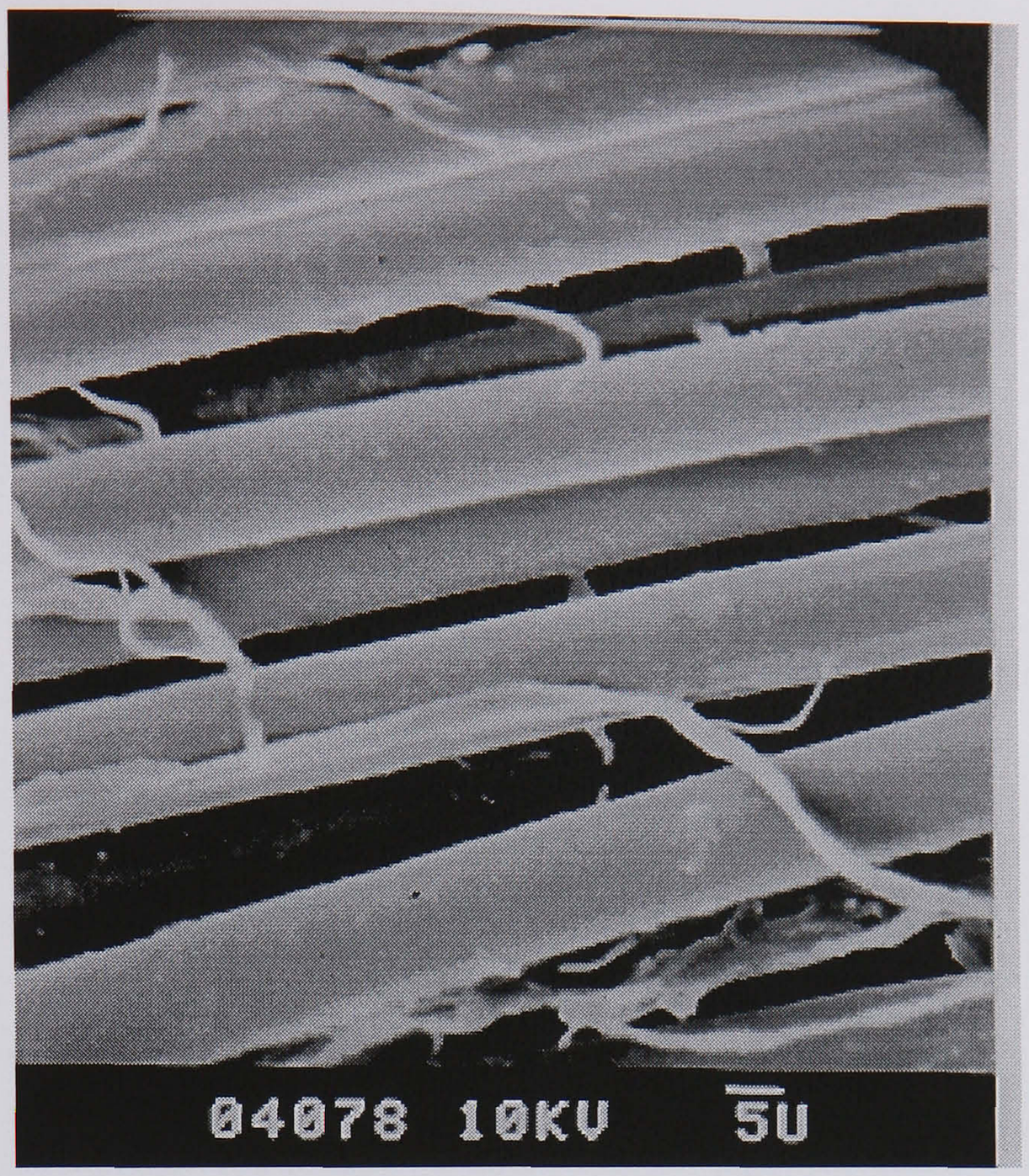

Plate 8.9: *SEM micrographs of uncovered 8 strand Technora showing the Peeling effect of fibre surfaces after tensile loading (1000×)*